CENTRO INTERNACIONAL DE ESTUDOS
DE DOUTORAMENTO E AVANZADOS
DA USC (CIEDUS)

TESE DE DOUTORAMENTO

# THERMAL AZIDE-ALKYNE CYCLOADDITION (TAAC) AS EFFICIENT CLICKED CHEMISTRY TOOL FOR THE FUNCTIONALIZATION OF DENDRIMERS AND POLYMERS

Hasan Haroon Tawara Ma'un

**ESCOLA DE DOUTORAMENTO INTERNACIONAL**
**PROGRAMA DE DOUTORAMENTO EN CIENCIA E TECNOLOXÍA QUÍMICA**

SANTIAGO DE COMPOSTELA
2019

USC
UNIVERSIDADE
DE SANTIAGO
DE COMPOSTELA

CENTRO INTERNACIONAL DE ESTUDOS DE DOUTORAMENTO E AVANZADOS DA USC (CIEDUS)

# DECLARACIÓN DO AUTOR DA TESE

Thermal Azide-Alkyne Cycloaddition (TAAC) as Efficient Clicked Chemistry Tool for the Functionalization of Dendrimers and Polymers

D. Ma'un Hasan Haroon Tawara

Presento a miña tese, seguindo o procedemento axeitado ao Regulamento, e declaro que:

1) A tese abarca os resultados da elaboración do meu traballo.
2) De selo caso, na tese faise referencia ás colaboracións que tivo este traballo.
3) A tese é a versión definitiva presentada para a súa defensa e coincide coa versión enviada en formato electrónico.
4) Confirmo que a tese non incorre en ningún tipo de plaxio doutros autores nin de traballos presentados por min para a obtención doutros títulos.

En Santiago de Compostela, 10 de octubre de 2019

Asdo: Ma'un Hasan Haroon Tawara

USC
UNIVERSIDADE
DE SANTIAGO
DE COMPOSTELA

CENTRO INTERNACIONAL DE ESTUDOS DE DOUTORAMENTO E AVANZADOS DA USC (CIEDUS)

# AUTORIZACIÓN DO DIRECTORE

Thermal Azide-Alkyne Cycloaddition (TAAC) as Efficient Clicked Chemistry Tool for the Functionalization of Dendrimers and Polymers

D. Eduardo Fernández Megía

INFORMAN:

Que a presente tese, correspóndese co traballo realizado por D. Ma'un Hasan Haroon Tawara, baixo a miña dirección, e autorizo a súa presentación, considerando que reúne os requisitos esixidos no Regulamento de Estudos de Doutoramento da USC, e que como director desta non incorre nas causas de abstención establecidas na Lei 40/2015.

En Santiago de Compostela, 10 de octubre de 2019

Asdo: Eduardo Fernández Megía

USC
UNIVERSIDADE
DE SANTIAGO
DE COMPOSTELA

# Dedication

Undoubtedly, the real and actual persons who sharing me the suffering, challenges and dreams of my life, are my lovely wife "Muna" and my wonderful son "Nadeem". For their endless support and patience along of my study time.

I dedicate this work

.

(رَبِّ أَوْزِعْنِي أَنْ أَشْكُرَ نِعْمَتَكَ الَّتِي أَنْعَمْتَ عَلَيَّ وَعَلَىٰ وَالِدَيَّ وَأَنْ أَعْمَلَ صَالِحًا تَرْضَاهُ وَأَصْلِحْ لِي فِي ذُرِّيَّتِي إِنِّي تُبْتُ إِلَيْكَ وَإِنِّي مِنَ الْمُسْلِمِينَ))15(

{سورة الأحقاف}

(وَمَا تَوْفِيقِي إِلَّا بِاللَّهِ ۚ عَلَيْهِ تَوَكَّلْتُ وَإِلَيْهِ أُنِيبُ)(88)

{سورة هود}

الحمد لله الذي بنعمته تتم الصالحات وبفضله تتنزل الرحمات وبشكره تزيد الخيرات، أفضل الصلاة وأتم التسليم على خير الكائنات، وسيد السادات، إمام المتقين وقائد الغر المحجلين، سيدنا ومحمد وعلى آله الطيبين الطاهرين. اللهم لك الحمد حمداً كثيراً كما ينبغي لجلال وجهك وعظيم سلطانك أن جعلتني من أمة خير الأنام، ولك الحمد على ما وفقتني إليه من بلوغ هذا المقام وأسبغت علي من نعمك الظاهرة والباطنة وصولي على درجة الدكتوراة. ولا حول ولا قوة إلا بالله العلي العظيم.

بأبي وأمي وعائلتي وإخوتي وكل عزيز على قلبي، رعاكم... الله جميعاً.

# ACKNOWLEDGEMENTS

The following pages involve a work that is an achievement of my nice family, parents, brothers, sisters, friends, coworkers and mentors whose great, unselfish support kept my hand steady in the most difficult of times. So, there are not enough words can fully express the gratitude I feel towards this fantastic group of people that I am proud to call my own.

First and foremost, my special, deep and sincere thankful to the essence of my life, my father and mother, with them whom I have grown up and to whom I owe more than I can ever repay, whom their honest continuous pray for me is one of the reasons of my success and happiness.

I wish to express my deep thanks and sincere gratitude to my wife Muna and my son Nadeem, for their love, support and constant encouragement during my study, undoubtedly, without their immense help and sacrifice, this work could not have been completed

I would like to express deep appreciation to my supervisor Dr. Eduardo Fernández Megía for the opportunity to work with him and benefit from his knowledge, experience and leadership. And his persistent confidence in me, particularly after I face many challenges along more than one year without tiny usefulness outcomes, but his continuous support and encourage in all professional and personal affairs, made all the difference.

During the last years, I was fortunate to work in Eduardo's group. First, I am extremely thankful to my closest friend Dr. Juan Correa, who always had the most patience to discuss my work in detail before our officinal meetings and providing innovative perspectives and thus

improving the quality of my research immensely, in addition of his help and follow up me when I was writing my thesis.

By their kindness, selflessness and willingness to help; my peers Muna Al-Ni'mat, Samuel Parcero, Roi López, and Dr. Petar Vukojicic, with whom I have shared everything and who will always stay in the circle of my closest friends. Furthermore, I thank Dr. Sandra Amaral, Dr. Sorel Jatunov, Dr. Marcos Fernandez, Noelia, Judith, Xade, Ulung and Dr. Flonja in our group, also thanks for all the members of the P2L3 lab, particularly Dr. Mohammad Saleh, Dr. Rafael Rodríguez, Dr. Sandra Arias, Esteban Suárez, Zulema Fernández, Kate Cobos, Elena Rivadulla and Manuel Núñez.

Express my sincere thanks to Dr. Manuel and Ramon in NMR unit, also to Noela and Pablo in materials supporting unit.

Finally, I would like to thank everyone else who provided me with advice, support and assistance throughout my study.

# Table of Contents

USC
UNIVERSIDADE
DE SANTIAGO
DE COMPOSTELA

# List of symbols and acronyms

| | |
|---|---|
| α | Alpha |
| β | Beta |
| δ | Chemical shift |
| ɀL | Microliter |
| ɀM | Micro molar |
| AAC | Azide-Alkyne Cycloaddition |
| AFM | Atomic force microscopy |
| ATR | Attenuated total reflection |
| BARAC | Biarylazacyclooctyne |
| Boc | *tert*-Butoxycarbonyl |
| br s | Broad singlet |
| CNDPs | Critical nanoscale design parameters |
| Con A | Concanavalin A |
| Conc | Concentration |
| COSS | Cube-octameric silsesquioxanes |
| CP | Cyclopentadienyl ligand |
| CP* | Pentamethylcyclopentadienyl ligand |
| CuAAC | Copper-catalyzed azide-alkyne-cycloaddition |
| d | Doublet |
| Da | Dalton |

| | |
|---|---|
| DBU | 1,8-Diazabicyclo[5.4.0]undec-7-ene |
| dd | Doublet of doublets |
| DDS | Drug delivery system |
| DIBAC | Dibenzoazacyclooctyne |
| DIBO | Dibenzocyclooctyn |
| DIFO | Diflourocyclooctyne |
| DL | Drug loading |
| DLS | Dynamic light scattering |
| DMC | Dimethyl chloride |
| DMF | Dimethyl formamide |
| DMM | Double-monomer methodology |
| DMSO | Dimethyl sulfoxide |
| DNA | Deoxyribonucleic acid |
| DOTA | 1,4,7,10-Tetraazacyclododecane-1,4,7,10-tetraacetic acid |
| DOX | Doxorubicin |
| DP | Degree of polymerization |
| DSC | Differential scanning calorimetric |
| DSC | N, N`-Disuccinimidyl carbonate |
| dt | Doublet of triplets |
| EDC | 1-Ethyl-3-(3-dimethyl aminopropyl) carbodiimide |
| EDG | Electron donating group |
| EE | Encapsulation efficiency |
| ESI-MS | Electrospray ionization- mass spectrometry |
| EWG | Electron withdrawing group |
| FDA | Food and Drug Administration |

| | |
|---|---|
| FIA | Flow injection |
| FITC | Fluorescein isothiocyanate |
| FT-IR | Fourier-transform-infrared spectroscopy |
| g | Gram |
| G | Generation |
| GATG | Gallic acid-triethylene glycol |
| GPC | Gel permeation chromatography |
| h | Hour |
| HIV | Human immunodeficiency virus |
| HOBt | Hydroxybenzotriazole |
| HPLC | High performance liquid chromatography |
| Hz | Hertz |
| IPr | Inverse procedure |
| IR | Infrared |
| J | Coupling constant |
| M | Molar concentration |
| m | Multiplet |
| MALDI-TOF | Matrix-assisted laser desorption/ionization - time-of-flight |
| mg | milligram |
| MHz | Mega hertz |
| mL | Milliliter |
| mM | millimolar |
| MPLC | Medium pressure liquid chromatography |
| MQ | Milli-Q |
| MRI | Magnetic resonance imaging |

| | |
|---|---|
| MW | Molecular weight |
| MWCO | Molecular weight cut off |
| n | Generation number |
| NHS | N-Hydroxysuccinimide |
| nm | Nanometer |
| NMR | Nuclear magnetic resonance |
| NPs | Nanoparticles |
| NPr | Normal procedure |
| $^{o}$C | Degrees celsius |
| PAMAM | Poly(amidoamine) |
| PB | Phosphate buffer |
| PBS | Phosphate-buffered saline |
| pDNA | Plasmid deoxyribonucleic acid |
| PEG | poly(ethylene glycol) |
| PHPMA | Poly(hydroxypropyl methacrylamide) |
| PIC | Polyion complex micelles |
| PLL | Poly-L-lysin |
| PPH | Phosphorus dendrimers |
| PPI | Poly(propylene imine) |
| ppm | Parts per million |
| PTP | Proton-transfer polymerization |
| Py | Pyridine |
| QS | Quorum sensing- |
| RNA | Ribonucleic acid |
| ROS | Reactive oxygen species |

| | |
|---|---|
| rt | Room temperature |
| RuAAC | Ruthenium-catalyzed azide-alkyne-cycloaddition |
| s | Singlet |
| SA | Streptavidin |
| SCROP | Self-condensing ring-opening polymerization |
| SCVP | Self-condensing vinyl polymerization |
| SEC | Size exclusion chromatography |
| siRNA | Silencing (small interfering) ribonucleic acid |
| SMM | Single-monomer methodology |
| SPAAC | Strain-promoted azide alkyne cycloaddition |
| t | Triplet |
| TAAC | Thermal azide-alkyne cycloaddition |
| TCEP | Tris(2-carboxyethyl) phosphine |
| TFA | Trifluoroacetic acid |
| THF | Tetrahydro furan |
| TKS | Thermal kinetic study |
| TLC | Thin layer chromatography |
| TMS | Tetramethylsilane |
| UV-vis | Ultraviolet–visible |

USC
UNIVERSIDADE
DE SANTIAGO
DE COMPOSTELA

**Abstract**

Dendrimers are synthetic tree-like macromolecules with distinct properties, built up from a multivalent core to which repetitive layers of branching units have been incorporated by a controlled and iterative fashion through generations. They are characterized by well-defined structures of null dispersity and adopt a globular architecture in the nanometer scale. These properties have rendered dendrimers with variety applications in a plethora of fields, including catalysis, biomedical applications, drug delivery and materials science.

In addition, the well-designed multivalent branched dendrimers with nanometer size, thus, providing the opportunity for the presence and incorporation of specific ligands, drug molecules, targeting moieties, imaging agents and enhance the solubility of the groups on the surface for drug delivery applications. Nevertheless, undesired limitation inherent to dendrimers, which is related to the synthetic cost of their preparation, and that demands strict and time-consuming protocols compared to classical polymers. This has led to a continuous research in the field of dendrimers synthesis during the last decade, towards the enhancement and development of more efficient synthetic methodologies for the seamless preparation and functionalization of dendrimers.

The nature is rich in examples of dendritic structures often utilized as a motif where a particular function needs to be enhanced or explored. The trees for instance, above ground, the dendritic pattern is used to enhance the exposure of the tree's leaves to the sunlight, which is necessary for photosynthesis. while the shadow of the tree provides a macroenvironment that maintain higher humidity and more fixed temperatures compared to the surrounding during the day. Underground, the large dendritic network of roots works to expose the maximum functional surface area for efficient nutrients and water collection from the soil. Another striking example discovered just

recently as a dendritic structure in nature is the foot-hair on the Gecko's feet, that enable the Gecko to stick easily and walk safely on surfaces. Gecko's foot hairs have proved that weakly quantum chemical forces can be amplified by millions of architectures in the form of dendritic structures. Other examples that represent the dendritic structure in the nature are bronchioles, alveoli, blood vessels and the central peripheral nervous system in humans and animals.

Inspired by the utilities provided by dendritic structures in nature, the scientists have been interested in obtaining dendritic structures in a synthetic way. The first attempt to design a dendritic structure via organic synthesis was carried out successfully in 1978. Dendrimer synthesis developed intensively from 1990 with poly(aryl ether) dendrimer and the convergent synthetic approach. After pioneering research and initial papers published on the design and synthesis of dendrimers, there was an enormous interest in the exploration of their properties and potential uses so far, mainly in chemistry and biology as a new class of polymeric nanomaterials characterized by cutting edge structural advantages and promising properties.

hyperbranched polymer are a highly branched tree-liked molecule with three-dimensional (3D) structure. They have gained more attention after the emergence of dendrimers. While the well-defined structure of dendrimers requires stepwise synthesis, hyperbranched polymers can be synthesized in one-pot processes, following two major strategies: the single-monomer methodology (SMM) or double-monomer methodology (DMM). Hyperbranched polymers have been utilized in many fields ranging from, nanotechnology, biomedicine, coating and so forth.

Block copolymers are a class of polymers in which two or more types of completely chemically different polymers incorporate into a new polymer chain in a statistical fashion. The properties of block copolymers mostly depend on the composition of the final product, and in general are intermediate between those of the parent starting materials. There are different types of block copolymers, such as A-B type diblock copolymers, A-B-A type triblock copolymers, A-B-C

type triblock copolymers, and so on, in addition they can be configured into several architectures involving linear, branched (graft and star), and cyclic molecular, with wide range of applications ranging from drug delivery to materials science.

Linear-block copolymers result from the combination of two or more fragments with fundamentally different molecular architectures and physical properties. This combination includes flexible linear chains and branched globular dendrimers yielding macromolecules with their own interesting and characteristic properties, that do not necessary match those of the initial constituents. The most known Linear-block copolymers in general, those consisting on the covalent incorporation at least with one of PEG chain, because of the attractive properties of PEG as a non-toxic, non-antigenic, non-immunogenic, highly water-soluble polymer.

Other types of the dendritic structure could be constructed, using more than one type of building blocks (repeating units or dendrons) arranged in a certain way within the dendrimer skeleton, this class is called dendritic copolymer, which is found in three different types of copolymers are segment-block dendrimer, layer-block dendrimer and surface-block dendrimer.

Dendrimers synthesis can be achieved following several approaches, basically, divergent and convergent approaches, additionally, to the alternative approaches derived from a combination of the previous two approaches in different ways, such as divergent/divergent, divergent/convergent and convergent/convergent approaches.

In divergent strategy, the dendrimer construction takes place in a step by step manner, starting from a reaction of the multivalent core with several repeating units to build up the dendrimer structure from the core towards the periphery, but it can be limited by an incomplete coupling of all activated peripheral groups on the surface, additionally, purification of the reaction, due to the similarity of byproducts and perfect product in term of diameter and the molecular weight.

While the convergent approach is oppositely to the divergent approach, here the dendrimer is constructed from the outside inwards, despite of this approach is restricted to the preparation of only low dendrimer generations, the most relevant features of this methodology that the presence of a limited number of reaction points per synthetic step provides a high reaction control, with ability to synthesize the so called segment-block dendrimers.

Alternatively, the divergent/divergent, convergent/convergent and combination of both in a certain way, can be used exclusively when a dendrimer with different peripheral group segments are desired. Many techniques are mostly used to find access to the precise characterization of dendrimers, in terms of the chemical composition, shape, molecular weight, purity and so forth. Among these tools are size exclusion chromatography, mass spectrometry (MALDI-TOF), Atomic force microscopy (AFM), dynamic light scattering (DLS), nuclear magnetic resonance (NMR), Infrared (IR). Additionally, Uv-vis, Raman, and differential scanning calorimetric (DSC) as routine techniques used for the analysis of dendrimers. However, the characterization of dendrimers is a synergistic process by spectroscopic and chromatographic tools.

GATG (Gallic Acid-Triethylene Glycol) dendrimers were described initially by the group of Roy through an ineffective synthesis up to G2, and different families with efficient synthetic improvements were developed by our group afterward. These dendrimers are composed of a repeating unit carrying a gallic acid core and three hydrophilic triethylene glycol (TEG) chains with terminal azide groups, that can be functionalized with a myriad of groups through very efficient reactions. In addition of the presence of carboxylic group in the repeating unit provides an opportunity the growing of the GATG dendrimer via classical amide chemistry with amine-terminated core.

Despite displaying great potential in a diverse range of applications, particularly when functionalized with different groups of interest, while the inefficient preparation of the repeating unit was

hampering the access to a larger scale of dendrimers and higher generations. Therefore, it undermined the growth of this dendritic family and made it a great challenge. To have an efficient and reliable synthesis of GATG dendrimers, our research group first turned the attention and exerted successfully great efforts to improve the preparation route of the GATG repeating unit, the first improvement started in 2006, while based on green chemistry principles, the route of GATG repeating unit preparation manifested in 2011 as efficient strategy to afford of the GATG repeating unit larger than 100 g..

In 2006, with the aim to evaluate click chemistry as a tool in functionalization, a study was performed to test the viability of Cu(I) catalyst as CuAAC [3+2] cycloaddition, our group reported the successful preparation of three generations of GATG dendrimers [Gn]-$N_3$, that was readily obtained from GATG repeating unit and *n*-$PrNH_2$, through amid linkage, and functionalized efficiently under aqueous solution, with unprotected prepared alkyne glycosides. In result, multivalent conjugations up to 27 peripheral group, and reproducible high yield. This successful by means of the using click chemistry, open the door for quick, efficient and reliable the on-surface functionalization of GATG dendrimers.

Soon after our group also described the preparation of linear-block copolymers combining GATG dendrimers and poly(ethylene glycol) (PEG). These dendritic polymers were decorated with unprotected carbohydrate units by means of click chemistry (room temperature, aqueous solution and an only catalytic amount of Cu). These PEGylated dendrimers have emerged a high capacity to aggregate the lectin upon increase the generation.

During the last decade, our group has exploited the advantageous presence of terminal azide groups in GATG to functionalize these dendrimers by means of the Cu(I)-catalyzed azide-alkyne cycloaddition (CuAAC) reaction, with different alkynes moieties, which give in turn products that could be used in many applications. This success by means of the using click chemistry, opened the door towards quick, efficient and reliable functionalization of GATG dendrimers.

To more exploration the importance and versatility of the GATG dendrimers, intensive studies were accomplished by our research group. The studies focused on the functionalization of PEG-GATG block copolymers synthesis, and exploit the terminated-azide groups for on-surface functionalization by means of CuAAC, as well, the applications that relevant to the functionalized dendrimers. Among of these studies, charged and neutral groups were used for decoration of PEGylated block copolymers, which displayed a strong effect of the charged surface on the cell uptake, moreover, PEGylated block copolymers have been used to prepare drug delivery carriers, such as polyion complex (PIC) micelles with potential applications, particularly in cancer therapy, and dendriplexes for gene therapy. Additionally, as carriers for contrast. agents in MRI such as gadolinium ion.

More recently, our research group has reported on the synthesis of new two families of symmetrical GATG dendrimers 2[Gn] and 3[Gn]. The generation of dendrimers is deemed as a powerful tool in controlling the size and biodistribution of polyion complexes (PIC). Using a combinatorial screening of six dendrimers and five oppositely charged PEGylated copolymers, a dendrimer-to-PIC hierarchical transfer of structural information was revealed with PIC sizes upon decrease the dendrimer generation. The increase in size, from micelle-to-vesicle transition, is interpreted according to a cone- to rod-shaped progression in the architecture of the unit PIC (uPIC). This precise size tuning enabled dendritic PICs to act as nanorulers for controlled biodistribution.

Cycloaddition is a chemical reaction in which two or more π systems combine to afford a stable cyclic adduct, without losing any fragment, and following a concerted mechanism. The Diels-Alder reaction and 1,3-dipolar cycloaddition are the most of such reaction that produce six and five membered rings respectively. Azide as dipole and alkynes as dipolarophiles are the most common examples of functional groups used in 1,3-dipolar cycloaddition reactions.

Click chemistry involves a set of powerful linking reaction that are straightforward to implement, give high yield, no or minimal

purification with versatile forming diverse structures without the necessity of protection steps. among of click chemistry reactions, the CuAAC and RuAAC have the advantage to exclusively afford the 1,4- and 1,5-regioisomer of 1,2,3-triazoles respectively, additionally, other metal-catalyzed azide-alkyne cycloaddition reactions (MAAC).

However, the metal-catalyzed azide-alkyne cycloaddition reactions were explored to overcome the regioselectivity issue, and limited reaction rate of the 1,3-dipolar Huisgen cycloaddition reaction, the metal's cytotoxicity limits their applications in living systems. The alternative, using free-metal click reactions, the strain-promoted azide-alkyne cycloaddition variant (SPAAC) and thermal conditions are examples of such alternatives. The SPAAC is deemed an example of the very few bioorthogonal reactions proper for the labeling of biomolecules in vivo. However, it has been noted that strained cyclooctyne can bind to some extent to biological functionalities in an azide-independent manner, thereby limiting the sensitivity of assays based on this reaction.

Accordingly, an alternative strategy towards accelerating the AAC reaction, which avoids catalysis and cyclooctynes is the thermal azide-alkyne cycloaddition (TAAC), chemistry that has been recently revisited, and used intensively in the synthesis of triazole derivatives.

The first part of this doctoral thesis involves modification and scaling up the preparation of the symmetrical 2G and 3G GATG dendritic families, that already prepared recently by our group. These new two GATG dendritic families were prepared after modification with very good yields and high scale, starting from symmetrical di- and trifunctionalized cores. High yielding reactions both of activation (azide reduction) and growing (amide formation), in addition, easy purifications (MPLC or ultrafiltration) has allowed the preparation of these two new families divergently up to the fourth generation with molecular weights ranging from 1 to 70 kDa (G1-G4), and the number of terminal azide groups up to 243.

Generally, the reactions series of the 2G family was going smoothly, while the second generation 2[G2] has hampered this sequence of the synthesis, because of the low percentage yield, it

became obviously important to look into developing this part of the approach. Consequently, to overcome this challenge, we started to change the reaction conditions of the synthesis for the second generation 2[G2] dendrimer, included using different solvents, temperatures and $Et_3N$ equivalent ratios. When DMSO was used as an alternative solvent of the reaction at rt, the reaction proceeded smoothly, to obtain pure 2[G2] in 91% yield. Moreover, many attempts for scaling up the preparation of the 2G GATG dendritic family were performed successfully on the scale of hundreds of milligrams (> 600 mg).

Regarding the preparation of the 3G family, the getting of planar core in high purity, after more than one purification cycle for the same patch, was the first and only big challenge in the whole preparation sequence of the 3G GATG dendrimers. In the modified route, chloride was replaced by tosylate as a leaving group in 1-azido-2-[2-(2-chloroethoxy)ethoxy]ethane, and the crude product was purified one time by MPLC with neutral alumina instead of silica gel, to obtain the pure core in 85% yield. Once the core of the 3G family in hand, four sequential generations of 3G GATG dendrimers were successfully prepared with scaling up, obtaining high yields of 93-96% with up to 243 peripherals azide/amino groups. However, these dendrimers could be purified by column chromatography, while ultrafiltration is possible for the third and fourth generations.

These GATG dendrimers were fully characterized by $^{1}H$ and $^{13}C$ NMR and GPC to confirm their purity, monodispersity, and successful growing steps, IR also confirmed the completion reduction terminated-azides dendrimer.

For thermal azide-alkyne cycloaddition reactions (TAAC), the activation of alkynes becomes an urgent need in the absence of chemical catalysts. Carbamate group was used to make the alkynes more electron-deficient, in order to activate their thermal reaction with terminated-azides dendrimer, furthermore, its stability against high temperatures and hydrolysis. For this aim, a library of new activated alkynes with different functional groups (alcohol, phenol, anionic, cationic, chromophore, biotic and chelating) to provide the greatest

diversity of functionality in various application fields, were prepared successfully under mild conditions in high yields, and fully characterized, starting from symmetrical synthesized Alk-NHS with amino moiety of the desired functional group reagent.

These activated alkynes were characterized very well. $^{1}$H NMR confirmed the successful synthesis and purity of the desired functionalized alkyne according to the change in the chemical shift of the characteristic signals of the starting materials and product, particularly, the characteristic signal for protons of methylene group adjacent to the triple bond in both Alk-NHS and functionalized alkyne. In addition, $^{13}$C NMR was also useful tool to characterize such reaction, based on the disappearance of the characteristic two signals of activated Alk-NHS, and appearance the specific signals for functionalized alkyne. In addition, elemental analysis and ESI-FIA-TOF-mass spectrometry were used to confirm the purity and exact molar mass of the alkynes.

However, some of the functionalized alkynes were derived from other alkynes with a new functional group. Furthermore, some privacy to a varying extent to specific reactions that need to carry out in a different way. Generally speaking, the purification of these functionalized alkynes ranging through on easy extraction to sometimes hard chromatography.

To apply the TAAC at optimum conditions, a thermal kinetic study (TKS) was adopted, using a model system to achieve the best conditions in term of the solvent, the temperature, the concentration of reaction solution and the time of reaction. As a result, the best conditions are 1 M concentration per azide group, 120 $^{o}$C and tBuOH/$H_2O$ solvent in volume ratio 1:1 and 6 h overall time of reaction.

To apply the TAAC in optimal conditions, it was decided to do a thermal kinetic study (TKS), using a model system to achieve the best conditions in terms of: solvent, temperature, concentration and reaction time. As a result, the best conditions are 1 M concentration per azide group, 120 oC and 6 h total reaction time. The best solvent was AcOtBu, however, the choice of solvent depended on the

solubility of the starting reagents and the final product for each of the reactions.

These conditions were applied to confirm the thermal stability of the functionalized alkynes, TLC and $^{1}$H NMR revealed their stability (no decomposition) at 120 ºC for 8 h, similar TAAC conditions.

With a library of different four types of dendrimers (2G2, 3G1, 3G3 and 3G4), eleven different types of synthetic functionalized alkynes and approved conditions of TKS in hand. Each dendrimer type was surface functionalized with a certain types activated alkynes, when 2G2 and 3G1 represented surface functionalization of the lower number of peripheral azides (18 and 9 peripheral groups respectively), 3G3 was the middle one (81 peripheral groups) that surface decorated with all types of activated alkynes, while surface functionalization of 3G4 to validate the functionalization of highest number of peripheral azides (243) by means of TAAC. Changing the solvent ration was imperative according to the particular solubility of reactants, the reaction time was ranging between 8-12 h, ultrafiltration was used in purification to afford the desired products (conjugates) in high yields (< 90%).

The conjugates were fully characterized. The disappearance of characteristic IR azide peak at around 2100 $cm^{-1}$ confirmed the reaction completion. Also, completion and full surface functionalization was clearly established by $^{1}$H NMR thanks to the disappearance of the characteristic signal that's related to the methylene adjacent to the azide group in dendrimer, to appear as multiplet signal in dendrimer conjugates (TAAC products), in addition, the appearance of two multiplet signals corresponding to the protons of the carbon alpha of the triazole, which originally were the protons of the methylene adjacent to the triple bond in functionalized alkyne, additionally, $^{13}$C NMR, was also used to follow the signal disappearance of the triple-bonded carbons in activated alkyne, and the appearance of the characteristic signals corresponding to the double-bonded carbons of triazole ring. DLS and GPC also confirmed the purity, monodispersity of conjugates and size increasing after functionalization compared with the native dendrimer size.

Some of the dendrimer conjugates were addressed in further study. It was verified the bioactivity of the mixed dendrimer 3[G4]-$(Man)_{60}$/$(Bio)_{16}$/$(FITC)_5$ by study the interaction of peripheral functionalized biotin with streptavidin in presence of FITC as imaging marker, moreover, 3[G4]-$(Man)_{60}$/$(Bio)_{16}$/$(FITC)_5$ when assayed with Con A, shown apparent recognition ability as glycodendrimer toward the protein receptor. This fact suggests that like functionalized dendrimers have a capability as a cell recognizable biomedical material. On the other hand, taking the advantage of the amphiphilic property of the functionalized dendrimer $PEG_{5k}$-[G3]-Cat with catechol groups, accordingly, a quick self-assembly of $PEG_{5k}$-[G3]-Cat in (PB pH 7.4, 150mM NaCl) into micelles was revealed. Hydrophobic anticancer drug DOX, was easily encapsulated into $PEG_{5k}$-[G3]-Cat micelles via dialysis with drug loading (DL) 29% and encapsulation efficiency 87%, which suggests these micelles as promising tools in drug delivery system.

USC
UNIVERSIDADE
DE SANTIAGO
DE COMPOSTELA

**Resumen**

Los dendrímeros son macromoléculas sintéticas de forma arborescente, construidos a partir de un núcleo multivalente al que capas repetitivas de unidades de ramificación se han incorporado de una manera controlada e iterativa a través de las generaciones. Los dendrímeros se caracterizan por presentar estructuras bien definidas, de dispersión nula y adoptan una arquitectura globular en la escala nanométrica. Estas propiedades han hecho que los dendrímeros sean estudiados para una variedad de aplicaciones en una gran cantidad de campos, incluyendo la catálisis, aplicaciones biomédicas, administración de fármacos y ciencia de materiales.

Además, la estructura única y el patrón de ramificación regular y perfecto, los dendrímeros aportan números bien definidos de grupos funcionales en la periferia, proporcionando un carácter multivalente y al mismo tiempo permite la incorporación de ligandos específicos, moléculas de medicamentos, fragmentos de reconocimiento específicos, agentes de contraste y grupos que favorecen la solubilidad en agua. lo cual los hace candidatos idóneos para aplicaciones en administración de fármacos. Sin embargo, la limitación no deseada inherente a los dendrímeros, se relaciona con el coste sintético de su preparación, ya que exige protocolos estrictos y consumen mucho tiempo en comparación con polímeros clásicos. Esto ha llevado, en la última década, a una continua investigación en el campo de la síntesis de dendrímeros, hacia la mejora y el desarrollo de metodologías sintéticas más eficientes para la preparación perfecta y funcionalización de dendrímeros.

La naturaleza es rica en ejemplos de estructuras dendríticas a menudo utilizadas como un motivo en el que una función particular necesita ser mejorada o explorada. En los árboles, por ejemplo, el patrón dendrítico se utiliza para mejorar la exposición de las hojas del árbol a la luz solar, que es necesaria para la fotosíntesis. mientras que la sombra del árbol proporciona un macroambiente que mantiene una mayor humedad y temperaturas más fijas en comparación con el entorno durante el día. Además, la gran red dendrítica de raíces trabaja

para exponer la superficie funcional máxima para la recolección eficiente de nutrientes y agua del suelo. Otro ejemplo sorprendente, descubierto recientemente. como una estructura dendrítica en la naturaleza es el pelo en los pies del Gecko, que permite que el Gecko se adhiera fácilmente y camine con seguridad en la superficie. Los pelos de los pies de Gecko han demostrado que las fuerzas químicas débiles pueden ser amplificados por millones de arquitecturas en forma de estructuras dendríticas. Otros ejemplos que representan la estructura dendrítica en la naturaleza son los bronquiolos, los alvéolos, vasos sanguíneos y el sistema nervioso periférico central en humanos y animales.

Inspirado por las propiedades de las estructuras dendríticas en la naturaleza, los científicos se han interesado en la obtención de estructuras dendríticas de una manera sintética. El primer intento de diseñar una estructura dendrítica a través de la síntesis orgánica se llevó a cabo con éxito en 1978. La síntesis de dendrímeros se ha desarrollado intensamente desde 1990 con la obtención de los dendrímeros poli (aril éter) y el enfoque sintético convergente. Después de la investigación pionera y documentos iniciales publicados en el diseño y la síntesis de dendrímeros, hubo un enorme interés en la exploración de sus propiedades y usos potenciales, principalmente en la química y la biología como una nueva clase de nanomateriales poliméricos poseedores de ventajas estructurales y propiedades prometedoras.

Los polímeros hiper-ramificado son moléculas tipo-árbol altamente ramificadas con la estructura tridimensional (3D). Estos polímeros han ganado más atención después de la aparición de los dendrímeros. Si bien la estructura bien definida de los dendrímeros requiere la síntesis paso a paso, los polímeros hiper-ramificados se pueden sintetizar en procesos de un solo paso, siguiendo dos estrategias principales: el método de monómero único (SMM) o metodología de doble monómero (DMM). Los polímeros hiper-ramificados se han utilizado en muchos campos los que incluye: la nanotecnología y la biomedicina entre otros.

Los copolímeros de bloque son una clase de polímeros en los que dos o más tipos de polímeros completamente diferentes químicamente se incorporan a una nueva cadena de polímeros de manera estadística. Las propiedades de los copolímeros de bloque dependen principalmente de la composición del producto final y, en general, son intermedias entre las de los materiales de partida originales. Existen diferentes tipos de copolímeros de bloque, como los copolímeros dibloque tipo AB, los copolímeros tribloque tipo ABA, los copolímeros tribloque tipo ABC, etc., además, se pueden configurar en varias arquitecturas que involucran lineal, ramificado (injerto y estrella) y cíclico. con una amplia gama de aplicaciones que van desde la administración de medicamentos hasta la ciencia de los materiales.

Los copolímeros de bloque lineal resultan de la combinación de dos o más fragmentos con arquitecturas moleculares y propiedades físicas fundamentalmente diferentes. Esta combinación incluye cadenas lineales flexibles y dendrímeros globulares ramificados que producen macromoléculas con sus propias propiedades interesantes y características, que no necesariamente coinciden con las de los constituyentes iniciales. Los copolímeros lineales de bloque más conocidos son aquellos que se basan en la incorporación covalente al menos de una cadena de polietilenglicol (PEG), debido a sus propiedades: no tóxico, no antigénico, no inmunogénico y altamente soluble en agua.

Cuando la estructura dendrítica tiene más de un tipo de bloques de construcción (unidades de repetición) dispuestos en un cierto modo dentro del esqueleto de dendrímero, esta clase se llama copolímero dendrítico. Existen tres tipos diferentes de copolímeros dendríticos: segmento-bloque dendrítico, capa-bloque dendrítico y la superficie-bloque. dendrítico

La síntesis de dendrímeros se puede lograr siguiendo varios enfoques, básicamente, enfoques divergentes y convergentes, y la combinación de éstos: divergentes / divergentes, divergentes / convergentes y convergentes / convergentes.

En una estrategia divergente, la construcción del dendrímero tiene lugar paso a paso, comenzando por una reacción del núcleo multivalente con varias unidades de repetición, así el dendrímero se construye desde el núcleo hacia la periferia. Esta estrategia puede estar limitada por un acoplamiento incompleto de los grupos periféricos, además, la purificación puede complicarse debido a la similitud de los subproductos y el producto final en términos de diámetro y peso molecular.

El enfoque convergente es opuesto al enfoque divergente, aquí el dendrímero se construye desde el exterior hacia el interior. Esta estrategia está limitada a la preparación de dendrímeros de baja generación debido al número limitado de puntos de reacción y al impedimento estérico al unir los dendrones al *core*.

Alternativamente, los enfoques / divergente, convergente / divergente convergente y la combinación de ambos en cierta manera, se pueden usar exclusivamente cuando se desean un dendrímero con diferentes segmentos de grupos periféricos.

Muchas técnicas se utilizan para garantizar una caracterización precisa de los dendrímeros, en términos de: composición química, forma, peso molecular y pureza. Entre estas herramientas las más usadas son: cromatografía de exclusión por tamaño, espectrometría de masas (MALDI-TOF), microscopía de fuerza atómica (AFM), dispersión de luz dinámica (DLS), resonancia magnética nuclear (RMN), infrarrojo (IR), UV-vis, Raman, y calorimetría diferencial de barrido (DSC). La caracterización de los dendrímeros es un proceso sinérgico por medios espectroscópicos y herramientas cromatográficas.

Los dendrímeros GATG (*Gallic Acid-Triethylene Glycol*) fueron preparados inicialmente por el grupo de Roy a través de una síntesis poco eficiente y obteniendo sólo dendrmíeros de baja generación (hasta G2). Posteriormente diferentes familias, con mejoras sintéticas eficientes. fueron desarrolladas por nuestro grupo de investigación. Estos dendrímeros están compuestos de una unidad de repetición que lleva un núcleo de ácido gálico y tres cadenas hidrófilas de trietilenglicol (TEG) con grupos azida terminales, que se pueden

funcionalizar con una variedad de grupos a través de reacciones muy eficientes. Además, la presencia del grupo carboxílico en la unidad de repetición proporciona un punto de crecimiento a través de la formación de la amida, por la reacción con los grupos aminos del material de partida.

Aunque los dendrimeros GATG mostraron un gran potencial en una amplia gama de aplicaciones, particularmente cuando fueron funcionalizados con diferentes grupos de interés, fue la preparación ineficiente de la unidad de repetición la que obstaculizó el acceso a mayor escala de dendrímeros y generaciones superiores. Para tener una síntesis eficiente y fiable de los dendrímeros GATG, nuestro grupo de investigación se planteó mejorar la preparación de la unidad de repetición GATG, que es el de paso crucial en la síntesis de dendrímeros GATG. A partir de un derivado de clorhidrina TEG disponible en el mercado, la unidad de repetición GATG podría obtenerse un rendimiento global del 87%.

Con un método de preparación fiable de la unidad de repetición GATG en la mano, en el año 2006 nuestro grupo describió la preparación con éxito de tres generaciones de dendrímeros GATG [Gn] -n3, con el objetivo de desarrollar dendrímeros para aplicaciones biomédicas. Ese mismo año, nuestro grupo también describió la preparación de copolímeros lineales de bloques combinando dendrímeros GATG y poli (etilenglicol) (PEG). Durante la última década, nuestro grupo ha explotado la presencia ventajosa de grupos azidas terminales en GATG para funcionalizar estos dendrímeros por medio de la reacción cicloadición azida-alquino catalizada por cobre (CuAAC). La reacción de las azidas terminales de los dendrímeros GATG con una variedad de alquinos, permitió la obtención de productos que se pudieron utilizar en muchas aplicaciones.

Para explorar más la importancia y versatilidad de los dendrímeros GATG, intensos estudios se llevaron a cabo por nuestro grupo de investigación. Los estudios se centraron en la síntesis de copolímeros de bloque de PEG-GATG, aprovechando los grupos-azida terminales para la funcionalización de la superficie por medio de CuAAC. Se prepararon diversos dendrímeros con grupos neutros y

cargados en la superficie de los copolímeros de bloque PEGilados, y se estudió su internalización celular. Por otra parte, los copolímeros de bloque PEGilados se han utilizado para preparar transportes de fármacos, tales como las micelas poliiónicas (PIC) con aplicaciones en terapia del cáncer. Además, se han usado los dendrímeros cargados para unir material genético y evaluar su potencial en terapia génica.

Más recientemente, nuestro grupo de investigación ha descrito la síntesis de dos nuevas familias de dendrímeros GATG simétricos: 2 [Gn] y 3 [Gn]. La generación de dendrímeros es una herramienta poderosa en el control del tamaño y la biodistribución de los complejos de poliiones (PIC). Utilizando un cribado combinatorio de seis dendrímeros (18–243 grupos terminales) y cinco copolímeros PEGilados con carga opuesta, se reveló una transferencia jerárquica desde el dendrímero a PIC con diámetros de PIC que aumentaron de 80 a 500 nm al disminuir la generación de dendrímeros. Este aumento de tamaño, que también estuvo acompañado por una transición de micela a vesícula, se interpreta de acuerdo con una progresión en forma de cono a barra en la arquitectura de la unidad PIC (uPIC). Este ajuste de tamaño preciso permitió que los PIC dendríticos actuaran como nanoreductores para una biodistribución controlada.

La cicloadición es una reacción química en la que dos o más sistemas *pi* se combinan para dar un aducto cíclico estable, sin perder ningún fragmento, y siguiendo un mecanismo concertado. La reacción de Diels-Alder y la cicloadición 1,3-dipolar son los ejemplos más conocidos de este tipo de reacción que producen anillos de seis y cinco miembros, respectivamente. La Azida como dipolo y el alquino como dipolarófilo son los ejemplos más comunes de los grupos funcionales utilizados en las reacciones de cicloadición 1,3-dipolar.

*Click Chemistry* implica un conjunto de poderosas reacciones que son fáciles de implementar, dan un alto rendimiento, con una mínima purificación y sin la necesidad de pasos de protección. Entre las reacciones *Click*, la CuAAC tiene la ventaja de proporcionar exclusivamente el 1,4-regioisómero de 1,2,3-triazoles.

Aunque se han explorado reacciones de cicloadición de azida-alquino catalizadas por metales para superar el problema de regioselectividad, y velocidad de reacción en la cicloadición 1,3-dipolar Huisgen, la citotoxicidad del metal limita sus aplicaciones en los sistemas vivos. La alternativa, para evitar el uso de metales en esta reacción, lo constituye la cicloadición promovida por un azida-alquino tenso (*Strain-promoted alkyne-azide cycloadditions:* SPAAC) Una estrategia alternativa para acelerar la reacción de AAC, lo que evita la catálisis y ciclooctinos es el empleo de la reacción térmica de cicloadición azida-alquino (TAAC), química que ha sido recientemente revisada, y se utiliza intensivamente en la síntesis de derivados de triazol.

La primera parte de esta tesis doctoral consiste en la modificación de la preparación de las familias GATG 2G y 3G, recientemente descritas por nuestro grupo de investigación. Estas dos familias dendríticas GATG se prepararon, después de la modificación, con muy buenos rendimientos y a gran escala, a partir de núcleos simétricos di- y tri-functionalizados. Los rendimientos fueron altos tanto en la etapa de activación (reducción de azida) y crecimiento (formación de la amida). Además, la facilidad de los procesos de purificación (MPLC o ultrafiltración) ha permitido la preparación divergente de estas dos nuevas familias hasta la cuarta generación con pesos moleculares que oscilan de 1 a 70 kDa (G1-G4), y el número de grupos azidas terminales hasta 243.

En general, la serie de reacciones de la familia 2G iba sin problemas, mientras que la segunda generación 2[G2] ha obstaculizado esta secuencia de la síntesis, debido al bajo rendimiento, obviamente fue necesario estudiar esta parte del enfoque. En consecuencia, para superar este desafío, comenzamos a cambiar las condiciones de reacción de la síntesis para la obtención del dendrímero 2[G2], incluido el uso de diferentes disolventes, temperaturas y equivalentes de $Et_3N$. Cuando se usó DMSO como disolvente alternativo en la reacción a temperatura ambiente, la reacción se desarrolló sin problemas, se obtuvo 2[G2] puro con un rendimiento del 91%. Además, se consiguió incrementar la escala en la preparación de la familia dendrítica 2[Gn] (> 600 mg).

Con respecto a la preparación de la familia 3G, la obtención del *core* fue el primer y único gran desafío en toda la secuencia de preparación de los dendrímeros 3G GATG. En la ruta modificada, el cloruro se reemplazó por tosilato como grupo saliente en 1-azido-2-[2- (2-cloroetoxi) etoxi] etano, y el producto bruto se purificó una vez por MPLC con alúmina neutra en lugar de gel de sílice, para obtener el *core* puro con un rendimiento del 85%. Una vez que el *core* fue obtenido completamente puro, cuatro generaciones secuenciales de dendrímeros 3G GATG se prepararon con altos rendimientos (93-96%) y con hasta 243 grupos periféricos azida / amino. Los dendrímeros de baja generación se purificaron por cromatografía en columna, mientras que la ultrafiltración permitió la purificación de la tercera y cuarta generación. Estos dendrímeros GATG fueron totalmente caracterizados por RMN $^{1}H$ y $^{13}C$ y GPC para confirmar su pureza, monodispersidad. IR confirmó la reducción de los grupos-azidas terminales en las etapas de activación.

Para las reacciones de cicloadición térmica de azida-alquino (TAAC), la activación de los alquinos se convierte en una necesidad urgente en la ausencia de catalizadores químicos. El grupo carbamato se usó para hacer los alquinos más deficientes en electrones, con el fin de activar su reacción térmica con dendrímeros funcionalizados con azidas terminales, aunado a su estabilidad frente a altas temperaturas e hidrólisis. Para este fin, una biblioteca de nuevos alquinos activados con diferentes grupos funcionales (alcohol, fenol, aniónicos, catiónicos, cromóforo, bióticos y quelate), fueron preparados, lo cual permite obtener una mayor diversidad de funcionalidad. La funcionalización de los dendrímeros con esta variedad de alquinos se consiguió con éxito bajo condiciones suaves y altos rendimientos.

Estos alquinos activados se caracterizaron muy bien. Por $^{1}H$ RMN se confirmó la síntesis exitosa y la pureza del alquino funcionalizado deseado de acuerdo con el cambio en el desplazamiento químico de las señales características de los materiales de partida y del producto, particularmente, la señal característica para los protones del grupo metileno adyacente al triple enlace en ambos Alk -NHS y alquino funcionalizado. Además, $^{13}C$ RMN también fue una herramienta útil para caracterizar dicha reacción, basada en la

desaparición de las dos señales características de Alk-NHS activado, y la aparición de las señales específicas para alquino funcionalizado. Además, el análisis elemental y la espectrometría de masas ESI-FIA-TOF se utilizaron para confirmar la pureza y la masa molar exacta de los alquinos.

Por otra parte, algunos de los alquinos funcionalizados se utilizaron en la preparación de otros alquinos con un nuevo grupo funcional. En términos generales, la purificación de estos alquinos funcionalizados se extiende desde la extracción liquido-liquido hasta la cromatografía por columna.

Para aplicar la TAAC en condiciones óptimas, se decidió hacer un estudio de cinética térmica (TKS), utilizando un sistema modelo para lograr las mejores condiciones en términos de: disolvente, temperatura, concentración y el tiempo de reacción. Como resultado, las mejores condiciones son 1 M de concentración por grupo azida, 120 $^{o}$C y 6 h de tiempo total de reacción. El mejor disolvente fue AcOtBu, sin embargo, la elección del disolvente dependió de la solubilidad de los reactivos de partida y del producto final para cada una de las reacciones.

Se aplicaron estas condiciones para confirmar la estabilidad térmica de los alquinos funcionalizados. TLC y $^{1}$H RMN revelaron su estabilidad (sin descomposición) a 120 $^{o}$C durante 8 h.

Con una biblioteca de cuatro tipos diferentes de dendrímeros (2G2, 3G1, 3G3 y 3G4), once tipos diferentes de alquinos y condiciones aprobadas de TKS en la mano, cada tipo de dendrímero se funcionalizó en la superficie con alquinos activados. Se funcionalizaron dendrímeros de diferente generación y distintas cantidades de grupos periféricos, Así por ejemplo 2[G2] y 3[G1] son los de menor grupos en la superficie (18 y 9 grupos periféricos respectivamente), 3G3 (81 grupos periféricos) y 3G4 el mayor número de azidas periféricas (243). La relación de disolventes y la concentración se ajustó de acuerdo con la solubilidad particular de los reactivos, el tiempo de reacción oscilaba entre 8-12 h. Se purificó por ultrafiltración obteniendo los productos deseados (conjugados) con altos rendimientos (<90%).

Los conjugados se caracterizaron completamente. La desaparición del pico característico azida IR (alrededor de 2100 $cm^{-1}$) confirmó la finalización de la reacción. Además, la funcionalización completa se corroboró claramente por $^{1}H$ RMN gracias a la desaparición de la señal característica del metileno adyacente al grupo azida en el dendrímero, para aparecer como multiplete la señal a alrededor de 4.60 a 4.50 ppm correspondiente a los conjugados de dendrímero (productos TAAC), y la aparición de dos señales multiplete a alrededor de 5.40 a 5.10 ppm correspondiente a los protones del carbono *alfa* del triazol. Adicionalmente, en el espectro de $^{13}C$ RMN, desaparece la señal asignable a los carbonos-del alquino activado a alrededor de 81 ppm, y aparecen señales alrededor de 133.0 y 142.0 ppm correspondientes a los carbonos del anillo de triazol. DLS y GPC también confirmaron la pureza, la monodispersidad de conjugados y aumento de tamaño después de funcionalización en comparación con el tamaño de dendrímero de partida.

Algunos de los conjugados de dendrímero se abordaron en estudios posteriores. Se verificó la bioactividad del dendrímero mixto 3[G4]-$(Man)_{60}$/$(Bio)_{16}$/$(FITC)_5$ mediante el estudio de la interacción de biotina periférica con estreptavidina en presencia de FITC como marcador. Por otra parte, 3[G4]-$(Man)_{60}$/$(Bio)_{16}$/$(FITC)_5$ cuando se ensayó con Con A, se muestra la capacidad de reconocimiento del glicodendrimero y la lectina. Este hecho sugiere que los dendrímeros funcionalizados tienen una capacidad como material biomédico de reconocimniento celular. Adicionalmente, aprovechando la propiedad anfifílica del dendrímero funcionalizado $PEG_{5k}$-[G3]-Cat con grupos catecol, se consiguió un auto-ensamblaje rápido en PB pH 7.4, 150 mM de NaCl. El fármaco anticancerígeno hidrofóbico DOX se encapsuló fácilmente en micelas de $PEG_{5k}$-[G3]-Cat mediante diálisis con carga de fármaco (DL) 29% y eficiencia de encapsulación del 87%, lo que sugiere que estas micelas son herramientas prometedoras como trasportes de fármacos.

# 1 Introduction

The last two decades have witnessed a tremendous development of dendritic materials and structures for diverse applications in fields like materials science, nanotechnology, biomedicine or catalysis.[1,2,3,4] In this introduction, we will highlight their properties, synthesis and biological applications.[5,6,7,8]

## 1.1 Dendrimers, hyperbranched polymers and block copolymers

### 1.1.1 Dendrimers

Dendrimers are monodisperse, synthetic polymers, characterized by a well-defined molecular weight, with regular three-dimensional architecture and roughly globular macromolecular structure.[9,10] The term dendrimer is derived from the Greek words *dendron* "tree" and *meros* "part", which graphically describe the architecture of this class of polymers. Cascade molecules, arborols, cauliflower or starburst polymers are some other names given to dendrimers.

---

[1] Liang, C.; Fréchet, J. M. *Progress in polymer science* **2005**, *30*, 385.
[2] Méry, D.; Astruc, D. *Coord. Chem. Rev.* **2006**, *250*, 1965.
[3] Rosen, B. M.; Wilson, C. J.; Wilson, D. A.; Peterca, M.; Imam, M. R.; Percec, V. *Chem. Rev.* **2009**, *109*, 6275.
[4] Astruc, D.; Boisselier, E.; Ornelas, C. *Chem. Rev.* **2010**, *110*, 1857.
[5] Tekade, R. K.; Kumar, P. V.; Jain, N. K. *Chem. Rev.* **2008**, *109*, 49.
[6] Rolland, O.; Turrin, C.-O.; Caminade, A.-M.; Majoral, J.-P. *New Journal of Chemistry* **2009**, *33*, 1809.
[7] Shcharbin, D.; Pedziwiatr, E.; Blasiak, J.; Bryszewska, M. *Journal of Controlled Release* **2010**, *141*, 110.
[8] Menjoge, A. R.; Kannan, R. M.; Tomalia, D. A. *Drug Discov. Today.* **2010**, *15*, 171.
[9] Tomalia, D. A. *Prog. Polym. Sci.* **2005**, *30*, 294. Reduce the line spacing
[10] Vögtle, F. R., G.; Werner, N *Dendrimer Chemistry*; Wiley-VCH: Weinheim, 2009.

The dendritic architecture is considered one of the most important and efficient frameworks that have evolved in the period life of plants and animals to enhance and improve some properties and functions of cells, tissues and organs. The nature is rich in examples of dendritic structures often utilized as a motif where a particular function needs to be enhanced or explored. In case of trees for instance (Figure 1), above ground, the dendritic pattern is used to enhance the exposure of the tree's leaves to the sunlight, which is necessary for photosynthesis, a crucial step to keep life and growth, and maintain the oxygen/carbon dioxide balance in the atmosphere. Per contra, the shadow of the tree provides a macroenvironment that maintain higher humidity and more fixed temperatures compared to the surrounding during the day. Underground, the large dendritic network of roots works to expose the maximum functional surface area for efficient water collection from the soil.[11]

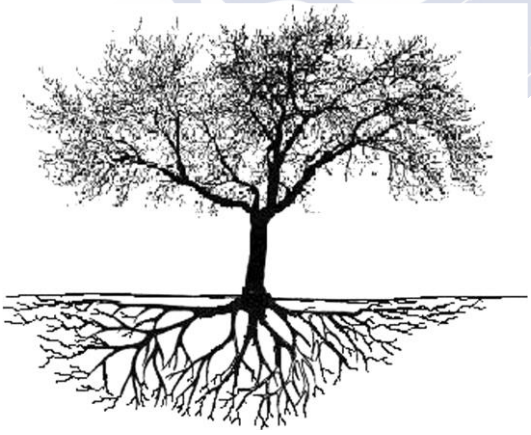

*Figure 1.* Dendritic architecture of tree and roots.[11]

.

In humans and animals, bronchioles, alveoli and blood vessels adopt the shape of an enormous dendritic network to provide a

[11] Boas, U.; Christensen, J. B.; Heegaard, P. M. H. *J. Math. Chem.* **2006**, *16*, 3785.

maximum surface for gas exchange. Similarly, the vascular system transfers the oxygen from the lungs and distribute it deeply into the tissues. Also, the central peripheral nervous system represents a massive network to gain the exchange of information with the surrounding tissues.[12] Another striking example discovered just recently as a dendritic structure in nature is the foot-hair on the Gecko's feet (Figure 2), this foot hair split up into amazing dendritic network of teeny hair, that enable the Gecko to stick easily and walk safely on surfaces, even dried ones through smart adhesives.[13] Gecko's foot hairs have proved that weakly quantum chemical forces can be amplified by millions of architectures in the form of dendritic structures.

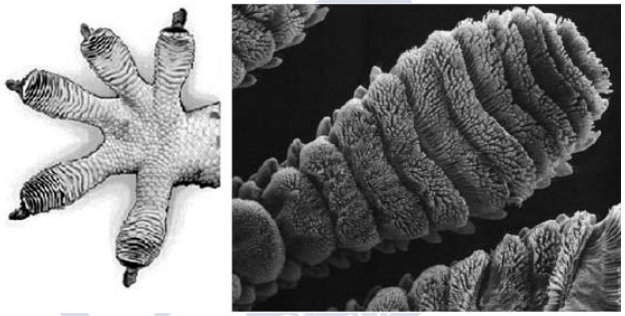

*Figure 2. Gecko's foot-hair [13]*

Inspired by the advantages provided by dendritic structures in nature, the scientific community has been interested in obtaining dendritic structures in a synthetic way. The first attempt to design a dendritic structure via organic synthesis was carried out successfully by Võgtle and co-workers[14] in 1978, which initially named "cascade molecules". Soon after this first report, Denkewalter reported a patent

[12] Narain, R. *Chemistry of Bioconjugates: Synthesis, Characterization, and Biomedical Applications.*; Wiley, 2014.

[13] Bhushan B., S. R. In *Gecko Feet: Natural Attachment Systems for Smart Adhesion-Mechanism, Modeling, and Development of Bio-Inspired Materials.*; Bhushan B., Ed.; Springer, Berlin, Heidelberg: 2008.

[14] Buhleier, E.; Wehner, W.; Vögtle, F. *Chemischer Informationsdienst* **1978**, *9*, 155.

in 1981 about the synthesis of branched polylysine derivatives.[15] It was in 1985 that Tomalia's group developed a new class of amide cascade poly(amidoamine) (PAMAM) polymers that were named by Tomalia as "dendrimers".[16] Other groups have expanded the field considerably. For instance, Newkome reported the synthesis of dendritic structures with saturated hydrocarbon chains and peripheral alcohol groups which were coined as "arborols", a term derived from the Greek word arbor (tree) and "alcohol".[17,18,19]

Dendrimer synthesis developed intensively from 1990 with Fréchet poly(aryl ether) dendrimer and the convergent synthetic approach.[20] In 1993, Wõrner and Mũlhaupt[21] at Freiburg University and Bravander-van der Berg and Meijer[22] from DSM simultaneously and independently developed a dendrimer synthesis based on Võgtle´s cascade but modified to overcome the problems derived from the poor yields of the reduction step, which limited the preparation of higher generations and complicated the purification. The new approach uses Raney/Nickel or Raney/Cobalt and $H_2$ to ease the reduction instead of Co(II)/$NaBH_4$. This modification leads to true dendrimers up to G5 of poly(propyleneimine, PPI) and poly(trimethyleneimine PTI) in large scale and high purity. A year later, Majoral and co-workers reported the synthesis of the first neutral phosphorus dendrimer (PPH);[23]

---

[15] Denkewalter, R. G.; Kolc, J. F.; Lukasavage, W. J.; U.S. Patent: 4,289,872; Sept 15; 1981.

[16] Tomalia, D. A.; Baker, H.; Dewald, J.; Hall, M.; Kallos, G.; Martin, S.; Roeck, J.; Ryder, J.; Smith, P. *Polymer Journal* **1985**, *17*, 117.

[17] Newkome, G. R.; Yao, Z.; Baker, G. R.; Gupta, V. K. *J. Org. Chem.* **1985**, *50*, 2003.

[18] Newkome, G. R.; Yao, Z.; Baker, G. R.; Gupta, V. K.; Russo, P. S.; Saunders, M. J. *J. Am. Chem. Soc.* **1986**, *108*, 849.

[19] Newkome, G. R.; Moorefield, C. N.; Baker, G. R.; Johnson, A. L.; Behera, R. K. *Angew. Chem.* **1991**, *103*, 1205.

[20] Hawker, C. J.; Frechet, J. M. J. *J. Am. Chem. Soc.* **1990**, *112*, 7638.

[21] Wörner, C.; Mülhaupt, R. *Angew. Chem., Int. Ed. Engl.* **1993**, *32*, 1306.

[22] de Brabander-van den Berg, E. M.; Meijer, E. *Angew. Chem., Int. Ed. Engl.* **1993**, *32*, 1308.

[23] Launay, N.; Caminade, A. M.; Lahana, R.; Majoral, J. P. *Angew. Chem., Int. Ed. Engl.* **1994**, *33*, 1589.

following a previous report on a charged dendrimer within phosphonium cascade structure in 1990.[24] After pioneering research and initial papers published on the design and synthesis of dendrimers, there was an enormous interest in the exploration of their properties and potential uses, mainly in chemistry and biology as a new class of polymeric nanomaterials characterized by cutting edge structural advantages and promising properties.[25,26,27] Most well-known structures of dendrimers are depicted in Figure 3.

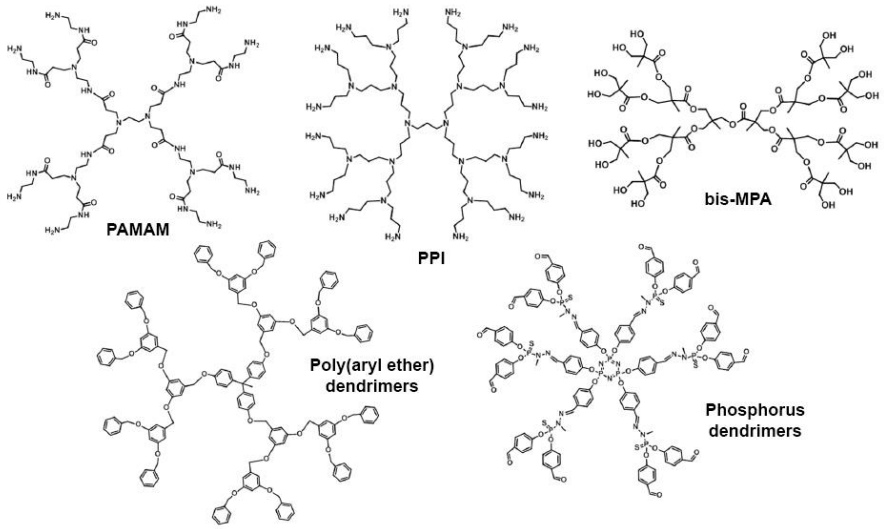


*Figure 3. Molecular structures of some of most well-known dendrimer families.*[14,16,23,28,29]

Structurally speaking, dendrimers, are well-designed multivalent branched macromolecules with nanometer size. They possess a

[24] Rengan, K.; Engel, R. *Journal of the Chemical Society, Chemical Communications* **1990**, 1084.

[25] Bosman, A. W.; Janssen, H. M.; Meijer, E. W. *Chem. Rev.* **1999**, *99*, 1665.

[26] Abbasi, E.; Aval, S. F.; Akbarzadeh, A.; Milani, M.; Nasrabadi, H. T.; Joo, S. W.; Hanifehpour, Y.; Nejati-Koshki, K.; Pashaei-Asl, R. *Nanoscale Research Letters* **2014**, *9*, 247.

[27] Gupta, V.; Nayak, S. K. *J. App. Pharm. Sci* **2015**, *5*, 117.

[28] Ihre, H.; Hult, A.; Söderlind, E. *J. Am. Chem. Soc.* **1996**, *118*, 6388.

[29] Hawker, C.; Fréchet, J. M. *Journal of the Chemical Society, Chemical Communications* **1990**, 1010.

distinguished molecular architecture that can be divided in three domains: (I) core, which is the initiator of dendrimer structure and determines the architecture in the space, (II) branches, that include the monomer units or repeating units, which are arranged and replicated around a core in a layer or generation (G) to build up an onion-like structure and, (III) the periphery, which can be functionalized with different functional groups to tune the chemical and physical properties to perform specific functions (Figure 4).

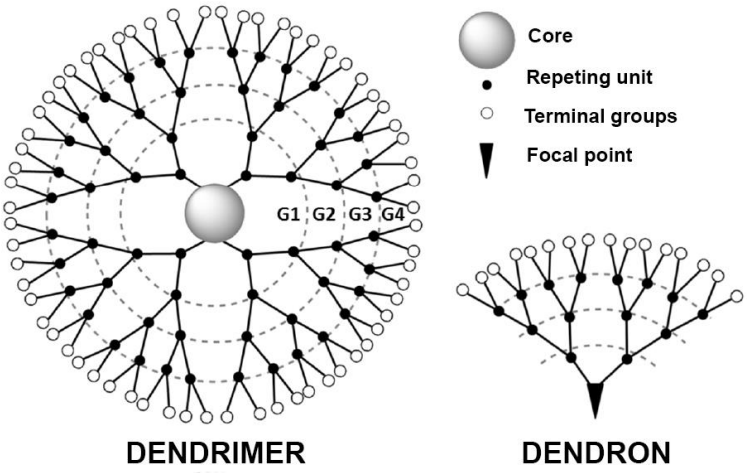


*Figure 4. Schematic representation of a dendrimer and a dendron and their structural components.*

The constituents of a dendritic structure are intimately interconnected. The core determines the primary number of branching points of the dendrimer growing in the space. The globular morphology of the dendrimer is highly affected by the geometry and the multivalency of the repeating units. The dendrimer generations (G1, G2, ĵ, G*n*, where n refers to the generation number) are defined from the number of iterative branch points from the core up to the periphery.

According to all the above, the size of the dendrimer increases in a linear fashion with generations. As a result, a huge steric hindrance emerges at the surface of high dendrimer generations, while

dendrimers of lower generations up to G2 or G3 possess more open, floppy structure with highly asymmetric shape as compared to higher generation dendrimers. At higher generations, dendrimers adopt a globular shape and the structure becomes densely packed.[6,30] A membrane-like structure is reached where steric effects hamper extra reactions of the terminal group. In this situation, reaction rates drop suddenly due to lack of space in what it has been referred as 'starburst effect'.[30]

Alternatively, when a monovalent core (usually called focal point) is used, a 'dendron' results with wedge-like structure (Figure 4) that can be independently functionalized both at the terminal and focal points with different groups of interest.

The number of terminal or end groups (Z) of a dendrimer can be determined by using the following mathematical expression:

$$Z = N_c (N_b)^G$$

where $N_c$ is the number of the branch points of the core, $N_b$ is the number of the branch points of the repeating unit and G is the number of generations.[31] Accordingly, the cartoon structure of dendrimer in (Figure 4) is built-up from a core with four branch points, and repeating unit with two branch points, which can be abbreviated systematically as 4G1 (8 end groups), 4G2 (16), 4G3 (32) and 4G4 (64).

### 1.1.2 Hyperbranched polymers

Flory[32] first introduced the hyperbranched polymer concept that later was coined by Kim and Webster[33] in 1990 as a highly branched tree-liked molecule with three-dimensional (3D) structure (Figure 5). Dendritic polymers, including hyperbranched polymers, dendrimers

---

[30] Fischer, M.; Vögtle, F. *Angew. chem., Int. Ed.* **1999**, *38*, 884.e

[31] Tomalia, D. A. *Soft Matter* **2010**, *6*, 456.

[32] Flory, P. J. *J. Am. Chem. Soc.* **1941**, *63*, 3083.

[33] Kim, Y. H.; Webster, O. W. *J. Am. Chem. Soc.* **1990**, *112*, 4592.

and other subclasses (Figure 6),[34] are the fourth class of polymer architectures following linear, branched and crosslinked polymers.[35]

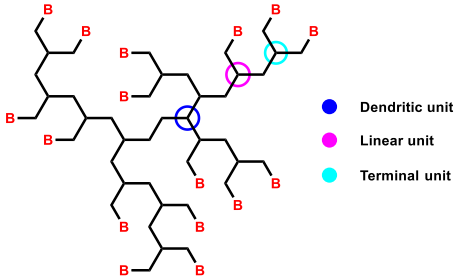


*Figure 5. Schematic structure of a hyperbranched polymer.*

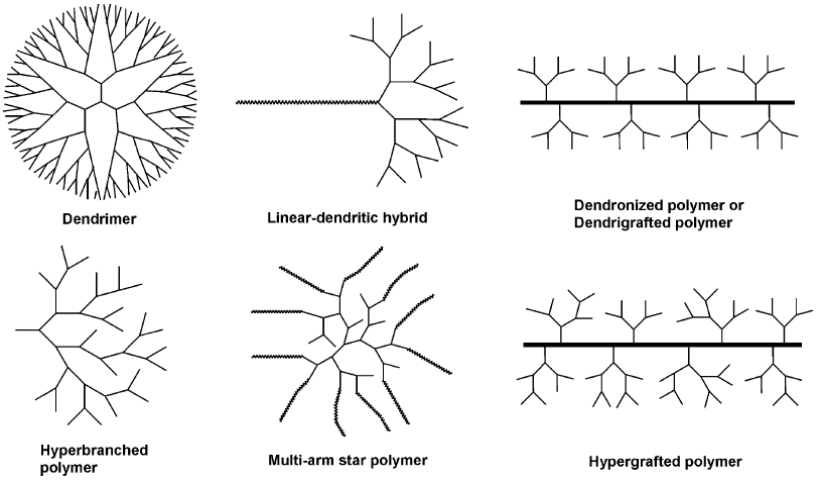


*Figure 6.* Schematic description of dendritic polymers.[34]

Interestingly, hyperbranched polymers have gained more attention after the emergence of dendrimers. While the well-defined structure of dendrimers requires stepwise synthesis, hyperbranched polymers can be synthesized in one-pot processes. Kim and Webster[33] and Fréchet *et al.*[36] published the first reports concerning the one-pot

[34] Gao, C.; Yan, D. *Progress in polymer science* **2004**, *29*, 183.
[35] Paez, J. I.; Martinelli, M.; Brunetti, V.; Strumia, M. C. *Polymers* **2012**, *4*, 355.
[36] Hawker, C. J.; Lee, R.; Frechet, J. M. J. *J. Am. Chem. Soc.* **1991**, *113*, 4583.

synthesis of hyperbranched polymers. Although with difference degree of branching,[36] hyperbranched polymers resemble dendrimers in most properties[37] such as highly branched structure,[38] plenty of functional groups, high solubility[39] and lower melt viscosity than linear polymers of the same molar mass,[40] Table ***1***[39] for more details. The relative ease of preparation, lower production cost and similar properties to dendrimer have led to hyperbranched polymers to become an alternative to dendrimers for applications where polydispersity is not an issue.



[37] Fréchet, J. M.; Hawker, C. J.; Gitsov, I.; Leon, J. W. *J. Macromol. Sci., Part A: Pure Appl. Chem.* **1996**, *33*, 1399.
[38] Kim, Y. H.; Webster, O. W. *Macromolecules* **1992**, *25*, 5561.
[39] Zheng, Y.; Li, S.; Weng, Z.; Gao, C. *Chemical Society Reviews* **2015**, *44*, 4091.
[40] Wooley, K. L.; Fréchet, J. M.; Hawker, C. J. *Polymer* **1994**, *35*, 4489.

Table 1. *Comparison of HP with a linear polymer and dendrimer.*[39]

| Polymer | Linear | Hyperbranched | Dendrimer |
|---|---|---|---|
| Structure | 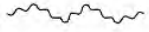 |  | 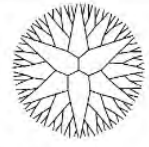 |
| Topology | 1D, linear | 3D, irregular | 3D, regular |
| Synthesis | One-step, facile | One-step, relatively facile | Multi-step, laborious |
| Purification | Precipitation | Precipitation or classification | Chromatography |
| Scaling-up | Already, easy | Already, easy | Difficult |
| MW | Discrepant | Discrepant | Identical |
| PDI | >1.1 | >1.1 | 1.0 (<1.05) |
| DB | 0 | 0.4–0.6 | 1.0 |
| Entanglement | Strong | Weak | Very weak or no |
| Viscosity | High | Low | Very low |
| Solubility | Low | High | High |
| Functional group | At two ends | At linear and terminal units | On periphery (terminal units) |
| Reactivity | Low | High | High |
| Strength | High | Low | Very low |

Hyperbranched polymers have been utilized in many fields ranging from, nanotechnology,[41,42] biomedicine,[43] coating,[44] adhesives,[45] modifiers[46] and so forth. Hyperbranched polymer can be synthesized following two major strategies: the single-monomer methodology (SMM) or double-monomer methodology (DMM). SMM includes at least four approaches according to the mechanism of reaction: 1) polycondensation of $AB_n$ monomers, where A and B are different functional groups; 2) self-condensing vinyl polymerization (SCVP); 3) self-condensing ring-opening polymerization (SCROP) and 4) proton-transfer polymerization (PTP), while DMM includes the direct polymerization of a monomer pair or two different types of monomers.[34]

With the development of hyperbranched polymers still in progress, improved reaction conditions are expected, for instance, to increase the control over the degree of branching (DB) to values closer to 1, that typically found in dendrimers. Indeed, it is now possible to overcome the theoretical DB limit of 0.5 imposed by statistics for $AB_2$ monomers, assuming the same reactivity for B groups independent of structure or location and discharging intramolecular condensation.[47,48] These conditions can be modulated by choosing the appropriate

[41] Duan, H.; Nie, S. *J. Am. Chem. Soc.* **2007**, *129*, 2412.

[42] Shi, Y.; Tu, C.; Zhu, Q.; Qian, H.; Ren, J.; Liu, C.; Zhu, X.; Yan, D.; Kong, E. S.-W.; He, P. *Nanotechnology* **2008**, *19*, 445609.

[43] Yan, D. *Nanomedicine: Nanotechnology, Biology, and Medicine* **2016**, *2*, 466.

[44] Gurunathan, T.; Mohanty, S.; Nayak, S. K. *Polymer-Plastics Technology and Engineering* **2016**, *55*, 92.

[45] Buonocore, G. G.; Schiavo, L.; Attianese, I.; Borriello, A. *Composites Part B: Engineering* **2013**, *53*, 187.

[46] Tomuta, A. M.; Ramis Juan, X.; de la Flor López, S.; Serra Albet, À. *Express polymer letters* **2013**, *7*, 595.

[47] Flory, P. J. *J. Am. Chem. Soc.* **1952**, *74*, 2718.

[48] Hobson, L. J.; Feast, W. J. *Polymer* **1999**, *40*, 1279.

reactivity of the functional groups involved in the synthesis, allowing to reach DB = 1 .[49,50,51,52]

### 1.1.3 Block Copolymers

Block copolymers are a class of polymers in which two or more types of chemically different polymers incorporate into a new polymer chain in a statistical fashion. The properties of block copolymers depend on the composition of the final product and are intermediate between those of the parent starting materials.[53] Various kinds of block copolymers have been synthesized since Szwarc in 1956 firstly synthesized a block copolymer by using a living-anionic polymerization.[54] There are A-B type diblock copolymers, A-B-A type triblock copolymers, A-B-C type triblock copolymers, and so on.[55,56] Block copolymers can be configured into linear, branched (graft and star), and cyclic molecular architectures, with wide range of applications ranging from drug delivery to materials science.[53]

#### 1.1.3.1 Linear-dendritic copolymer

Linear-block copolymers result from the combination of two or more fragments with fundamentally different molecular architectures and physical properties. This combination includes flexible linear chains and branched globular dendrimers yielding macromolecules with their own interesting and characteristic properties, that do not necessary match those of the initial constituents.[57]

---

[49] Fu, Y.; Van Oosterwijck, C.; Vandendriessche, A.; Kowalczuk-Bleja, A.; Zhang, X.; Dworak, A.; Dehaen, W.; Smet, M. *Macromolecules* **2008**, *41*, 2388.
[50] Sinananwanich, W.; Higashihara, T.; Ueda, M. *Macromolecules* **2009**, *42*, 994.
[51] Sinananwanich, W.; Segawa, Y.; Higashihara, T.; Ueda, M. *Macromolecules* **2009**, *42*, 8718.
[52] Segawa, Y.; Higashihara, T.; Ueda, M. *J. Am. Chem. Soc.* **2010**, *132*, 11000.
[53] Feng, H.; Lu, X.; Wang, W.; Kang, N.-G.; Mays, J. *Polymers* **2017**, *9*, 494.
[54] Szwarc, M. *Nature* **1956**, *178*, 1168.
[55] Zhang, M.; June, S.; Long, T.; Kong, J. **2016**.
[56] Shibayama, M. In *Elsevier Experimental Methods in the Physical Sciences*; Felix Fernandez-Alonso, Ed.; Elsevier Inc: 2017; Vol. 49, p 459.
[57] Roovers, J. C., B *Advances in Polymer Science* Springer: Berlin, 1999; Vol. 142.

The architecture of the polymer can be tailor-made in order to get the desired properties by manipulating the relative portion of the components, position in the dendritic skeleton or position in the copolymer (Figure 4)[58,59] The ability of this type of materials to self-assemble in solution, according of the different solubility of the blocks, attracts a big deal of attention in the field of nanotechnology and biomedicine, particularly in drug delivery.[60]

Hybrid macromolecules prepared from lineal polymers and dendrimers can be divided in four big families (Figure 7):

- Diblock copolymers DL (D: dendritic block, L: linear block).
- Triblock copolymers LDL, where L is a linear polymer.
- Dendronized copolymers, where dendrons emerge from fixed points along a linear chain.
- Star polymers, where several linear chains are connected at a central core using different synthetic routes: core-first, coupling-onto and arm-first.[61]

The first synthesis of a linear-dendritic block copolymer was reported by the group of Fréchet.[62] In this work, DL and DLD structures were synthesized with L being poly (ethylene glycol) (PEG) and D a G3 or G4 poly (benzyl ether) dendron. Since then, an exponential number of publications have emerged describing the synthesis and applications of linear-dendritic block copolymers.

PEGylation was described firstly by Davies and Abuchowski in the 1970s.[63,64] It is a modification process of natural and synthetic

[58] Gitsov, I. *J. Polym. Sci., Part A: Polym. Chem* **2008**, *46*, 5295.

[59] Wurm, F.; Frey, H. *Linear–dendritic block copolymers: The state of the art and exciting perspectives*, 2011; Vol. 36.

[60] Sousa-Herves, A.; Riguera, R.; Fernandez-Megia, E. *New Journal of Chemistry* **2012**, *36*, 205.

[61] Gao, H.; Matyjaszewski, K. *Macromolecules* **2008**, *41*, 1118.

[62] Gitsov, I.; Wooley, K. L.; Fréchet, J. M. *Angew. Chem., Int. Ed. Engl.* **1992**, *31*, 1200.

[63] Abuchowski, A.; Van Es, T.; Palczuk, N.; Davis, F. *Journal of Biological Chemistry* **1977**, *252*, 3578.

macromolecules (proteins, peptides, polymers in general) consisting on the covalent incorporation of one or more PEG chains. The advantages of PEGylation relate those of PEG as a non-toxic, non-antigenic, non-immunogenic, highly water-soluble polymer, approved by the Food and Drug Administration (FDA).

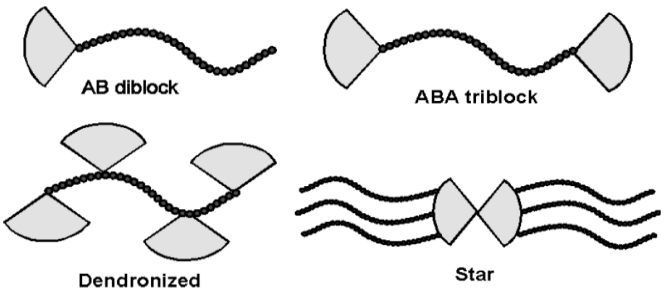


*Figure 7. Pictorial representation of different linear-dendritic copolymer structures.*

The conjugation systems composed of a PEG-drug have several advantages: a decreased degradation by metabolic enzymes, a prolonged circulation in the body, and reduction or sometimes elimination of protein immunogenicity. Thanks to these unique properties, PEGylation plays nowadays an important role in drug delivery system, enhancing the potential of proteins and peptides to be used as therapeutic agents.[65]

### 1.1.3.2 Dendritic-block copolymer

Because of the three-dimensional globular structure of dendritic macromolecules, several novel architectures can be designed for block copolymers. When the dendritic structure has more than one type of building blocks (repeating units) arranged in a certain way within the

---

[64] Abuchowski, A.; McCoy, J. R.; Palczuk, N. C.; van Es, T.; Davis, F. F. *Journal of Biological Chemistry* **1977**, *252*, 3582.

[65] Suk, J. S.; Xu, Q.; Kim, N.; Hanes, J.; Ensign, L. M. *Adv. Drug Delivery Rev.* **2016**, *99*, 28.

dendrimer skeleton, this class is called dendritic copolymer, which is found in three different types of copolymers[66] (Figure 8):

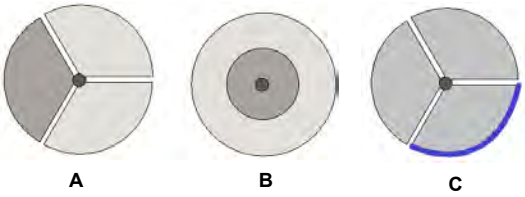


*Figure 8. Copolymers of dendrimer: A) Segment-block dendrimer, B) Layer-block dendrimer and C) surface-block dendrimer.*

(A) Segment-block dendrimer built up with completely different dendritic segments, starting from a polyfunctional core molecule to obtain dendritic segments of different constitutions. Segment-block dendrimers can be synthesized only by the convergent method (*vide infra*). The first example of a segment-block dendrimer was reported by Hawker and Fréchet, which included one ether segment and two ester-linked segments.[67] (B) Layer-block dendrimers are built up with concentric spheres (layers) of completely different repeating unit or different chemistries, while each layer consists of a homogeneous chemical structure. Layer-block dendrimers can be synthesized by both convergent and divergent methods. The first layer-block dendrimer was synthesized by Hawker and Fréchet, where the first two generations were ester-linked while the external one was ether-linked.[67] (C)The third class is surface-block dendrimer, which can be synthesized by the convergent method only. The synthesis of this type of block copolymer relies on the use of identical dendrons in the interior part, while one of the used dendrons is different in the surface functional groups. The first example of surface-block dendrimer was prepared again by Hawker and Fréchet, a dendrimer where the periphery of one dendron was fully substituted with bromide, while

[66] Hawker, C. J.; Wooley, K. L.; Fréchet, J. M. In *Macromolecular Symposia*; Wiley Online Library: 1994; Vol. 77, p 11.
[67] Hawker, C. J.; Frechet, J. M. *J. Am. Chem. Soc.* **1992**, *114*, 8405.

the remaining surface was totally devoid of any substitutions.[68] Other examples of this type of architecture were reported by Wooley *et al*.,[69] Okada *et al*.,[70] Caminade *et al*.[71] and Twyman *et al*.[72] On the other hand, the concept of surface-block was utilized for building up 'unimolecular micelles' in case of the substituted part is hydrophilic.[73] In a study yielding new 'unimolecular micelles', Okada *et al*. reported the synthesis of three different amphiphilic functionalized PAMAM dendrimers getting G4 amino/hexyl PAMAM, G4 hydroxyl/hexyl PAMAM and glucose amine/hexyl PAMAM dendrimers.[74]

## 1.2 Dendrimer synthesis and characterization

Monodispersity is one of the major characteristics that make dendrimers unique nano-tools and represents a feature when comparing them with easier to prepare hyperbranched polymers. The precise control of generation growing leads to monodisperse products with expected molecular weights and high reproducibility.[75]

### 1.2.1 Divergent approach

In the early times of dendrimers, the synthetic routes followed by Tomalia,[16] Newkome[17,18,19] and Vögtle[14] relied on a stepwise divergent approach. In this strategy, the dendrimer construction takes place in a step by step manner, starting from a reaction of the multivalent core with several repeating units to build up the dendrimer structure from

[68] Wooley, K. L.; Hawker, C. J.; Fréchet, J. M. J. *J. Chem. Soc., Perkin Trans. 1.* **1991**, 1059.
[69] Wooley, K. L.; Hawker, C. J.; Frechet, J. M. J. *J. Am. Chem. Soc.* **1993**, *115*, 11496.
[70] Aoi, K.; Itoh, K.; Okada, M. *Macromolecules* **1997**, *30*, 8072.
[71] Maraval, V.; Laurent, R.; Donnadieu, B.; Mauzac, M.; Caminade, A.-M.; Majoral, J.-P. *J. Am. Chem. Soc.* **2000**, *122*, 2499.
[72] Martin, I. K.; Twyman, L. J. *Tetrahedron Lett* **2001**, *42*, 1119.
[73] Hawker, C. J.; Wooley, K. L.; Fréchet, J. M. J. *J. Chem. Soc., Perkin Trans. 1.* **1993**, 1287.
[74] Ito, M.; Imae, T.; Aoi, K.; Tsutsumiuchi, K.; Noda, H.; Okada, M. *Langmuir* **2002**, *18*, 9757.
[75] Mintzer, M. A.; Grinstaff, M. W. *Chemical Society Reviews* **2011**, *40*, 173.

the core towards the periphery. Under this strategy the employed repeating units have one reactive site and two or more unreactive/protected end-groups. Subsequent activation/deprotection of the unreactive end-groups creates a new reactive surface for further functionalization with an additional layer (generation) of repeating units (Figure 9). This divergent approach involves an iterative two-step process of coupling and activation to achieve each generation. It typically generates dendrimers with $AB_2$ or $AB_3$ branching architectures.

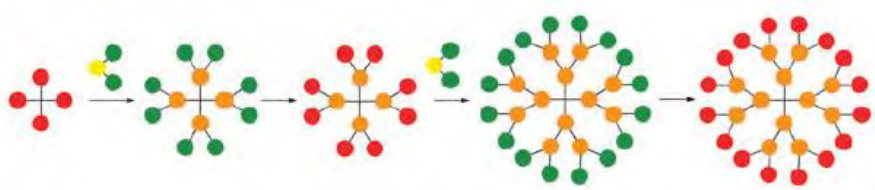

*Figure 9. Pictorial representation of dendrimer synthesis by the divergent approach.*[75]

Despite this methodology being a flexible tool for the synthesis of a broad spectrum of different dendrimers, it can be limited by an incomplete coupling of all activated peripheral groups on the surface, leading to defects in the branching structure that make difficult the achievement of perfect monodisperse dendrimers, Additionally, such strategy in case of defects is challenging from a purification point of view due to the similarity in diameter and the molecular weight of byproducts compared to the perfect product. To overcome this obstacle, prolonged reaction times, suitable solvents and an excess of repeating unit are usually implemented, which might complicate purification of final products.

As example, the synthesis of PPI dendrimers is challenged by retro-Michael reactions and intramolecular amine cyclization during the growing step that severely compromises the monodispersity of the dendrimer structure. Thus, even when the selectivity per reaction step is close to 99.5%, only a 29% of the fifth generation dendrimer will be defect-free. In a similar way, the synthesis of PAMAM dendrimer

suffers from retro-Michael and intermolecular lactam side reactions,[75] which limit the overall dendrimer synthesis.

Despite these limitations in PPI and PAMAM dendrimers, if the reaction conditions are selected carefully, this methodology of synthesis proceeds smoothly, without major challenges, particularly in growth step, thus, this strategy is considered the number one of the most methods that used for dendrimers synthesis efficiently.

### 1.2.2 Convergent approach

The second common method used for the synthesis of dendrimers is the convergent approach, which was pioneered by Hawker and Fréchet in 1990.[20,29,73] Oppositely to the divergent approach, here the dendrimer is constructed from the outside inwards. A small branching dendron of desired generation having a single reactive site at the focal point is first prepared following a divergent approach. Subsequently, it is used in excess to react with a multivalent core to yield the desired dendrimer (Figure 10).

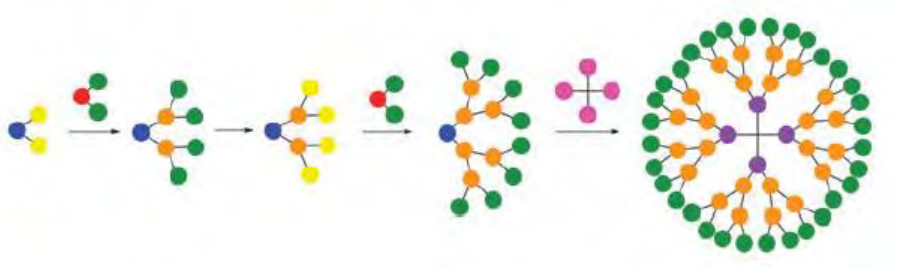

*Figure 10.* Pictorial representation of dendrimer synthesis by the convergent approach.[75]

The most relevant feature of this methodology is that allows high reaction control by the presence of a limited number of reaction points per synthetic step, which reduces the possibility of defects in the product structure. As a result, high yields of pure (defect-free) and monodisperse products are usually obtained, accompanied by easier purifications. Another appealing feature which is restricted to the convergent methodology is the ability to synthesize the so called segment-block dendrimers previously mentioned in section 1.1.3.2-a. Despite these advantages, the convergent approach is generally

restricted to the preparation of only low dendrimer generations because of the steric effects associated to large dendron skeletons reacting with small cores.[76]

### 1.2.3 Alternative synthetic approaches

Despite all the features and advantages shown by dendrimers for biomedical applications compared to linear polymers, it is now obvious that the latter have entered into clinical trials at a faster rate. The major limitation to use dendrimers in the clinical area is their preparation costs and long synthetic processes. To overcome these challenges, several attempts have been recently performed which aim to develop new synthetic strategies, encompassing user-friendly reactions and acceleration of synthetic approaches with a view to reduce the number of synthetic steps, the reaction times and/or to remove purifications.[77,78] Within this vision, several strategies have crystallized into synthetic procedures avoiding the linearity of repetitive syntheses. For instance, the "double-stage" strategy[79,80,81,82,83,84] implies the coupling of a dendron to the surface of small dendrimers (first- or second-generation maximum) called "hypercores" (Figure 11). Although this approach overcomes the steric hindrance effect, the total number of reaction steps to obtain both dendron and hypercore is identical to classical stepwise approaches. Following this methodology many dendrimers have been

[76] Grayson, S. M.; Fréchet, J. M. J. *Chem. Rev.* **2001**, *101*, 3819.
[77] Brauge, L.; Magro, G.; Caminade, A.-M.; Majoral, J.-P. *J. Am. Chem. Soc.* **2001**, *123*, 6698.
[78] Carlmark, A.; Hawker, C.; Hult, A.; Malkoch, M. *Chemical Society Reviews* **2009**, *38*, 352.
[79] Wooley, K. L.; Hawker, C. J.; Frechet, J. M. J. *J. Am. Chem. Soc.* **1991**, *113*, 4252.
[80] Miller, T. M.; Neenan, T. X.; Zayas, R.; Bair, H. E. *J. Am. Chem. Soc.* **1992**, *114*, 1018.
[81] Xu, Z.; Kahr, M.; Walker, K. L.; Wilkins, C. L.; Moore, J. S. *J. Am. Chem. Soc.* **1994**, *116*, 4537.
[82] Ihre, H.; Hult, A.; Fréchet, J. M. J.; Gitsov, I. *Macromolecules* **1998**, *31*, 4061.
[83] Forier, B.; Dehaen, W. *Tetrahedron* **1999**, *55*, 9829.
[84] Maraval, V.; Laurent, R.; Donnadieu, B.; Mauzac, M.; Caminade, A.-M.; Majoral, J.-P. *J. Am. Chem. Soc.* **2000**, *122*, 2499.

successfully synthesized such as polyester,[82] polyamide[85] and triazine[86] dendrimers

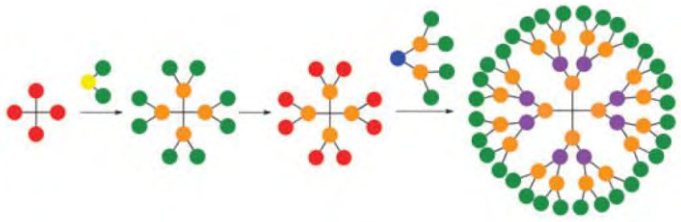

*Figure 11.* Pictorial representation of dendrimer synthesis by the double stage approach.[75]

A second approach used in improvement the synthesis of dendrimers is known as "double-exponential growth".[87,88,89,90] In this approach, the dendron growth occurs bidirectionally (periphery and focal point) (Scheme 1).[87] This type of approaches could be suitable for the synthesis of large dendrimers because of the reduction in the total number of steps. For instance, the synthesis of the fourth generation dendrimer needs seven steps following this approach compared to eight steps by classical ways.

[85] Ishida, Y.; Jikei, M.; Kakimoto, M.-a. *Macromolecules* **2000**, *33*, 3202.
[86] Lim, J.; Mintzer, M. A.; Perez, L. M.; Simanek, E. E. *Org. Lett* **2010**, *12*, 1148.
[87] Kawaguchi, T.; Walker, K. L.; Wilkins, C. L.; Moore, J. S. *J. Am. Chem. Soc.* **1995**, *117*, 2159.
[88] Chang, H. T.; Chen, C. T.; Kondo, T.; Siuzdak, G.; Sharpless, K. B. *Angew. Chem., Int. Ed. Engl.* **1996**, *35*, 182.
[89] Klopsch, R.; Schlüter, A. D.; Franke, P. *Chem.--Eur. J.* **1996**, *2*, 1330.
[90] Ashton, P. R.; Anderson, D. W.; Brown, C. L.; Shipway, A. N.; Stoddart, J. F.; Tolley, M. S. *Chem.--Eur. J.* **1998**, *4*, 781.

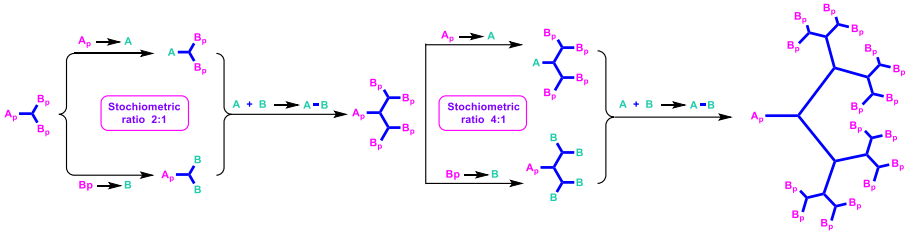


*Scheme 1.* The first two generations of double exponential dendrimer growth.[87]

The third method of acceleration of dendrimer synthesis involves the use of hypermonomers[91,92,93,94,95,96,97,98] of the type $AB_4$ or $AB_8$ instead of the classical $AB_2$ or $AB_3$ monomers. Such an approach increases the number of peripheral groups without diminishing the total number of reaction steps to obtain a desired generation.

A fourth method is called "orthogonal coupling strategy" (Figure 12),[75,85,99,100,101,102,103] which consists of coupling two different orthogonal monomers $AB_2$ and $CD_2$ with complementary functionalities to ensure spontaneous reaction without needing for activation or protection-deprotection steps. Developed in 1993, the orthogonal coupling strategy was reported by Spindler and Fréchet for the synthesis of poly (ether urethane) dendrimers.[99] Soon after this seminal paper, many other dendrimers were synthesized following this strategy, including

[91] Wooley, K. L.; Hawker, C. J.; Fréchet, J. M. *Angew. Chem., Int. Ed. Engl.* **1994**, *33*, 82.
[92] Twyman, L. J.; Beezer, A. E.; Mitchell, J. C. *J. Chem. Soc., Perkin Trans. 1.* **1994**, 407.
[93] L'Abbé, G.; Forier, B.; Dehaen, W. *Chemical Communications* **1996**, 2143.
[94] Bo, Z.; Zhang, X.; Zhang, C.; Wang, Z.; Yang, M.; Shen, J.; Ji, Y. *J. Chem. Soc., Perkin Trans. 1.* **1997**, 2931.
[95] Morgenroth, F. *Chemical Communications* **1998**, 1139.
[96] Wiesler, U.-M.; Müllen, K. *Chemical Communications* **1999**, 2293.
[97] Gilat, S. L.; Adronov, A.; Fréchet, J. M. J. *J. Org. Chem.* **1999**, *64*, 7474.
[98] Scott, D. A.; Krülle, T. M.; Finn, M.; Fleet, G. W. *Tetrahedron Lett* **2000**, *41*, 3959.
[99] Spindler, R.; Fréchet, J. M. J. *J. Chem. Soc., Perkin Trans. 1.* **1993**, 913.
[100] Xu, Z.; Moore, J. S. *Angew. Chem., Int. Ed. Engl.* **1993**, *32*, 1354.
[101] Zeng, F.; Zimmerman, S. C. *J. Am. Chem. Soc.* **1996**, *118*, 5326.
[102] Deb, S. K.; Maddux, T. M.; Yu, L. *J. Am. Chem. Soc.* **1997**, *119*, 9079.
[103] Klopsch, R.; Koch, S.; Schlüter, A. D. *Eur. J. Org. Chem.* **1998**, *1998*, 1275.

phosphorous-containing dendrimers by Caminade *et al*. in 2001.[77,104] This synthesis is based on previous work by the group on the condensation between aldehydes and phosphorhydrizides[105,106] on the one hand, and on the other hand the Staudinger reaction between phosphine and azide[71,107] (only water and nitrogen byproducts are produced, respectively). Having these reactions in hand, two different $AB_2$ and $CD_2$ monomers were designed, one containing aldehyde and azide functions, and the other one containing hydrazine and phosphine groups. Since then, this strategy has been adopted by other groups; several orthogonal syntheses have been published based both on divergent and convergent approaches.[108,109]

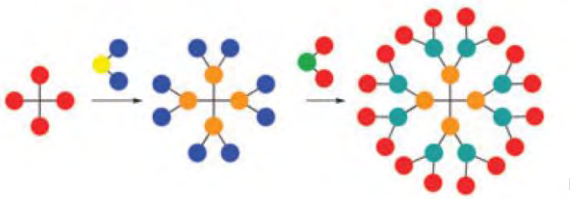

*Figure 12.* Pictorial representation of dendrimer synthesis by the orthogonal coupling strategy.[75]

Other general methods useful for the synthesis of dendrimers are: (a) the divergent/convergent approach developed by Okada *et al*.[70] and (b) a divergent/divergent approach proposed by Twyman *et al*.[110] Both approaches start with a multivalent core having protected and

[104] Brauge, L.; Magro, G.; Caminade, A.-M.; Majoral, J.-P. *Journal of the American Chemical Society* **2001**, *123*, 8446.
[105] Launay, N.; Caminade, A.-M.; Majoral, J.-P. *J. Am. Chem. Soc.* **1995**, *117*, 3282.
[106] Slany, M.; Bardaji, M.; Casanove, M.-J.; Caminade, A.-M.; Majoral, J.-P.; Chaudret, B. *J. Am. Chem. Soc.* **1995**, *117*, 9764.
[107] Sebastián, R.-M. a.; Magro, G.; Caminade, A.-M.; Majoral, J.-P. *Tetrahedron* **2000**, *56*, 6269.
[108] Antoni, P.; Nyström, D.; Hawker, C. J.; Hult, A.; Malkoch, M. *Chemical Communications* **2007**, 2249.
[109] Antoni, P.; Robb, M. J.; Campos, L.; Montanez, M.; Hult, A.; Malmström, E.; Malkoch, M.; Hawker, C. J. *Macromolecules* **2010**, *43*, 6625.
[110] Martin, I. K.; Twyman, L. J. *Tetrahedron Lett* **2001**, *42*, 1119.

deprotected sites at the same time. The active ones are used to build up the dendrimer structure divergently until a desired generation. Subsequent activation of the protected site allows to construct the remaining dendrimer structure through a convergent way (Scheme 2-path A) or divergently (Scheme 2-path B). Okada *et al.*[70] used the divergent/convergent approach to obtain an AB-type surface-block dendrimer, where the A-block was covered with a hydrophilic layer formed by sugar while the B-block surface was hydrophobic. Both hemispheres were prepared divergently from a PAMAM core and then coupled via a convergent pathway.

The divergent/divergent approach was applied by Twyman *et al.*[110] to synthesize an unsymmetric dendrimer with both DNA binding and cell recognition groups. They started with a core partially protected from which a conventional PAMAM dendron with terminal esters was grown. After deprotection of the core, a second PAMAM dendron was grown. The final dendrimer has an ester terminated and an amine terminated hemisphere.

The divergent/divergent approach was also explored by Okada *et al.*[74] allowing them to obtain three different G4 PAMAM dendrimers with amphiphilic properties. One with amino and hexyl terminal groups, another with hydroxyl and hexyl terminal groups, and the last one with amine and hexyl terminal groups (to form layers over flat surfaces).

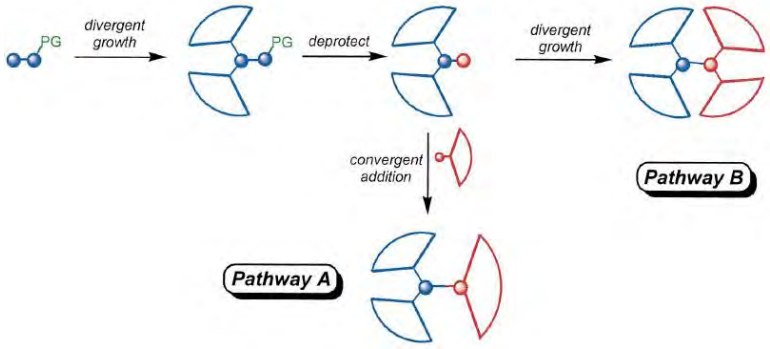


*Scheme 2.* Schematic representation of the two general methods for the construction of unsymmetrical dendrimers, the divergent/convergent approach, pathway A, and the divergent/divergent approach, pathway B.[110]

The third method to synthesize unsymmetrical dendrimers is (c) convergent/convergent. This methodology was developed by Wooley, Hawker and Fréchet.[111,112] It is a stepwise process that allows the growth of a large diversity of dendritic surface block copolymers. Each dendron or dendritic wedge is grown separately, each with its own surface functionalization, then the focal point is activated to attach the dendron to the polyfunctional core. In this way it is possible to prepare micellar (all carboxylate groups), amphiphilic (carboxylate hydrophilic and benzyl hydrophobic) and dipolar (cyano EWG and benzyl ethers EDG) dendrimers with high control of number, nature and to a certain extent the position of functional groups at the surface of the dendritic structure.

### 1.2.4 Characterization of dendrimers

The successful synthesis and purification of any dendritic product requires analytical evidence for its chemical structure and purity. A vast array of analytical tools and techniques are available to verify the chemical structure, purity, and composition. Among these tools are

[111] Wooley, K. L.; Hawker, C. J.; Fréchet, J. M. *J. Chem. Soc., Perkin Trans. 1.* **1991**, 1059.

[112] Fréchet, J. M.; Hawker, C. J.; Wooley, K. L. *Journal of Macromolecular Science, Part A* **1994**, *31*, 1627.

size exclusion chromatography (SEC)[113] or gel permeation chromatography (GPC)), which is mostly used to determine the purity, and monodispersity of dendrimers. MALDI-TOF mass spectrometry[114,115,116] can be used to determine the molecular weight of dendrimers. Atomic force microscopy (AFM) is used for imaging nanoscale structures at different surfaces and interfaces, which complements the use of dynamic light scattering (DLS) for the analysis of hydrodynamic diameters in solution. Undoubtedly, nuclear magnetic resonance (NMR)[117,118] is the most common used method for identification and structure elucidation in modern synthetic organic chemistry. In dendrimer synthesis, it is utilized to monitor the disappearance /appearance of specific moieties before and after coupling/activation reactions. Our group has described the use of NMR to study the dynamics of dendrimers based on recording relaxation time data $T_1$ at various temperatures (and fields)[119]. Infrared (IR) is also a good tool to monitor and confirm the completion of reactions of dendrimers according to the appearance/disappearance of characteristic signals of certain functional groups. Uv-vis, Raman, and differential scanning calorimetric (DSC)[120] are also routine techniques used for the analysis of dendrimers. It should be noted, however, that characterization of dendrimers is a synergistic process by spectroscopic and chromatographic tools.

---

[113] Gavrilov, M.; Monteiro, M. J. *Eur. Polym. J.* **2015**, *65*, 191.

[114] Baytekin, B.; Werner, N.; Luppertz, F.; Engeser, M.; Brüggemann, J.; Bitter, S.; Henkel, R.; Felder, T.; Schalley, C. A. *International Journal of Mass Spectrometry* **2006**, *249*, 138.

[115] Krupková, A.; Čermák, J.; Walterová, Z.; Horský, J. *Anal. Chem.* **2007**, *79*, 1639.

[116] Räder, H. J.; Nguyen, T.-T.-T.; Müllen, K. *Macromolecules* **2014**, *47*, 1240.

[117] Deloncle, R.; Coppel, Y.; Rebout, C.; Majoral, J. P.; Caminade, A. M. *Magn. Reson. Chem.* **2008**, *46*, 493.

[118] Caminade, A. M. T., C.O.; Laurent, R.; Ouali, A.; Delavaux-Nicot., B. *Dendrimers: Towards catalytic, material and biomedical uses*; 1 ed.; Wiley & Sons: New York, 2011.

[119] Pinto, L. F.; Correa, J.; Martin-Pastor, M.; Riguera, R.; Fernandez-Megia, E. *J. Am. Chem. Soc.* **2013**, *135*, 1972.

[120] Valdés Lizama, O.; Vilos, C.; Durán-Lara, E. *Curr. Org. Chem.* **2016**, *20*, 2591.

## 1.3 GATG Dendrimers and their applications

Gallic acid-triethylene glycol (GATG) dendrimers (abbreviated as [G*n*]-$N_3$, where *n* is the generation number) are a dendritic family firstly described by Roy and co-workers in 1995.[121,122] These dendrimers are composed of a repeating unit carrying a gallic acid core and three hydrophilic triethylene glycol (TEG) chains with terminal azide groups (

Scheme *3*). GATG dendrimers are characterized by a high tunability, regarding to the presence of the terminal azide groups that can be functionalized with a myriad of groups through very efficient reactions. Moreover, the presence the carboxylic group in the repeating unit allows the growing of the dendrimers via classical amide chemistry with amine-terminated cores.[123]

To make the synthesis of GATG dendrimers[121,122] efficient and reliable, our group first turned the attention to improve the preparation of the GATG repeating unit,[121,122] that with a reported overall 23% yield after four steps from TEG, revealed a bottleneck in the synthesis and development of this dendritic family. As shown in Scheme 3 starting from a commercially available TEG chlorohydrin derivative, the GATG repeating unit could be obtained in a 87% overall yield.

[121] Roy, R.; Park, W. K.; Wu, Q.; Wang, S.-N. *Tetrahedron Lett* **1995**, *36*, 4377.
[122] Meunier, S. J.; Wu, Q.; Wang, S.-N.; Roy, R. *Can. J. Chem.* **1997**, *75*, 1472.
[123] Sousa-Herves, A.; Novoa-Carballal, R.; Riguera, R.; Fernandez-Megia, E. *The AAPS journal* **2014**, *16*, 948.

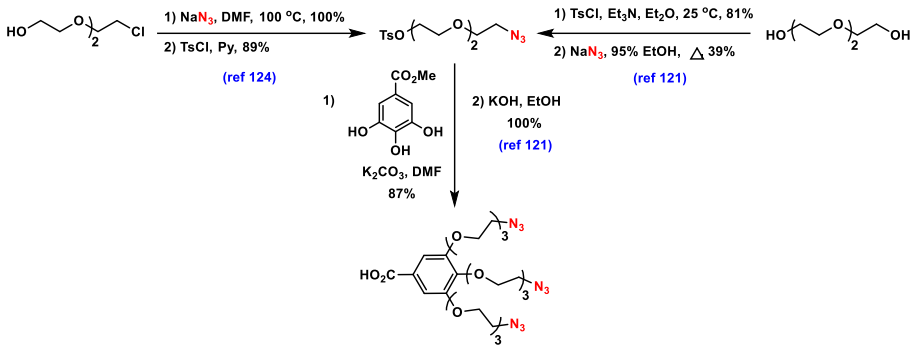


*Scheme 3, Preparation of GATG repeating unit.*

Figure 13 illustrates the diverse applications of GATG dendrimers and their PEGylated block copolymers.[123]

With a robust method for the preparation of the GATG repeating unit[124,125] in 2006 our group reported the successful preparation of three generations of GATG dendrimers [Gn]-$N_3$[124] starting from 1-propylamine. Soon after, with the aim of developing dendritic structures for biomedical applications, our group also described the preparation of linear-block copolymers combining GATG dendrimers and poly(ethylene glycol) (PEG). The resulting PEG-[Gn]-$N_3$ copolymers[126,127] were obtained up to G4. During the last decade, our group has exploited the advantageous presence of terminal azide groups in GATG for their functionalization by means of the Cu(I)-catalyzed azide-alkyne cycloaddition (CuAAC) reaction, with different alkynes moieties, which give in turn products that could be used in many applications.

---

[124] Fernandez-Megia, E.; Correa, J.; Rodríguez-Meizoso, I.; Riguera, R. *Macromolecules* **2006**, *39*, 2113.

[125] Amaral, S. P.; Fernandez-Villamarin, M.; Correa, J.; Riguera, R.; Fernandez-Megia, E. *Org. Lett* **2011**, *13*, 4522.

[126] Fernandez-Megia, E.; Correa, J.; Riguera, R. *Biomacromolecules* **2006**, *7*, 3104.

[127] Fernandez-Villamarin, M.; Sousa-Herves, A.; Correa, J.; Munoz, E. M.; Taboada, P.; Riguera, R.; Fernandez-Megia, E. *ChemNanoMat* **2016**, *2*, 437.

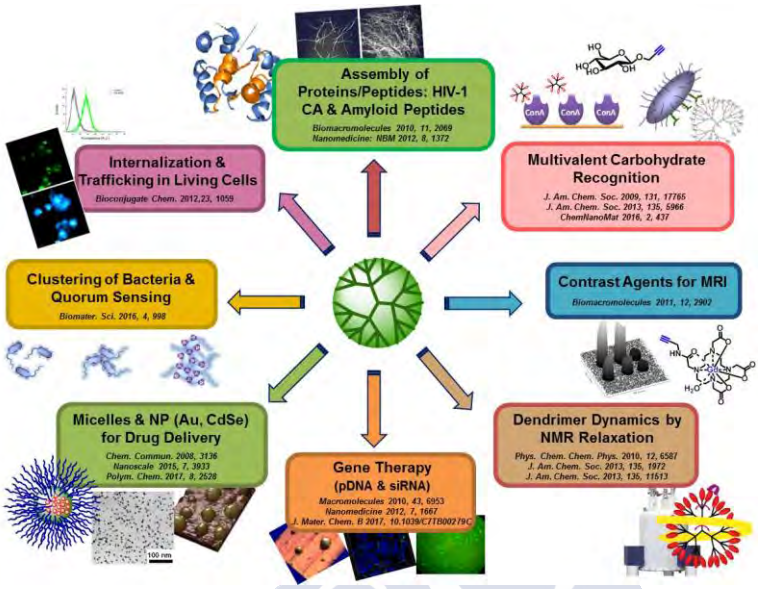


*Figure 13.* Applications of functionalized GATG dendrimers.[123]

First, to evaluate click chemistry as a tool in the functionalization of GATG dendrimers, a study was performed focused on the CuAAC. To this aim, three generations of GATG dendrimers ([G1]-$N_3$, [G2]-$N_3$ and [G3]-$N_3$) were prepared and functionalized efficiently under aqueous conditions with unprotected alkynated glycosides derived from α-L-fucose, α-D-mannose, and β-D-lactose.[124] As a result, multivalent conjugations with up to 27 peripheral groups were obtained in reproducible, very high yields. This successful use of click chemistry opened the door for a quick, efficient and reliable functionalization of GATG dendrimers. Further exploration of CuAAC for the functionalization of GATG dendrimers and block copolymers involved diverse peripheral groups, including charged ($OSO_3^-$, $NH_3^+$) and neutral (acetylated) ones, and biologically relevant ligands (carbohydrates and peptides). All these conjugates were also labeled with an alkynated fluorescein isothiocyanate (FITC), to analyzing the effect of surface functionalization on cell uptake and

intracellular trafficking.[128] This study showed a strong effect of the charged surface on the cell uptake, which agrees to previous results with alternative dendritic families.[129,130]

More recently, PEG-GATG block copolymers have also been used to template the preparation of metal nanoparticles (NPs),[131] to polyplex pDNA and siRNA for gene delivery[123,132,133,134] and participate in the preparation of drug delivery systems, particularly, polyion complex (PIC) micelles.[135,136] Thus, our research group has reported the preparation PIC micelles from an anionic PEG-GATG block copolymer of G3 functionalized with 27 sulfates and poly-L-lysine (PLL) as oppositely charged polymer. These micelles are envisioned as appealing delivery systems of low molecular weight drug, proteins, nucleic acids, and imaging agents.[133] In addition, our research group exploited CuAAC for the anionic decoration of PEG-GATG block copolymers with carboxylates, which provided an opportunity for the preparation of pH-sensitive PIC micelles with potential applications in tumor therapy.[135,137]

---

[128] Albertazzi, L.; Fernandez-Villamarin, M.; Riguera, R.; Fernandez-Megia, E. *Bioconjugate. Chem* **2012**, *23*, 1059.

[129] Perumal, O. P.; Inapagolla, R.; Kannan, S.; Kannan, R. M. *Biomaterials* **2008**, *29*, 3469.

[130] Albertazzi, L.; Serresi, M.; Albanese, A.; Beltram, F. *Mol. Pharm* **2010**, *7*, 680.

[131] Sousa-Herves, A.; Espinel, C. S.; Fahmi, A.; González-Fernández, Á.; Fernandez-Megia, E. *Nanoscale* **2015**, *7*, 3933.

[132] Ravina, M.; de La Fuente, M.; Correa, J.; Sousa-Herves, A.; Pinto, J.; Fernandez-Megia, E.; Riguera, R.; Sanchez, A.; Alonso, M. J. *Macromolecules* **2010**, *43*, 6953.

[133] De La Fuente, M.; Raviña, M.; Sousa-Herves, A.; Correa, J.; Riguera, R.; Fernandez-Megia, E.; Sánchez, A.; Alonso, M. J. *Nanomedicine* **2012**, *7*, 1667.

[134] Leiro, V.; Garcia, J. P.; Moreno, P. M.; Spencer, A. P.; Fernandez-Villamarin, M.; Riguera, R.; Fernandez-Megia, E.; Pêgo, A. P. *Journal of Materials Chemistry B* **2017**, *5*, 4901.

[135] Fernandez-Villamarin, M.; Sousa-Herves, A.; Porto, S.; Guldris, N.; Martínez-Costas, J.; Riguera, R.; Fernandez-Megia, E. *Polym. Chem.* **2017**, *8*, 2528.

[136] Sousa-Herves, A.; Fernandez-Megia, E.; Riguera, R. *Chemical Communications* **2008**, 3136.

[137] Sousa-Herves A, R. R., Fernandez-Megia E. In *PCT Int Appl* 2010; Vol. WO 2010018286 A1 20100218

Cationic synthetic carriers and dendrimers have been exceedingly assayed as an alternative to viral vectors for the delivery of nucleic acids.[138] Among them, cationic GATG dendrimers and block copolymers, easily obtained by reduction of GATG terminal azides, have revealed as excellent candidates for gene delivery applications. PEGylated block copolymers excel dendrimers by masking the dendriplex positive charge[139] as well as for overcoming aggregation with blood components. The ability of amino-functionalized GATG dendrimers and block copolymers to complex pDNA was evaluated[123,132,133,134] in collaboration with Alonso's group. This study revealed that GATG dendriplexes are stable, biocompatible and able to protect pDNA from degradation.[133]

Recently our research group has reported on the synthesis of two new families of symmetrical GATG dendrimers 2[Gn] and 3[Gn].[140] It has been revealed that the generation of these globular dendrimers is a powerful tool in tuning the size of the PIC assemblies, which in turn controls their pharmacokinetics and biodistribution. A library of oppositely charged GATG dendrimers and commercial linear PEGylated copolymers has led to a hierarchical transfer of structural information from dendrimer-to-PIC assemblies, with average size 80 to 500 nm upon decreasing the generation of the dendrimer. Two different PIC assemblies were revealed, which is interpreted according to the progression of the unit-PIC from cone- to rod-shaped. As expected, because of the precise size tuning of PICs, the smaller size assembles showed faster kinetics, broader organ distributions and longer distribution time than larger aseembles.[140]

A G1 GATG dendrimer functionalized with peripheral benzoate groups ([G1]-$CO_2Na$) was able to hamper the capside assembly of the

[138] Mintzer, M. A.; Simanek, E. E. *Chem. Rev.* **2008**, *109*, 259.
[139] Wood, K. C.; Little, S. R.; Langer, R.; Hammond, P. T. *Angew. chem., Int. Ed.* **2005**, *44*, 6704.
[140] Amaral, S. P.; Tawara, M. H.; Fernandez-Villamarin, M.; Borrajo, E.; Martinez-Costas, J.; Vidal, A.; Riguera, R.; Fernandez-Megia, E. *Angew Chem Int Ed Engl* **2018**, *57*, 5273.

HIV in vitro.[141] In a related investigation in collaboration with the group of Klajnert, a G3 GATG dendrimer decorated with morpholine groups ([G3]-Mor) significantly reduced the toxicity of amyloid peptides.[142] In another report, the synthesis of dendritic Magnetic Resonance Imaging (MRI) contrast agents was accomplished, taking advantage of CuAAC as an efficient prelabeling coupling technology using an alkynated Gd chelate. After intravenous injection, these dendrimers displayed an enhancement of their ionic relaxivity as contrast agents for MRI.[143]

The multivalent interaction of decorated GATG with specific ligands has been exploited, to study the multivalent nature of carbohydrate-lectin interactions. Three generations of GATG dendrimers, functionalized with 3-27 mannose residues, associated with concanavalin A, provided a precise nanotool for gaining insight into the fundamental mechanisms of their multivalent carbohydrate recognition.[127,144] The models that describe surface plasmon resonance (SPR) sensograms of monovalent interactions are well established and commercially available. Unfortunately, multivalent interactions lacked such models. Recently our group has developed a new method of analysis of multivalent interactions by SPR which is based on the kinetic analysis of the early association and late dissociation phases of the sensograms. This system provides important information on the mechanisms governing multivalent interactions by obtaining kinetic and thermodynamic parameters of the binding.[145]

---

[141] Doménech, R.; Abian, O.; Bocanegra, R.; Correa, J.; Sousa-Herves, A.; Riguera, R.; Mateu, M. G.; Fernandez-Megia, E.; Velázquez-Campoy, A.; Neira, J. L. *Biomacromolecules* **2010**, *11*, 2069.

[142] Klajnert, B.; Wasiak, T.; Ionov, M.; Fernandez-Villamarin, M.; Sousa-Herves, A.; Correa, J.; Riguera, R.; Fernandez-Megia, E. *Nanomedicine: Nanotechnology, Biology and Medicine* **2012**, *8*, 1372.

[143] Fernandez-Trillo, F.; Pacheco-Torres, J.; Correa, J.; Ballesteros, P.; Lopez-Larrubia, P.; Cerdan, S.; Riguera, R.; Fernandez-Megia, E. *Biomacromolecules* **2011**, *12*, 2902.

[144] Munoz, E. M.; Correa, J.; Fernandez-Megia, E.; Riguera, R. *J. Am. Chem. Soc.* **2009**, *131*, 17765.

[145] Munoz, E. M.; Correa, J.; Riguera, R.; Fernandez-Megia, E. *J. Am. Chem. Soc.* **2013**, *135*, 5966.

More recently, to explore the precise size effect of GATG dendrimers, three generations 3[G1]-$N_3$, 3[G2]-$N_3$ and 3[G3]-$N_3$ with 9, 27 and 81 primary amines, were selected in order to investigate their effects on the aggregation of the bacteria *V. harveyi*. The study showed that cationic GATG dendrimers induced clustering in *V. harveyi*, which is greater than that induced by a cationic linear polymer.[146,147] Also they induced the expression of quorum sensing (QS) controlled luminescence. As a result, this study highlighted the potential of the GATG dendrimers as a platform in the development of new antimicrobial agents.[148]

### 1.4 Huisgen azide-alkyne cycloaddition (AAC)

Cycloaddition is a chemical reaction in which two or more π systems combine to afford a stable cyclic adduct with formation of new sigma bonds between the termini of the π systems, without losing any fragment, and following a concerted mechanism. This type of chemical reaction has proved to be a powerful tool in the formation of cyclic systems. The Diels-Alder reaction, extensively used for the stereospecific construction of six-membered rings, and the 1,3-dipolar cycloaddition, exploited in the preparation of five-membered rings, are the most familiar examples of cycloadditions.

The 1,3-dipolar cycloaddition is known as Huisgen reaction[149,150] who described this type of cyclization reactions in 1960s. Here, the formation of a five-member ring involves a three atom entity (a-b-c) and a two atom entity (d-e) (Figure 14); for this reason it is called [3+2] cycloaddition reaction.

---

[146] Lui, L. T.; Xue, X.; Sui, C.; Brown, A.; Pritchard, D. I.; Halliday, N.; Winzer, K.; Howdle, S. M.; Fernandez-Trillo, F.; Krasnogor, N. *Nature chemistry* **2013**, *5*, 1058.

[147] Louzao, I.; Sui, C.; Winzer, K.; Fernandez-Trillo, F.; Alexander, C. *Eur. J. Pharm. Biopharm.* **2015**, *95*, 47.

[148] Leire, E.; Amaral, S. P.; Louzao, I.; Winzer, K.; Alexander, C.; Fernandez-Megia, E.; Fernandez-Trillo, F. *Biomaterials science* **2016**, *4*, 998.

[149] Huisgen, R. *Angew. Chem., Int. Ed. Engl.* **1963**, *2*, 565.

[150] Huisgen, R. *in 1,3-Dipolar Cycloaddition Chemistry*; Wiley: New York, 1984.

A 1,3-dipole is a reactive molecule with distributed charge, that forms a five-membered ring via a concerted pericyclic mechanism[151] with dipolarophile (Figure 14). The resonance structure allows them to react as electrophiles and nucleophiles (Figure 15). Azide as dipole and alkynes as dipolarophiles are the most common examples of functional groups used in 1,3-dipolar cycloaddition reactions.

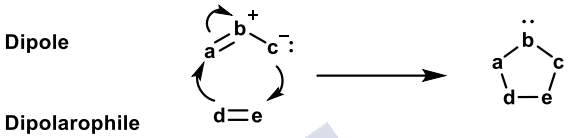


*Figure 14. 1,3-Cycloaddition reaction mechanism.*

*Figure 15. Resonance structures of 1,3-dipoles.*

Five-membered nitrogen-containing heterocycles are major structures in a diversity of natural products and drugs. Among the five-membered nitrogen-containing heterocycles stands the triazole, which is the main outcome of the Huisgen azide-alkyne cycloaddition (AAC).[149] This reaction is 1,3-dipolar cycloaddition of organic azides and terminal or internal alkynes to produce triazoles as a mixture of 1,4- and 1,5-adducts (Figure 16).

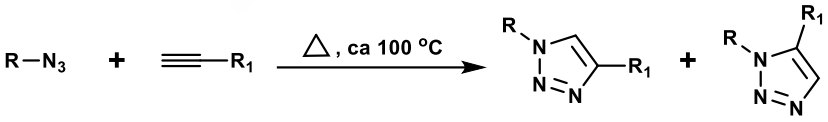


*Figure 16. Schematic of the Huisgen cycloaddition.*

[151] Huisgen, R. *J. Org. Chem.* **1968**, *33*, 2291.

## 1.5 Click chemistry and CuAAC

The concept of click chemistry was introduced by K. B. Sharpless[152] in 2001 to describe reactions with an optimum set of properties, such as "j wide in scope, afford very high yield, generate inoffensive byproducts that can be easily removed by nonchromatographic means and stereospecific. The characteristics of the required process include simple reaction conditions (ideally, insensitive to water and oxygen), readily available chemical reagents and starting materials, using no solvent or benign solvent (such as water) or volatile solvent to be removed easily and simple isolation of product. Purification, if necessary, must be with simple methods such as crystallization or simple distillation while chromatographic should be excluded, and the obtained product must be stable under physiological conditions".[152]

Click chemistry involves a set of powerful linking reaction that are straightforward to implement, give high yield, no or minimal purification with versatile forming diverse structures without the necessity of protection steps. To date, click reactions have been identified in four major classifications (Figure 17), cycloaddition,[153] nucleophilic ring-opening,[153] carbonyl chemistry of the non-aldol type,[152] and addition to carbon-carbon multiple bond.[152,153,154]

[152] Kolb, H. C.; Finn, M.; Sharpless, K. B. *Angew. chem., Int. Ed.* **2001**, *40*, 2004.
[153] Kolb, H. C.; Sharpless, K. B. *Drug Discov. Today.* **2003**, *8*, 1128.
[154] Lallana, E.; Fernandez-Trillo, F.; Sousa-Herves, A.; Riguera, R.; Fernandez-Megia, E. *Pharm. Res* **2012**, *29*, 902.

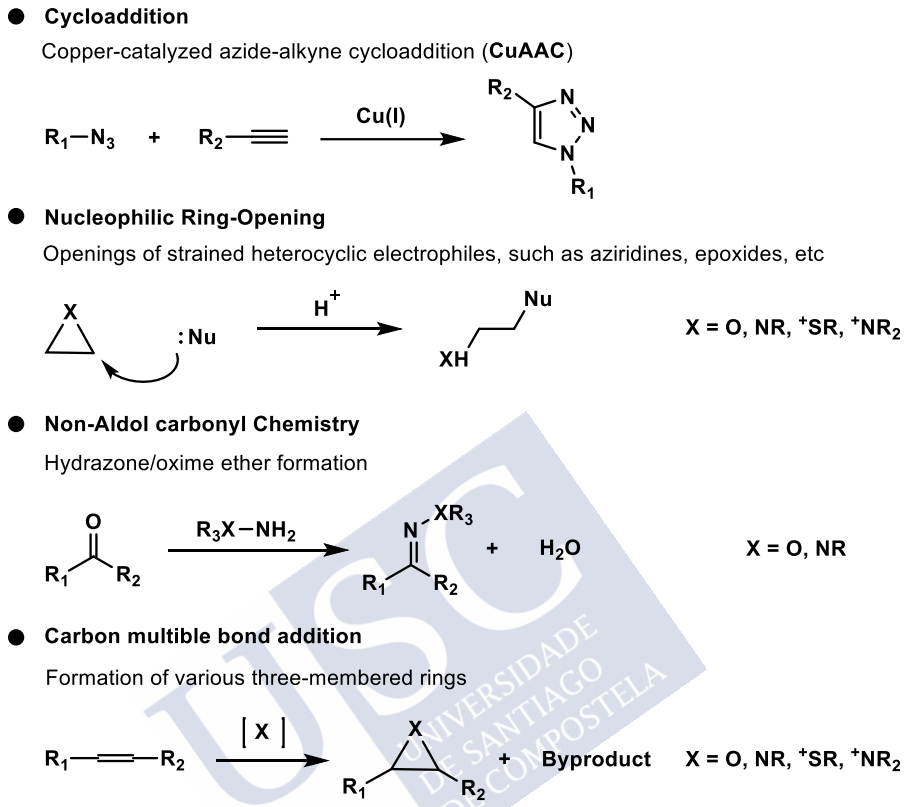


*Figure 17. Major classifications of click reactions.*

Among these reactions, cycloadditions, particularly the Cu(I) catalyzed azide-alkyne cycloaddition (CuAAC) has the advantage to exclusively afford the 1,4-regioisomer of 1,2,3-triazoles.[149] The CuAAC, independently introduced by Sharpless[155] and Meldal[156] in 2002, represents the most widely used click reaction with applications across many research areas, compared with the other metal-catalyzed azide-alkyne cycloaddition reactions.[157]

[155] Rostovtsev, V. V.; Green, L. G.; Fokin, V. V.; Sharpless, K. B. *Angew. chem., Int. Ed.* **2002**, *41*, 2596.
[156] Tornøe, C. W.; Christensen, C.; Meldal, M. *J. Org. Chem.* **2002**, *67*, 3057.
[157] Wang, C.; Ikhlef, D.; Kahlal, S.; Saillard, J.-Y.; Astruc, D. *Coord. Chem. Rev.* **2016**, *316*, 1.

The CuAAC undergoes a mechanism (Figure 18) that is completely different to the concerted pericyclic mechanism of the uncatalyzed reaction (Figure 14). It perfectly fulfills the whole click chemistry criteria. Typically, it doesn't require high temperature (possibility to be performed over a wide temperature range, 0-160 ºC), it can be performed under a variety of solvents, including water, and over a wide pH domain (5-12). In addition, CuAAC reactions benefit from short workup and purification (filtration and precipitation).[155,158,159,160] Furthermore, this reaction is unaffected by steric factors (tertiary, secondary, primary substituents and aromatic azides are allowed), and both azides and terminal alkynes are extremely stable under standard reaction conditions.[161,162]

The most common approach to generate Cu(I) is by reducing Cu(II) salts such as $CuSO_4 \cdot 5H_2O$ in situ by using a reducing agent such as sodium ascorbate,[160] while hydrazine[163] and tris(2-carboxyethyl) phosphine (TCEP)[164] have been also used with success. Using water as solvent is possible, without requiring deoxygenated atmosphere[160,165] or protecting steps; furthermore, it's environmentally safe.[152] The major challenge in CuAAC is to keep the Cu(I) oxidation state , which can be obtained by using a proper ratio of reducing agent to catalyst or addition of a copper stabilizing agent.[160]

---

[158] Rodionov, V. O.; Fokin, V. V.; Finn, M. *Angew. Chem.* **2005**, *117*, 2250.

[159] Himo, F.; Lovell, T.; Hilgraf, R.; Rostovtsev, V. V.; Noodleman, L.; Sharpless, K. B.; Fokin, V. V. *J. Am. Chem. Soc.* **2005**, *127*, 210.

[160] Bock, V. D.; Hiemstra, H.; Van Maarseveen, J. H. *Eur. J. Org. Chem.* **2006**, *2006*, 51.

[161] Kolb, H. C.; Sharpless, K. B. *Drug Discov. Today.* **2003**, *8*, 1128.

[162] Bräse, S.; Gil, C.; Knepper, K.; Zimmermann, V. *Angew. chem., Int. Ed.* **2005**, *44*, 5188.

[163] Golas, P. L.; Tsarevsky, N. V.; Sumerlin, B. S.; Matyjaszewski, K. *Macromolecules* **2006**, *39*, 6451.

[164] Zhan, W.-h.; Barnhill, H. N.; Sivakumar, K.; Tian, H.; Wang, Q. *Tetrahedron Lett* **2005**, *46*, 1691.

[165] Orgueira, H. A.; Fokas, D.; Isome, Y.; Chan, P. C.-M.; Baldino, C. M. *Tetrahedron Lett* **2005**, *46*, 2911.

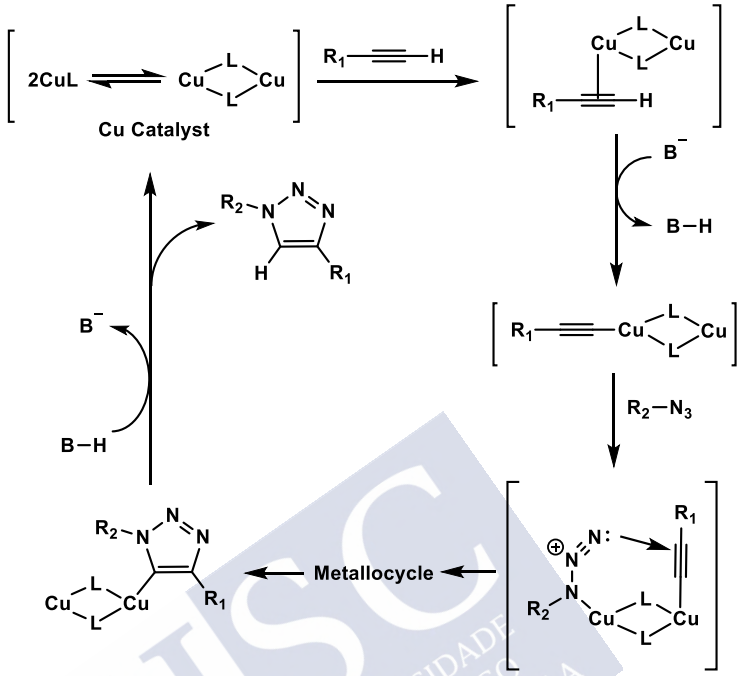


*Figure 18. Mechanism of CuAAC.*[160]

Alternatively, the direct addition of Cu(I) salts, such as CuBr, CuI or CuOTf·$C_6H_6$ represents an alternative source of Cu catalyst.[155] Nevertheless, under these conditions, reactions are typically restricted to organic solvents and sometimes require deoxygenated conditions. Formation of by-products such as primarily diacetylenes, bistriazoles and 5-hydroxytriazoles has been often observed, which can be minimized by addition of 2,6-lutidine.[155] In addition, Cu(I)-halides require at least an amine base or high temperature to form the Cu-acetylide complex, while catalytically active Cu(I), directly generated from $CuSO_4$ in situ by reduction with ascorbate, instantly produces the Cu-acetylide.[166] Overall, the Cu(II)/ascorbate system results more reliable, less costly and affords purer products than Cu(I) salts.[155] Another way to generate Cu(I) is via oxidation of copper metal with

[166] Meldal, M.; Tornøe, C. W. *Chem. Rev.* **2008**, *108*, 2952.

an amine salt.[159,167] Still, this route has resulted in considerable disadvantages that include longer reaction times, larger amounts of copper metal, and an acidic environment to dissolve copper which in turn damage potentially acidic-sensitive functional groups.[164] With a lot of attempts to implement CuAAC via different ways to generate Cu(I), the reduction approach of Cu(II) salts to Cu(I) is recognized as the most valuable approach.[155]

In 2005, Fokin, Jia and coworkers[168] showed that an exchange of copper Cu(I) for a ruthenium Ru(II) complex could be applied in the AAC reaction. The first attempts of a Ru(II) catalysts screening involved benzyl azide and phenylacetylene, with different Ru(II) complexes. Although initial attempts with Ru(II) catalyst complexes produced the same 1,4-isomers as in CuAAC, when the complex contained cyclopentadienyl ligands (CP), the 1,5-isomer was produced albeit with some of 1,4-isomer. Switching the attention to the more sterically hindered pentamethylcyclopentadienyl derivative (CP*), the 1,5-disubstituted triazole was selectivity obtained (Figure 19). Depending on the catalyst loading, this reaction could be run under a wide range of temperature (ambient to 80 ºC) and solvent (polar and nonpolar) conditions.[169]

In contrast to the CuAAC, that is limited to terminal alkynes, the RuAAC was found tolerant to both terminal alkynes to produce 1,5-disubstituted 1,2,3-triazoles, and internal alkynes to produce 1,5-disubstituted 1,4,5-triazoles,[168,170] but conditions required are often harsh compared to those for CuAAC.

---

[167] Orgueira, H. A.; Fokas, D.; Isome, Y.; Chan, P. C.-M.; Baldino, C. M. *Tetrahedron Lett* **2005**, *46*, 2911.

[168] Zhang, L.; Chen, X.; Xue, P.; Sun, H. H.; Williams, I. D.; Sharpless, K. B.; Fokin, V. V.; Jia, G. *J. Am. Chem. Soc.* **2005**, *127*, 15998.

[169] Oakdale, J. S.; Fokin, V. V.; Umezaki, S.; Fukuyama, T. *Organic syntheses; an annual publication of satisfactory methods for the preparation of organic chemicals* **2013**, *90*, 96.

[170] Boren, B. C.; Narayan, S.; Rasmussen, L. K.; Zhang, L.; Zhao, H.; Lin, Z.; Jia, G.; Fokin, V. V. *J. Am. Chem. Soc.* **2008**, *130*, 8923.

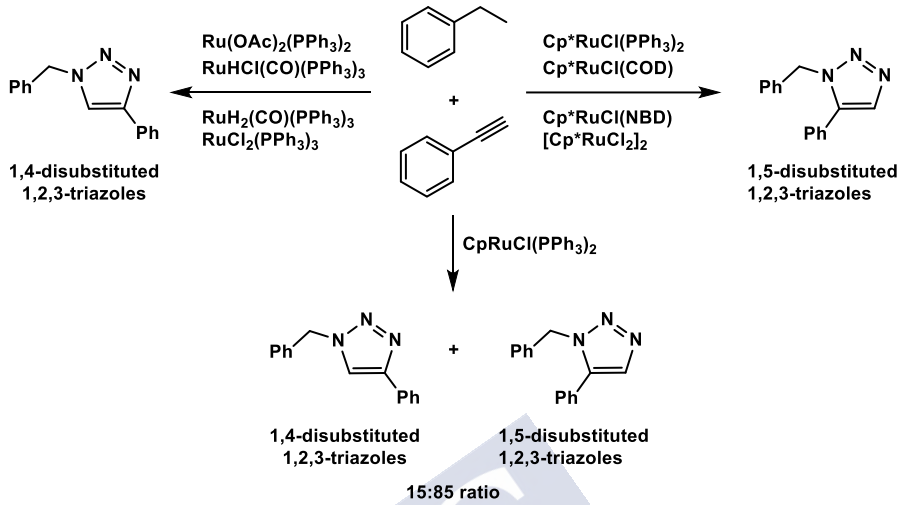


*Figure 19. Regiochemical outcome using different Ru catalysts.*[168]

## 1.6 Catalyst-free Huisgen cycloaddition reaction

While CuAAC and RuAAC were explored to overcome the regioselectivity issue and limited reaction rate of the 1,3-dipolar Huisgen cycloaddition reaction, the metal's cytotoxicity limits their applications in living systems. To enhance the cycloaddition rate without catalyst, attention has been paid to the chemical structure and electronic effects of both dipole and dipolarophile. According to the frontier molecular orbital theory (FMO), 1,3-dipole and dipolarophile overlap in symmetry-allowed $_{\pi}4_{s} + _{\pi}2_{s}$ manner, that can be achieved in three ways;[171] the dominant interaction possessing the lowest HOMO-LUMO energy gap. Azide as a dipole belongs to type II, where the energy gap in either direction is similar; i.e., HOMO of dipole overlaps with LUMO of dipolarophile evenly with opposite pathway. A dipole in this class is referred as HOMO-LUMO controlled dipole or an ambiphilic dipole. Accordingly, any substituent on the dipolarophile would accelerate the two overlapping orbitals, where EWG would lower the LUMO and EDG rise the HOMO.[172]

[171] Sustmann, R. *Pure Appl. Chem.* **1974**, *40*, 569.
[172] Huisgen, R.; Szeimies, G.; Möbius, L. *Chemische Berichte* **1967**, *100*, 2494.

In addition to running the reaction at elevated temperatures, an alternative strategy to speed up the reaction rate relies on strained cyclooctynes. The bond angle of the sp-hybridized carbons in cyclooctyne is around 160º, the triple bond is distorted toward the transition state of the cycloaddition reaction, resulting in a dramatic rate acceleration with azides.[173,174]

### 1.6.1 Strain promoted azide-alkyne cycloaddition (SPAAC)

In 1953, Blomquist and Liu[175] firstly described AAC as a benign strategy between cyclooctyne and azides that doesn't require cytotoxic metals or additives. This strain-promoted azide-alkyne cycloaddition variant, abbreviated SPAAC (Figure 20), has been recently recognized for use in biological milieu.[176,177,178,179] In addition, it has gained significance in polymer/materials science and drug delivery system, where the use of Cu is not desired.[180,181] Different attempts for rate optimization of SPAAC for faster bioconjugation under mild conditions have been described by the groups[182] of Bertozzi, Boons, and vant Hest and vant Delft by using different modified cyclooctyne structures such as diflourocyclooctyne (DIFO),[183,184]

[173] Ess, D. H.; Jones, G. O.; Houk, K. *Org. Lett* **2008**, *10*, 1633.
[174] Schoenebeck, F.; Ess, D. H.; Jones, G. O.; Houk, K. *J. Am. Chem. Soc.* **2009**, *131*, 8121.
[175] Blomquist, A.; Liu, L. H. *J. Am. Chem. Soc.* **1953**, *75*, 2153.
[176] Agard, N. J.; Prescher, J. A.; Bertozzi, C. R. *J. Am. Chem. Soc.* **2004**, *126*, 15046.
[177] Sletten, E. M.; Bertozzi, C. R. *Angew. chem., Int. Ed.* **2009**, *48*, 6974.
[178] Sletten, E. M.; Bertozzi, C. R. *Accounts of chemical research* **2011**, *44*, 666.
[179] Debets, M. F.; Van Berkel, S. S.; Dommerholt, J.; Dirks, A. J.; Rutjes, F. P.; Van Delft, F. L. *Accounts of chemical research* **2011**, *44*, 805.
[180] Debets, M. F.; van der Doelen, C. W.; Rutjes, F. P.; van Delft, F. L. *ChemBioChem* **2010**, *11*, 1168.
[181] Baskin, J. M.; Bertozzi, C. R. *ChemInform* **2011**, *42*, no.
[182] Lallana, E.; Sousa-Herves, A.; Fernandez-Trillo, F.; Riguera, R.; Fernandez-Megia, E. *Pharm. Res* **2012**, *29*, 1.
[183] Baskin, J. M.; Prescher, J. A.; Laughlin, S. T.; Agard, N. J.; Chang, P. V.; Miller, I. A.; Lo, A.; Codelli, J. A.; Bertozzi, C. R. *Proceedings of the National Academy of Sciences* **2007**, *104*, 16793.

dibenzocyclooctyne (DIBO),[185] dibenzoazacyclooctyne (DIBAC)[186] and biarylazacyclooctyne (BARAC)[187] derivatives (Figure 20). The group of Heemstra has also demonstrated that micellar catalysis can be used to accelerate the reaction of cyclooctynes with azides. Anionic and cationic surfactants provide an efficient catalysis, with reaction rate enhancements up to 179-fold for the reaction of benzyl azide as a model and DIBAC.[188]

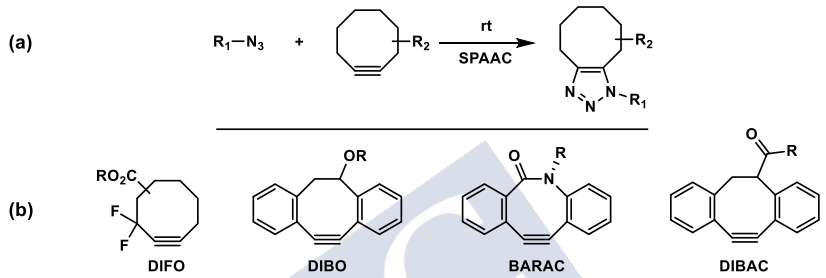


*Figure 20. SPAAC (a), and various activated cyclooctyne derivatives used in bioconjugation (b).*[182]

### 1.6.2 Thermal azide-alkyne cycloaddition (TACC)

An 1960s, Huisgen *et al.*[149,189] investigated a family of 1,3-dipolar cycloaddition reactions and elaborated a general synthetic approach for the synthesis 1,2,3-triazoles from organic azides and terminal/internal alkynes, a chemistry that has been recently revisited under the click chemistry umbrella.

---

[184] Codelli, J. A.; Baskin, J. M.; Agard, N. J.; Bertozzi, C. R. *J. Am. Chem. Soc.* **2008**, *130*, 11486.

[185] Ning, X.; Guo, J.; Wolfert, M. A.; Boons, G. J. *Angew. chem., Int. Ed.* **2008**, *47*, 2253.

[186] Debets, M. F.; Van Berkel, S. S.; Schoffelen, S.; Rutjes, F. P.; van Hest, J. C.; van Delft, F. L. *Chemical communications* **2010**, *46*, 97.

[187] Jewett, J. C.; Sletten, E. M.; Bertozzi, C. R. *J. Am. Chem. Soc.* **2010**, *132*, 3688.

[188] Anderton, G. I.; Bangerter, A. S.; Davis, T. C.; Feng, Z.; Furtak, A. J.; Larsen, J. O.; Scroggin, T. L.; Heemstra, J. M. *Bioconjugate. Chem* **2015**, *26*, 1687.

[189] Huisgen, R. *Angew. Chem., Int. Ed. Engl.* **1963**, *2*, 633.

Several attempts on the use of this metal-free chemistry for the preparation of polymers and dendrimers have been reported taking advantage of the enhanced reactivity of acetylenedicarboxylates. In 2000, Wim Dehaen *et al.*[190] reported a synthesis of dendrimers from polyazide cores (Figure 21-A) and commercial dimethyl and di-*tert*-butyl acetylenedicarboxylates, which afforded cycloadducts (G0) in excellent yield and purity. For the synthesis of higher generations G1, G2, and G3, they used a convergent approach. Firstly, G1, G2 and G3 dendrons of the acetylenedicarboxylate esters were synthesized from 2,3-dibromofumaric acid, following Mitsunobu esterification with Fréchet dendritic wedges. Then, each acetylenedicarboxylate ester G1, G2, and G3 dendron was mixed separately with two different polyazide cores (Figure 21-A) and heated at 70 $^{o}$C for several days. As a result, G1 and G2 dendrimers were successfully synthesized, while the G3 dendron failed to add to the polyazide cores, indicating that the cycloaddition reaction is sterically hindered at higher generations. Slightly improved yields of G2 with an hexaazide core (Figure 21-B) were obtained after introduction of flexible diethylene glycol spacers in the acetylene ester structure to limit steric hindrance.

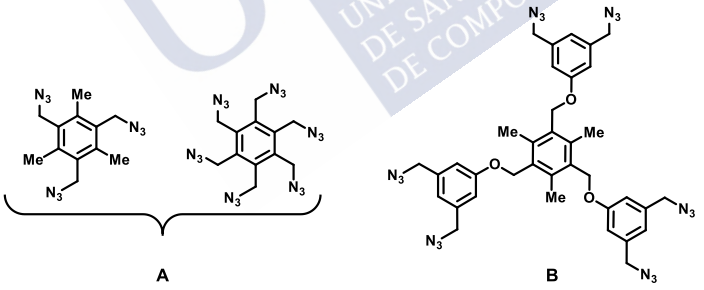


*Figure 21. Polyazide cores.*

In the polymer field, the azide-alkyne cycloaddition reaction has gained an important role for synthesizing novel polymers with appealing properties: azide end group polymers[191,192,193,194] and alkyne

[190] Van Wuytswinkel, G.; Verheyde, B.; Compernolle, F.; Toppet, S.; Dehaen, W. *J. Chem. Soc., Perkin Trans. 1.* **2000**, 1337.

[191] Tsarevsky, N. V.; Sumerlin, B. S.; Matyjaszewski, K. *Macromolecules* **2005**, *38*, 3558.

end group polymers.[191,192,199,194] In one example, Katritzky and co-workers[195] reported a set of 1,3-dipolar cycloaddition reactions of different acetylenic esters with azides for the preparation of triazole polymers. The reaction time of cycloadditions under neat conditions was significantly enhanced while heating, from days at room temperature to hours at 50-75 $^{o}$C. Also, in the same study, a three-component reaction system was tested, involving a stoichiometric azide/alkyne ratio between a triazide and two different acetylene components, with and without heating.

Multivalency is a key principle in biological systems. Cube-octameric silsesquioxanes (COSS) is a hybrid inorganic-organic nanocluster $(RSiO_{1.5})_8$. With a unique eight-fold symmetry, rigid globular architecture and biocompatibility, COSS has recently been used in biological studies by conjugation with peptides and glycosides.[196,197] One of the challenges in COSS is the requirement of full conjugation, that limits the repertoire of useful reactions. In addition to the CuAAC, the thermal version of the Huisgen 1,3-dipolar cycloaddition of organic azides and alkynes has recently gained prominent importance for the decoration of COSS. Fessner *et al*. reported conditions for the functionalization of COSS with acetylenedicarboxylate esters at 80 $^{o}$C, requiring higher temperatures for less activated internal alkynes (toluene/xylene, at 110/140 $^{o}$C respectively).[198]

Silicon (polysiloxanes) elastomers are a class of polymers that could be prepared by different two metal-catalyzed or radical cure at

---

[192] Dirks, A. T.; van Berkel, S. S.; Hatzakis, N. S.; Opsteen, J. A.; van Delft, F. L.; Cornelissen, J. J.; Rowan, A. E.; van Hest, J. C.; Rutjes, F. P.; Nolte, R. J. *Chemical communications* **2005**, 4172.

[193] Opsteen, J. A.; van Hest, J. C. *Chemical Communications* **2005**, 57.

[194] Binder, W. H.; Kluger, C. *Macromolecules* **2004**, *37*, 9321.

[195] Katritzky, A. R.; Meher, N. K.; Hanci, S.; Gyanda, R.; Tala, S. R.; Mathai, S.; Duran, R. S.; Bernard, S.; Sabri, F.; Singh, S. K. *J. Polym. Sci., Part A: Polym. Chem* **2008**, *46*, 238.

[196] Gao, Y.; Eguchi, A.; Kakehi, K.; Lee, Y. C. *Org. Lett* **2004**, *6*, 3457.

[197] Kaneshiro, T. L.; Wang, X.; Lu, Z.-R. *Mol. Pharm* **2007**, *4*, 759.

[198] Heyl, D.; Rikowski, E.; Hoffmann, R. C.; Schneider, J. J.; Fessner, W. D. *Chem.--Eur. J.* **2010**, *16*, 5544.

high temperature. All three methods exhibit some deficiencies, such as using expensive platinum and leaching of metal residues from elastomers. Thanks to the triazole ring as a stable linker between two precursors,[152,155] Brook *et al*. described the first cross-linking of azido- and alkyne-substituted polymers via thermal 1,3-dipolar cycloaddition reactions. The thermal click ligation between activated alkyne-terminated siloxanes and a polyazide occurred at a temperature ranging between 20-95 $^{o}$C. Many parameters were explored to enhance the thermal cycloadditions, including the molar ratio and solvent-free conditions. These authors showed that the thermal cycloaddition is highly dependent on the electronic properties of the alkyne, with electron-deficient alkynes reacting at lower temperature.[199]

In the same context of the crosslinking of polymers. Van Hest *et al*. have developed the first metal-free click procedure for both the synthesis and functionalization of a polymeric coating. Azide group was suggested to be used because of its improved stability compared to reactive groups such as isocyanate.[200] A stable network was formed by thermally reacting diacetylene crosslinkers with excess of azides from an azide-functionalized polymer on a glass substrate. The more reactive crosslinker that structurally includes cyclooctyne allowed the curing temperature to be dropped when terminal alkyne was used from 120 to 65 $^{o}$C.[201]

The dipolar cycloaddition of azides and alkynes under thermal conditions is expected to deliver a regioisomeric mixture of 1,4 and 1,5-disubstituted triazoles. Using symmetrical alkynes represents an easy approach to get rid of this inconvenience.[202] Alternative methods of regiodirecting TAAC rely on electronic as well as steric

[199] Gonzaga, F.; Yu, G.; Brook, M. A. *Macromolecules* **2009**, *42*, 9220.
[200] Groll, J.; Amirgoulova, E. V.; Ameringer, T.; Heyes, C. D.; Röcker, C.; Nienhaus, G. U.; Möller, M. *J. Am. Chem. Soc.* **2004**, *126*, 4234.
[201] Canalle, L. A.; van Berkel, S. S.; de Haan, L. T.; van Hest, J. C. *Adv. Funct. Mater.* **2009**, *19*, 3464.
[202] Arseneault, M.; Levesque, I.; Morin, J.-F. o. *Macromolecules* **2012**, *45*, 3687.

effects.[203,204,205,206] For instance, Jingyue Ju *et al.*[204] evaluated the reaction between ethyl 5-azidovalerate and different electron-deficient internal and terminal alkynes in water at room temperature; only the 1,4-regioisomer was produced selectively when terminal alkynes were used, which implies that the reaction was mainly controlled by steric effects. Encouraged by these results, they successfully exploited this approach to react an azido-DNA with electron-deficient alkynes.[204]

In accordance with click chemistry criteria, Morin *et al.*[202] have described the preparation of ethylene oxide dendrimers containing triazole units by means of free-metal 1,3-dipolar cycloaddition reaction (Figure 22) between terminal azide and symmetrical activated disubstituted alkyne (acetylenedicarboxylate ester).[190] In another example, Zhang and Guo[207] reported the use of TAAC as cross-linking reaction for styrenic polymer dielectric layers between an azide-containing styrenic polymer and alkyne-containing styrenic polymer. The group of Tang has also described a sequential azidation/metal-free 1,3-dipolar cycloaddition reaction for the synthesis of polymers at 100 $^{o}$C with regioregularities ($F_{1,4}$ up to 92% in high yield 98%), without restrictions regard atmospheric oxygen and moisture.[208,209]

With the aim of establishing an efficient and highly regioselective TAAC for 1,2,3-triazoles, the group of Schubert and coworkers[205] has reported that a high 1,5-adduct can be obtained by using alkyne trimethylsilyl moieties, supporting the strategy of electron-donating alkyne substituents.

---

[203] Hlasta, D. J.; Ackerman, J. H. *J. Org. Chem.* **1994**, *59*, 6184.
[204] Li, Z.; Seo, T. S.; Ju, J. *Tetrahedron Lett* **2004**, *45*, 3143.
[205] Kloss, F.; Köhn, U.; Jahn, B. O.; Hager, M. D.; Görls, H.; Schubert, U. S. *Chemistry–An Asian Journal* **2011**, *6*, 2816.
[206] Miners, S. A.; Fay, M. W.; Baldoni, M.; Besley, E.; Khlobystov, A. N.; Rance, G. A. *J. Phys. Chem* **2019**, *123*, 6294.
[207] Li, S.-X.; Feng, L.-R.; Guo, X.-J.; Zhang, Q. *Journal of Materials Chemistry C* **2014**, *2*, 3517.
[208] Qin, A.; Jim, C. K.; Lu, W.; Lam, J. W.; Häussler, M.; Dong, Y.; Sung, H. H.; Williams, I. D.; Wong, G. K.; Tang, B. Z. *Macromolecules* **2007**, *40*, 2308.
[209] Li, H.; Wang, J.; Sun, J. Z.; Hu, R.; Qin, A.; Tang, B. Z. *Polym. Chem.* **2012**, *3*, 1075.

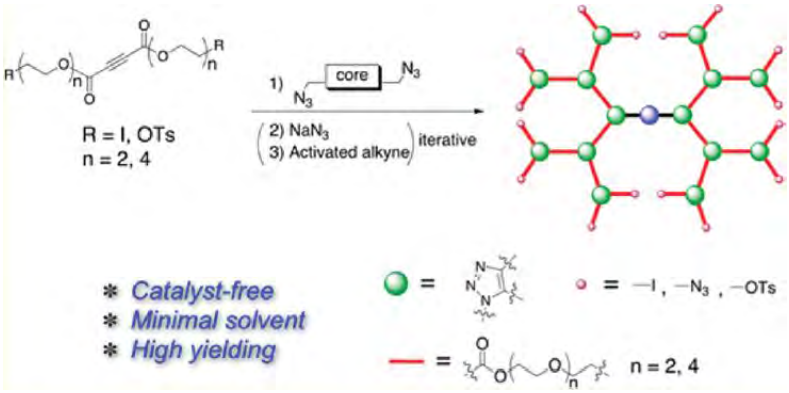


*Figure 22. schematic preparation of ethylene oxide dendrimers containing triazole units.*[202]

# 2 Objectives

The aim of this thesis is to develop a method to functionalize azide-terminated GATG dendrimers with a set of different functional groups/ligands under metal-free AAC conditions. The following objectives have been set to fulfil this aim.

The **first objective** is focused on the scaling up the preparation of symmetrical 2G and 3G GATG dendrimers, with a higher number of terminal azides compared with the previously developed families by our group.

The **second objective** is to develop reliable and efficient conditions for the synthesis of functionalized alkynes that being thermally stable and not readily hydrolyzed, could carry different ligands/functional groups of biological interest to be used in the decoration of azide-terminated GATG dendrimers.

The **third objective** of this doctoral thesis is to develop efficient conditions for the functionalization of 2G and 3G GATG dendrimers with a wide array of functional groups and ligands through a thermal azide-alkyne cycloaddition (TAAC) reaction with the alkynes develop in the second objective. The final aim is obtaining functional dendritic tools for nanotechnology and the biomedical field.

USC
UNIVERSIDADE
DE SANTIAGO
DE COMPOSTELA

# 3 Results and Discussion

## 3.1 GATG Dendrimers synthesis and characterization

Different core structures are typically used in dendrimer preparation, mostly planar or linear molecules such as ammonia, lactic acid, succinic acid, adipic acid, ethylene glycol, ethylenediamine, 1,4-diamino butane and benzene derivatives, or three-dimensional structure such as adamantane.[25,210,211,212,213,214] Aware of this fact, with a reliable synthesis of the GATG repeating unit in hand,[124,125] two different families of symmetrical GATG dendrimers that are abbreviated as 2[Gn] and 3[Gn] were synthesized by Dr. Sandra P. Amaral in our group,[140] using di- and trivalent cores, following a divergent method involving an iterative sequence of growing step represented by amide coupling with the GATG repeating unit (EDC, HOBt, 91-96%), and activation step accomplished by reduction of the terminal azides ($Ph_3P$, 90-100%), to successfully obtain four generations for each family (Scheme 4).

[210] Carnahan, M. A.; Grinstaff, M. W. *J. Am. Chem. Soc.* **2001**, *123*, 2905.
[211] Carnahan, M. A.; Grinstaff, M. W. *Macromolecules* **2001**, *34*, 7648.
[212] Carnahan, M. A.; Grinstaff, M. W. *Macromolecules* **2006**, *39*, 609.
[213] Tang, S.; Martinez, L. J.; Sharma, A.; Chai, M. *Org. Lett* **2006**, *8*, 4421.
[214] Akiyama, H.; Miyashita, K.; Hari, Y.; Obika, S.; Imanishi, T. *Tetrahedron* **2013**, *69*, 6810.

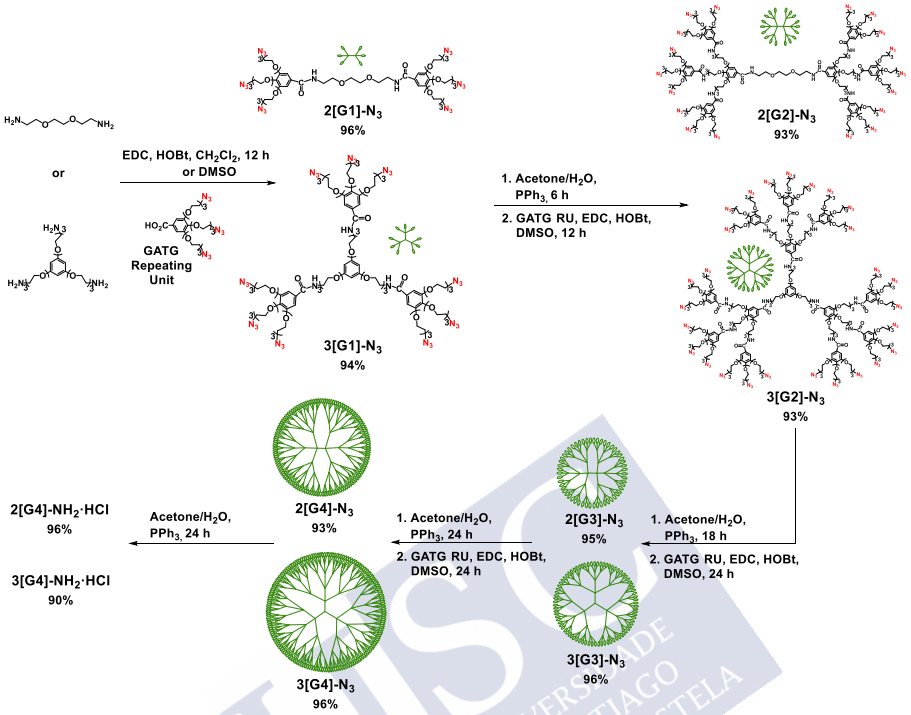


*Scheme 4. Synthesis of 2[Gn] and 3[Gn] GATG dendrimers.*[140]

The construction of the 2G family began with commercially available linear 2,2`-(ethylenedioxy)bis(ethylamine), to obtain the dendrimer generations in excellent yields with up to 162 terminals azide/amino groups: 2[G1] (6 terminal groups), 2[G2] (18), 2[G3] (54) and 2[G4] (162).

The amide coupling reactions towards 2[G1], 2[G3] and 2[G4] proceeded smoothly, while synthesis of the second generation 2[G2] sometimes resulted in low yield (< 30-40%). Despite of this, it was enough to keep running the production of dendrimers and subsequent experiments. However, as higher amounts of dendrimers were required, it became obvious to improve the synthesis of 2[G2]. To this end, we started evaluating different reaction conditions towards this dendrimer (Table 2). In addition, during the scaling up of this sequence, reaction and purification conditions had to be adapted to maintain the high reaction yields and recoveries typically found in

small scale. In the next paragraphs an optimization of these procedures is described.

*Table 2. Optimized conditions for the synthesis of 2[G2] dendrimer.*

| Trial No | Solvent | T (ºC) | $Et_3N$ eq | % yield |
|---|---|---|---|---|
| 1 | $CH_2Cl_2$ | rt | 2 | 40 |
| 2 | $CH_3CN$ | rt | 2 | 40 |
| | | | 3 | 40 |
| 3 | $CH_3CN$ | 60 | 2 | 45 |
| | | | 3 | 45 |
| 4 | DMSO | rt | 3 | 91 |

First attempts to increase the reproducibility of the 2[G2] synthesis were oriented to change the solvent from $CH_2Cl_2$ to MeCN, while heating from rt up to 60 ºC. Unfortunately, no enhancement of the yield of pure product was observed, even after increasing the number of $Et_3N$ equivalents. When DMSO was used instead as alternative solvent at rt, the reaction proceeded smoothly, affording pure 2[G2] in 91% after completely removing DMSO solvent from the crude product by aqueous extraction with $H_2O$/EtOAc. Under these conditions, scaling up the preparation of the 2G GATG dendritic family was successfully performed to hundreds of milligrams (> 600 mg).

The first two generations 2[G1] and 2[G2] were purified with MPLC flash chromatography, while the next two generations 2[G3] and 2[G4] were purified successfully by ultrafiltration. While chromatography is also possible for 2[G3] and 2[G4], ultrafiltration resulted more convenient since no work-up of the reaction is required and any loss of material due to sticking to the stationary phase is avoided. Ultrafiltration was unsuitable for purification of the first two generations. When Amicon YM1 membrane was used, both GATG repeating unit and the dendrimers were retained inside the ultrafiltration device, while in case of Amicon YM3, both GATG repeating unit and the dendrimers were released from the system.

As for the 3G GATG family, the preparation started from a synthetic core, namely 3[G0]-$NH_2$ (Scheme 5). Getting this core in high purity represented the only challenge in the synthesis of these dendrimers. The initial route of our group relied on the chloride as a leaving group in 1-azido-2-[2-(2-chloroethoxy)ethoxy]ethane[125] (Scheme 5 first route), which after several purification cycles by MPLC with silica allowed to obtain the core in 76% yield. In a modified route, chloride was replaced by tosylate as a leaving group (Scheme 5, modified route), affording a crude product that after a single MPLC in neutral alumina led to pure 3[G0]-$NH_2$ in 85% yield.

With a trustworthy synthesis of the 3G GATG core in hand, four generations of 3G dendrimers were successfully prepared while scaling up, in high yields (93-96%), and with up to 243 terminals azide/amino groups 3[G1] (9 terminal groups), 3[G2] (27), 3[G3] (81) and 3[G4] (243).[140] Similarly to the 2[Gn] family, 3[Gn] dendrimers were purified by MPLC in 10-15 min, with the possibility of ultrafiltration for 3[G3] and 3[G4], which is the best option due to the advantages of ultrafiltration over chromatography.

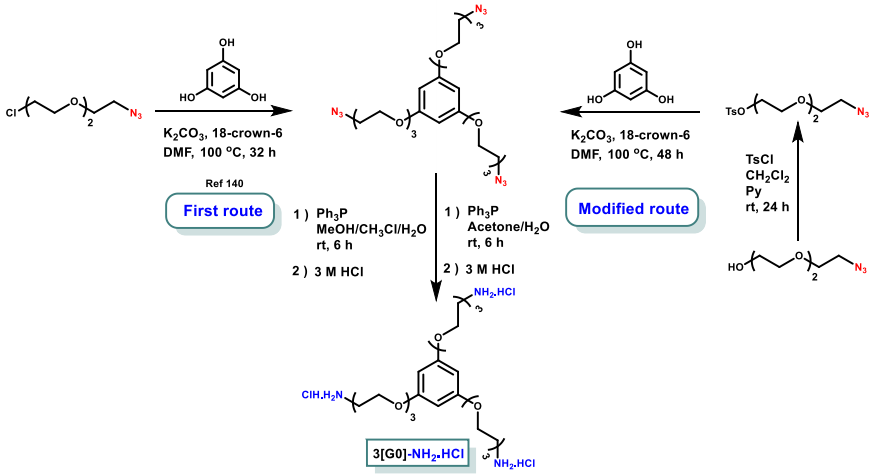


*Scheme 5. Preparation routes of the 3G GATG family core: 3[G0]-$NH_2$·HCl.*

The spectral data of 2[Gn] and 3[Gn] families matched well those previously reported.[140] The completion of both synthetic steps for all generations of both families were monitored easily by $^1$H NMR,

according to the appearance-disappearance of the characteristic signals of the methylene protons that are adjacent to the azide group at 3.4 ppm, and appearance-disappearance of the characteristic signals of the methylene protons that are adjacent to the ammonium group at 3.2 ppm (Figure 23-a). IR confirmed the complete reduction of dendrimer azides to amines by disappearance of the intense signal of azide at around 2100 $cm^{-1}$ (Figure 23-b).

Purity, monodispersity and successful growing steps were confirmed by GPC (Figure 24) in accordance to the difference in the retention time of particular dendrimer generation, and also DLS (Figure 25) that displayed the expected size increase with generations growth. Table 3 shows characteristic data related to the dendrimers such as the hydrodynamic values of [Gn]-$NH_2$·HCl, and Z-potentials.

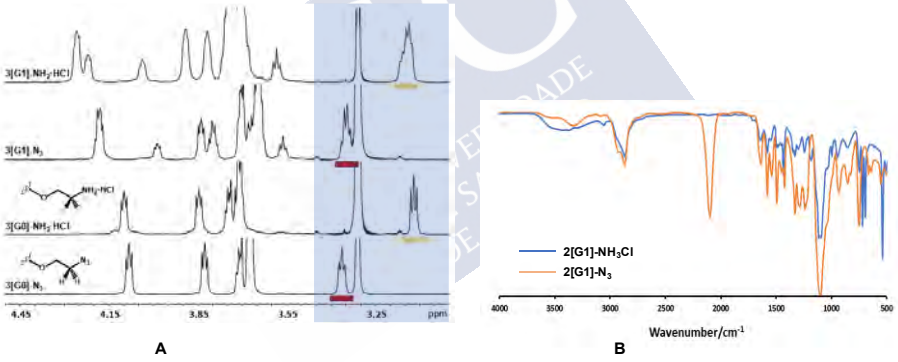


*Figure 23. (A). Monitoring of dendrimer growth by $^1H$ NMR ($CD_3OD$, 300 MHz, 25 $^oC$). (B). Monitoring the efficiency of the azide reduction by IR (disappearance of the azide peak at ca. 2100 $cm^{-1}$)*

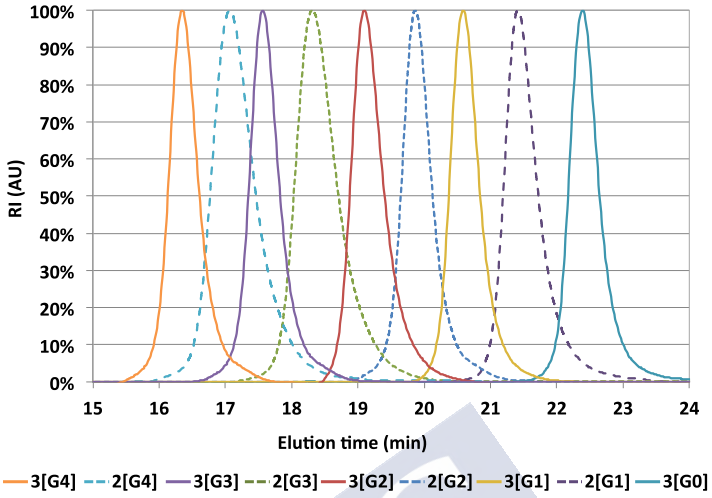


*Figure 24. Normalized GPC elugrams of 2[Gn]-$N_3$ and 3[Gn]-$N_3$ (THF).*

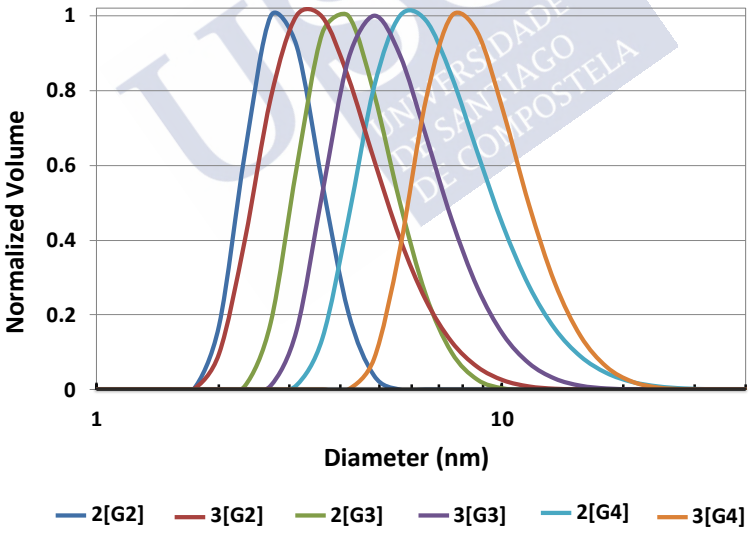


*Figure 25. DLS size distribution of [Gn]-$NH_2$·HCl [1.5 mg/mL in 10 mM $NaH_2PO_4$, 0.1 M HCl (10% v/v)].*

*Table 3. Dendrimers characterization data.*

| dendrimer Family | G | Terminal groups | MW (g/mol)[a] | Z-potential (mV)[b] | Hydrodynamic Diameter (nm)[c] |
|---|---|---|---|---|---|
| 2[Gn]-$NH_2$·HCl | 1 | 6 | 1394 | ..... | ..... |
| | 2 | 18 | 4978 | 35 | 3.01 |
| | 3 | 54 | 15729 | 43 | 4.45 |
| | 4 | 162 | 48012 | 57 | 7.45 |
| 3[Gn]-$NH_2$·HCl | 1 | 9 | 2389 | ..... | ..... |
| | 2 | 27 | 7765 | 40 | 3.62 |
| | 3 | 81 | 23891 | 54 | 5.68 |
| | 4 | 243 | 74855 | 61 | 8.82 |

[a] Theoretical molecular weight of [Gn]-$NH_2$·HCl.

[b] [Gn]-$NH_2$·HCl (0.5mg/mL in 10 mM $NaH_2PO_4$, 10mM NaCl).

[c] DLS: [Gn]$NH_2$·HCl [1.5mg/mL in 10 mM $NaH_2PO_4$, 0.1 M HCl (10% v/v)].

## 3.2 Functionalized alkynes synthesis

### 3.2.1 Overview

The second objective of this thesis is to develop reliable and efficient conditions for the synthesis of functionalized alkynes that being thermally stable and not readily hydrolyzed, could carry different ligands/functional groups of biological interest to be used in the decoration of azide-terminated GATG dendrimers. Among the possible ligands/functional groups we focused our attention into solubilizing groups (such alcohols), anionic and cationic groups for application in the preparation of polyelectrolyte complexes and PIC assembles (sulfates and ammonium), phenol and catechol with interest in the preparation of polyphenols, ligands of biological relevance (such as glucose, mannose and biotin), fluorophores (FITC) and metal complexing agents (DOTA) with interest as contrast agents in diagnosis (MRI, PET and SPECT) and radiotherapy.

The selection of internal alkynes was proposed to get a regiospecific product when reacted under thermal AAC conditions, rather than regioselective isomers. In addition, this strategy allows to duplicate the number of peripheral groups, which in turn enhances the functionality of the dendritic structure.

Internal alkynes bearing electron-deficient groups should be used in order to conduct metal-free click chemistry.[152] Alkynes activated by ester groups were investigated,[202,215,216] but their easy hydrolysis represents a drawback that inspired us to think on the use of a different electron-deficient group that combines easy purifications, high yielding reactions, thermal stability and lack of hydrolysis. The alternative proposed involved replacing the ester with a carbamate group as seen in Figure 26.

---

[215] Gonzaga, F.; Sadowski, L. P.; Rambarran, T.; Grande, J.; Adronov, A.; Brook, M. A. *J. Polym. Sci., Part A: Polym. Chem* **2013**, *51*, 1272.

[216] Arseneault, M.; Leung, N. L.; Fung, L. T.; Hu, R.; Morin, J.-F.; Tang, B. Z. *Polym. Chem.* **2014**, *5*, 6087.

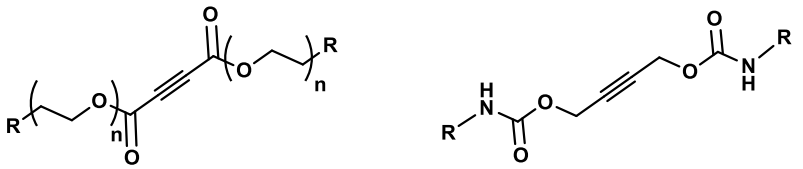

*Figure 26. Alkyne with ester group (left) and carbamate group (right).*

Accordingly, alkynes double activated by carbamate groups were synthesized as dipolarophiles for TAAC reactions. As seen in the retrosynthetic Scheme 6, functionalized alkynes were obtained by nucleophilic substitution following reaction of 2-butyne-1,4-diol with N, N`-disuccinimidyl carbonate (DSC). The intermediate activated Alk-NHS product carrying a good leaving group (NHS) reacts with a variety of amino-functionalized ligands to afford the desired functionalized alkynes shown in (Scheme 7).

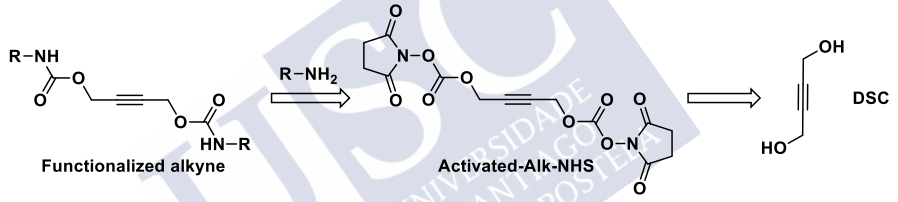


*Scheme 6. Retrosynthesis of functionalized alkyne with carbamate group.*

The alkynes functionalized with electron deficient carbamate groups have a characteristic $^{1}H$ NMR signature. Propargyl protons in the activated Alk-NHS lie around 5.21 ppm, which are shifted to 4.70 ppm in the functionalized alkynes (Figure 27). Moreover, the disappearance of the proton signal of NHS at around 2.81 ppm confirmed the purity of the product and the completion of the reaction (Figure 27). $^{13}C$ NMR was also useful as a tool to confirm the completion of the reactions and purity of the functionalized alkynes thanks to the disappearance of two NHS specific signals at ca 170.0 ppm and 25.4 ppm, as well as the shifting of two signals at ca 151.0 and 58.0 ppm to ca 155.5 and 52.5 ppm, respectively (Figure 28). In the IR spectrum of the activated Alk-NHS, there are no bands near 3500-3300 $cm^{-1}$ of NH-bond stretching that appear in the case of activated alkynes, providing further evidence of successful coupling.

For IR and $^{1}H$ and $^{13}C$ NMR spectra of each product, see the experimental part.

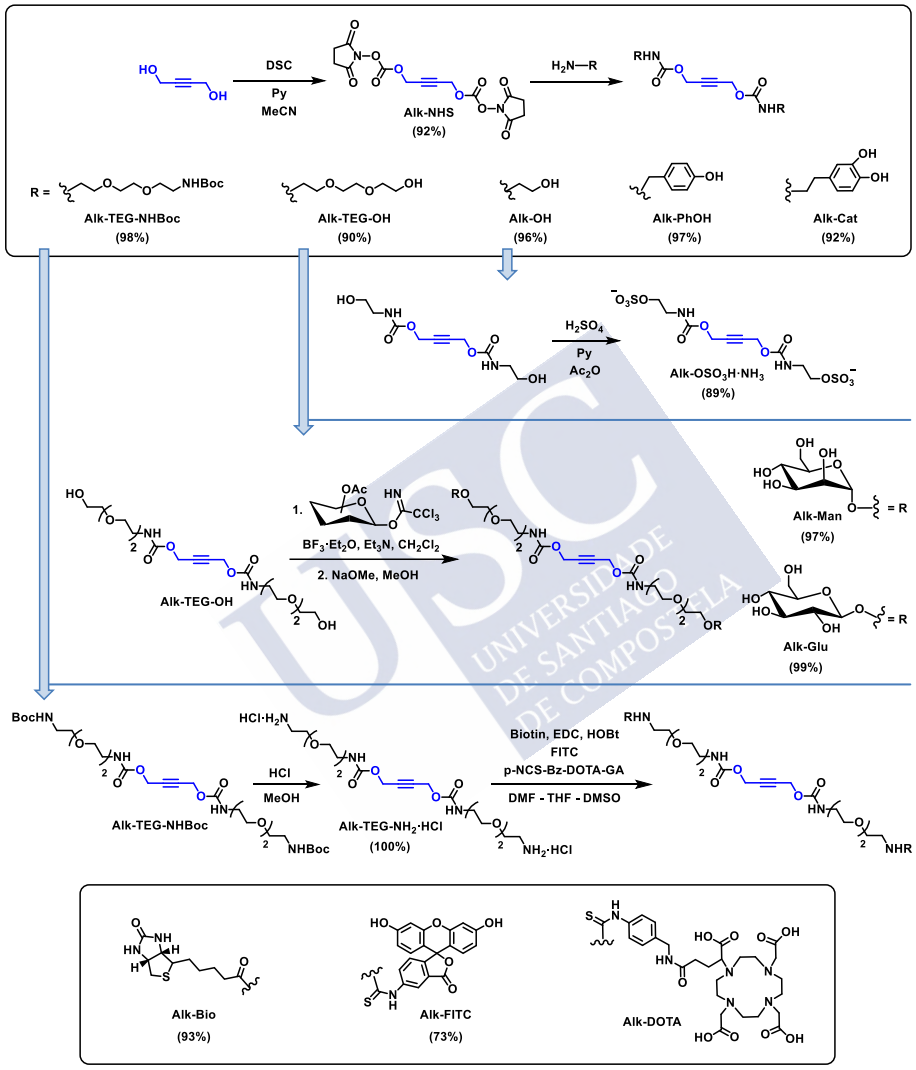


*Scheme 7. Synthesis of functionalized alkynes*

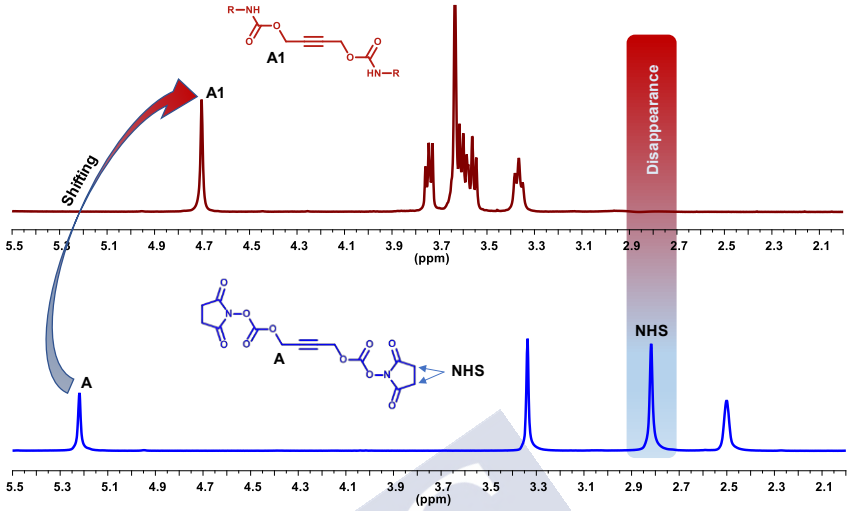


*Figure 27. $^{1}H$ NMR conversion in the synthesis of functionalized alkynes. Spectra of Alk-NHS (blue) and a functionalized alkyne Alk-TEG-OH (red).*

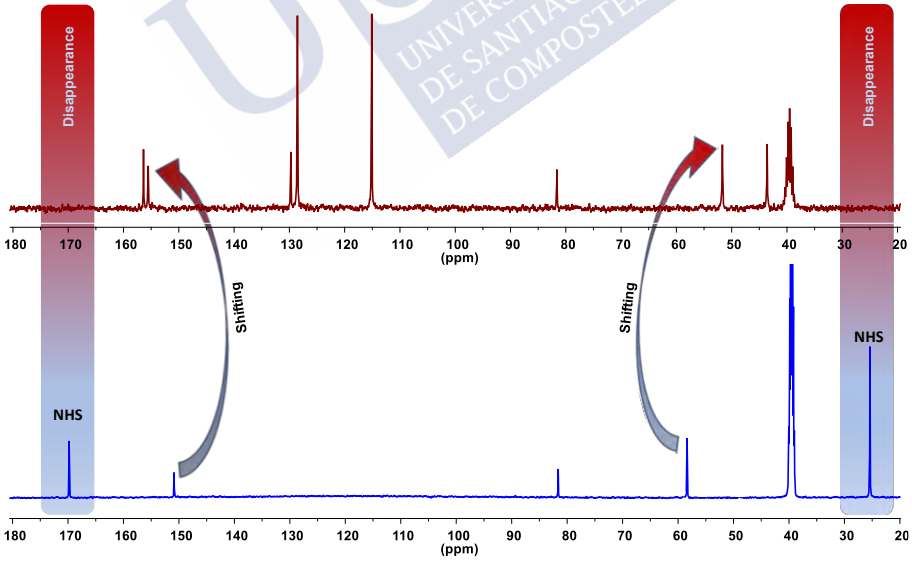


*Figure 28. $^{13}C$ NMR conversion in the synthesis of functionalized alkynes. Spectra of Alk-NHS (blue) and a functionalized alkyne Alk-PhOH (red).*

Activated Alk-NHS is highly soluble in polar organic solvents like DMSO, DMF, MeOH and MeCN. Reactions with the amino reagents were run using a good solvent for both reactants and product. Since alcohols are weaker nucleophiles than amines, in order to avoid any competition reaction with amine nucleophile, MeOH was excluded. As a result, MeCN was the solvent of choice because of its higher volatility, followed by DMF and DMSO.

### 3.2.2 Activated Alk-NHS synthesis

The first step in the synthesis of the functionalized alkynes was the preparation of the starting activated Alk-NHS.[217] DSC is used to activate 2-butyne-1,4-diol (Scheme 7), where the OH groups of diol attacks in a nucleophilic substitution reaction the carbonyl group of the DSC in the presence of pyridine as catalyst (Figure 29). The reaction mixture was purified by aqueous workup to remove pyridine, NHS byproduct, and excess of DSC. Using DSC in excess avoids the formation of dimers, trimers or higher polymers. The activated Alk-NHS product was obtained in excellent yield (92%). It was characterized by $^{1}$H NMR, $^{13}$C NMR, IR and ESI-MS, and the spectral data matched well those previously reported.[217]

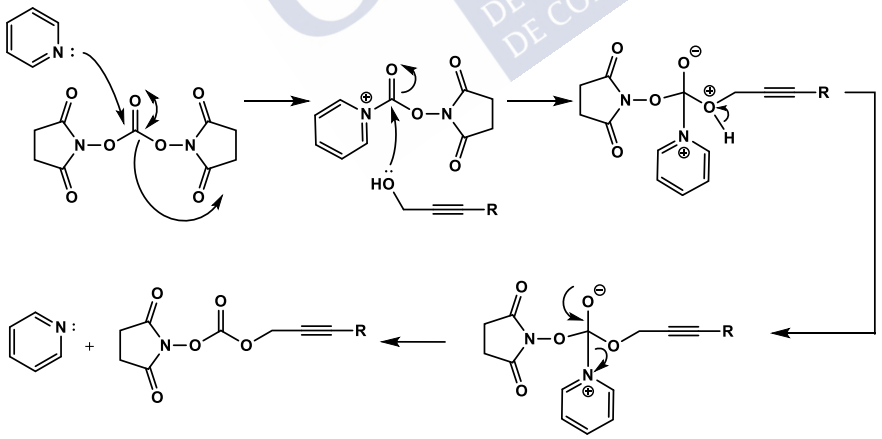

*Figure 29. Mechanism of Alk-NHS formation.*

[217] Fujimoto, K.; Oimoto, N.; Katsuno, K.; Inouye, M. *Chem. Commun. (Cambridge, U. K.)* **2004**, 1280.

In the second step, activated Alk-NHS reacts with a set of amino ligands (Figure 30) to produce functionalized alkynes with different peripheral groups (R': alcohol, phenol, anionic, cationic, chromophore, biotic and chelating) (Scheme 7). Considering, the presence of OH groups in the amino moiety, these reagents aren't considered a nucleophilic rival to the amine nucleophilicity. Starting from the activated Alk-NHS a wide range of functionalized alkynes with different peripheral functional groups have been prepared (Scheme 7)

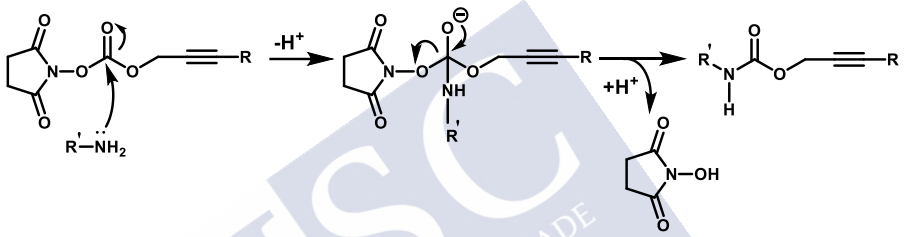

*Figure 30. Mechanism of the reaction of amines with activated Alk-NHS.*

### 3.2.3 Alk-TEG-NHBoc synthesis

The t-butoxycarbonyl (Boc) group is deemed as one of the most common amine protecting groups.[218] With the aim of avoiding polymerization of the amino moiety reagent, monoprotected tris(ethylene glycol)-diamine linker was prepared first (Scheme 8),[219] and its spectral data matched well those previously reported. $^{1}$H NMR confirmed the purity of the monoprotected tris(ethylene glycol)-diamine by appearance of the Boc group signal at 1.44 ppm, and the methylene protons alpha to the amine and carbamate at 2.83 ppm and 3.30 ppm, respectively. $^{13}$C NMR also confirmed the appearance of the Boc group signal at 28.5 ppm (Figure 31).

[218] Wang, J.; Liang, Y.-L.; Qu, J. *Chemical communications* **2009**, 5144.

[219] Sigal, G. B.; Mammen, M.; Dahmann, G.; Whitesides, G. M. *J. Am. Chem. Soc.* **1996**, *118*, 3789.

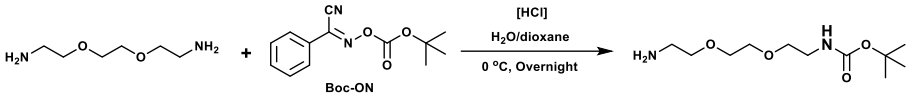


*Scheme 8. Monoprotected tris(ethylene glycol)-diamine.*

A coupling reaction between this monoprotected diamine and Alk-NHS ($Et_3N$, MeCN) led to the protected amine derivative Alk-TEG-NHBoc in an excellent yield of 98% (Scheme 7). This product was characterized by $^1$H NMR, $^{13}$C NMR, IR and elemental analysis.

The completion of the reaction was confirmed by following the specific protons signals by $^1$H NMR: disappearance of alpha amine protons at 2.83 ppm and appearance at 3.39 ppm, also the disappearance of characteristic NHS signal at 2.81 ppm, and shifting the protons signal of activated Alk-NHS at around 5.21 ppm to appear in the product at around 4.70 ppm. Further confirmation was achieved by the disappearance of the characteristic $^{13}$C NMR signals of NHS at ca 170.0 ppm and ca 25.4 ppm.

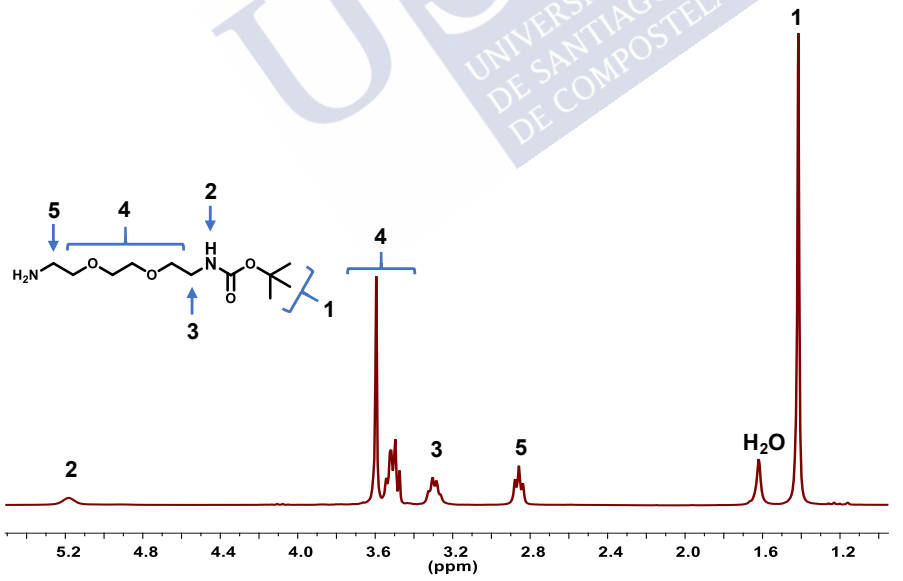


*Figure 31. $^1$NMR spectrum (300 MHz, $CDCl_3$) of tris(ethylene glycol)-diamine linker*

### 3.2.4 Alk-TEG-OH synthesis

The preparation of Alk-TEG-OH required two synthetic steps before conjugation to Alk-NHS. The first one involved preparation of 2-(2-(2-azidoethoxy)ethoxy)ethan-1-ol in quantitative yield ($NaN_3$, $H_2O$) as previously reported by our group[143] (Scheme 9). The spectral data matched well those previously reported, particularly, the replacement of chloride by the azide was confirmed by the appearance of specific $^1$H NMR signal at chemical shift 3.40 ppm which refers to protons of the methylene linked directly to the azide group. In addition, appearance of a strong stretching band of azide at ca 2100 $cm^{-1}$ was observed in the IR spectrum.

Reduction of azide to amine was done by hydrogenation with Pd-C as catalyst, following a reported protocol,[220] to produce 2-(2-(2-aminoethoxy)ethoxy)ethan-1-ol in quantitative yield (Scheme 9). The complete conversion was clearly seen in the IR spectrum by disappearance of the azide band at ca 2100 $cm^{-1}$, and the appearance of two strong bands near 3500-3300 $cm^{-1}$ due to -$NH_2$ stretching (due to primary amine).

Once 2-(2-(2-aminoethoxy)ethoxy)ethan-1-ol was in hand, coupling with activated Alk-NHS was carried out to produce Alk-TEG-OH in excellent yield (90%) (Scheme 7). Because of the high water solubility of (2-(2-(2-aminoethoxy)ethoxy)ethan-1-ol) in excess and the products (Alk-TEG-OH and NHS), aqueous workup was discouraged as purification method. Silica chromatography was used instead (DCM to MeOH 10% in silica), to obtain Alk-TEG-OH in 90% yield. Alk-TEG-OH was characterized by $^1$H NMR, $^{13}$C NMR, IR and ESI-MS. Completion of the reaction and product purity were confirmed by $^1$H NMR by disappearance of the NHS signal at around 2.81 ppm, appearance of TEG signals in the range 3.76-3.73 ppm, in addition to the aforementioned shift of the propargyl proton signal from around 5.21 ppm in activated Alk-NHS to 4.70 ppm in the new product Alk-TEG-OH.

[220] Heller, K.; Ochtrop, P.; Albers, M. F.; Zauner, F. B.; Itzen, A.; Hedberg, C. *Angew Chem Int Ed Engl* **2015**, *54*, 10327.

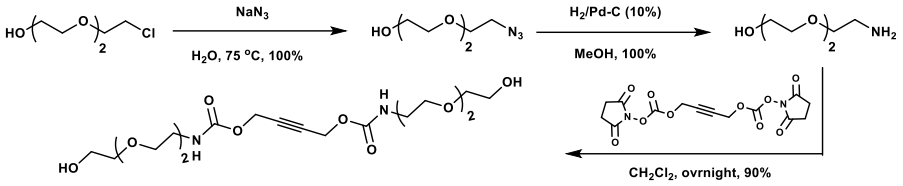


*Scheme 9. Preparation of Alk-TEG-OH.*

### 3.2.5 Alk-OH synthesis

Following a similar protocol, reaction of ethanolamine with Alk-NHS in dry MeCN afforded after just 4 h Alk-OH in excellent 96% yield after purification by chromatography. This product was fully characterized by $^{1}$H NMR, $^{13}$C NMR, IR and elemental analysis, which all confirmed the purity of the product. In the $^{1}$H NMR spectrum, the disappearance of NHS signals at 2.81 ppm was observed, along with a shifting of the propargyl protons from 5.21 ppm to 4.70 ppm. Also, $^{13}$C NMR showed the disappearance of NHS signals at 170.0 ppm and 25.4 ppm, in addition to a shifting of the signals at 150.0 ppm and 58.0 ppm to 155.5 ppm and 52.5 ppm.

### 3.2.6 Alk-PhOH synthesis

Polyphenols are a category of natural products with a number of phenolic structural units,[221] an aromatic ring bearing one or more OH groups.[222] Recently, polyphenols have gained importance because of their potential to prevent cellular damage.[223] Also, antioxidant activity is one of the most important features of phenolic compounds.[224] Phenol and catechol are the simplest structures of polyphenols that are used in a vast range of applications. Because of this growing interest, we proposed to synthesize two functionalized alkynes carrying phenol and catechol groups.

Following the same chemistry as for the synthesis of the above functionalized alkynes, commercial 4-hydroxybenzylamine was proposed to react with Alk-NHS to obtain Alk-PhOH carrying phenol groups. Thanks to the insolubility of the product in aqueous phase, $Et_3N$ and excess of 4-hydroxybenzylamine were removed easily by washing with 0.5 M HCl. Alk-PhOH was obtained with an excellent yield of 96%. In addition to elemental analysis, purity confirmation was gained by $^1H$ NMR by disappearance of the NHS signals at 2.81 ppm, shifting of the propargyl protons from 5.21 ppm to 4.70 ppm, and appearance of specific aromatic signals at 7.04 and 6.69 ppm.$^{13}C$ NMR also confirmed the purity by disappearance of the specific NHS carbons at 170.0 ppm and 25.4 ppm, and appearance of new signals that matched well aromatic carbons at around 155.5, 129.7, 128.5 and 115.1 ppm.

[221] Lima, G. P. P.; Vianello, F.; Corrêa, C. R.; Campos, R. A. d. S.; Borguini, M. G. *Food and Nutrition sciences* **2014**, 1065.
[222] Ozcan, T.; Akpinar-Bayizit, A.; Yilmaz-Ersan, L.; Delikanli, B. *Int. J. Chem. Eng. Appl.* **2014**, *5*, 393.
[223] Hasegawa, U.; Moriyama, M.; Uyama, H.; van der Vlies, A. J. *Polymer* **2015**, *66*, 1.
[224] Michalak, A. *Pol. J. Environ. Stud* **2006**, *15*.

### 3.2.7 Alk-Cat

Similar to phenol, catechol is one of the most common structural motifs in natural polyphenols, which inspired us to synthesize a functionalized alkyne with catechol groups. The synthesis started by dissolving dopamine hydrochloride and $Et_3N$ in dry MeCN. After complete dissolution, Alk-NHS was added. Unfortunately, both TLC and NMR confirmed uncomplete reaction, even after long reaction times and heating. By replacing MeCN as solvent with DMF, the reaction was successfully completed in 24 h. After aqueous work-up and purification by column chromatography, the product was obtained in an excellent 92% yield. $^1$H NMR spectroscopy, $^{13}$C NMR and FT-IR measurements were employed to demonstrate the successful synthesis and purity of the product. In addition to the disappearance of the $^1$H NMR signal of NHS at 2.81 ppm and shifting the propargyl protons from 5.21 ppm to 4.65 ppm, appearance of specific aromatic multiplet protons signals at 6.71-6.56 ppm confirmed the identity of Alk-Cat. Also, $^{13}$C NMR was a complementary characterization tool confirming the purity of the product by disappearance of the NHS signals at 170.0 ppm and 25.4 ppm, and the appearance of aromatic signals at around 145.6, 144.1, 121.7, 117.0, 116.5 ppm. These results were confirmed by elemental analysis that matched well the expected values.

### 3.2.8 Alk-$OSO_3H{\cdot}NH_3$ synthesis

Several attempts were made to get an anionic activated alkyne of the type Alk-$OSO_3^-$. The initial proposal was to sulfonate a phenolic or alcoholic moiety present in a previously prepared alkyne. Starting with Alk-PhOH, several trials were run using $ClSO_3H$, Py and $SO_3Py$, Py in different solvents (DCM, THF, DMF) at different temperatures. Unfortunately, the reaction didn't proceed well according to TLC monitoring. Similar results were obtained using Alk-OH as starting material. Gratifyingly, using $H_2SO_4$, $Ac_2O$, Py as sulfonation reagent,[225] the reaction was completed with Alk-OH after 16 h. After

[225] Bureeva, S.; Andia-Pravdivy, J.; Petrov, G.; Igumnov, M.; Romanov, S.; Kolesnikova, E.; Kaplun, A.; Kozlov, L. *Bioorg Med Chem* **2005**, *13*, 1045.

purification by sublimation at 40 ºC, 0.1 mm Hg, Alk-$OSO_3^-$ was obtained in 89% yield.

$^1$H NMR confirmed the reaction completion by the shift of the characteristic signals of Alk-OH from 3.60 and 3.24 ppm to 4.04 and 3.40 ppm of Alk-$OSO_3^-$ (Figure 32). $^{13}$C NMR supported reaction completion according to a shift of the methylene carbon alpha to the hydroxyl from 60.6 to 69.3 ppm. In addition to the $^1$H NMR and $^{13}$C NMR, purity was further confirmed by elemental analysis.

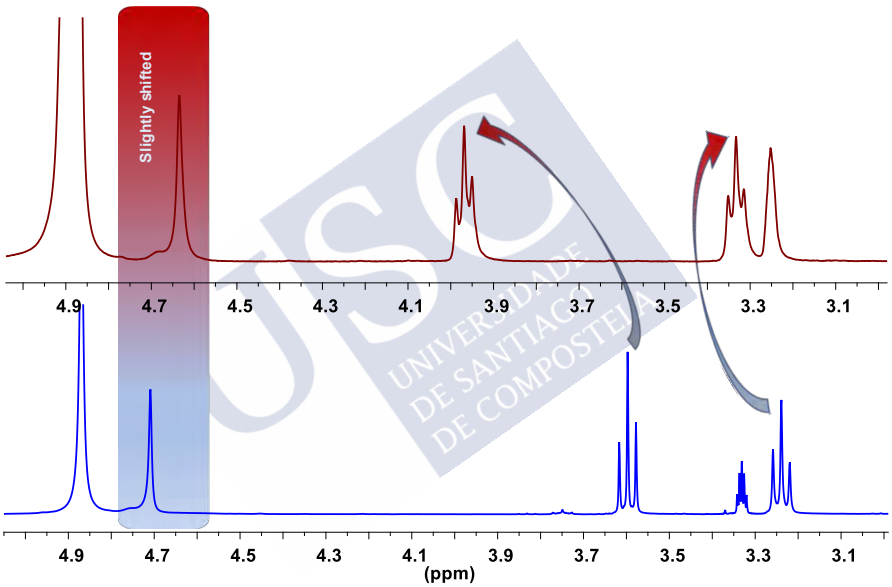


*Figure 32. $^1$H NMR conversion of Alk-OH (blue) to Alk-$OSO_3H{\cdot}NH_3$ (red).*

### 3.2.9 Alk-Man and Alk-Glu synthesis

Carbohydrates and glycoconjugates are the most abundant biomolecules on earth.[226] They play a significant role in many biological processes, such as molecular recognition.[227] For instance,

[226] Das, R.; Mukhopadhyay, B. *ChemistryOpen* **2016**, *5*, 401.
[227] Hu, Y.; Tabor, R. F.; Wilkinson, B. L. *Org. Biomol. Chem.* **2015**, *13*, 2216.

bacteria strongly bind to glycopolymers,[228] making carbohydrates highly active reagents for bacteria sequestration through carbohydrate-lectin binding.[229,230]

Glycosylation is a synthetic process that involves a coupling of two reagents, which are termed glycosyl donor and glycosyl acceptor. It takes place at the anomeric position of a donor (C1-OH) to form a glycoside.[231] When the acceptor is a saccharide, the glycoside is termed oligosaccharide. The donor in glycosylation is the electrophile, therefore, the reactive groups (nucleophiles) that are available on the donor must be protected to avoid self-coupling. The acceptor molecule is the nucleophile, so if contains extra nucleophilic groups, they must be protected. The stereochemistry and yield of glycosylation reactions are influenced by the Lewis acid catalyst used,[232,233] and the protecting groups on acceptor[234] and donor building blocks.[232,233] In addition, yield is significantly affected by applying the normal (NPr) or inverse procedure (IPr).[231] As a result, glycosylation is a cumbersome process.

With the objective of preparing carbohydrate functionalized alkynes, D-mannose and D-glucose were selected as monosaccharides. Tetraacetate mannose trichloroacetimidate was synthesized from D-mannose in a three-step process (Scheme 10), while tetraacetate glucose-trichloroacetimidate was synthesized from D-glucose pentaacetate in two steps (Scheme 11).[235,236,237] Both sugars were fully protected with acetyl groups using $Ac_2O$. Then, the

[228] Pieters, R. J. *Med. Res. Rev.* **2007**, *27*, 796.
[229] Pasparakis, G.; Cockayne, A.; Alexander, C. *J. Am. Chem. Soc.* **2007**, *129*, 11014.
[230] Pasparakis, G.; Alexander, C. *Angew. Chem.* **2008**, *120*, 4925.
[231] Schmidt, R. R.; Toepfer, A. *Tetrahedron Lett* **1991**, *32*, 3353.
[232] Boltje, T. J.; Buskas, T.; Boons, G.-J. *Nature chemistry* **2009**, *1*, 611.
[233] Demchenko, A. V. *Synlett* **2003**, *2003*, 1225.
[234] van der Vorm, S.; van Hengst, J. M.; Bakker, M.; Overkleeft, H. S.; van der Marel, G. A.; Codée, J. D. *Angew. chem., Int. Ed.* **2018**.
[235] Ichikawa, S.; Sato, T. *Tetrahedron Lett* **1986**, *27*, 45.
[236] Cai, T. B.; Lu, D.; Tang, X.; Zhang, Y.; Landerholm, M.; Wang, P. G. *J. Org. Chem.* **2005**, *70*, 3518.
[237] van der Peet, P.; Gannon, C. T.; Walker, I.; Dinev, Z.; Angelin, M.; Tam, S.; Ralton, J. E.; McConville, M. J.; Williams, S. J. *ChemBioChem* **2006**, *7*, 1384.

anomeric acetate was selectively removed by treatment with $BnNH_2$. The mannose and glucose trichloroacetimidates were prepared from the corresponding hemiacetals in the presence of DBU, following the Schmidt approach who developed trichloroacetimidoyl derivatives as strong donors.[238] A catalytic amount of a Lewis acid is typically required in glycosylation with trichloroacetimidates. $BF_3{\cdot}OEt_2$ was used to activate the anomeric leaving group, which is present in two conformations, α and β, at the anomeric position (Scheme 10 and Scheme 11).

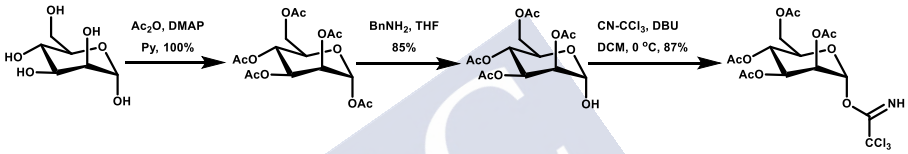


*Scheme 10. Synthesis of Man-trichloroacetimidate.*

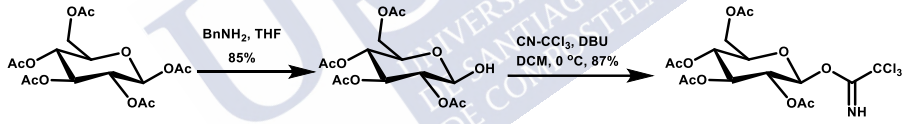


*Scheme 11. Synthesis of Glu-trichloroacetimidate.*

Because of the presence of an acetyl group at the C2 position, the formation of a more stable five member acetoxonium ion ring will be formed (Figure 33 and Figure 34). In the case of mannose, that acetoxonium ion can only be formed in an equatorial conformation, so the alcohol acceptor will attack the anomeric position with an axial orientation, leading to the selective formation of an α-linked glycoside (Figure 33). Likewise, in the case of glucose, due to the C2 neighboring group being equatorial, the Schmidt's glycosylation will lead to the selective formation of β-linked products with anomeric carbon substituent group in the equatorial position[232] (Figure 34).

[238] Schmidt, R. R.; Castro-Palomino, J. C.; Retz, O. *Pure Appl. Chem.* **1999**, *71*, 729.

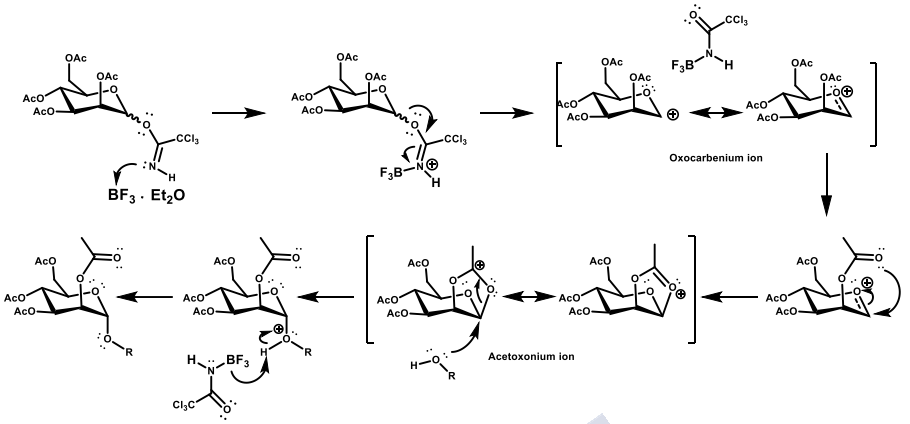


*Figure 33. Mechanism of glycosylation of alcohol with $BF_3{\cdot}Et_2O$ as catalyst. Selective formation of α-mannose derivative.*

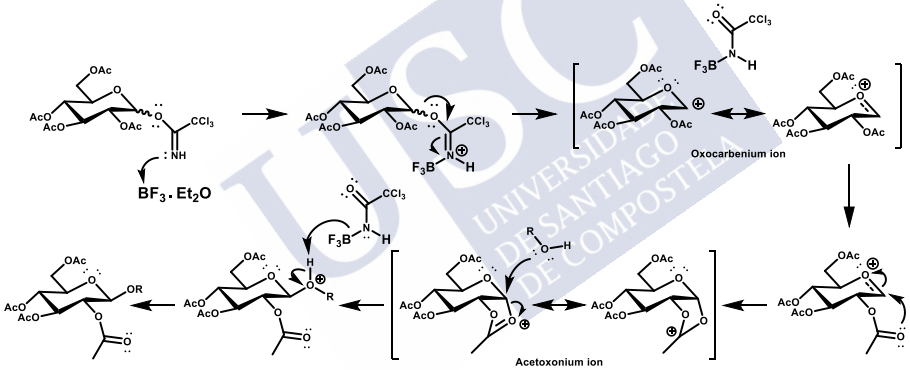


*Figure 34. Mechanism of glycosylation of alcohol with $BF_3{\cdot}Et_2O$ as catalyst. Selective formation of β-glucose derivative.*[239]

With both mannose and glucose trichloroacetimidates in hand, the production of alkynated carbohydrates was straightforward starting from Alk-TEG-OH in a process catalyzed by $BF_3{\cdot}Et_2O$ (

Scheme *12* and Scheme 13). Both reactions were performed in collaboration with Dr. Emma Leire. After purification by chromatography in silica acetylated Alk-Man and Alk-Glu were

[239] Bergeron-Brlek, M.; Shiao, T. C.; Trono, M. C.; Roy, R. *Carbohydr. Res.* **2011**, *346*, 1479.

obtained in 48% and 76% yield, respectively. Improved yield for the mannose derivative up to 82% could be reached using neutral alumina instead of silica.

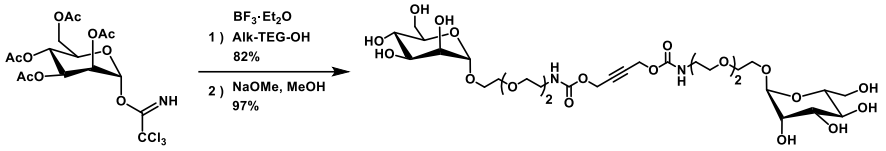


*Scheme 12. Synthesis of Alk-Man.*

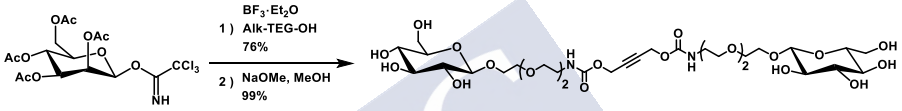


*Scheme 13. Synthesis of Alk-Glu.*

The NMR *J*-coupling constants represent a powerful tool in the study of the conformational properties of pairs of nuclei which are chemically bonded to each other. α and β-sugar configurations are completely different in the angle between the hydrogens at C1 and C2 and so, they have characteristic *J*-coupling constants.[240] In case of mannose, the reported *J*-coupling constants of anomeric protons for α- and β-configurations are 1.6 Hz and 0.8 Hz respectively. For acetylated Alk-Man, the measured *J*-coupling of the anomeric proton was 1.6 Hz (Figure 35), which matches the expected α-mannose configuration (Figure 36). Likewise, the reported *J*-coupling of anomeric protons for α- and β-glucose lie in the ranges 2-4 Hz and 7-9 Hz, respectively.[240,241] In our case, the measured *J*-coupling of the anomeric proton was 7.9 Hz (Figure 35), compatible with a β-configuration in acetylated Alk-Glu (Figure 36). Lastly, acetylated Alk-Man and Alk-Glu were completely deprotected under Zemplén

[240] Jacobsen, N.E **(2007)** *NMR Spectroscopy Explained: Simplified Theory, Applications and Examples for Organic Chemistry and Structural Biology*, Wiley.
[241] Bubb, W. A. *Concepts in Magnetic Resonance Part A: An Educational Journal* **2003**, *19*, 1.

conditions (NaOMe in MeOH)[242] to give the desired products in excellent yield (97-99%).

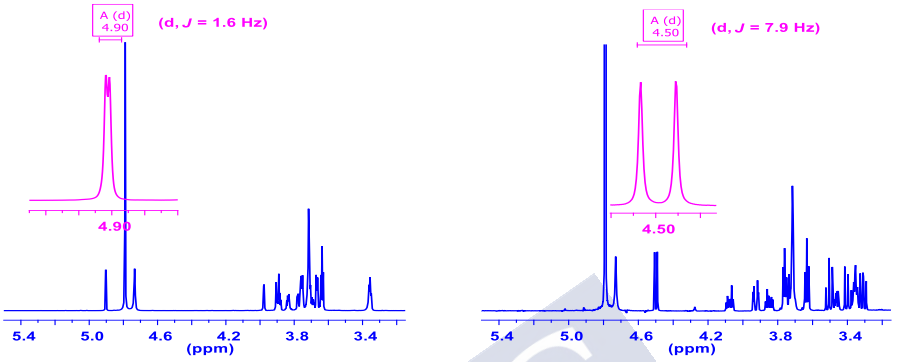


*Figure 35. $^{1}$H NMR Spectrum, J-coupling constant of anomeric proton peak for α-mannose (left) and β-glucose (right).*


*Figure 36. H1-H2 relationship in α-mannose ang β-glucose.*

Characterization of the acetylated products was done by mass spectrometry and IR. $^{1}$H NMR confirmed the successful glycosylation by appearance of four singlets of the acetyl groups at 2.12-1.96 ppm and the specific anomeric proton at 4.85 ppm. By $^{13}$C NMR, characteristic signals were observed for the acetyl groups at 170.7-169.7 ppm and 20.9-20.6 ppm, as well as anomeric carbon at 97.7 ppm. Alk-Glu-OAc showed similar spectra with the only difference in the chemical shift of the anomeric proton which appears at 4.59 ppm.

[242] Wang Z., Zemlén Deacetylation. *Comprehensive Organic Name Reactions and Reagents*. W.Z, Editor. **2010**, John Wiley & Sons.: Hoboken NJ.

Successful deprotection of Alk-Man and Alk-Glu was confirmed by disappearance of the acetyl signals by $^{1}H$ NMR and $^{13}C$ NMR.

### 3.2.10 Alk-TEG-$NH_2$·HCl synthesis

In 3.2.3, the preparation of Alk-TEG-NHBoc was described. Herein, the deprotection of the Boc group is reported either using HCl in MeOH for 30 min. The resulting ammonium salt will be subsequently functionalized with fluorophores and ligands of biomedical interest as biotin, FITC and DOTA. After the reaction was completed, the crude product was evaporated to afford pure Alk-TEG-$NH_2$·HCl.

As is illustrated in Figure 37, the successful deprotection of Alk-TEG-NHBoc was confirmed by disappearance of the Boc signals by $^{13}C$ NMR at 155.6, 79.3 and 28.5 ppm, purity of Alk-TEG-$NH_3$·Cl was promoted by elemental analysis.

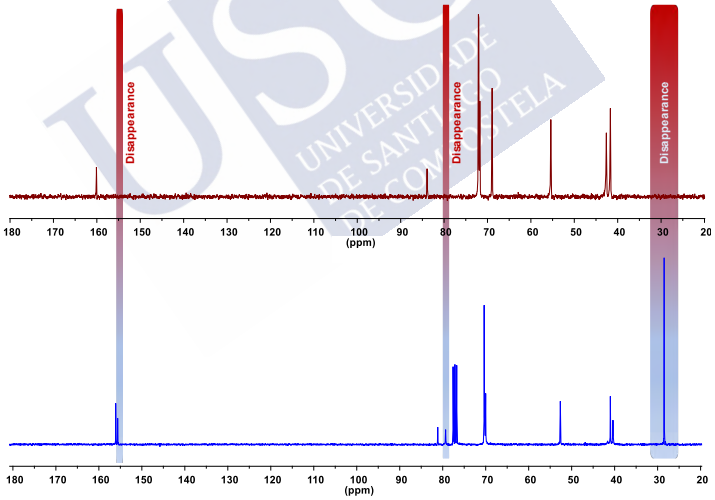


*Figure 37. $^{13}C$ NMR conversion in the synthesis of Alk-TEG-$NH_2$·HCl. Spectrum of Alk-TEG-NHBoc (blue), spectrum of Alk-TEG-$NH_2$·HCl (red).*

### 3.2.11 Alk-Bio synthesis

Biotin is called vitamin H or vitamin B7, it is available in low concentrations in most living organisms. Since it is water-soluble, a daily intake is required; it is not stored in the body. Deficiency of

biotin in humans is rare, because it is available in many different food types, and the good gut bacteria can normally synthesize more biotin than the body needs.

Biotin exists in two forms, biotin itself and biocytin (Figure 38), a conjugate between biotin and L-lysine.[243] Biotin helps the body to metabolize[244] fats, carbohydrates, and proteins. It may also be helpful in keeping a fixed level of blood sugar.[245]

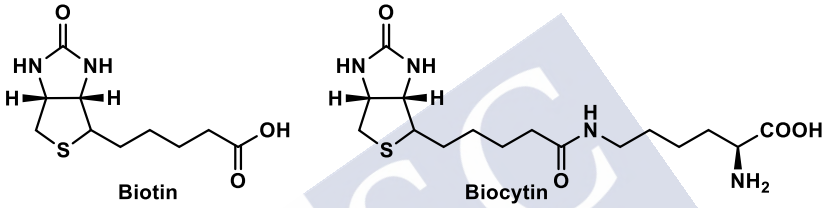


*Figure 38. Biotin forms.*

Alk-Bio was synthesized following two different routes. The route **A** included four sequential steps illustrated in the Scheme 14. Preparation of monoprotected tris(ethylene glycol)-diamine[219] was the first step in this route, followed by amide coupling with biotin (HOBt, EDC, DMF) to afford the protected biotin derivative (*N*-Boc-*N'*-biotinyl-3,6-dioxaoctane-1,8-diamine) in 93% yield.[246] This product was purified by chromatography in gradient from EtOAc to MeOH 5% in silica.[246] The $^{1}$H NMR spectrum matched well those previously reported,[219] particularly, the appearance of the specific biotin and Boc signals (Figure 39, red). Deprotection of Boc with TFA in DCM[219,246] was the third step to afford the amino-functionalized biotin (*N*-biotinyl-3,6-dioxaoctane-1,8-diamine) in quantitative yield. The $^{1}$H

[243] Perez-Ruiz, T.; Martinez-Lozano, C.; Sanz, A.; Bravo, E. *Chromatographia* **2003**, *58*, 757.
[244] Huskisson, E.; Maggini, S.; Ruf, M. *J. Int. Med. Res* **2007**, *35*, 277.
[245] Pour, H. A.; Branch, S.; Sarab, I. *Scholars Research library* **2012**, *3*, 1929.
[246] Fernandez-Megia, E.; Novoa-Carballal, R.; Quiñoá, E.; Riguera, R. *Biomacromolecules* **2007**, *8*, 833.

NMR spectrum of this product matched well those previously reported,[219] in particular, the disappearance Boc signal at ca 1.44 ppm (Figure 39, blue). The last step was the coupling of the obtained amino-functionalized biotin with Alk-NHS. Crude Alk-Bio was purified using EtOAc to MeOH 10% in alumina to afford pure the product in 77% yield.

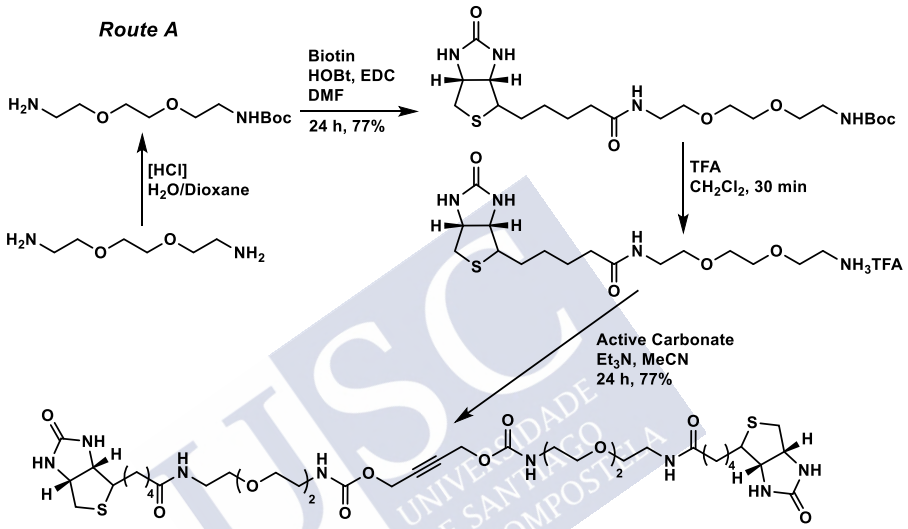


*Scheme 14. Alk-Bio synthesis by route A.*

In the route **B** depicted in Scheme 15, it was used the sequence of Alk-TEG-$NH_2$·HCl synthesis that was discussed previously in section 3.2.10). With Alk-TEG-$NH_2$·HCl in hand, amide coupling with biotin was carried out (HOBt, EDC, $Et_3N$, DMF). The resulting crude product was purified as above to obtain Alk-Bio in 93% yield. Although both routes involve the same number of steps, route **B** is considered more favorable to prepare Alk-Bio because of its higher overall yield and reduced number of chromatographic purifications (one for route **B** compared to two for **A**).

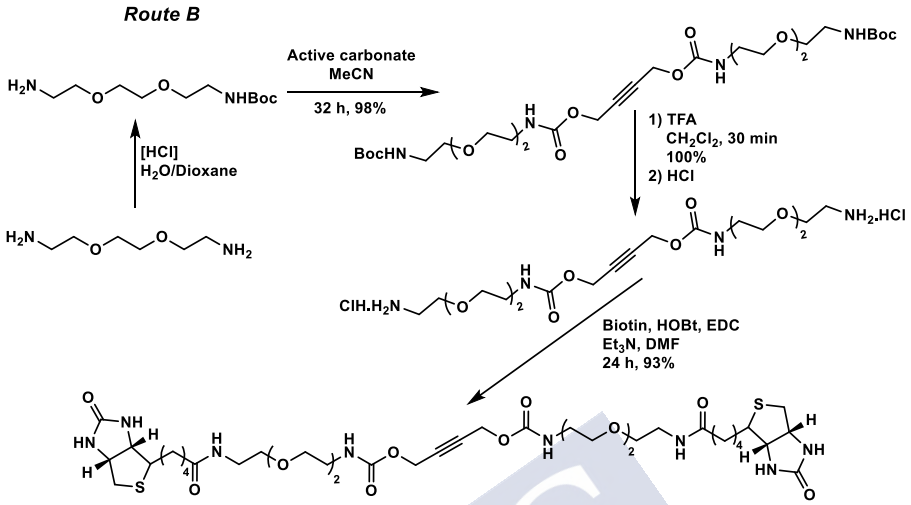


*Scheme 15. Alk-Bio synthesis by route B.*

Alk-Bio was fully characterized by elemental analysis, NMR and IR that confirmed its purity. The $^{1}H$ NMR spectrum contains the expected biotin signals, in agreement with a successful coupling with activated Alk-NHS: (i) appearance of the α-alkyne proton at around 4.70 ppm when the route **A** was followed, (ii) coupling confirmed in route **B** by appearance of Alk-TEG-$NH_2$ and biotin expected signals (Figure 39). Likewise,$^{13}C$ NMR confirmed the completion of the coupling reaction, particularly, the appearance of biotin carbonyl groups and the other characteristic biotin carbons. The matching of TLC and NMR spectral data of the final product obtained by the two routes was additional evidence to the identity of Alk-Bio

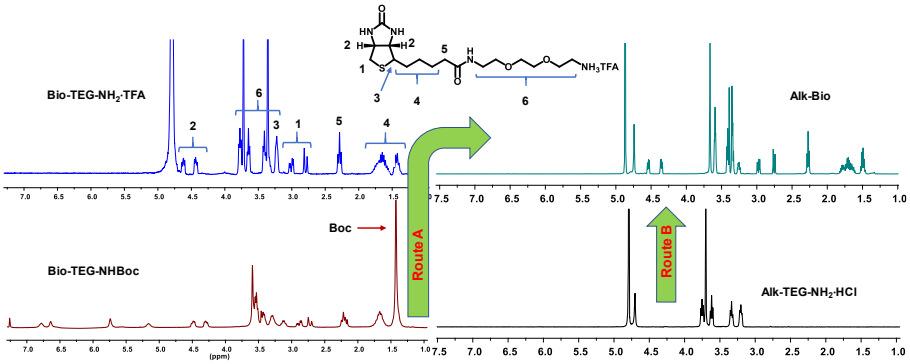


*Figure 39. $^1$H NMR spectrum. Route (A) the appearance of biotin and Boc signals (red) and disappearance of Boc signal (blue). Route (B) the appearance of Alk-TEG-$NH_2$·HCl and biotin signals (green).*

### 3.2.12 Alk-FITC synthesis

Fluorescent dyes are considered basic and major tools in biomolecule labeling,[247] Fluorescein and its derivatives, particularly fluorescein isothiocyanate (FITC) are among those commonly used in conjugation, especially with proteins, due to their excellent absorption and emission properties.[248] FITC is found in two indistinguishable spectrally isomers (Figure 40). Isomer **A** is more easily to isolate, and this explains its extensive use.

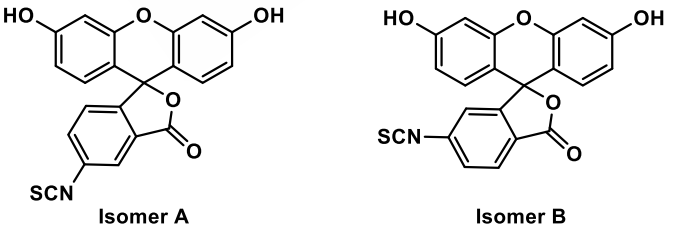


*Figure 40. Structures of FITC isomers.*

[247] Jullian, M.; Hernandez, A.; Maurras, A.; Puget, K.; Amblard, M.; Martinez, J.; Subra, G. *Tetrahedron Lett* **2009**, *50*, 260.

[248] Tsien, R.; Ernst, L.; Waggoner, A.; 3 ed.; James, Ed.; Spring: New York, 2006, p 338.

FITC displays a wide range of applications in biochemistry, it is an amine-reactive fluorescein dye, and because of the isothiocyanate is more reactive than carboxyl derivatives that need activation before use.[247] The isothiocyanate group reacts easily and efficiently with amines in proteins.

Breen and co-workers[249] demonstrated that the fluorescence of FITC and its conjugates is significantly affected by pH. As depicted in Figure 41, there is no distinguishable fluorescence below pH 5, and the optimum absorbance is at pH 8.5. In the case of FITC itself, the reversibility of fluorescence is possible only in the pH range 0 to 7, but irreversibly loses its fluorescence at high pH (Figure 41, a) since $OH^-$ ions react with FITC to form aminofluorescein.[250] However, when FITC is conjugated to amine, the irreversible loss of fluorescence does not occur at high pH since the thiourea linkage is not vulnerable to attack by $OH^-$ ions.[249]

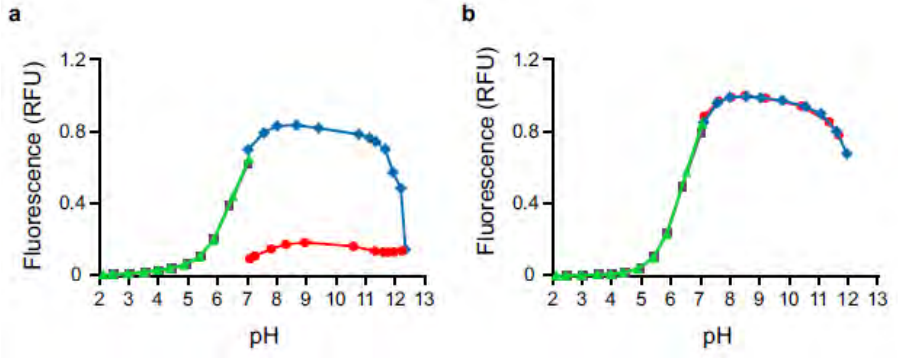


*Figure 41. Fluorescence of (a) FITC and (b) FITC-methylamine, as a pH function: upward titration from pH 7 with NaOH (blue) and return to neutral pH with HCl (red), downward titration from pH 7 with HCl (green) and return to neutral pH with NaOH (gray). Figure adapted from reference* 249.

[249] Breen, C. J.; Raverdeau, M.; Voorheis, H. P. *Scientific Reports* **2016**, *6*, 25769.
[250] Mckinney, R. M.; Spillane, J. T.; Pearce, G. W. *The Journal of Immunology* **1964**, *93*, 232.

The preparation of an Alk-FITC molecule was envisioned very interesting as a fluorophore marker for the decoration of dendrimers requiring fluorescence monitoring, as for cell internalization studies. Accordingly, Alk-FITC was prepared from Alk-TEG-$NH_2$·HCl (Section 3.2.10) and FITC. The completion of the reaction was confirmed by TLC after 16 h. The crude product was purified by column chromatography, using DCM to MeOH 15% in neutral alumina, to obtain the desired product in 73% yield. The complete amine-isothiocyanate coupling was clearly indicated in the IR spectrum by disappearance of a strong band of isothiocyanate group[251] at ca 2110 $cm^{-1}$. Furthermore, $^{1}H$ NMR and $^{13}C$ NMR spectra confirmed the appearance the characteristic aromatic signals of FITC, especially C=S at ca 181.0 ppm.

Once this collection of alkynes was prepared, their thermal stability was assessed. Their $^{1}H$ NMR spectra was compared before and after a heating procedure that involved 8 h at 120 ºC in tBuOH/$H_2O$. No changes by NMR or TLC were observed for any of the alkynated ligands prepared, confirming their high thermal stability under the expected conditions to be used in their thermal AAC coupling to dendrimers and polymers.

## 3.3 Functionalization of GATG dendrimers by TAAC

### 3.3.1 Overview

Dendrimer functionalization is a process that involves the incorporation of different functional groups in the dendritic architecture.[252] There are six well defined nanoscale features, named Critical Nanoscale Design Parameters (CNDPs) including, size, shape, surface chemistry, flexibility, rigidity, architecture and elemental composition that define the properties of nanomaterials.[20] The

[251] McKinney, R. M.; Churchill II, F. C.; Spillane, J. T.; Pearce, G. W. *Anal. Biochem.* **1969**, *29*, 526.

[252] Augustus, E. N.; Allen, E. T.; Nimibofa, A.; Donbebe, W. *American Journal of Polymer Science* **2017**, *7*, 8.

functionalization of macromolecules, such as dendrimers, is crucial to control their CNDPs and produce interesting features and properties of application in different fields.[253]

Dendrimers and dendritic structures offer an amazing palette of unique properties. To exploit these features, the functionalization of dendrimers has proceeded over native (nonfunctionalized) dendrimers[254] for specific high-end applications, particularly, in biotechnology,[255] nanotechnology[256] complexation of transition metals,[257] catalysis,[258] and drug delivery systems.[259,260,261,262]

As shown above, our research group has mainly relied on the use of CuAAC for the functionalization of dendrimers. Despite the undouble advantages of this reaction, there are certain limitations that should not be obviated. The most important is the presence of residual Cu traces potentially leading to reactive oxygen species (ROS) and biological damage during applications.[144,263,264] Consequently, we have turned our attention to alternative ways for the functionalization of GATG dendrimers that do not require the presence of metal catalysts. Functionalization under thermal AAC conditions has been envisioned as a potential substitute of CuAAC for dendrimers and polymers.

---

[253] Chow, H.-F.; Mong, T. K.-K.; Nongrum, M. F.; Wan, C.-W. *Tetrahedron* **1998**, *54*, 8543.

[254] Smith, D. K.; Diederich, F. *Chem.--Eur. J.* **1998**, *4*, 1353.

[255] Grinstaff, M. W. *Chem.--Eur. J.* **2002**, *8*, 2838.

[256] Tully, D. C.; Fréchet, J. M. *Chemical Communications* **2001**, 1229.

[257] Slany, M.; Caminade, A.-M.; Majoral, J. P. *Tetrahedron Lett* **1996**, *37*, 9053.

[258] Oosterom, G. E.; Reek, J. N.; Kamer, P. C.; van Leeuwen, P. W. *Angew. chem., Int. Ed.* **2001**, *40*, 1828.

[259] Stiriba, S. E.; Frey, H.; Haag, R. *Angew. chem., Int. Ed.* **2002**, *41*, 1329.

[260] Madaan, K.; Kumar, S.; Poonia, N.; Lather, V.; Pandita, D. *Journal of pharmacy & bioallied sciences* **2014**, *6*, 139.

[261] Chowdhury, R.; Berg, E. A.; Fishman, J. B.; Al Sayeghº, H. A.; Blackwelderº, P. *Cancer Res.* **2011**, *71*, 7452.

[262] Bai, C. Z.; Choi, S.; Nam, K.; An, S.; Park, J.-S. *Int. J. Pharm* **2013**, *445*, 79.

[263] Halliwell, B.; Gutteridge, J. M. In *Methods in enzymology*; Elsevier: 1990; Vol. 186, p 1.

[264] Lallana, E.; Riguera, R.; Fernandez-Megia, E. *Angew. chem., Int. Ed.* **2011**, *50*, 8794.

Thus, as opposed to biopharmaceuticals, dendrimers and polymers are generally stable to heating for long periods of time, which entitle them as ideal substrates for this reaction.

With a reliable synthesis of azide-terminated 2[Gn]-$N_3$ and 3[Gn]-$N_3$[140] dendrimers and a collection of alkynated ligands in hand, conditions for the TAAC reaction were optimized regarding concentration, temperature, solvent and time using 2-(2-(2-azidoethoxy)ethoxy)ethan-1-ol as organic model azide, mimicking the terminal arm of GATG, and but-2-yne-1,4-diyl bis (propyl-carbamate) as a model alkynated carbonate (Scheme 16). A kinetic study was performed by taking aliquots of the reactions at different times. Conversion values determined by $^1$H NMR were adjusted to a second-order reaction kinetics from which the time estimated for a 99% conversion was determined (Table 4).

As shown in Table 4, using the azide at 1 M concentration and 2 equivalents of alkyne at 100 ºC afforded quantitative conversion in 16-17 h, independently on the nature of the solvent (tBuOH or tBuOAc; entries 1 and 2). Reaction time could be reduced to 8 h either by increasing the concentration of azide to 2 M or the temperature to 110 ºC (entries 3 and 4). A further 10 ºC temperature increase allowed reducing the reaction time to just 6 h. While the incorporation of $H_2O$ as cosolvent in mixtures with tBuOH reduced the reaction kinetics for the propyl-carbamate model due to solubility issues, no such effects were revealed when dealing with water soluble ligands (data not shown). As a result, a set of conditions were obtained for application to the functionalization of dendrimers: 1 M concentration of terminal azide, 2 equivalents of alkyne per azide, 120 ºC in tBuOH/$H_2O$. Under these conditions, TAAC should be completed in 6 h, but to ensure full dendrimer functionalization, reactions were allowed to run for 8 h.

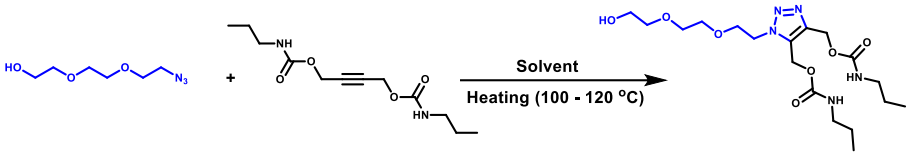


*Scheme 16 . Kinetic study of a model TAAC reaction.*

*Table 4. Optimization conditions of the TAAC.*

| Exp | Solvent | Temp (°C) | Conc. (M) | Estimated time (h) for 99% conv. |
|---|---|---|---|---|
| 1 | tBuOH | 100 | 1 | 16.91 |
| 2 | AcOtBu | 100 | 1 | 15.97 |
| 3 | AcOtBu | 100 | 2 | 8.41 |
| 4 | AcOtBu | 110 | 1 | 7.50 |
| 5 | AcOtBu | 120 | 1 | 6.05 |
| 6 | AcOtBu | 120 | 0.5 | 12.94 |

Several generations of azido-terminated GATG dendrimers (2[Gn] and 3[Gn]) amenable to surface functionalization with internal alkynes by means of TAAC were tested under the optimized conditions shown above. The reaction progress was easily monitored by FT-IR by following the disappearance of the characteristic azide band at ca 2100 $cm^{-1}$ (Figure 42). After purification by ultrafiltration, reaction completion and full surface functionalization was also clearly established by $^{1}H$ NMR thanks to the disappearance of the characteristic signal at ca. 3.40 ppm due to the methylene protons adjacent to the azide group that are shifted to 4.50-4.60 ppm in the dendrimer conjugates. The appearance of two new set of multiplets at ca. 5.10-5.40 ppm, corresponding to the methylene protons alpha of the triazole (protons originally at the propargylic position in the alkyne), also confirmed the structure and integrity of the functionalized dendrimers (Figure 43). Purity and success of the

TAAC reaction were also confirmed by $^{13}C$ NMR thanks to the disappearance of the alkyne carbons at around 81 ppm that are shifted to around 130-145 ppm, characteristic of the triazole ring (Figure 44). Gel permeation chromatography (GPC) (Figure 45) and dynamic light scattering (DLS) (Figure 46) further confirmed the monodispersity, purity, lack of aggregation and successful surface functionalization. Summary of characterization is presented in (Table 5). As seen in Table 6, after TAAC reaction, the size of the dendrimers increases the equivalent to one generation difference in GATG. For IR, $^{1}H$ and $^{13}C$ NMR spectra of each dendrimer conjugate, see the experimental part.

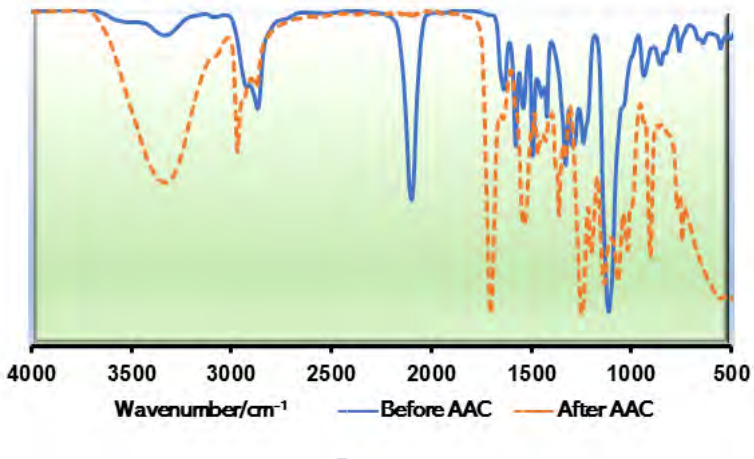


*Figure 42. IR spectra of azide-terminated GATG dendrimer (blue) and TAAC conjugate (doted orange).*

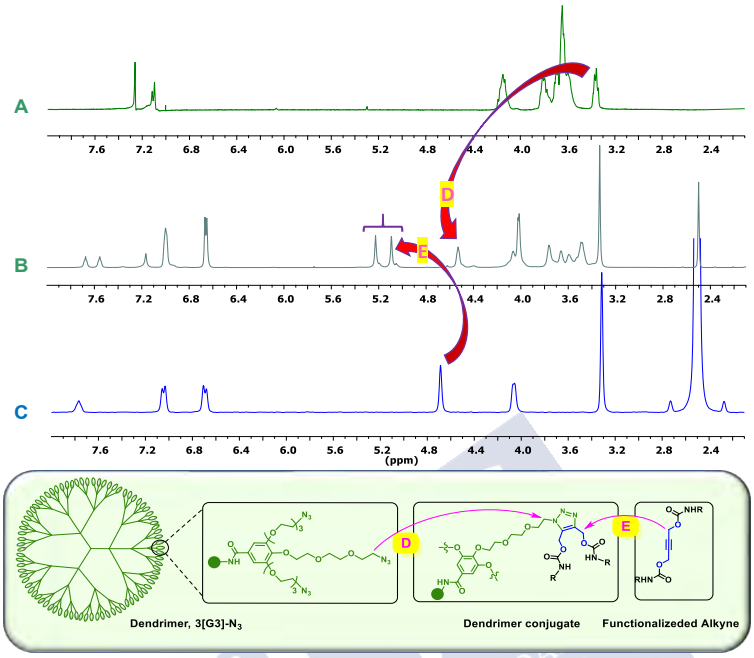


*Figure 43. TAAC conversion by $^{1}H$ NMR. Spectra of starting GATG azido-dendrimer (A), a TAAC dendrimer conjugate (B), and a functionalized alkyne (C).*

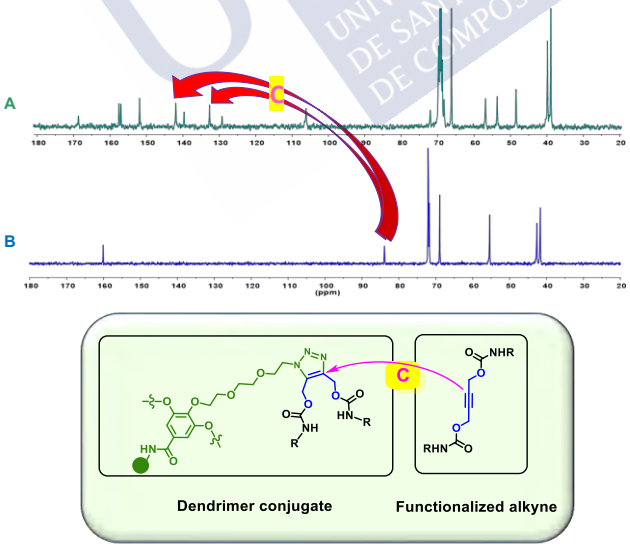


*Figure 44. TAAC conversion by $^{13}C$ NMR. Spectra of a TAAC dendrimer conjugate (A), and a functionalized alkyne (B).*

Table 5. *TAAC Functionalization of Dendrimers and Polymers.*

| Dendrimer/Polymer | Alkyne | Dendrimer conjugate | Yield (%) |
|---|---|---|---|
| 3[G1]-$N_3$ | Alk-OH | 3[G2]-OH | 93 |
| | Alk-Glu | 3[G2]-Glu | 91 |
| 2[G2]-$N_3$ | Alk-OH | 2[G3]-OH | 94 |
| | Alk-TEG-$NH_2$·HCl | 2[G3]-TEG-$NH_2$·HCl | 93 |
| 3[G3]-$N_3$ | Alk-TEG-OH | 3[G4]-TEG-OH | 92 |
| | Alk-OH | 3[G4]-OH | 91 |
| | Alk-PhOH | 3[G4]-PhOH | 91 |
| | Alk-$OSO_3H$·$NH_3$ | 3[G4]-$OSO_3Na$ | 91 |
| | Alk-Man | 3[G4]-Man | 93 |
| | Alk-Glu | 3[G4]-Glu | 92 |
| | Alk-TEG-$NH_2$·HCl | 3[G4]-TEG-$NH_2$·HCl | 92 |
| | Alk-DOTA | 3[G4]-DOTA | 90 |
| | Alk-Man, Alk-Bio, Alk-FITC | 3[G4]-$(Man)_{60}$/$(Bio)_{16}$/$(FITC)_5$ | 96 |
| 3[G4]-$N_3$ | Alk-Man | 3[G5]-Man | 94 |
| $PEG_{5k}$-[G2]-$N_3$ | Alk-Cat | $PEG_{5k}$-[G3]-Cat | 86 |
| $PEG_{5k}$-$PGA_{25}$-$N_3$ | Alk-OH | $PEG_{5k}$-$PGA_{25}$-[G1]-OH | 92 |

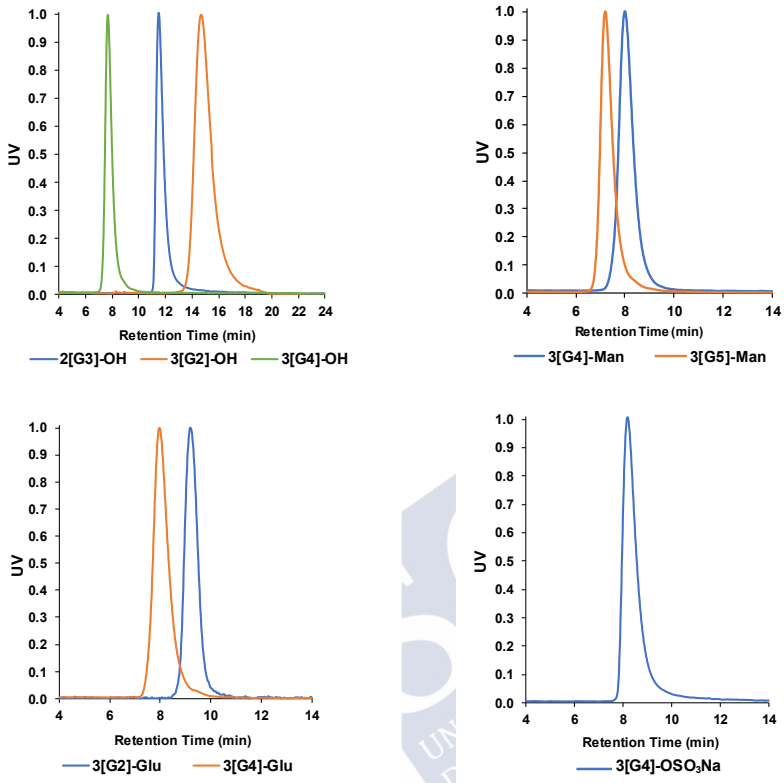


*Figure 45. Normalized GPC elugrams of dendrimer conjugates (UV signal at 254 nm, 10 mM PB pH 7.4, 150 mmol LiCl).*

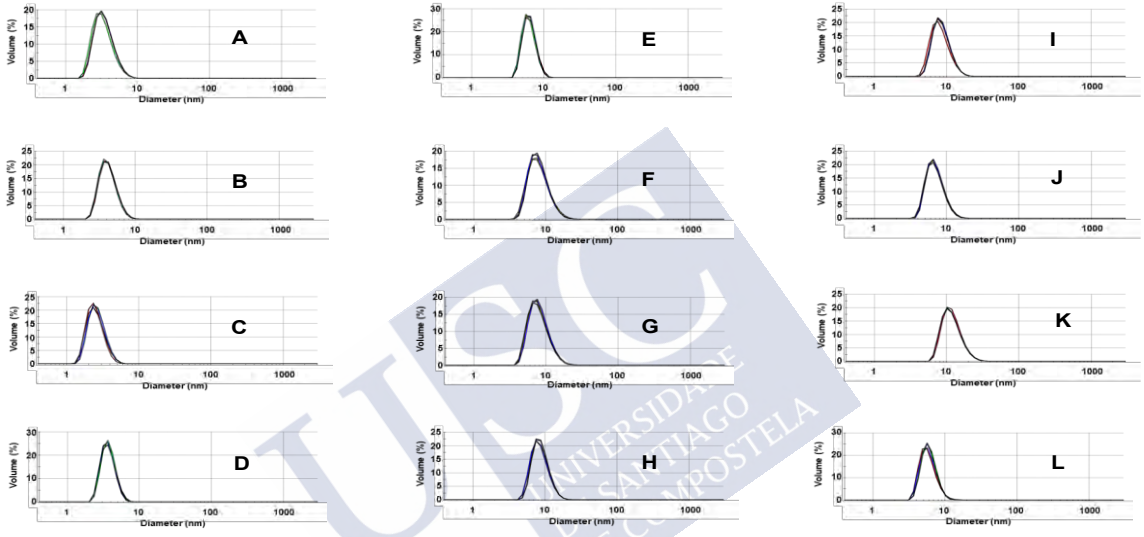


**A :** 2[G3]-OH
**B :** 2[G3]-TEG-$NH_2$·HCl
**C :** 3[G2]-OH
**D :** 3[G2]-Glu
**E :** 3[G4]-OH
**F :** 3[G4]-TEG-OH
**G :** 3[G4]-TEG-$NH_2$·HCl
**H :** 3[G4]-Glu
**I :** 3[G4]-Man
**J :** 3[G4]-$OSO_3Na$
**K :** 3[G5]-Man
**L :** $PEG_{5K}$-$PGA_{25}$-[G1]-OH

*Figure 46. Dynamic light scattering (DLS) of dendrimer conjugates (size distribution by volume; 1 mg/mL, 150 mM LiCl, 25 ºC).*

*Table 6. Size of dendrimer conjugates measured by DLS (1 mg/mL, 150 mM LiCl, 25 $^{o}$C).*

| Dendrimer conjugate | Size (nm) |
|---|---|
| 3[G2]-OH | 2.63 |
| 3[G2]-Glu | 3.71 |
| 2[G3]-OH | 3.42 |
| 2[G3]-TEG-$NH_2$·HCl | 4.31 |
| 3[G4]-TEG-OH | 8.20 |
| 3[G4]-OH | 6.14 |
| 3[G4]-$OSO_3Na$ | 6.99 |
| 3[G4]-Man | 8.71 |
| 3[G4]-Glu | 8.71 |
| 3[G4]-TEG-$NH_2$·HCl | 8.21 |
| 3[G5]-Man | 12.01 |
| $PEG_{5k}$-$PGA_{25}$-[G1]-OH | 5.96 |

### 3.3.2 Dendrimer functionalization with alcohols

#### 3.3.2.1 Functionalization with Alk-OH

To verify the applicability of the reaction conditions develop for the model azide to azide-terminated GATG dendrimers, three dendrimers with increasing number of terminal azides, namely 3[G1]-$N_3$ (9 azides), 2[G2]-$N_3$ (18 azides) and 3[G3]-$N_3$ (81 azides), were functionalized with the alkynated diol Alk-OH under standard conditions: 1 M azide group, 2 equiv of Alk-OH per azide, 120 ºC in tBuOH/$H_2O$ 5:1. The progress of the reactions was monitored by IR, which confirmed completeness after 8 h by disappearance of the azide band at ca 2100 $cm^{-1}$. The reaction mixtures were purified by ultrafiltration to obtain the expected dendrimer conjugates 3[G2]-OH, 2[G3]-OH and 3[G4]-OH in excellent yields (Table 5). Full characterization of the polyol dendrimers by $^1H$ NMR, $^{13}C$ NMR, GPC (Figure 45) and DLS (Figure 46) confirmed their purity and monodispersity.

The scope of the TAAC conditions herein described were also tested for the dendronization of linear polymers. To this end, we selected $PEG_{5k}$-$PGA_{25}$-$N_3$, a PEG-polyglutamic acid block copolymer derivative that carries pendant azide groups from the glutamic acid residues. Following procedures previously described by our group,[135] amide coupling of commercial $PEG_{5k}$-$PGA_{25}$ with 1-azido-3-aminopropane [265] afforded $PEG_{5k}$-$PGA_{25}$-$N_3$ (Scheme 17). With the block copolymer in hand, functionalization (dendronization) with Alk-OH was carried out under standard TAAC conditions. In this case, due to the high viscosity of the reaction mixture, azide concentration was lowered down to 0.5 M, while keeping the remaining conditions untouched (tBuOH/$H_2O$ 1:1). Gratifyingly, reaction monitoring by IR confirmed full functionalization after 12 h of reaction time (disappearance azide peak at around 2100 $cm^{-1}$). Purification by

[265] Carboni, B.; Benalil, A.; Vaultier, M. *J. Org. Chem.* **1993**, *58*, 3736.

ultrafiltration afforded $PEG_{5k}$-$PGA_{25}$-[G1]-OH in excellent yield (92%).

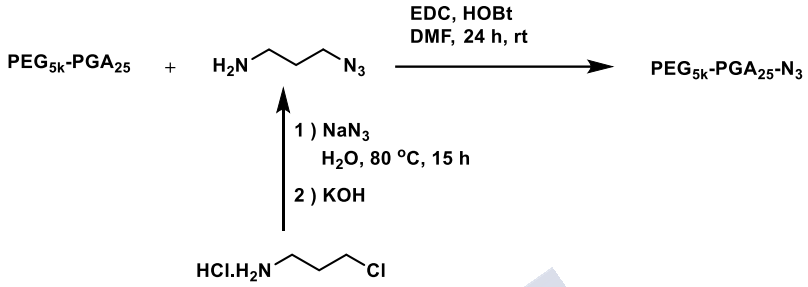


*Scheme 17. $PEG_{5k}$-$PGA_{25}$-[G1]-$N_3$ preparation.*

### 3.3.2.2 Functionalization with Alk-TEG-OH

Application of TAAC conditions for the functionalization of dendrimers with a diol alkyne having longer spacer linkers, such as Alk-TEG-OH, also revealed successful. TAAC between 3[G3]-$N_3$ and Alk-TEG-OH under similar conditions as above (1 M azide, tBuOH/$H_2O$ 2:1) afforded 3[G4]-TEG-OH in 92% after 8 h of stirring at 120 ºC. $^1$H NMR, $^{13}$C NMR, GPC (Figure 45) and DLS (Figure 46) confirmed the purity and monodispersity of the material.

## 3.3.3 Dendrimer functionalization with charged moieties

### 3.3.3.1 Functionalization with Alk-TEG-$NH_2$·HCl

Functionalization of azido-dendrimers with alkynated ammonium groups was envisaged as a straightforward strategy for the preparation of cationic dendrimers with plenty of applications in materials science. To this end, Alk-TEG-$NH_2$·HCl was clicked onto two different GATG dendrimers, 2[G2]-$N_3$ and 3[G3]-$N_3$, by means of TAAC, to produce the corresponding dendrimer conjugates 2[G3]-TEG-$NH_2$·HCl and 3[G4]-TEG-$NH_2$·HCl, with full surface functionalization and doubled number of positively charged terminal groups.

Functionalization of 2[G2]-$N_3$ with Alk-TEG-$NH_2$·HCl was performed at a 1 M concentration of azide groups and 120 ºC, in a tBuOH/$H_2O$ 5:1 solvent mixture. IR monitoring confirmed reaction completeness after 8 h. Then, the reaction mixture was purified by ultrafiltration using 0.1 M HCl followed by water to afford 2[G3]-TEG-$NH_3Cl$ in 93% yield. $^1H$ NMR, $^{13}C$ NMR, GPC (Figure 45) and DLS (Figure 46) confirmed its purity and monodispersity. In a similar way, 3[G3]-$N_3$ was peripherally functionalized with Alk-TEG-$NH_2$·HCl to give 3[G4]-TEG-$NH_2$·HCl in an excellent 92%yield.

#### 3.3.3.2 Functionalization with Alk-$OSO_3Na$

To evaluate the surface functionalization of dendrimers with negatively charged moieties, 3[G3]-$N_3$ was clicked with Alk-$OSO_3H$·$NH_3$ by means of TAAC. As above, the concentration of azides was set at 1 M and the temperature to 120 ºC. As solvent mixture, tBuOH/$H_2O$ 1:1 was used. The reaction was monitored by IR that confirmed completion after 8 h. Then, the reaction mixture was purified by ultrafiltration using 0.1 M NaOH, followed with water, to obtain the desired dendrimer conjugate 3[G4]-$OSO_3Na$ in 91% yield. $^1H$ and $^{13}C$ NMR, GPC (Figure 45) and DLS (Figure 46) confirmed its purity and monodispersity.

### 3.3.4 Dendrimer functionalization with phenols

#### 3.3.4.1 Functionalization with Alk-PhOH

Following TAAC conditions, surface functionalization of 3[G3]-$N_3$ was carried out with Alk-PhOH to yield the dendrimer conjugate 3[G4]-PhOH in 91% yield. Again, in this case, the concentration of azides was set at 1 M and the temperature at 120 ºC. A solvent mixture MeOH/$H_2O$ 5:1 was used (MeOH was used instead of tBuOH because of the poor solubility of Alk-PhOH in tBuOH). The reaction was monitored by IR that confirmed completion after 8 h. The reaction mixture was purified by ultrafiltration using acetone/water to obtain the 3[G4]-PhOH in 91% yield.

#### 3.3.4.2 Functionalization with Alk-Cat

With the aim of investigating the ability of the dendrimer conjugates to form micelles and their subsequent potential applications in drug delivery, $PEG_{5k}$-[G2]-$(N_3)_9$ with 9 peripheral azides was selected for functionalization with Alk-Cat. Because of the higher viscosity of PEGylated copolymers, the azide concentration of this TAAC reaction was set at 0.5 M, leaving untouched all other experimental conditions (120 ºC, tBuOH/$H_2O$ 1:1). IR monitoring indicated that the reaction was finished after 20 h. The reaction mixture was purified by ultrafiltration to obtain $PEG_{5k}$-[G3]-Cat in 86% yield as a product completely soluble in water and phosphate buffer (PB). In addition to the characteristic $^1H$ NMR signals of the conjugates mentioned above, the $^1H$ NMR spectrum of $PEG_{5k}$-[G3]-Cat showed the characteristic catechol protons at 6.31-6.66 ppm. When analyzed by DLS, the aqueous solutions of $PEG_{5k}$-[G3]-Cat revealed the presence of micelles of ca. 20 nm (Scheme 18 and Figure 47), which have been exploited for the encapsulation of the anticancer drug doxorubicin (DOX).

Micelles are nanoassembles used in drug delivery for the encapsulation of poorly water-soluble drugs. They consist of a hydrophobic core that solubilizes and stabilizes hydrophobic molecules and a hydrophilic shell that makes the whole assembly soluble in water. In the case of $PEG_{5k}$-[G3]-Cat, the catechol units located on the dendritic periphery grant the system with amphiphilic character that promotes the spontaneous formation of micelles.

DOX is a widely-used chemotherapeutic agent for the treatment of cancer (bladder, breast, lung, stomach, ovarian), lymphomas and certain leukemias, which unfortunately produces severe side-effects, including cardiac toxicity and myelosuppression.[266] Although improved pharmacokinetics and reduced toxicity have been achieved by encapsulation within liposomes (Myocet, Doxil/Caelyx), clinical data do not suggest enhanced antitumor efficacy compared to free

[266] Tacar, O.; Sriamornsak, P.; Dass, C. R. *Journal of pharmacy and pharmacology* **2013**, *65*, 157.

DOX,[267] which has prompted the search of more efficient drug delivery systems. With this aim, DOX was encapsulated into $PEG_{5k}$-[G3]-Cat via a dialysis method that afforded micelles of ca 27 nm in size. Evaluation of the encapsulation by fluorescence revealed an encapsulation efficiency (EE) of 87% and drug loading (DL) of 29%. Preliminary experiments on the efficiency of the DOX-loaded $PEG_{5k}$-[G3]-Cat micelles for cell internalization are currently underway.

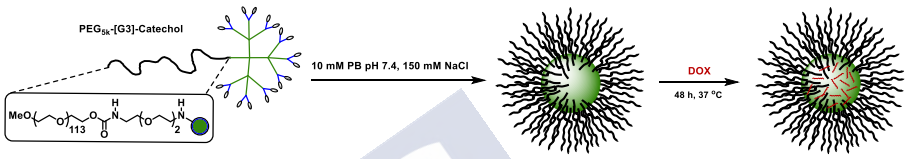


*Scheme 18. Schematic representation of the formation of $PEG_{5k}$-[G3]-Cat micelles and the encapsulation of DOX.*

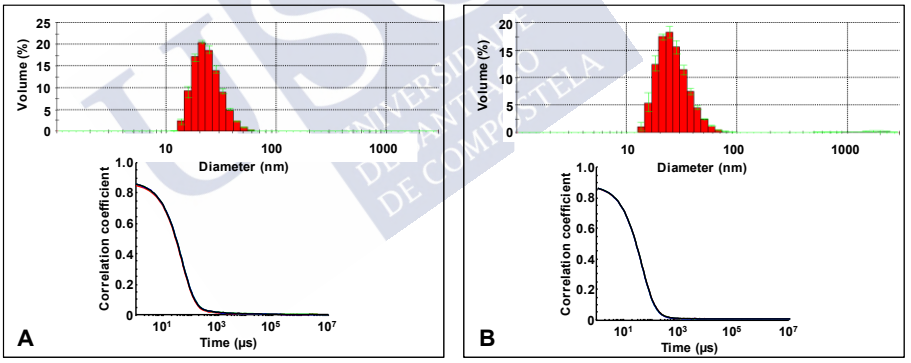


*Figure 47. DLS histograms (10 mM PB pH 7.4, 150 mM NaCl) of $PEG_{5k}$-[G3]-Cat micelles at 25 ºC (A) and DOX-loaded PEG5k-[G3]-Cat micelles at 37 ºC (B).*

[267] Hofheinz, R.-D.; Gnad-Vogt, S. U.; Beyer, U.; Hochhaus, A. *Anti-cancer drugs* **2005**, *16*, 691.

### 3.3.5 Dendrimer functionalization with carbohydrates

#### 3.3.5.1 Functionalization with Alk-Glu

Because of the role of sugars in biology (see sections 3.3.7 and 3.4), it was proposed to functionalize several dendrimer generations with sugars such as glucose and mannose. Following TAAC conditions, two different dendrimers 3[G1]-$N_3$ and 3[G3]-$N_3$ were surface functionalized with Alk-Glu at 120 $^oC$. The concentration for both reactions was 0.5 M because of the high viscosity of the reaction mixture at higher concentrations. The reactions were monitored with IR that confirmed their completion after 12-14 h. Both reactions were purified by ultrafiltration to yield the dendrimer conjugates in 91% and 92% yields, respectively. Beside of the characteristic $^1H$ NMR signals of new protons at 5.36-5.11 ppm, $^1H$ NMR also confirmed the purity and reaction completion according to the spectral data that matched the dendrimer and glucose part, particularly the anomeric protons at around 4.38-4.54 ppm. $^{13}C$ NMR additionally confirmed the success of functionalization by appearance of the characteristic anomeric carbon signal at around 106.5 ppm, GPC (Figure 45) and DLS (Figure 46) also confirmed the purity, monodispersity and reaction compilation.

#### 3.3.5.2 Functionalization with Alk-Man

Similar to section 3.3.5.1, functionalization of 3[G3]-$N_3$ with Alk-Man afforded the expected mannosylated dendrimer in excellent (93%) yield. To explore the scope and limitations of the current TAAC reaction for the functionalization of high dendrimer generations with sterically demanding, large ligands, 3[G4]-$N_3$ with 243 terminal azides was selected to be functionalized with Alk-Man. Following reaction conditions as above (0.5 M of azides, 120 $^oC$, tBuOH/$H_2O$ 5:1), reaction completion was confirmed by IR after just 12 h. The reaction was purified by ultrafiltration to obtain the corresponding adduct in 94% yield.

$^1H$ NMR confirmed in both cases the purity and full functionalization according to the integration of characteristic proton

signals at ca. 5.10-5.36 ppm, and the appearance of anomeric protons at ca. 4.83-4.88 ppm. Moreover, $^{13}C$ NMR was an additional tool confirming the clicking of Alk-Man onto dendrimers based on the appearance of characteristic anomeric carbons at around 100.00 ppm. Finally, GPC (Figure 45) and DLS (Figure 46) data also confirmed the purity and monodispersity of the conjugates.

### 3.3.6 Dendrimer functionalization with DOTA chelating agents

The high solubility of Alk-DOTA in water made challenging its isolation. Therefore, for the preparation of dendrimers functionalized with DOTA ligands, it was proposed to rely on a one-pot alkyne preparation-TAAC conjugation strategy. Accordingly, Alk-DOTA was synthesized by coupling of Alk-TEG-$NH_2$·HCl with a commercial isothiocyanate-DOTA derivative (p-NCS-Bz-DOTA-GA) in DMSO. The reaction was monitored by TLC using ninhydrin staining, which confirmed no free amino groups after 24 h of reaction time. Then, TAAC coupling was immediately carried out by simply adding a dendrimer like 3[G3]-$N_3$, followed by stirring at 120 $^oC$. IR monitoring confirmed reaction completion after 32 h. Then, the reaction was ultrafiltered to afford the dendrimer conjugate 3[G4]-DOTA in 90% overall yield. $^1H$ NMR spectral data matched very well with those of the dendrimer and DOTA, particularly at 2.26-2.55 and 1.82-2.11 ppm, in addition to the appearance of the characteristic signals produced after cycloaddition at 5.40-5.10 ppm.

To verify the absence of free amino groups in the final product coming from an incomplete first step, the reaction product was subjected to a ninhydrin test, consisting of reaction of any potential amino group with ninhydrin, followed by determination of the resulting chromophore (Ruhemann dye) (Figure 48) by absorbance at 570 nm. To this end, a calibration curve of Ruhemann's dye was realized first with a series of solutions of known concentration of 2-(2-(2-aminoethoxy)ethoxy)-ethanol as a model amine mimicking the terminal amino groups in the alkynated ligands. Gratifyingly, application of the calibration curve to 3[G4]-DOTA confirmed the absence of free amino groups.

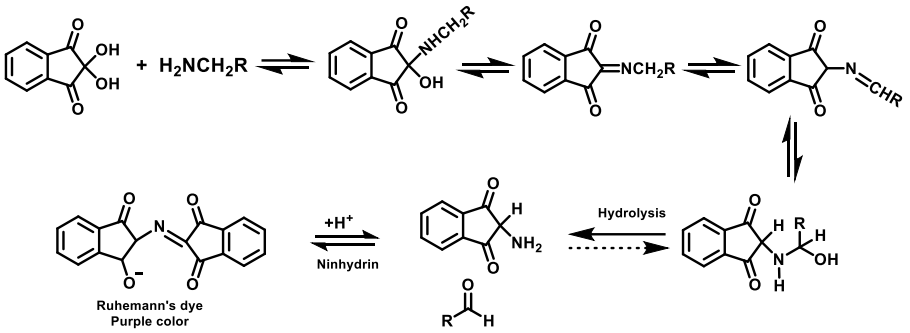


*Figure 48. Mechanism of reaction of a primary amine with ninhydrin to produce Ruhemann's dye (purple color).*[268]

### 3.3.7 Dendrimer multifunctionalization: simultaneous conjugation with alkynated mannose, biotin and FITC ligands

Having functionalized GATG dendrimers of several families and generations by means of TAAC with alkynated ligands of different nature, it was obvious that neither the dendrimer generation nor ligand functionality had an impact on the kinetics of TAAC. Based on this experimental fact, it was decided to exploit this advantage for the preparation of multifunctionalized dendrimers in a one-pot procedure. It was hypothesized that mixing any dendrimer with different ligands in a certain proportion (azide:total alkyne ratio, 1:2) would afford a dendrimer functionalized with those ligands in the same feeding ratio.

With the aim of exploring this possibility, biotin and mannose were selected as recognition ligands of biomedical interest, along with FITC as fluorescent probe. The objective was to prepare a multifunctionalized dendrimer with the three ligands in a ratio determined by the feeding ratio of these ligands in solution.

Indeed, although vitamins are required for living cell survival, the rapid division, growth, and proliferation of cancer cells results in an extra necessity of certain vitamins to sustain their rapid

[268] Friedman, M. *Journal of agricultural and food chemistry* **2004**, *52*, 385.

metabolism.[269] Consequently, receptors of vitamins are usually overexpressed on cancer cells surface, which converts them into useful biomarkers for diagnosis and tumor-targeting drug delivery.[270] Biotin is one of these vitamin class. It is a growth promoter, with content in cancer cells higher than that in normal tissues.[269] Accordingly, the biotin receptor has emerged as a newer tumor-specific target besides the widely recognized folate receptor.[271]

On the other hand, protein-carbohydrate interactions on the surface of cells play important roles in cellular processes.[272] The functionalization of dendrimers with sugars, particularly mannose, affords useful tools to study protein-carbohydrate interactions.[144,145,273] Remarkably, changing the size of the dendrimer and controlling the amount of mannose functionalization on the surface of a dendrimer, affect significantly the number of lectins that can be bound with the dendrimer, and control the relative activity of the dendrimer for the lectin.[274,275,126]

Accordingly, to verify our hypothesis about multifunctionalization, 3[G3]-$N_3$ (with 81 terminal azides) was challenged to be peripherally decorated with three functionalized alkynes: Alk-Man, Alk-Bio, and Alk-FITC in ratio 60:16:5, respectively. The TAAC reaction was performed under 0.5 M concentration of azides (as for 100% Alk-Man) at 120 ºC, in tBuOH/$H_2O$ 1:1. The reaction was monitored by IR that confirmed completion after 14 h. The reaction was purified by ultrafiltration to

[269] Russell-Jones, G.; McTavish, K.; McEwan, J.; Rice, J.; Nowotnik, D. *Journal of inorganic biochemistry* **2004**, *98*, 1625.
[270] Chen, S.; Zhao, X.; Chen, J.; Chen, J.; Kuznetsova, L.; Wong, S. S.; Ojima, I. *Bioconjugate. Chem* **2010**, *21*, 979.
[271] Chen, J.; Chen, S.; Zhao, X.; Kuznetsova, L. V.; Wong, S. S.; Ojima, I. *J. Am. Chem. Soc.* **2008**, *130*, 16778.
[272] Schlick, K. H.; Udelhoven, R. A.; Strohmeyer, G. C.; Cloninger, M. J. *Mol. Pharm* **2005**, *2*, 295.
[273] Roy, R. *Trends in Glycoscience and Glycotechnology* **2003**, *15*, 291.
[274] Woller, E. K.; Cloninger, M. J. *Org. Lett* **2002**, *4*, 7.
[275] Woller, E. K.; Walter, E. D.; Morgan, J. R.; Singel, D. J.; Cloninger, M. J. *J. Am. Chem. Soc.* **2003**, *125*, 8820.

afford 3[G4]-$(Man)_{60}$/$(Bio)_{16}$/$(FITC)_5$ as a red foam in 96% yield. The incorporation of 5 Alk-FITC on average was determined by absorbance at 519 nm in DMSO (applying an extinction coefficient of 60800 $M^{-1}$ $cm^{-1}$) to calculate the degree labeling of the dendrimer. $^1H$ NMR characteristic signals of mannose at 4 90 ppm and the two signals of biotin at 2.93-2.64 ppm and 2.30-2.12 ppm were integrated to quantify the ratio of the both ligands, which matched the expected degrees of substitution: 16 and 60 for biotin and mannose, respectively. In addition, $^1H$ and $^{13}C$ NMR confirmed the purity of the dendrimer conjugate based on the characteristic signals of the three types of ligands.

### 3.4 Agglutination assay: interaction of the multifunctionalized dendrimer 3[G4]-$(Man)_{60}$/$(Bio)_{16}$/$(FITC)_5$ with concanavalin A

Carbohydrates participate in many biological processes, like intercellular recognition and pathogen identification via carbohydrate-protein (lectin) interactions.[272,276] Many viral and bacterial infections and fertilization are examples of these interactions.[277] While monovalent carbohydrate interactions are usually weak, nature applies multivalency to increase the strength of binding and specificity,[278] a phenomenon known as cluster-glycoside effect.[279]

Presentation of multivalent carbohydrates to different receptors has been achieved by using natural and synthetic scaffolds, like glycoproteins[280,281] and polymers.[282,283] Recently, dendrimers have

[276] Ambrosi, M.; Cameron, N. R.; Davis, B. G. *Org. Biomol. Chem.* **2005**, *3*, 1593.
[277] Lis, H.; Sharon, N. *Chem. Rev.* **1998**, *98*, 637.
[278] Mann, D. A.; Kanai, M.; Maly, D. J.; Kiessling, L. L. *J. Am. Chem. Soc.* **1998**, *120*, 10575.
[279] Lundquist, J. J.; Toone, E. J. *Chem. Rev.* **2002**, *102*, 555.
[280] Lundquist, J. J.; Debenham, S. D.; Toone, E. J. *J. Org. Chem.* **2000**, *65*, 8245.
[281] Allen, J. R.; Harris, C. R.; Danishefsky, S. J. *J. Am. Chem. Soc.* **2001**, *123*, 1890.
[282] Fraser, C.; Grubbs, R. H. *Macromolecules* **1995**, *28*, 7248.
[283] Ponader, D.; Wojcik, F.; Beceren-Braun, F.; Dernedde, J.; Hartmann, L. *Biomacromolecules* **2012**, *13*, 1845.

emerged as an alternative multivalent architecture with globular structure.[284] Many examples of saccharide-functionalized dendrimers have been reported.[145,285,286,287,288,289]

Concanavalin A (Con A) is a lectin (carbohydrate binding protein) commonly used to probe multivalent carbohydrate-receptor interactions.[290] Con A shows a pH-dependent dissociation equilibrium between dimeric and tetrameric forms. Below pH 5 Con A exists as a dimer with monomeric subunits prevailing at even lower pH values. At pH higher than 6, Con A reconstructs as a tetramer.[291] Con A shows specificity for α-D mannose and α-D glucose.[292] The presence of calcium and a transition metal ion is necessary for the carbohydrate-binding activity.[293,294,295,296]

To demonstrate the ability of our multifunctionalized dendrimer [G4]-$(Man)_{60}$/$(Bio)_{16}$/$(FITC)_5$ carrying 60 copies of mannose to recognize a natural receptor like Con A, a solution of the dendrimer with concentration 1.67 mM of terminal mannoses was incubated with increasing concentrations of Con A (10 τL aliquots of a 17 τ M Con A solution) and the interaction was monitored in a turbidity assay by measuring the absorbance at 700 nm (highest transmittance of the

[284] He, H.; Yuan, Q.; Bie, J.; Wallace, R. L.; Yannie, P. J.; Wang, J.; Lancina III, M. G.; Zolotarskaya, O. Y.; Korzun, W.; Yang, H. *Translational Research* **2018**, *193*, 13.
[285] Esfand, R.; Tomalia, D. A. *Drug Discov. Today.* **2001**, *6*, 427.
[286] Boas, U.; Heegaard, P. M. *Chemical Society Reviews* **2004**, *33*, 43.
[287] Wolfenden, M. L.; Cloninger, M. J. *J. Am. Chem. Soc.* **2005**, *127*, 12168.
[288] Wolfenden, M. L.; Cloninger, M. J. *Bioconjugate. Chem* **2006**, *17*, 958.
[289] Vasu, K.; Naresh, K.; Bagul, R.; Jayaraman, N.; Sood, A. *Appl. Phys. Lett.* **2012**, *101*, 053701.
[290] Zatta, P. F.; Cummings, R. D. *Biochem. Educ.* **1992**, *20*, 2.
[291] AUER, H. E.; SCHILZ, T. *International journal of peptide and protein research* **1984**, *24*, 462.
[292] Mandal, D. K.; Kishore, N.; Brewer, C. F. *Biochemistry* **1994**, *33*, 1149.
[293] Hardman, K. D.; Agarwal, R. C.; Freiser, M. J. *Journal of molecular biology* **1982**, *157*, 69.
[294] Loris, R.; Hamelryck, T.; Bouckaert, J.; Wyns, L. *Biochimica et biophysica acta (BBA)-Protein structure and molecular enzymology* **1998**, *1383*, 9.
[295] Brown, R. D.; Brewer, C. F.; Koenig, S. H. *Biochemistry* **1977**, *16*, 3883.
[296] Brewer, C. F.; Brown III, R. D.; Koenig, S. H. *Biochemistry* **1983**, *22*, 3691.

dendrimer solution).[126,229] In this experiment, lysosome was selected as control non-aggregating protein. Figure 49 clearly illustrates that aggregation already starts after the second addition of Con A, with increasing aggregation being observed up to 120 τL of the Con A solution, after which no further increases in absorbance are observed. Interestingly, when a saturated solution of α-methyl-D-mannopyranoside (10 τL) was added, the mixture recovered the original absorbance value (no aggregation), indicating complete disaggregation. When the experiment was applied to a 17 τM solution of lysozyme in the same buffer as a control protein, no aggregation was seen in agreement with the expected lack of mannose recognition.

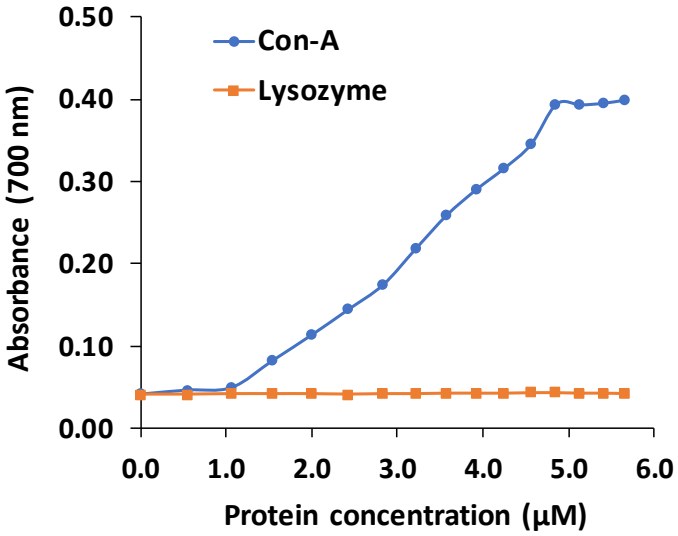


*Figure 49. Aggregation of 3[G4]-$(Man)_{60}$/$(Bio)_{16}$/$(FITC)_5$ with Con A in 20 mM Tris-HCl, 250 mM NaCl, 1 mM $CaCl_2$, 1 mM $MnCl_2$, as determined by absorbance at 700 nm. Lysozyme was used as control non-interacting protein.*

### 3.5 Incubation of 3[G4]-$(Man)_{60}$/$(Bio)_{16}$/$(FITC)_5$ with streptavidin-agarose beads

Streptavidin (SA) is a biotin-binding protein found as homotetramer (one biotin per SA subunit) (Figure 50). The high affinity of the biotin-streptavidin binding makes the system a useful and attractive technology for bioconjugation.[297] Indeed, with a dissociation constant ca. $10^{-15}$ M, the biotin-SA interaction is recognized as the strongest noncovalent interaction.[298,299,300] As a result, it has been exploited in the detection of proteins, lipids and nucleic acids, as well as for the purification of proteins.[301,302] A high stability over a wide range of pH and temperature, great tolerance to organic solvents and denaturing agents, and a high specificity are advantages provided by the SA-biotin binding.[303,304,305]

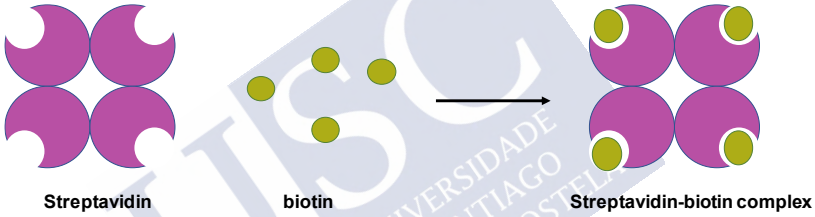


*Figure 50. Schematic representation of streptavidin-biotin interaction.*

[297] Vajda, S.; Wheng, Z.; Rosenfeld, R.; DeLisi, C. *Biochemistry* **1994**, *33*, 13977.
[298] Weber, P.; Wendoloski, J.; Pantoliano, M.; Salemme, F. *J. Am. Chem. Soc.* **1992**, *114*, 3197.
[299] Chilkoti, A.; Stayton, P. S. *J. Am. Chem. Soc.* **1995**, *117*, 10622.
[300] Chaiet, L.; Wolf, F. J. *Arch. Biochem. Biophys.* **1964**, *106*, 1.
[301] de Boer, E.; Rodriguez, P.; Bonte, E.; Krijgsveld, J.; Katsantoni, E.; Heck, A.; Grosveld, F.; Strouboulis, J. *Proceedings of the National Academy of Sciences* **2003**, *100*, 7480.
[302] Wu, S.-C.; Wong, S.-L. *PloS one* **2013**, *8*, e69530.
[303] Sano, T.; Vajda, S.; Cantor, C. R. *Journal of Chromatography B: Biomedical Sciences and Applications* **1998**, *715*, 85.
[304] Stayton, P. S.; Freitag, S.; Klumb, L. A.; Chilkoti, A.; Chu, V.; Penzotti, J. E.; To, R.; Hyre, D.; Le Trong, I.; Lybrand, T. P. *Biomol. Eng.* **1999**, *16*, 39.
[305] Laitinen, O.; Hytönen, V.; Nordlund, H.; Kulomaa, M. *Cell. Mol. Life Sci.* **2006**, *63*, 2992.

To verify the bioactivity of the biotin molecules on the surface of the multifunctionalized dendrimer 3[G4]-$(Man)_{60}/(Bio)_{16}/(FITC)_5$, a recognition assay using agarose beads functionalized with SA was devised that exploits the fluorescent signal of the FITC probes on the dendrimer. To this end, SA-agarose beads and unfunctionalized blank beads taken as control (no SA) were incubated separately with 3[G4]-$(Man)_{60}/(Bio)_{16}/(FITC)_5$ for 2 h. After removal of the supernatant by centrifugation washing with PBS, both bead samples were analyzed by fluorescence microscopy that revealed the SA-agarose beads as green (FITC), while no fluorescence was seen in the control beads (Figure 51). This result confirms that a selective interaction exits between the biotin ligands on the surface of the dendrimer and the SA supported on the beads. Overall, both mannose and biotin ligands on the surface of the dendrimer are selectively recognized by specific protein receptors in solution and the interaction can be monitored thanks to a fluorescent probe (FITC) also on the dendrimer.

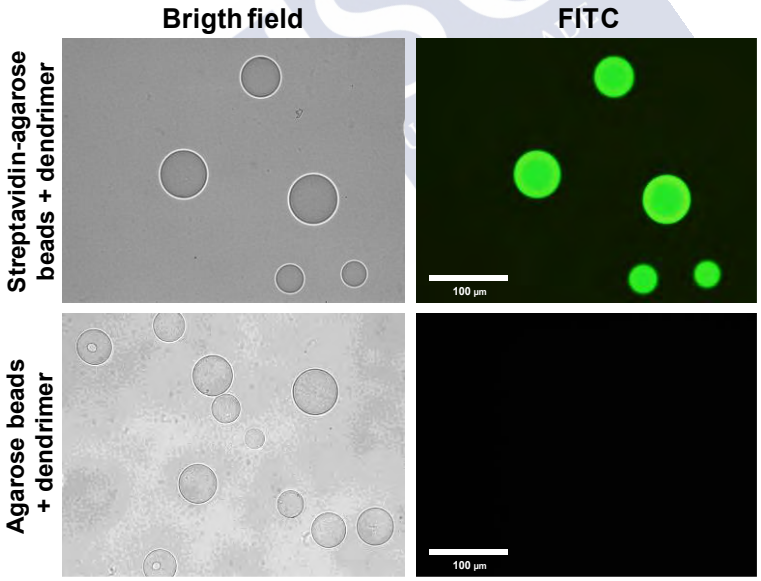


*Figure 51. Fluorescence microscopy images of streptavidin-agarose beads treated with the biotinylated, fluorescently labelled dendrimer 3[G4]-$(Man)_{60}/(Bio)_{16}/(FITC)_5$. A control with unfunctionalized beads (no streptavidin) is shown.*

# 4 Experimental and Methods

## 4.1 Materials

2-Butyne-1,4-diol, N,N′-disuccinimidyl carbonate (DSC), biotin, agarose beds, concanavalin A (Con A), 2-(Boc-oxyimino)-2-phenylacetonitrile, 2,2`-(ethylenedioxy)bis(ethylamine), 2-[2-(2-chloroethoxy)ethoxy]ethanol, 4-hydroxybenzylamine, D-(+)-mannose, D-(+)-glucose, ethanolamine, and fluorescein-5-isothiocyanate (FITC) were purchased from Sigma-Aldrich. p-NCS-Bz-DOTA-GA was purchased from CheMatech. All other chemicals were purchased from Sigma-Aldrich or Acros Organics and were used without further purification. All solvents were HPLC grade, purchased from Scharlab, Sigma-Aldrich or Acros Organics and used without further purification. DMSO, $Et_3N$ and pyridine were dried under 4Å molecular sieves. MeCN, DMF, THF and $CH_2Cl_2$ were dried using a SPS800 solvent purification system from MBRAUN. $H_2O$ was Milli-Q grade and was obtained using a Millipore water purification system. $PEG_{5k}$-$PGA_{25}$-$N_3$,[135] $PEG_{5k}$-[G2]-$N_3$,[127] GATG repeating unit,[125] GATG-dendrimers[140] and 2-[2-(2-azidoethoxy)ethoxy]ethanol[143] were prepared following previously reported procedures by our group. 2-[2-(2-Aminoethoxy)ethoxy]-ethanol[125,306] and tert-butyl (2-(2-(2-aminoethoxy)ethoxy)ethyl)carbamate[219] were prepared following known procedures. Mannose and glucose trichloroacetimidates were prepared following known procedures.[307,308,309]

---

[306] Airoldi, C.; Zona, C.; Sironi, E.; Colombo, L.; Messa, M.; Aurilia, D.; Gregori, M.; Masserini, M.; Salmona, M.; Nicotra, F. *Journal of biotechnology* **2011**, *156*, 317.

[307] Montanez, M. I.; Hed, Y.; Utsel, S.; Ropponen, J.; Malmstrom, E.; Wagberg, L.; Hult, A.; Malkoch, M. *Biomacromolecules* **2011**, *12*, 2114.

[308] Ren, T.; Liu, D. *Tetrahedron Lett* **1999**, *40*, 7621.

[309] Nagahori, N.; Nishimura, S.-I. *Biomacromolecules* **2001**, *2*, 22.

## 4.2 Instrumentation

### 4.2.1 Column chromatography

Automated column chromatography was performed on a MPLC Teledyne ISCO CombiFlash RF 200 psi with RediSep Rf normal-phase 4 g or 12 g silica columns and columns refilled with neutral aluminium oxide 70–230 mesh from Merck. Samples were adsorbed onto silica gel 40-63 $\tau$m or neutral aluminium oxide 70–230 mesh from Merck and loaded into solid cartridges.

### 4.2.2 Ultrafiltration

Purifications by ultrafiltration were performed on Millipore Amicon stirred cells with Amicon YM3 and YM5 regenerated cellulose membranes under a 5 psi $N_2$ pressure.

### 4.2.3 NMR spectroscopy

NMR spectra were recorded on Varian Mercury 300 MHz, Varian Inova 500 MHz or Varian NMR Innova 750 MHz spectrometers. Chemical shifts were reported in ppm (δ units) downfield from internal tetramethylsilane (TMS) ($CDCl_3$), the HOD residual solvent peak ($CD_3OD$ and $D_2O$), or residual solvent peak (DMSO-$d_6$, and $CD_3CN$). All spectra were analyzed using MestReNova software.

### 4.2.4 Infrared spectroscopy

FT-IR spectra were recorded on a Bruker IFS-66v using KBr pellets or neat samples (CsI window), or on a Perkin-Elmer Spectrum Two spectrophotometer.

### 4.2.5 UV-Vis spectroscopy

UV-Vis measurements were recorded on a Jasco V-630 spectrophotometer.

### 4.2.6 ESI-FIA-TOF Mass spectrometry

Electrospray Ionization (ESI) Flow injection Analysis (FIA) Time-of-flight (TOF) mass spectrometry was carried out on a Tandem HPLC (Agilent 1100)-MS (Bruker Microtof). The ESI source was equipped with a gas flow counter current of 1 τL/min under temperature control.

### 4.2.7 Elemental analysis

Samples were analyzed in a Thermo Finnigan Flash 1112 elemental analyzer.

### 4.2.8 Gel permeation chromatography (GPC)

GPC experiments were performed on an Agilent 1100 series separation module using a polyanionic and neutral column type composed of a PSS SDV pre-column (5 τm, 8 x 50 mm) and a Suprema Lux 100A connected to an Agilent 1100 series UV detector. A 10 mM PB pH 7.4, 150 mmol LiCl solution was used as eluent at 1 mL/min. Samples at 1 mg/mL were filtered through 0.45 τm PTFE filters before injection.

### 4.2.9 Dynamic light scattering (DLS)

DLS measurements were carried out on a Malvern Nano ZS (Malvern Instruments, U.K.) operating at 633 nm with a 173º scattering angle, at 25 ºC. Hydrodynamic diameters of the dendrimer conjugates were measured in 10 mM PB pH 7.4, 150 mM LiCl at a concentration 1.0 mg/mL and 25 ºC. Mean diameters were obtained from the volume particle size distribution provided by Malvern Zetasizer Software.

### 4.2.10 Fluorescence microscopy

Samples were observed by fluorescence microscopy using an Olympus BX-51 microscope equipped with an Olympus DP-71 camera. The following parameters of the fluorescent channels were used. Blue channel: ultraviolet excitation U-MWU2; excitation filter 360-370 nm, emission filter 420 nm and dichromatic mirror 400 nm. Green channel: blue excitation U-MWB2; excitation filter 460-490 nm, emission filter 520 nm and dichromatic mirror 500 nm. Red channel: green excitation UMNG2; excitation filter 530-550- nm, emission filter 590 nm and dichromatic mirror 570 nm. Images were processed with Adobe Photoshop software.

## 4.3 Synthesis of Gn GATG dendrimers

### 4.3.1 General procedure for the synthesis of 2[Gn] GATG dendrimers

GATG repeating unit (1.25 equiv per amine group), HOBt (1.25 equiv per amine group) and EDC (1.25 equiv per amine group) were added to a solution of (i) 2,2'-(ethylenedioxy)bis(ethylamine) in $CH_2Cl_2$ (0.1 M per amino group) or (ii) 2[G1]-$NH_2$·HCl, 2[G2]-$NH_2$·HCl or 2[G3]-$NH_2$·HCl dendrimers and $Et_3N$ (2.4 equiv per amine group) in DMSO (0.1 M per amino group) (Scheme 4). After stirring at rt for 12-24 h, (i) $CH_2Cl_2$ was removed by evaporation and the reaction mixture was dissolved in $CH_2Cl_2$ (30 mL) and washed with $H_2O$ (3 x 30 mL), or (ii) an extraction was done with $H_2O$/EtOAc (5 x 30 mL) followed by $H_2O$ (3 x 30 mL) when DMSO was used. In both cases, then, the organic layer was dried ($MgSO_4$) and concentrated to give a crude product that was purified by (i) automated MPLC (gradient from hexane to 30% MeOH/EtOAc, neutral alumina, 10 min) to afford 2[G1]-$N_3$ and 2[G2]-$N_3$. Alternatively (ii), purification of 2[G3]-$N_3$ and 2[G4]-$N_3$ was done by ultrafiltration (acetone/$H_2O$ 3:1, 3 x 50 mL; Amicon YM3-YM5).

### 4.3.2 Synthesis of 3[G0]-$N_3$ and 3[G0]-$NH_2$·HCl (core of 3[Gn] GATG dendrimers)

Phloroglucinol (1 equiv), dry $K_2CO_3$ (10 equiv) and 18-crown-6 (0.1 equiv) were added to a solution of 2-(2-(2-azidoethoxy)ethoxy)ethyl 4-methylbenzenesulfonate (1.1 equiv per OH) in DMF (Scheme 5). The resulting mixture was heated at 100 ºC for 48 h under Ar. After cooling down to rt, the solvent was evaporated, and the resulting crude product was filtered through a pad of neutral alumina (eluent gradient from hexane to acetone). The filtrate was concentrated and purified by MPLC (neutral alumina, gradient from hexane to EtOAc) to afford 3[G0]-$N_3$ as a colorless oil in 85% yield

$Ph_3P$ (1.25 equiv per azide group) was added to a solution of 3[G0]-$N_3$ in acetone/$H_2O$ (10:1 v/v) and the mixture was stirred at rt

for 6 h. Then, 3 M HCl (2 equiv per azide group) was added and the solvent was evaporated. The crude product was dissolved in $H_2O$ (30 mL) and the solution was filtered through a cotton plug and washed with $CHCl_3$ (3 x 30 mL). The aqueous phase was lyophilized to give 3[G0]-$NH_2$·HCl as a white foam (99%).

### 4.3.3 General procedure for the synthesis of 3[Gn] GATG dendrimers

GATG repeating unit (1.25 equiv per amine group), HOBt (1.25 equiv per amine group) and EDC (1.25 equiv per amine group) were added to a solution of 3[G0]-$NH_2$·HCl, 3[G1]-$NH_2$·HCl, 3[G2]-$NH_2$·HCl or 3[G3]-$NH_2$·HCl and $Et_3N$ (2.4 equiv per amine group) in DMSO (0.1 M per amino group) (Scheme 4). After stirring at rt for 12-24 h, the reaction mixture was distributed between $H_2O$ and EtOAc (5 x 30 mL) followed by washing with $H_2O$ (3 x 30 mL). The organic layer was dried ($MgSO_4$) and concentrated to give a crude product that was purified by automated MPLC (gradient from hexane to 30% MeOH/EtOAc, neutral alumina, 10 min) to afford 3[G1]-$N_3$ and 3[G2]-$N_3$, while 3[G3]-$N_3$ and 3[G4]-$N_3$ were purified by ultrafiltration (acetone/$H_2O$ 3:1, 3 x 50 mL; Amicon YM3-YM5).

## 4.4 Synthesis of functionalized alkynes

### 4.4.1 Alk-NHS

2-Butyne-1,4-diol (1.0 g, 12 mmol) was dissolved in dry $CH_3CN$ (36 mL). DSC (5.95 g, 23 mmol) and dry pyridine (1.9 mL, 23 mmol) were added and the reaction was stirred under argon at rt overnight. After evaporation under reduced pressure, the crude product was dissolved in EtOAc (90 mL) and washed with 1 M HCl (2 x 60 mL), $H_2O$ (3 x 60 mL) and brine (50 mL). The organic phase was dried ($MgSO_4$) and concentrated to afford Alk-NHS as a white solid (3.92 g, 92%) $^1$H-NMR (300 MHz, DMSO-$d_6$) δ: 5.22 (s, 4H), 2.81 (s, 8H). $^{13}$C-NMR (75 MHz, DMSO-$d_6$) δ: 169.8, 150.9, 81.6, 58.4, 25.4. ESI-HRMS *m/z*: found 391.0492. Calcd for $[M+Na]^+$ $C_{14}H_{12}N_2O_{10}Na$: 391.0384. IR: (KBr): 1793, 1788, 1730, 1197, 1092 $cm^{-1}$.

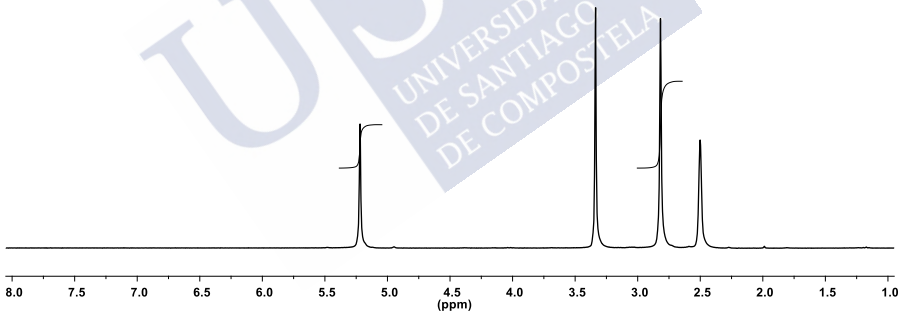


*Figure 52. $^1$H NMR spectrum (300 MHz, DMSO-$d_6$) of Alk-NHS.*

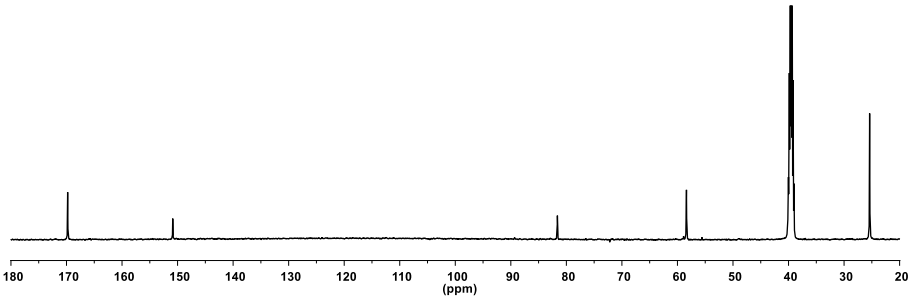


*Figure 53. $^{13}C$ NMR spectrum (75 MHz, DMSO-$d_6$) of Alk-NHS.*

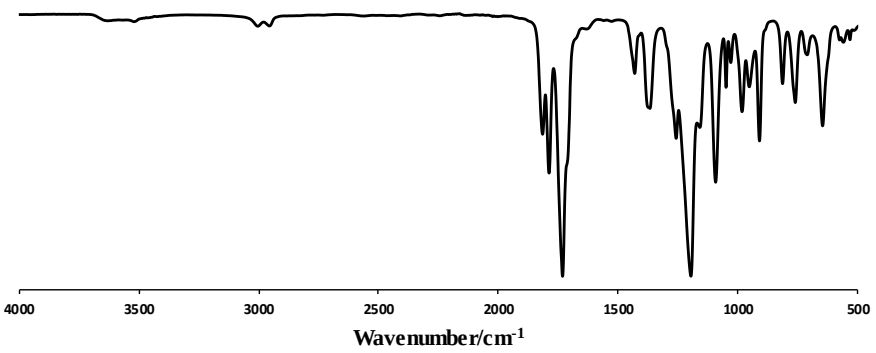


*Figure 54. IR (KBr) spectrum of Alk-NHS.*

### 4.4.2 Alk-TEG-NHBoc

Tert-butyl (2-(2-(2-aminoethoxy)ethoxy)ethyl)carbamate (1.18 g, 4.75 mmol) and $Et_3N$ (662 ɀ L, 4.75 mmol) were added to a solution of Alk-NHS (0.50 g, 1.36 mmol) in dry $CH_3CN$ (3.4 mL). The reaction was stirred at rt for 32 h under argon. After evaporation under reduced pressure, the crude product was dissolved in EtOAc (50 mL) and washed with 1 M HCl (2 x 50 mL), $H_2O$ (2 x 50 mL) and brine (50 mL). The organic phase was dried ($MgSO_4$) and concentrated to afford Alk-TEG-NHBoc as a yellow oil (848 mg, 98%).$^1$H NMR (300 MHz, $CDCl_3$) δ: 5.41 (br s, 1H), 5.06 (br s, 1H), 4.73 (s, 4H), 3.60 (s, 8H), 3.57-3.53 (m, 8H), 3.39 (dd, *J*=10.5, 5.2 Hz, 4H), 3.34-3.31 (m,

4H), 1.44 (s, 18H). $^{13}C$ NMR (75 MHz, $CDCl_3$) δ: 156.1, 155.6, 81.2, 79.3, 70.4, 70.2, 70.0, 52.6, 41.0, 40.4, 28.5. Elem. Anal. Found: C, 52.68; H, 8.12; N, 8.99, Calcd. for $C_{28}H_{50}N_4O_{12}$: C, 52.98; H, 7.94; N, 8.83. IR (neat, ATR): 3332, 1689, 1671, 1265 $cm^{-1}$.

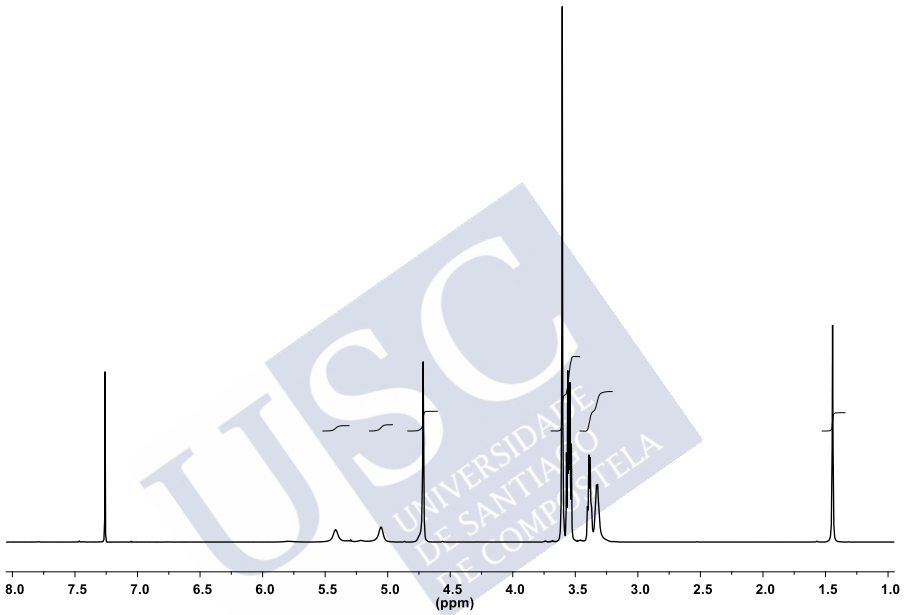


*Figure 55. $^1H$ NMR spectrum (300 MHz, $CDCl_3$) of Alk-TEG-NHBoc.*

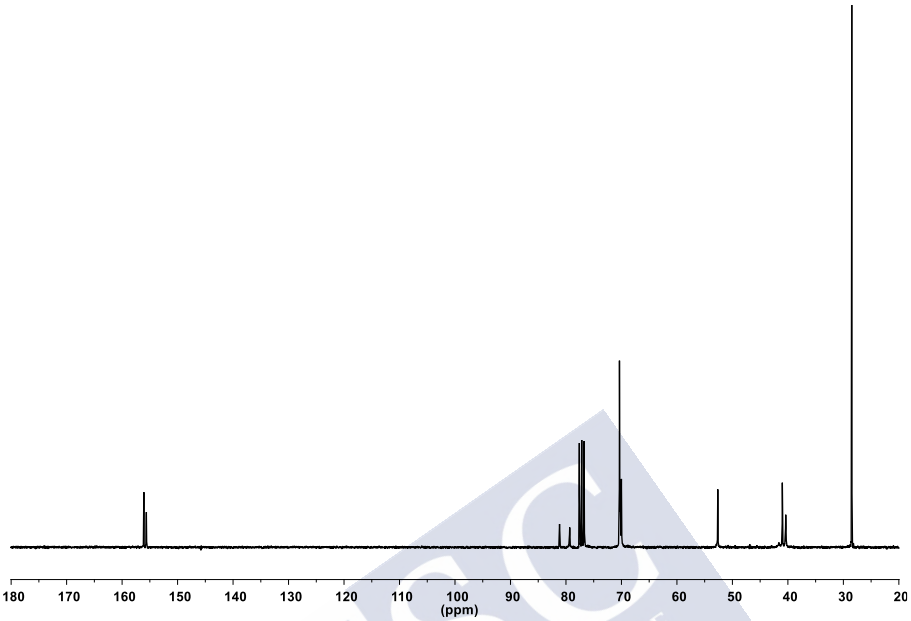


*Figure 56. $^{13}C$ NMR spectrum (75 MHz, $CDCl_3$) of Alk-TEG-NHBoc.*

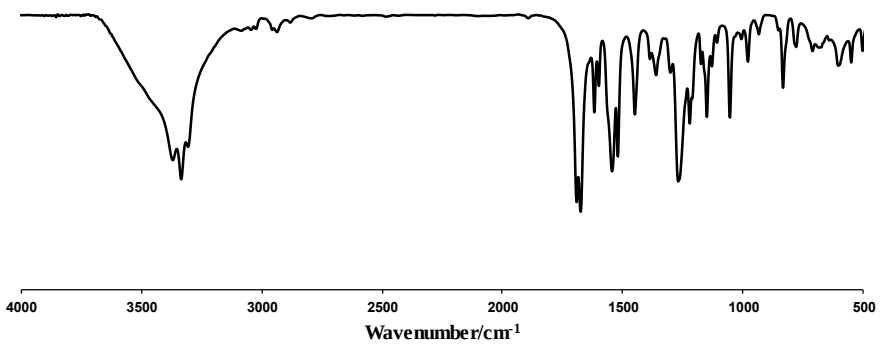


*Figure 57. IR (neat, ATR) spectrum of Alk-TEG-NHBoc.*

### 4.4.3 Alk-TEG-OH

Alk-NHS (420 mg, 1.14 mmol) was added to a solution of 2-(2-(2-aminoethoxy)ethoxy)ethanol (1.0 g, 6.83 mmol) in dry $CH_2Cl_2$ (5.7 mL) under argon. The reaction was stirred at rt overnight. The solvent was evaporated under reduced pressure and the crude product was purified by automated MPLC (gradient from $CH_2Cl_2$ to 10% MeOH/$CH_2Cl_2$, silica gel, 10 min) to afford Alk-TEG-OH as a clear oil (450 mg, 90%). $^1$H NMR (300 MHz, $CDCl_3$) δ: 5.70 (br s, 2H), 4.73 (s, 4H), 3.76-3.73 (m, 4H), 3.66-3.55 (m, 16H), 3.37 (t, *J*=4.9 Hz, 4H). $^{13}$C NMR (75 MHz, $CDCl_3$) δ: 155.7, 81.1, 72.6, 70.7, 70.2, 69.9, 61.4, 52.5, 40.8. ESI-HRMS *m/z* found 459.1950. Calcd for $[M+Na]^+$ $C_{18}H_{32}N_2NaO_{10}Na$: 459.1949. IR: (neat, ATR): 3331, 2875, 1703, 1536, 1252, 1098 $cm^{-1}$.

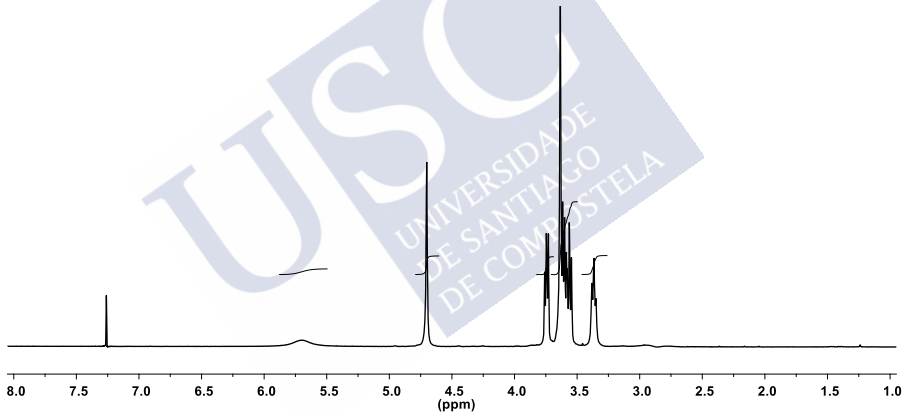


*Figure 58. $^1$H NMR spectrum (300 MHz, $CDCl_3$) of Alk-TEG-OH.*

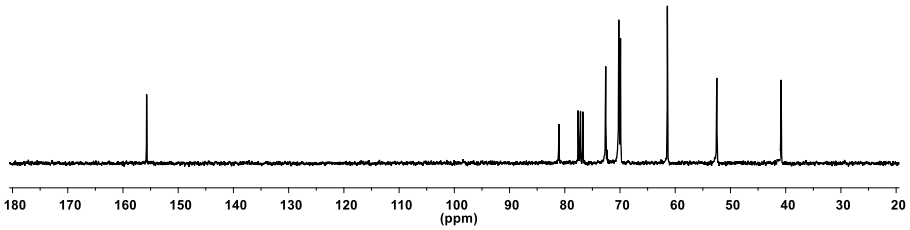


*Figure 59. $^{13}C$ NMR spectrum (75 MHz, $CDCl_3$) of Alk-TEG-OH.*

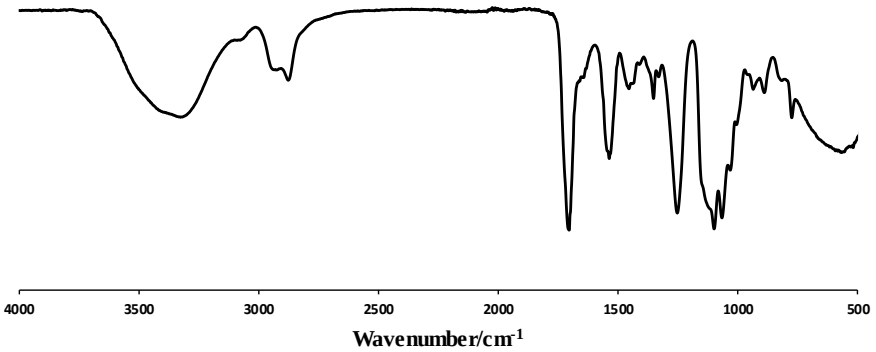


*Figure 60. IR (neat, ATR) spectrum of Alk-TEG-OH.*

### 4.4.4 Alk-OH

Ethanolamine (329 ɀ L, 5.44 mmol) was added to a solution of Alk-NHS (500 mg, 1.36 mmol) in dry $CH_3CN$ (6.2 mL) at 0 °C under argon. The reaction was stirred at rt for 4 h. The solvent was evaporated under reduced pressure and the crude product was purified by automated MPLC (gradient from $CH_2Cl_2$ to 10% MeOH/$CH_2Cl_2$, silica gel, 20 min) to afford Alk-OH as a white solid (340 mg,

96%).$^{1}$H NMR (300 MHz, $CD_3OD$) δ: 4.71 (s, 4H), 3.60 (t, *J*=5.8 Hz, 4H), 3.24 (t, *J*=5.8 Hz, 4H). $^{13}$C NMR (75 MHz, $CD_3OD$) δ: 158.1, 82.1, 61.8, 53.2, 44.3. Elem. Anal. Found: C, 45.87; H, 6.03; N, 10.92, Calcd. for $C_{10}H_{16}N_2O_6$: C, 46.15; H, 6.20; N, 10.76. IR (KBr): 3330, 2933, 1694, 1517, 1244, 1096 $cm^{-1}$.

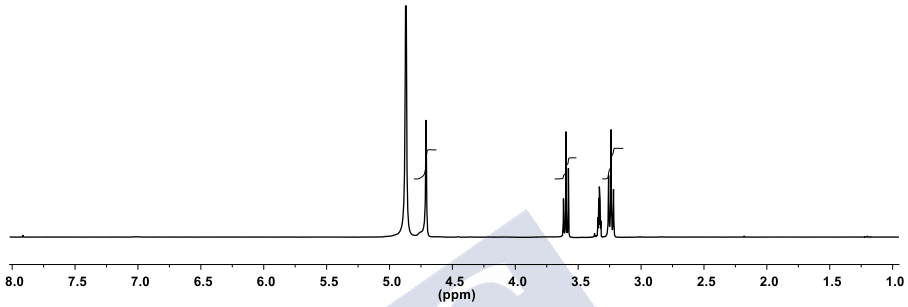


*Figure 61. $^{1}$H NMR spectrum (300 MHz, $CD_3OD$) of Alk-OH.*

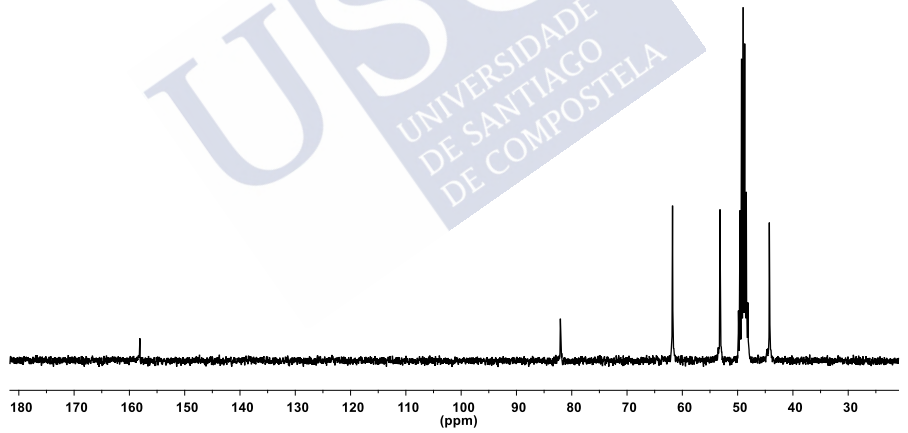


*Figure 62. $^{13}$C NMR spectrum (75 MHz, $CD_3OD$) of Alk-OH.*

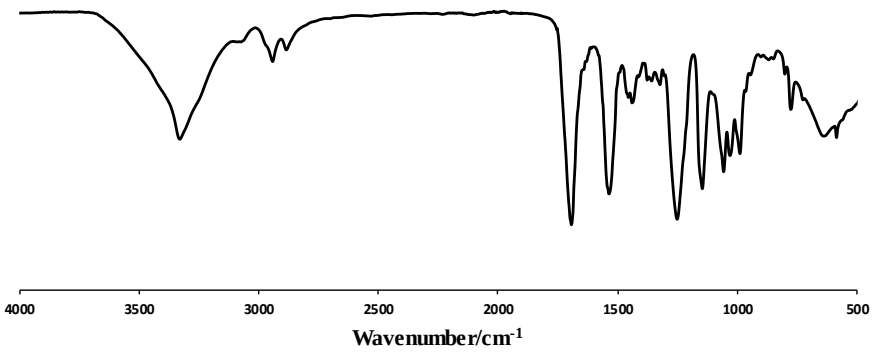


*Figure 63. IR (KBr) spectrum of Alk-OH.*

### 4.4.5 Alk-PhOH

4-Hydroxybenzylamine (293 mg, 2.38 mmol) was added to a solution of Alk-NHS (250 mg, 0.68 mmol) and $Et_3N$ (331 mL, 2.38 mmol) in dry DMF (3.4 mL). The reaction was stirred at rt for 32 h under argon. The reaction mixture was added to EtOAc (50 mL) and washed with 0.5 M HCl (3 x 30 mL), $H_2O$ (5 x 30 mL) and brine (30 mL). The organic phase was dried ($MgSO_4$) and concentrated to afford Alk-PhOH as a white solid (514 mg, 97%). $^1$H NMR (300 MHz, DMSO-$d_6$) δ: 9.26 (br s, 2H), 7.77 (br s, 2H), 7.04 (d, *J*=7.4 Hz, 4H), 6.69 (d, *J*=7.4 Hz, 4H), 4.70 (s, 4H), 4.08 (s, 4H). $^{13}$C NMR (75 MHz, DMSO-$d_6$) δ: 156.4, 155.5, 129.7, 128.5, 115.1, 81.6, 51.7, 43.6. Elem. Anal. Found: C, 62.11; H, 5.61; N, 6.99, Calcd. for $C_{20}H_{20}N_2O_6$: C, 62.49; H, 5.24; N, 7.29. IR (KBr): 3332, 1673, 1538, 1265, 1051 cm$^{-1}$

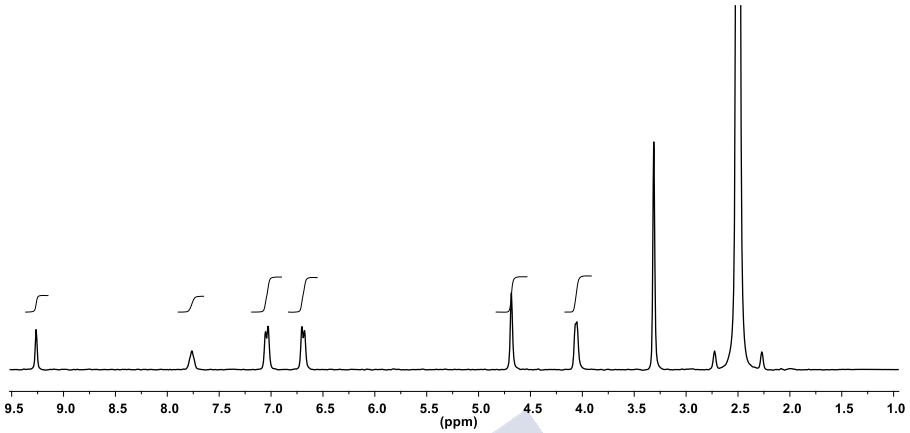


*Figure 64. $^{1}H$ NMR spectrum (300 MHz, DMSO-$d_6$) of AIk-PhOH.*

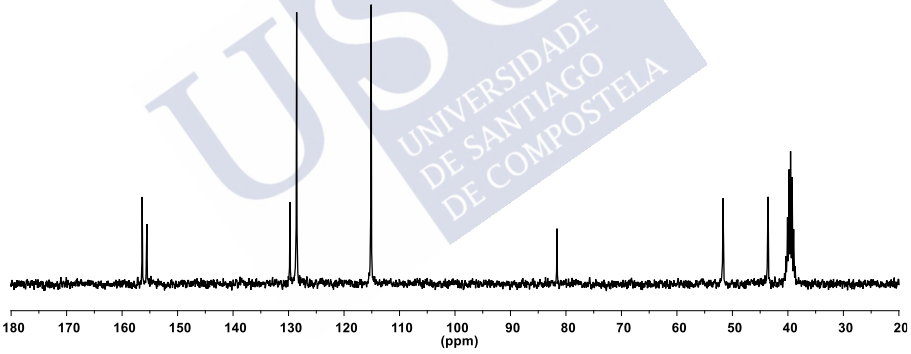


*Figure 65. $^{13}C$ NMR spectrum (75 MHz, DMSO-$d_6$) of AIk-PhOH.*

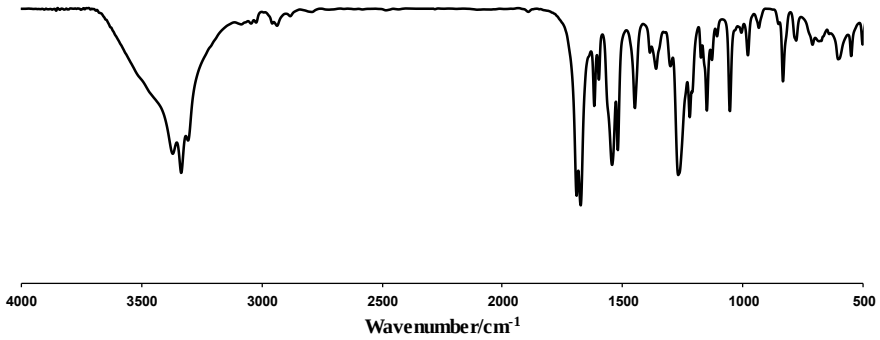


*Figure 66. IR (KBr) spectrum of Alk-PhOH.*

### 4.4.6 Alk-Cat

Alk-NHS (150 mg, 0.41 mmol) was added to a solution of dopamine hydrochloride (232 mg, 1.22 mmol) and $Et_3N$ (230 ɀ L, 1.63 mmol) in dry DMF (2.75 mL) under argon. The reaction was stirred at rt for 24 h. After evaporation under reduced pressure, the crude product was dissolved in EtOAc (50 mL) and washed with sat $NaHCO_3$ (3 x 50 mL) and $H_2O$ (2 x 50 mL). The organic phase was dried ($MgSO_4$) and concentrated to give a crude product that was purified by automated MPLC (gradient from hexane to EtOAc, silica gel, 30 min) to afford Alk-Cat as a yellow oil (167 mg, 92%). $^1H$ NMR (300 MHz, $CD_3CN$) δ: 6.74-6.47 (m, 6H), 5.65 (br s, 2H), 4.62 (s, 4H), 3.22 (dd, *J*=13.2, 6.7 Hz, 4H), 2.59 (t, *J*=7.0 Hz, 4H). $^{13}C$ NMR (75 MHz, $CD_3CN$) δ: 156.8, 145.6, 144.1, 132.4, 121.7, 117.0, 116.5, 82.4, 53.2, 43.6, 36.0. Elem. Anal. Found: C, 59.81; H, 5.23; N, 5.97, Calcd. for $C_{22}H_{24}N_2O_8$: C, 59.46; H, 5.44; N, 6.30. IR (neat, ATR): 3344, 1694, 1517, 1242 $cm^{-1}$.

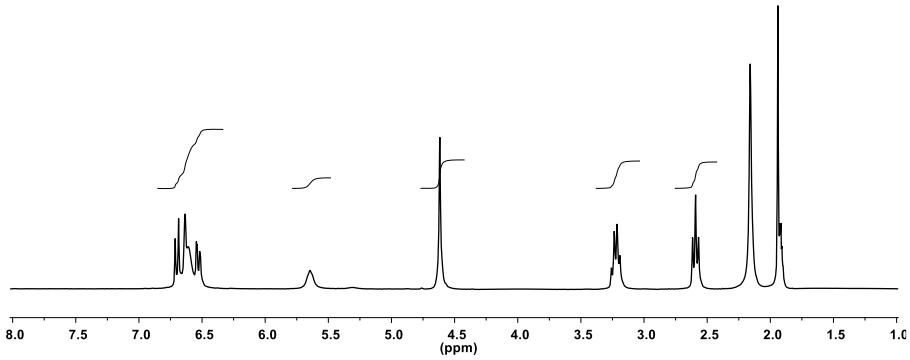


*Figure 67. $^{1}H$ NMR spectrum (300 MHz, $CD_3CN$) of Alk-Cat.*

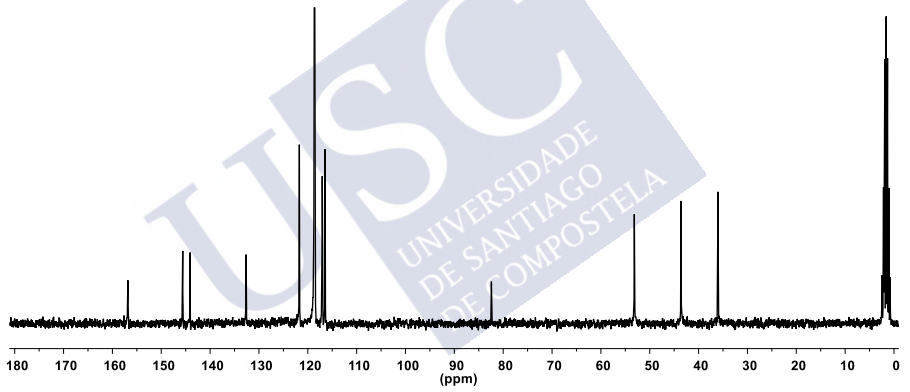


*Figure 68. $^{13}C$ NMR spectrum (75 MHz, $CD_3CN$) of Alk-Cat.*

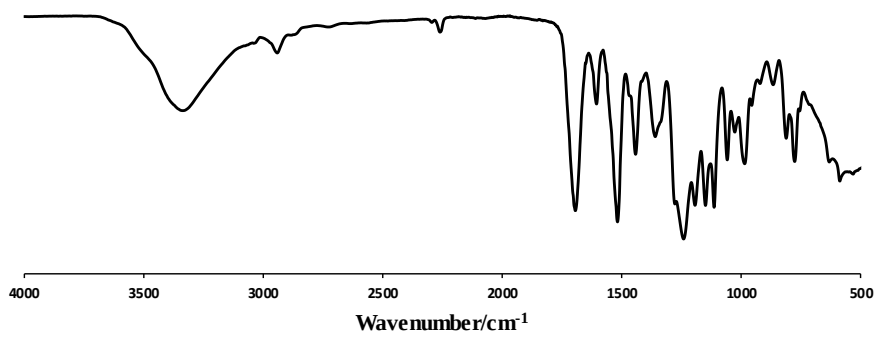


*Figure 69. IR (neat, ATR) spectrum of Alk-Cat.*

### 4.4.7 Alk-$OSO_3H \cdot NH_3$

$H_2SO_4$ (0.614 mL, 11.54 mmol) and $Ac_2O$ (1.08 mL, 11.54 mmol) were added to dry pyridine (9.6 mL). After 5 min of stirring at 55 ºC, Alk-OH (250 mg, 0.961 mmol) was added. The mixture was stirred at 55 ºC for 16 h and then cooled down to 0 ºC. Ammonium hydroxide (3.5 mL, 25%) was added and after 15 min of stirring at 0 ºC, the reaction mixture was concentrated under reduced pressure and lyophilized. Sublimation of ammonium acetate (40 ºC, 0.1 mmHg) afforded Alk-$OSO_3H \cdot NH_3$ as a white solid (359 mg, 89%). $^1$H NMR (300 MHz, $CD_3OD$) δ: 4.62 (s, 4H), 3.95 (t, *J*=5.5 Hz, 4H), 3.31 (t, *J*=5.5 Hz, 4H). $^{13}$C NMR (75 MHz, $CD_3OD$) δ: 157.8, 81.8, 69.5, 52.9, 44.0. Elem. Anal. Found: C, 26.06; H, 5.27; N, 12.05, Calcd. for $C_{10}H_{22}N_4O_{12}S_2$: C, 26.43; H, 4.88; N, 12.33. IR (KBr): 3341, 2979, 1701, 1364, 1067 cm$^{-1}$.

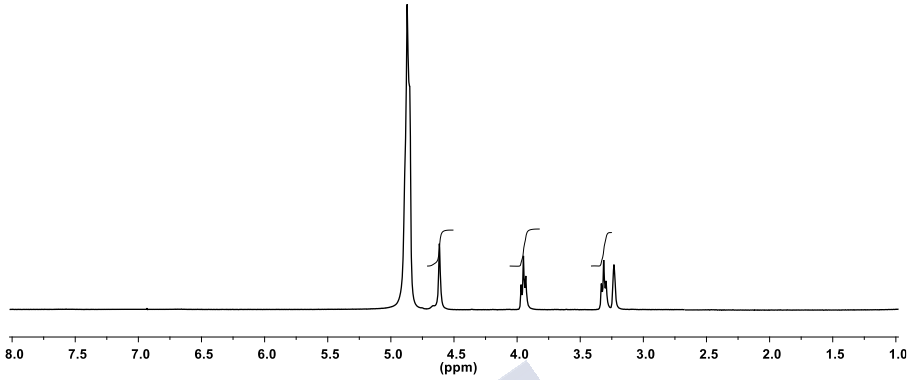


*Figure 70. $^{1}H$ NMR spectrum (300 MHz, $CD_3OD$) of Alk-$OSO_3H{\cdot}NH_3$.*

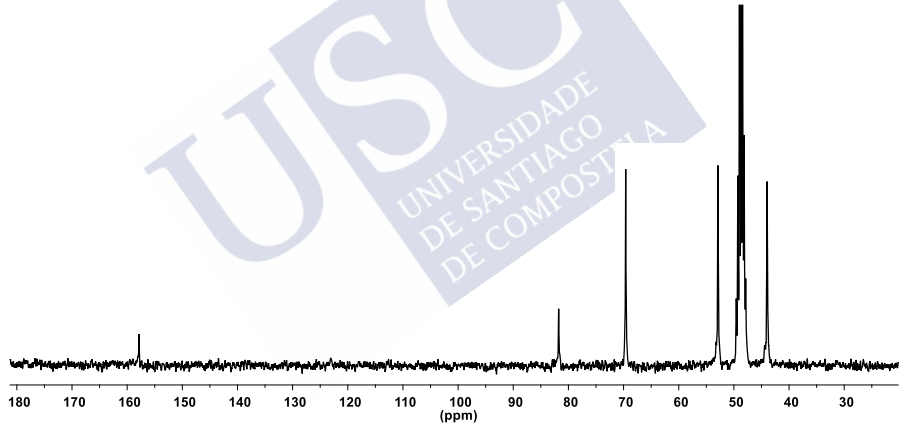


*Figure 71. $^{13}C$ NMR spectrum (75 MHz. $CD_3OD$) of Alk-$OSO_3H{\cdot}NH_3$.*

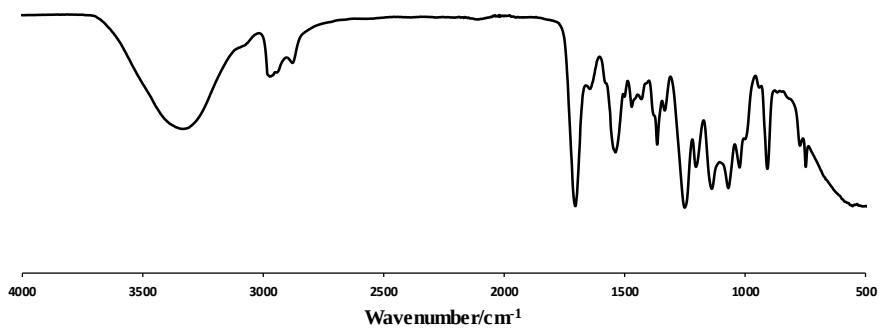


*Figure 72. IR (KBr) spectrum of Alk-$OSO_3H \cdot NH_3$.*

### 4.4.8 Alk-Man-OAc

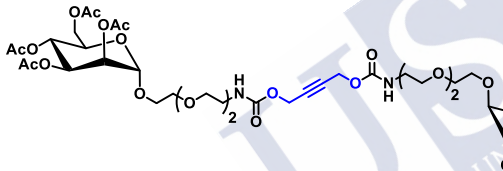

Alk-TEG-OH (330 mg, 0.76 mmol) and 2,3,4,6-tetra-O-acetyl-α-D-mannopyranosyl trichloroacetimidate (1.5 g, 3.04 mmol) were dissolved in dry $CH_2Cl_2$ (30 mL) and cooled down to 0 °C under argon. Dry 4Å molecular sieves were added and the mixture was stirred at 0 °C for 20 min. Then, $BF_3 \cdot Et_2O$ (380 ɀ L, 0.31 mmol) was added dropwise and the reaction was stirred at 0 °C for 1 h and at rt for 4 h. After addition of $Et_3N$ (150 ɀ L), the solvent was evaporated under reduced pressure and the crude product was purified by automated MPLC (gradient from hexane to 60% EtOAc/hexane, neutral alumina, 30 min) to give Alk-Man-OAc as an off-white solid (683 mg, 82%). $^1$H NMR (750 MHz, CDCl3) δ: 5.43 (t, *J*=5.1 Hz, 2H)5.31 (dd, *J*=10, 3.5 Hz, 2H), 5.26 (d, *J*= 9.9 Hz, 2H), 5.22 (dd, *J*=3.4, 1.7 Hz, 2H), 4.85 (d, *J*=1.7 Hz, 2H), 4.67 (s, 4H), 4.24 (dd, *J*=12.2, 5 Hz, 2H), 4.07 (dd, *J*=12.2, 2.4 Hz, 2H), 4.04-4.01 (m, 2H), 3.80 (d, *J*=2.9 Hz, 2H), 3.78 (d, *J*=1.9 Hz, 2H), 3.67-3.57 (m, 12H),

3.52 (t, *J*=5.2 Hz, 4H), 3.35 (dd, *J*=10.2, 4.9 Hz, 4H), 2.12, 2.07, 2.01 and 1.96 (each s, 24H). $^{13}$C NMR (125 MHz, CDCl3) δ: 170.7, 170.0, 169.9, 169.7, 155.5, 97.7, 81.1, 70.6, 70.3, 70.0, 69.9, 69.5, 69.0, 68.4, 67.4, 66.1, 62.4, 52.5, 40.9, 20.9, 20.73, 20.67, 20.66. ESI-HRMS *m/z*: found 1097.4035. Calcd for $[M+H]^+$ C46H69N2O28: 1097.4037. IR (MeOH, CsI): 1739, 1368, 1217, 1043 $cm^{-1}$.

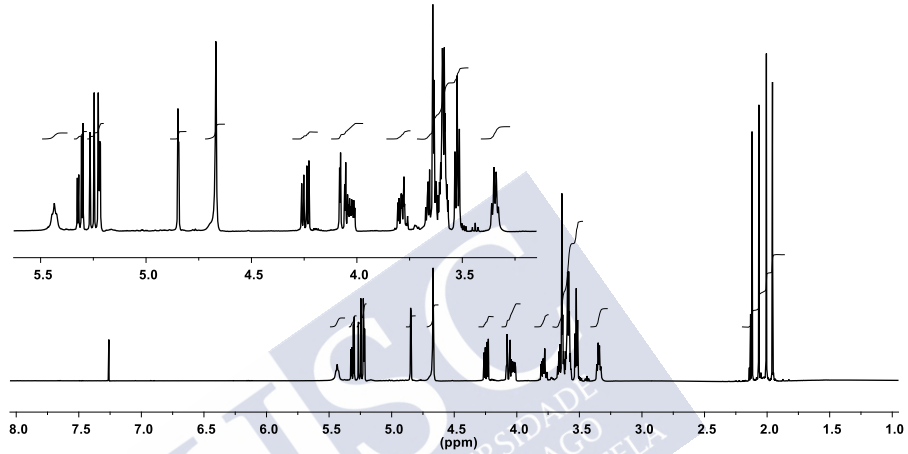


*Figure 73. $^{1}$H NMR spectrum (750 MHz, $CDCl_3$) of AIk-Man-OAc.*

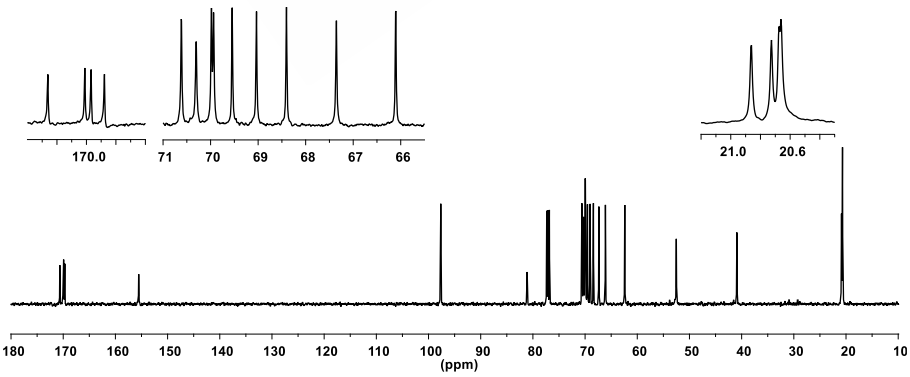


*Figure 74. $^{13}$C NMR spectrum (125 MHz, $CDCl_3$) of AIk-Man-OAc.*

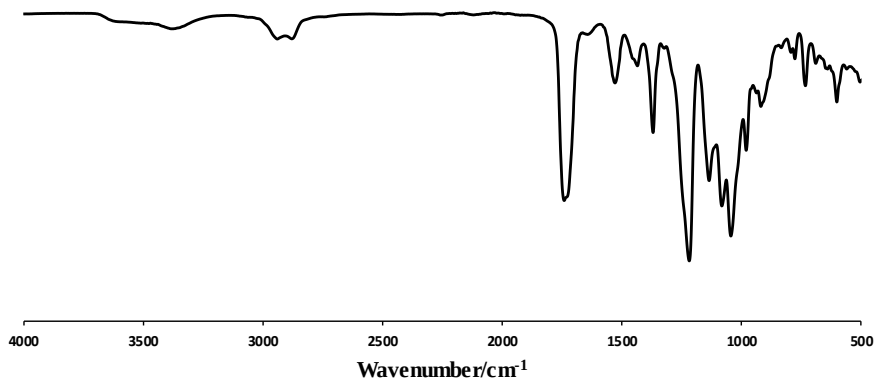


*Figure 75. IR (MeOH, CsI) spectrum of Alk-Man-OAc.*

### 4.4.9 Alk-Man

Alk-Man-OAc (432 mg, 0.4 mmol) was dissolved in dry MeOH (60 mL). A solution of NaOMe (1 M in dry MeOH) was added until pH 9 and the reaction was stirred at rt for 1 h. Then, Amberlite IR-120 was added until neutral pH. The mixture was filtered and the solvent was evaporated. Alk-Man was obtained as a white foam after lyophilization (301 mg, 97 %). $^{1}$H NMR (750 MHz, $D_2O$) δ: 4.9 (d, *J*=1.7 Hz, 2H), 4.73 (s, 4H), 3.98 (dd, *J*=3.4, 1.7 Hz, 2H), 3.91-3.87 (m, 4H), 3.86-3.81 (m, 2H), 3.78 (dd, *J*=4.3, 1.3 Hz, 2H), 3.77-3.74 (m, 4H), 3.74-3.68 (m, 12H), 3.67 (dd, *J*=4.2, 2.1 Hz, 2H), 3.64 (t, *J*=5.4 Hz, 4H), 3.36 (t, *J*=4.7 Hz, 4H). $^{13}$C NMR (125 MHz, D2O) δ: 157.5, 99.9, 81.3, 72.7, 70.5, 70.0, 69.6, 69.5, 69.4, 69.2, 66.7, 66.3, 60.9, 52.8, 40.1. ESI-HRMS *m/z*: found 783.3009. Calcd for $[M+Na]^+$ $C_{30}H_{52}N_2NaO_{20}$: 783.3011. IR (MeOH, CsI): 3342, 2928, 1706,1255,1057 $cm^{-1}$.

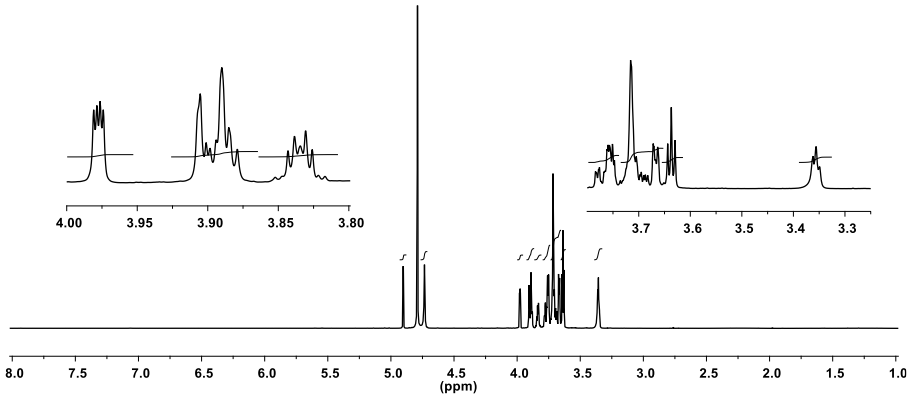


*Figure 76. $^{1}H$ NMR spectrum (750 MHz, $D_2O$) of Alk-Man.*

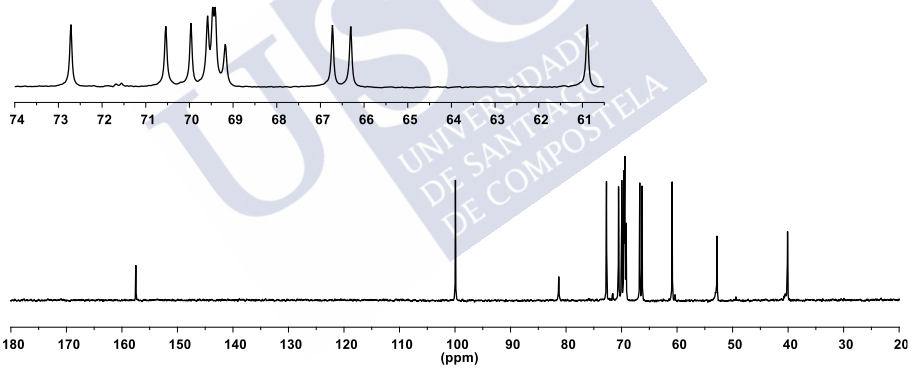


*Figure 77. $^{13}C$ NMR spectrum (125 MHz, $D_2O$) of Alk-Man.*

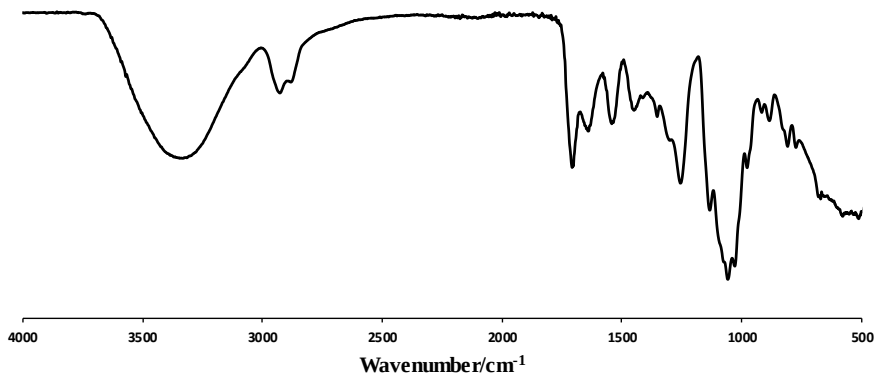


*Figure 78. IR (MeOH, CsI) spectrum of Alk-Man.*

### 4.4.10 Alk-Glu-OAc

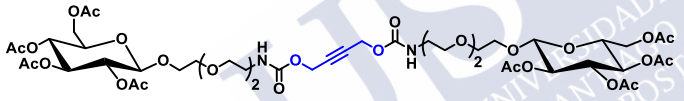

Alk-TEG-OH (110 mg, 0.26 mmol) and 2,3,4,6-tetra-O-acetyl-β-D-glucopyranosyl trichloroacetimidate (0.51 g, 1.04 mmol) were dissolved in dry $CH_2Cl_2$ (10 mL) and cooled down to 0 °C under argon. Dry 4Å molecular sieves were added and the mixture was stirred at 0 °C for 20 min. Then $BF_3{\cdot}Et_2O$ (130 ɀ L, 0.10 mmol) was added drop wise and the reaction was stirred at 0 °C for 1 h and at rt for 4 h. After addition of $Et_3N$ (150 ɀ L), the solvent was evaporated under reduced pressure and the crude product was purified by automated MPLC (gradient from hexane to 60% EtOAc/hexane, neutral alumina, 30 min) to give Alk-Glu-OAc as an off-white solid (210 mg, 76%.). $^1$H-NMR (500 MHz, $CDCl_3$) δ: 5.42 (br s, 2H), 5.17 (t, *J*=9.5 Hz, 2H), 5.05 (t, *J*=9.7 Hz, 2H), 4.96 (dd, *J*=9.6, 8.0 Hz, 2H), 4.69 (s, 4H), 4.59 (d, *J*=8.0 Hz, 2H), 4.23 (dd, *J*=12.3, 4.7 Hz, 2H), 4.11 (dd, *J*=12.3, 2.4 Hz, 2H), 3.96–3.89 (m, 2H), 3.76–3.66 (m, 4H), 3.65–3.54 (m, 10H), 3.52 (t, *J*=5.2 Hz, 4H), 3.35 (dd, *J*=10.6, 5.4 Hz, 4H), 2.06, 2.02, 1.99 and 1.97 (each s, 24H). $^{13}$C NMR (125 MHz,

$CDCl_3$) δ: 170.2, 170.1, 169.4, 169.3, 155.5, 100.7, 81.1, 72.7, 71.7, 71.2, 70.5, 70.2, 69.8, 69.0, 68.3, 61.9, 52.5, 40.9, 20.66, 20.59, 20.53, 20.51. ESI-HRMS *m/z*: found 1119.3913. Calcd for $[M+Na]^+$ $C_{46}H_{68}N_2O_{28}Na$: 1119.3856. IR (MeOH, CsI): 1739, 1368, 1217,1043 $cm^{-1}$.

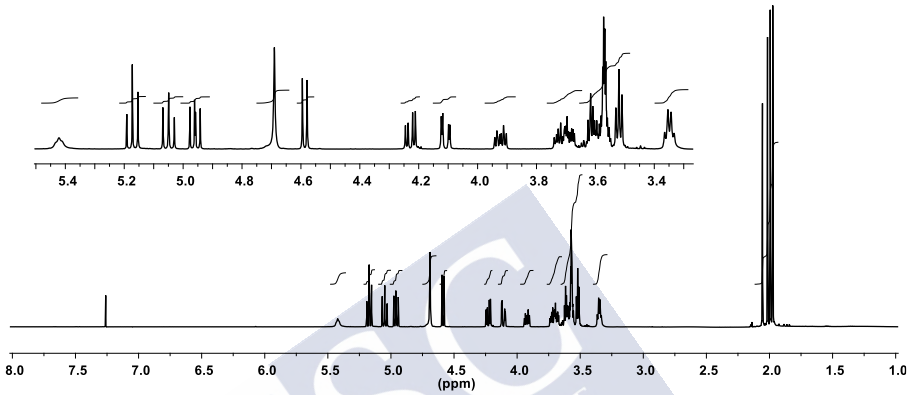


*Figure 79. $^1H$ NMR spectrum (500 MHz, $CDCl_3$) of Alk-Glu-OAc.*

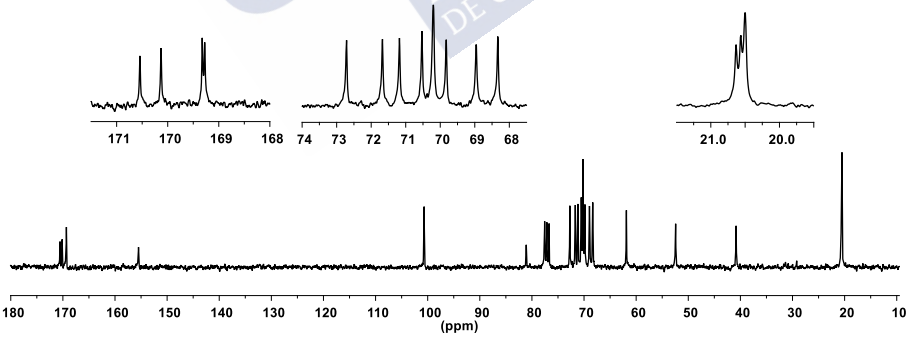


*Figure 80. $^{13}C$ NMR spectrum (125 MHz, $CDCl_3$) of Alk-Glu-OAc.*

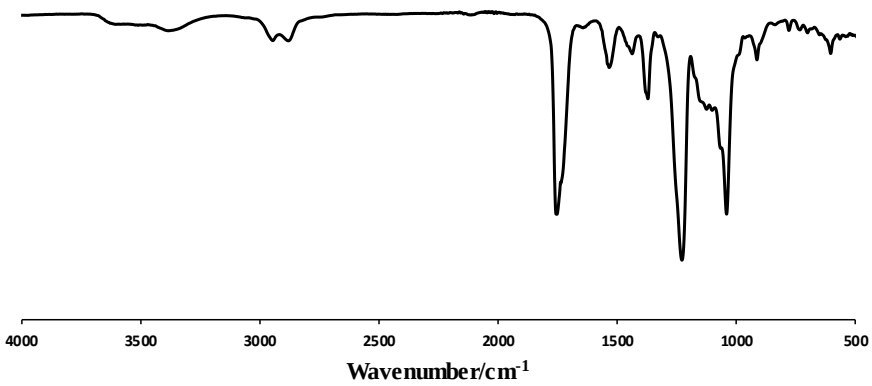


*Figure 81. IR (MeOH, CsI) spectrum of Alk-Glu-OAc.*

### 4.4.11 Alk-Glu

Alk-Glu-OAc (410 mg, 3.7 mmol) was dissolved in dry MeOH (56 mL). A solution of NaOMe (1 M in dry MeOH) was added until pH 9 and the reaction was stirred at rt for 1 h. Then, Amberlite IR-120 was added until neutral pH. The mixture was filtered and the solvent was evaporated. Alk-Glu was obtained as a white foam after lyophilization (281 mg, 99%). $^{1}$H NMR (500 MHz, $D_2O$) δ: 4.73 (s, 4H), 4.50 (d, *J*=7.9 Hz, 2H), 4.08 (m, 2H), 3.93 (dd, *J*=12.3, 2.2 Hz, 2H), 3.89-3.81 (m, 2H), 3.79-3.66 (m, 14H), 3.63 (t, *J*=5.4 Hz, 4H), 3.51 (dd, *J*=9.2, 8 Hz, 2H), 3.48-3.44 (m, 2H), 3.40 (dd, *J*=9.4, 8 Hz, 2H), 3.35 (t, *J*=5.2 Hz, 4H), 3.31 (dd, *J*=9.4, 8 Hz, 2H). $^{13}$C-NMR (75 MHz, $D_2O$) δ: 157.6, 102.2, 81.4, 75.9, 75.7, 73.1, 69.81, 69.79, 69.61, 69.36, 69.20, 68.7, 60.8, 52.9, 40.1. ESI-HRMS *m/z* found 783.2988. Calcd for $[M+Na]^+$ $C_{30}H_{52}N_2NaO_{20}$: 783.3006. IR (MeOH, CsI): 3369, 2921, 1708, 1257, 1038 cm$^{-1}$.

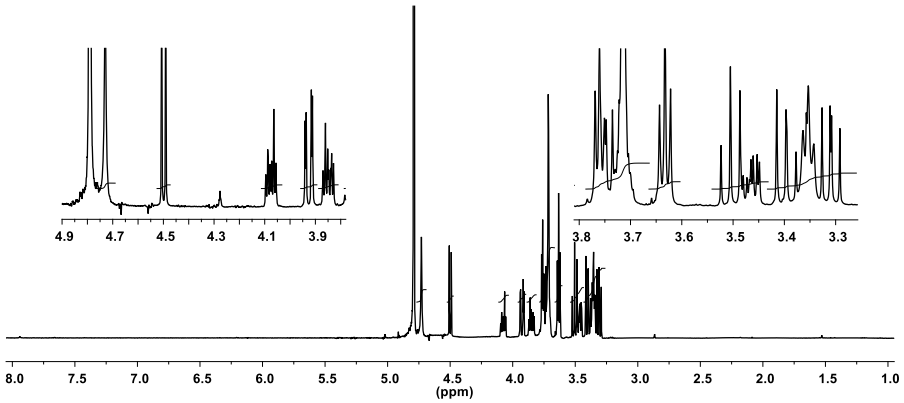


*Figure 82. $^{1}H$ NMR spectrum (500 MHz, $D_2O$) of Alk-Glu.*

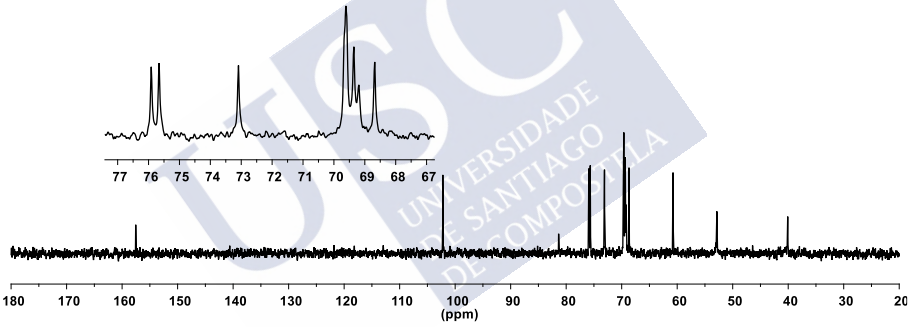


*Figure 83. $^{13}C$ NMR spectrum (75 MHz, $D_2O$) of Alk-Glu.*

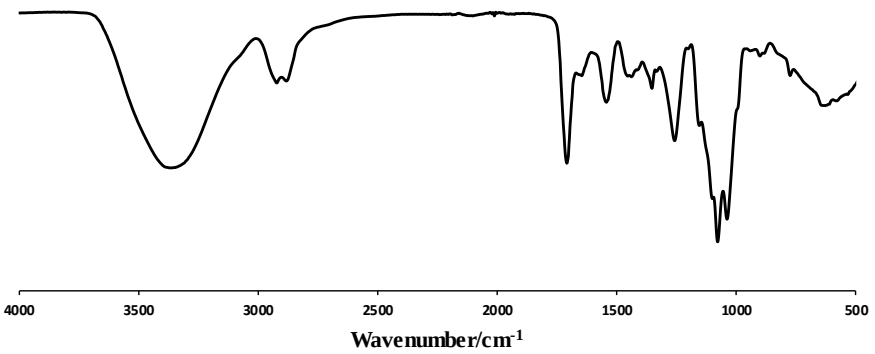


*Figure 84. IR (MeOH, CsI) spectrum of Alk-Glu.*

### 4.4.12 Alk-TEG-$NH_2$·HCl

HCl (2.8 mL, 8.4 mmol, 3 M in MeOH) was added to a solution of Alk-TEG-NHBoc (0.553 g, 0.836 mmol) in MeOH (15 mL). The mixture was stirred for 30 min and the solvent was evaporated. Alk-TEG-$NH_2$·HCl was obtained as a white foam after lyophilization (423 mg, 100%). $^1$H NMR (300 MHz, $D_2O$) δ: 4.70 (s, 4H), 3.75 (t, *J*=5.3 Hz, 4H), 3.70 (s, 8H), 3.62 (t, *J*=5.3 Hz, 4H), 3.34 (t, *J*=5.3 Hz, 4H), 3.20 (t, *J*=5.3 Hz, 4H). $^{13}$C NMR (75 MHz, $D_2O$) δ: 160.1, 83.9, 72.1, 72.0, 71.8, 68.9, 55.4, 42.6, 41.7. Elem. Anal. Found: C, 42.83; H, 7.41; N, 10.88, Calcd. for $C_{18}H_{36}Cl_2N_4O_8$: C, 42.61; H, 7.15; N, 11.04. IR (KBr): 2878, 1703, 1525, 1251, 1089 $cm^{-1}$.

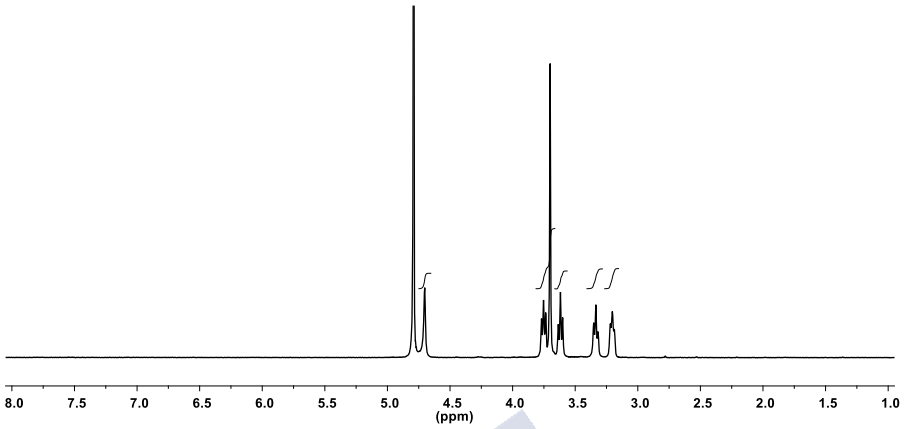


*Figure 85. $^{1}H$ NMR spectrum (300 MHz, $D_2O$) of Alk-TEG-$NH_2$·HCl.*

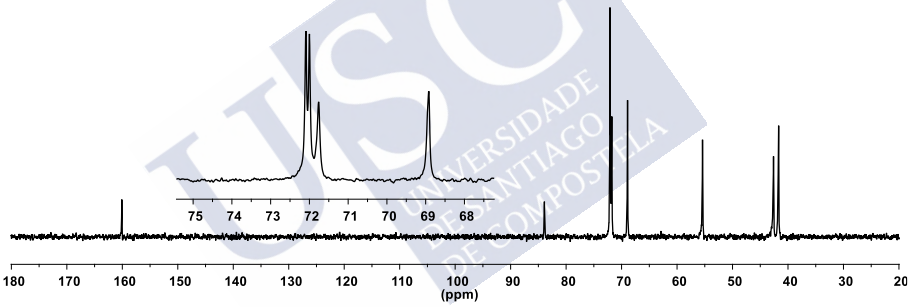


*Figure 86. $^{13}C$ NMR spectrum (75 MHz, $D_2O$) of Alk-TEG-$NH_2$·HCl.*

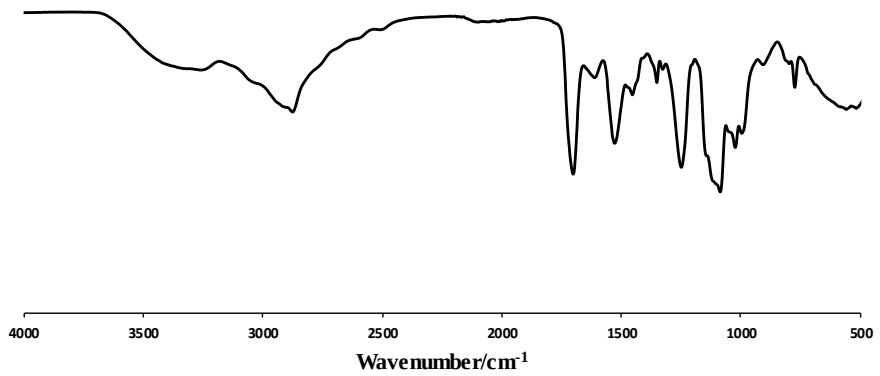


*Figure 87. IR (KBr) spectrum of Alk-TEG-$NH_2$·HCl.*

### 4.4.13 Alk-Bio

EDC·HCl (105 mg, 0.550 mmol) was added to a solution of biotin (134 mg, 0.550 mmol), Alk-TEG-$NH_2$·HCl (93 mg, 0.183 mmol), HOBt (74 mg, 0.550 mmol) and $Et_3N$ (102 µL, 0.734 mmol) in dry DMF (4.6 mL) at 0 °C under argon. The reaction mixture was stirred at 0 °C for 1.5 h and then allowed to reach rt. After 24 h of additional stirring, the solvent was evaporated, and the resulting yellow oil was purified by automated MPLC (gradient from $CHCl_3$ to 25% MeOH/$CHCl_3$, neutral alumina, 30 min) to afford Alk-Bio as a yellow oil (131 mg, 93%). $^1$H NMR (500 MHz, $CD_3OD$, 50 ms DOSY filter) δ: 4.74 (s, 4H), 4.54 (dd, *J*=6.4, 5.9 Hz, 2H), 4.36 (dd, *J*=7.4, 4.1 Hz, 2H), 3.67 (s, 8H), 3.59 (dd, *J*=5.1, 3.7 Hz, 8H), 3.42 (t, *J*=5.3 Hz, 4H), 3.34 (t, *J*=5.5 Hz, 4H), 3.29-3.22 (m, 2H), 2.98 (dd, *J*=12.8, 4.1 Hz, 2H), 2.76 (d, *J*=12.8 Hz, 2H), 2.28 (t, *J*=7.2 Hz, 4H), 1.84-1.59 (m, 8H), 1.54-1.44 (m, 4H). $^{13}$C NMR (125 MHz, $CD_3OD$) δ: 176.2, 166.1, 157.9, 82.2, 71.3, 71.2, 70.9, 70.6, 63.3, 61.6, 57.0, 53.3, 41.8, 41.1, 40.3, 36.8, 29.8, 29.5, 26.8. Elem. Anal. Found: C, 51.63; H, 6.78; N, 12.29, Calcd. for $C_{38}H_{62}N_8O_{12}S_2$: C, 51.45; H, 7.05; N, 12.63. IR (MeOH, CsI): 3281, 2934, 1693, 1645, 1257 cm$^{-1}$.

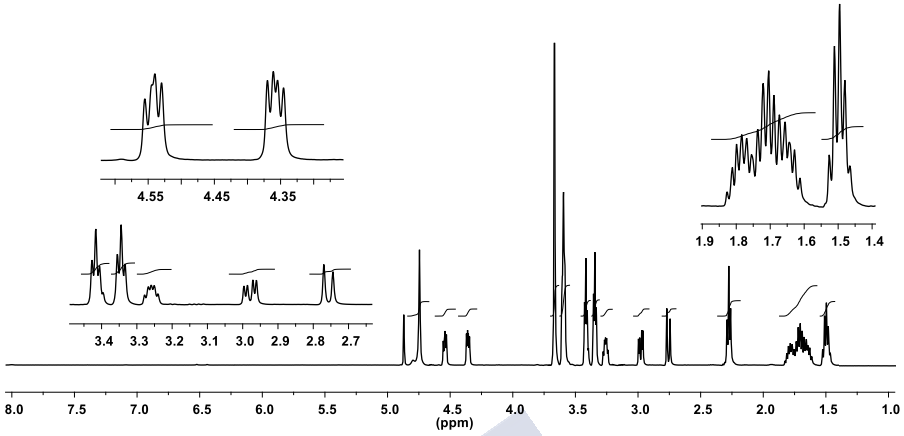


*Figure 88. $^{1}H$ NMR spectrum (500 MHz, $CD_3OD$) of Alk-Bio.*

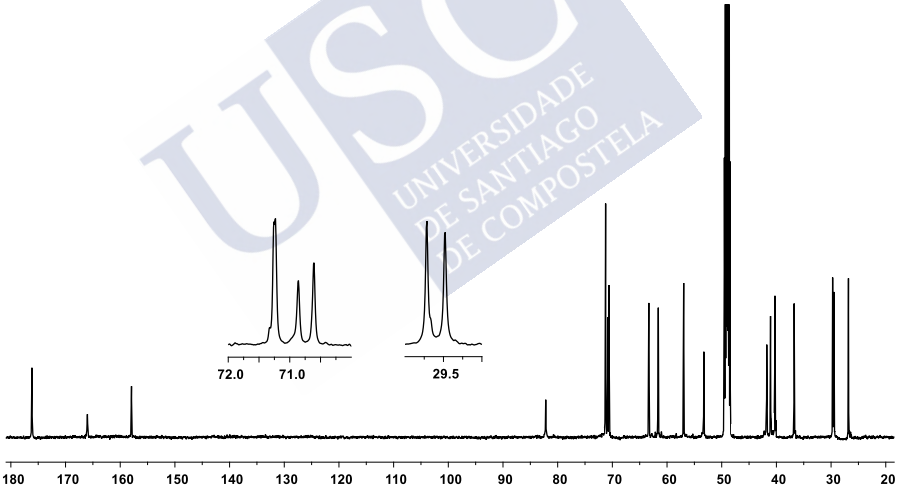


*Figure 89. $^{13}C$ NMR spectrum (125 MHz, $CD_3OD$) of Alk-Bio.*

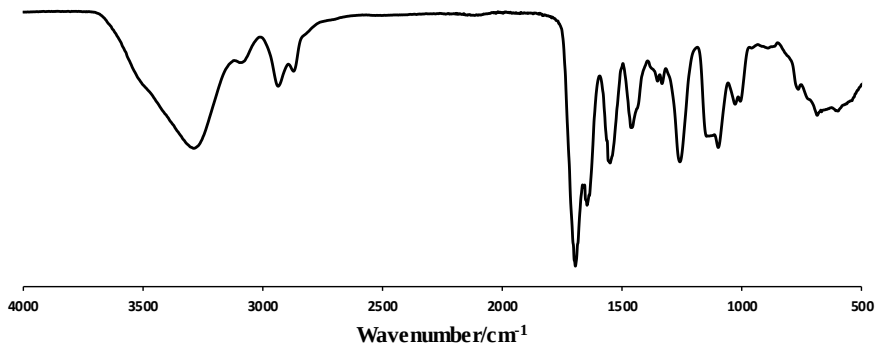


*Figure 90. IR (MeOH, CsI) spectrum of Alk-Bio.*

### 4.4.14 Alk-FITC

Fluorescein 5-isothiocyanate (190 mg, 0.489 mmol; FITC) was added to a solution of Alk-TEG-$NH_2$·HCl (100 mg, 0.196 mmol) and $Et_3N$ (109 μL, 0.783 mmol) in dry THF (3.9 mL) under argon. After 16 h of stirring at rt in the dark, the solvent was evaporated and the resulting yellow oil was purified by automated MPLC (gradient from $CH_2Cl_2$ to 15% MeOH/$CH_2Cl_2$, neutral alumina, 30 min) to afford Alk-FITC as a yellow foam (173 mg, 73%). $^1$H NMR (500 MHz, DMSO-$d_6$) δ: 10.11 (br s, 4H), 8.28 (s, 2H), 8.14 (br s, 2H), 7.72 (d, *J*=11.9 Hz, 2H), 7.35 (t, *J*=4.1 Hz, 2H), 7.16 (t, *J*=6.3 Hz, 2H), 6.73-6.45 (m, 10H), 4.66 (s, 4H), 3.75-3.21 (m, 20H), 3.14 (dd, *J*=10.6, 4.8 Hz, 4H). $^{13}$C NMR (75 MHz, DMSO-$d_6$) δ: 181.0, 169.1, 159.8, 155.9, 152.3, 147.7, 141.7, 130.1, 129.4, 126.9, 124.4, 117.2, 113.1, 110.1, 102.7, 83.6, 81.8, 70.0, 69.9, 69.4, 68.7, 52.0, 46.3, 44.1. IR (MeOH, CsI): 3296, 2926, 1712, 1456, 1111 cm$^{-1}$.

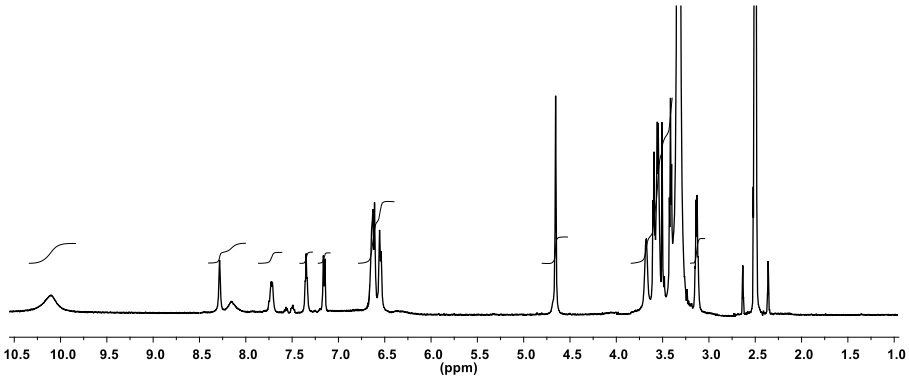


*Figure 91. $^{1}H$ NMR spectrum (500 MHz, DMSO-$d_6$) of Alk-FITC.*

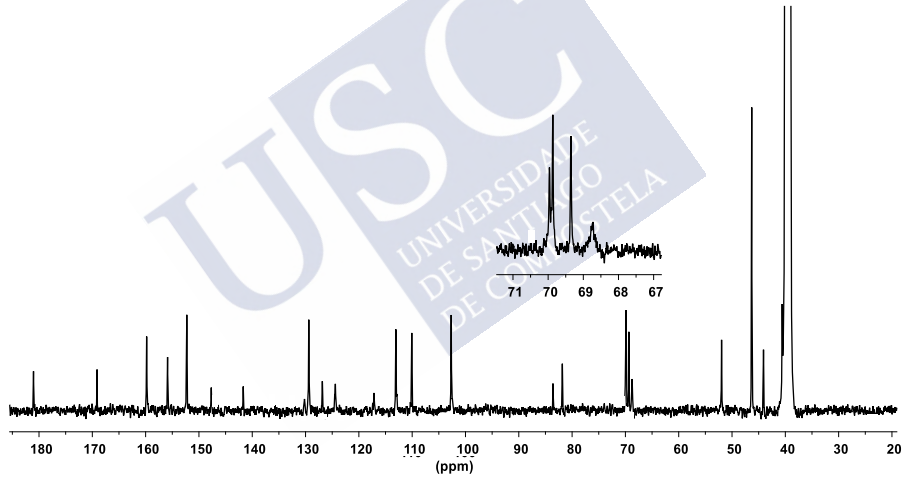


*Figure 92. $^{13}C$ NMR spectrum (75 MHz, DMSO-$d_6$) of Alk-FITC.*

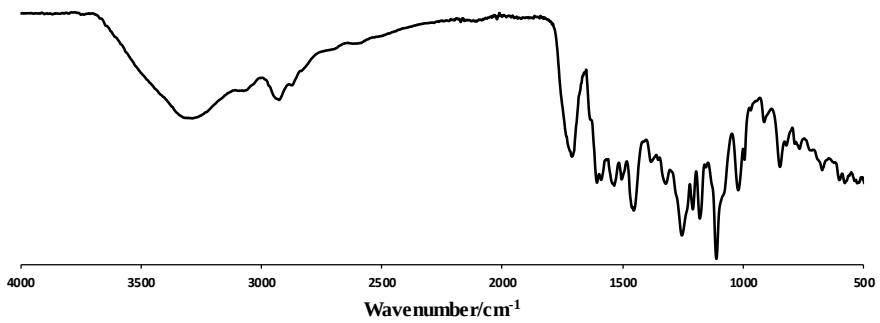


*Figure 93. IR (MeOH, CsI) spectrum of Alk-FITC.*

## 4.5 Synthesis of conjugates

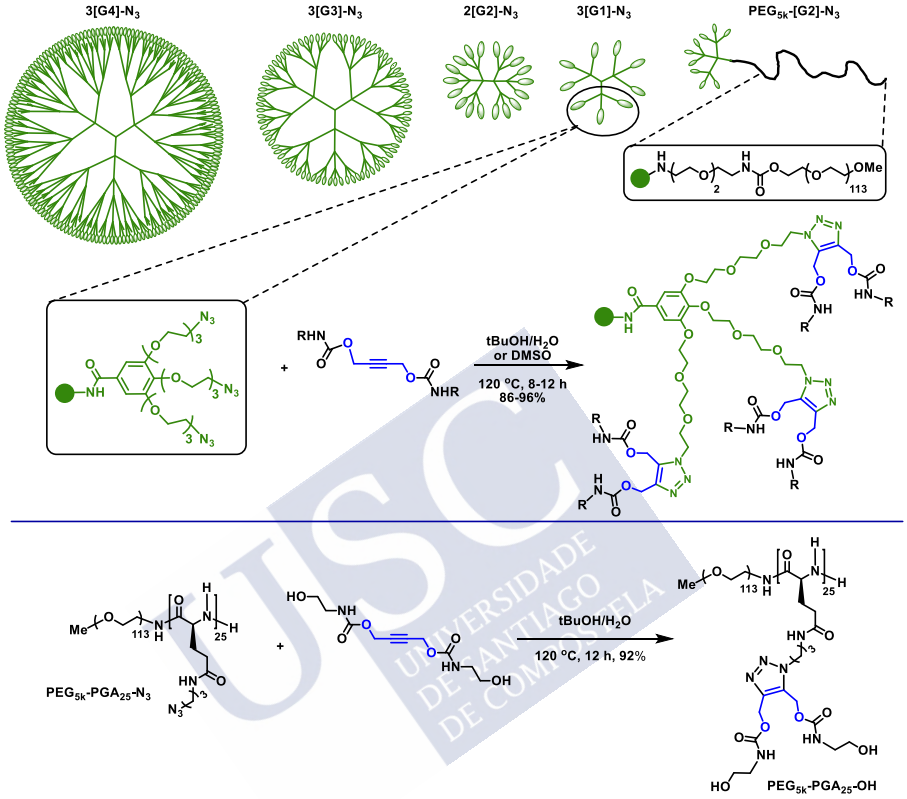


*Scheme 19. Functionalization of dendrimers and polymers.*

### 4.5.1 3[G2]-OH

In a Schlenk-flask, Alk-OH (98 mg, 377 τmol) was added to a solution of 3[G1]-$N_3$ (50 mg, 21 τmol) in tBuOH/$H_2O$ 5:1 (188 τL). The reaction was stirred at 120 ºC for 8 h and then was purified by ultrafiltration (4 x 30 mL $H_2O$, Amicon YM3) and lyophilized to afford 3[G2]-OH as a white foam (92 mg, 93%). $^1$H NMR (500 MHz, $D_2O$) δ: 7.10 (br s, 6H), 5.93 (br s, 3H), 5.37-5.07 (m, 36H), 4.67-4.52 (m, 18H), 4.20-4.00 (m, 24H), 3.98-3.39 (m, 138H), 3.28-3.07 (m, 36H). $^{13}$C NMR (125 MHz, DMSO-$d_6$) δ: 166.0, 160.0, 156.1, 155.5, 151.9, 141.7, 139.9, 132.1, 129.2, 106.2, 94.9, 72.0, 70.0, 69.8, 69.5,

69.1, 68.9, 68.4, 59.9, 56.8, 52.7, 48.0, 43.1. IR (KBr): 3338, 2972, 1704, 1251, 1068 $cm^{-1}$.

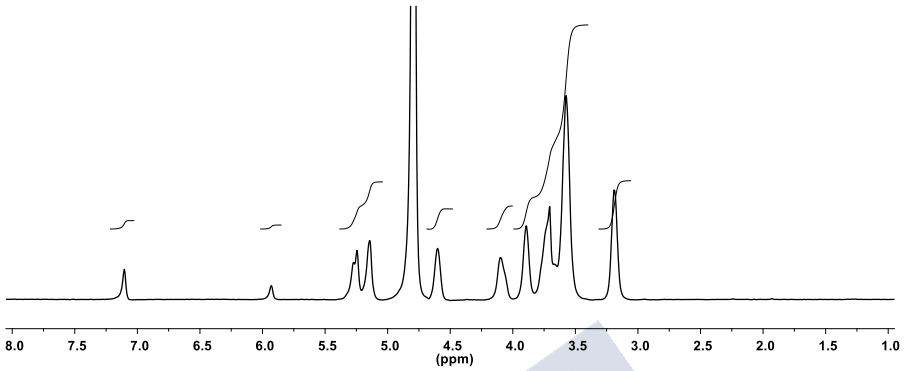


*Figure 94. $^{1}H$ NMR spectrum (500 MHz, $D_2O$) of 3[G2]-OH.*

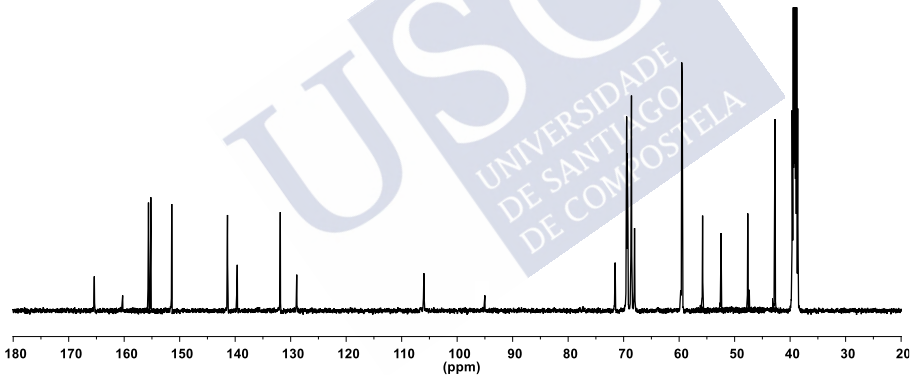


*Figure 95. $^{13}C$ NMR spectrum (125 MHz, DMSO-$d_6$) of 3[G2]-OH.*

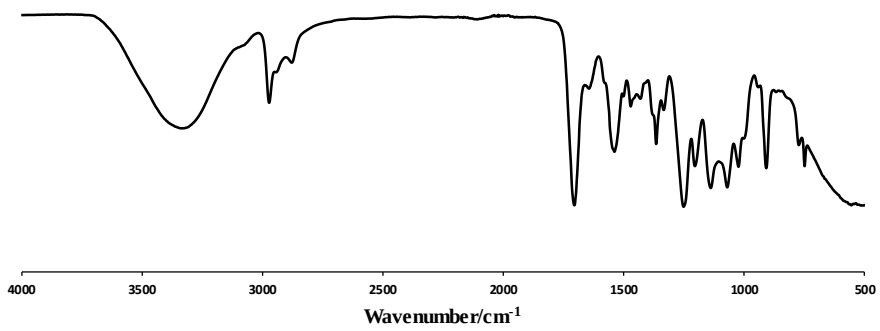


*Figure 96. IR (KBr) spectrum of 3[G2]-OH.*

### 4.5.2 3[G2]-Glu

In a Schlenk-flask, Alk-Glu (114 mg, 151 ɀmol) was added to a solution of 3[G1]-$N_3$ (20 mg, 8.4 ɀmol) in tBuOH/$H_2O$ 5:1 (150 ɀL). The reaction was stirred at 120 $^oC$ for 12 h and then was purified by ultrafiltration (4 x 30 mL $H_2O$, Amicon YM3) and lyophilized to afford 3[G2]-Glu as a brown foam (70 mg, 91%). $^1H$ NMR (500 MHz, $D_2O$) δ: 7.13 (br s, 6H), 5.98 (br s, 3H), 5.37-5.07 (m, 36H), 4.68-4.56 (m, 18H), 4.54-4.39 (m, 18H), 4.20-3.98 (m, 24H), 3.98-3.33 (m, 390H), 3.32-3.12 (m, 36H). $^{13}C$ NMR (125 MHz, $D_2O$) δ: 168.7, 160.0, 157.5, 156.9, 151.8, 141.9, 139.7, 132.7, 129.2, 106.2, 102.2, 94.2, 75.9, 75.7, 73.1, 72.1, 71.7, 69.9, 69.6, 69.3, 69.1, 68.9, 68.6, 68.4, 67.2, 60.8, 60.3, 56.9, 53.8, 48.7, 40.1. IR (KBr): 3348, 2874, 1705, 1252, 1074 $cm^{-1}$.

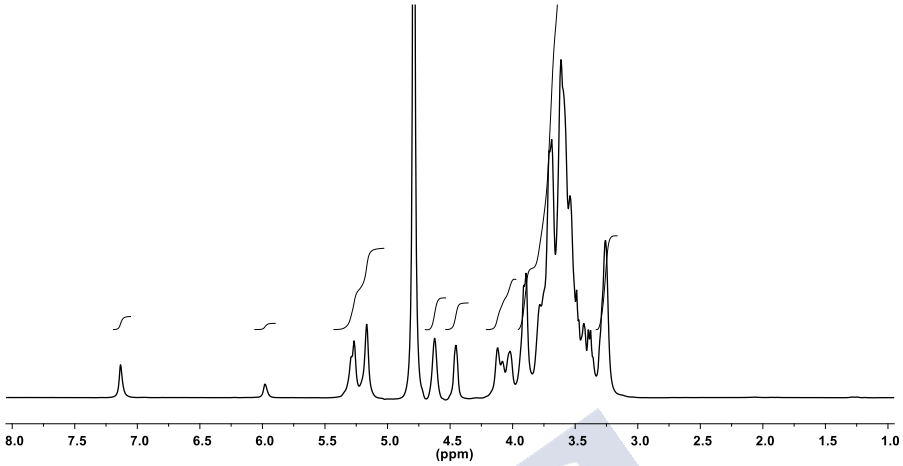


*Figure 97. $^{1}H$ NMR spectrum (500 MHz, $D_2O$) of 3[G2]-Glu.*

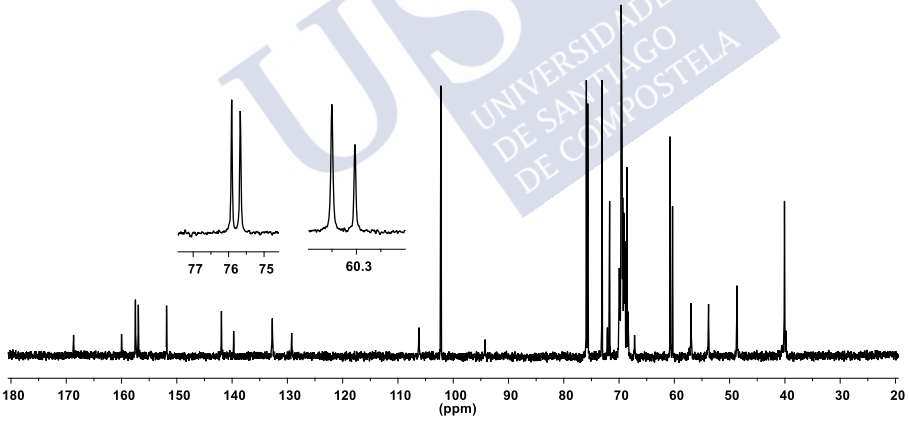


*Figure 98. $^{13}C$ NMR spectrum (125 MHz, $D_2O$) of 3[G2]-Glu.*

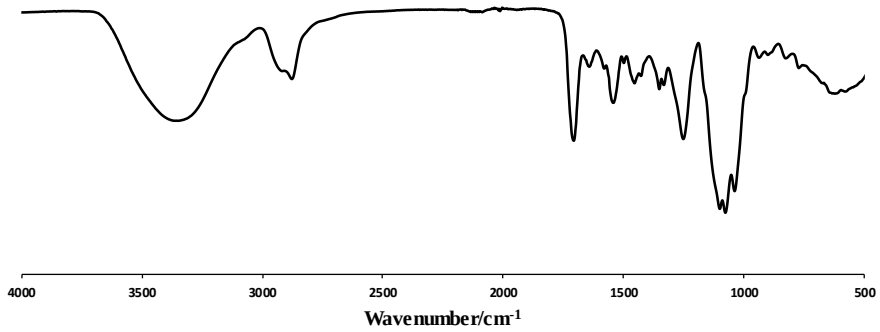


*Figure 99. IR (KBr) spectrum of 3[G2]-Glu.*

### 4.5.3 2[G3]-OH

In a Schlenk-flask, Alk-OH (94 mg, 362 τmol) was added to a solution of 2[G2]-$N_3$ (50 mg, 10 τmol) in tBuOH/$H_2O$ 5:1 (181 τL). The reaction was stirred at 120 °C for 8 h and then was purified by ultrafiltration (4 x 30 mL $H_2O$, Amicon YM3) and lyophilized to afford 2[G3]-OH as a white foam (91 mg, 94%). $^1$H NMR (500 MHz, $D_2O$, 50 ms DOSY filter) δ: 7.21-7.01 (m, 16H), 5.39-5.09 (m, 72H), 4.68-4.56 (m, 36H), 4.19-3.96 (m, 48H), 3.95-3.47 (m, 288H), 3.27-3.12 (m, 72H). $^{13}$C NMR (125 MHz, DMSO-*d6*) δ: 165.5, 155.9, 155.5, 151.8, 141.7, 140.0, 132.2, 129.3, 106.4, 71.9, 69.8, 69.7, 69.5, 69.0, 68.8, 68.4, 66.8, 59.8, 56.1, 52.9, 48.1, 43.2. IR (KBr): 3330, 2972, 1705, 1538, 1250 cm$^{-1}$.

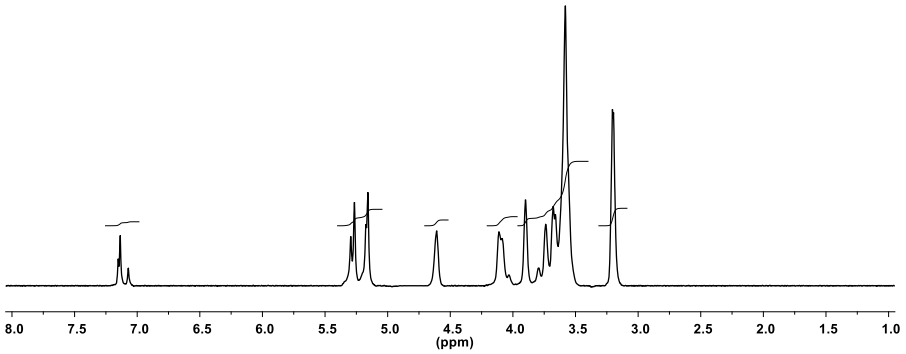


*Figure 100. $^{1}H$ NMR spectrum (500 MHz, $D_2O$) of 2[G3]-OH.*

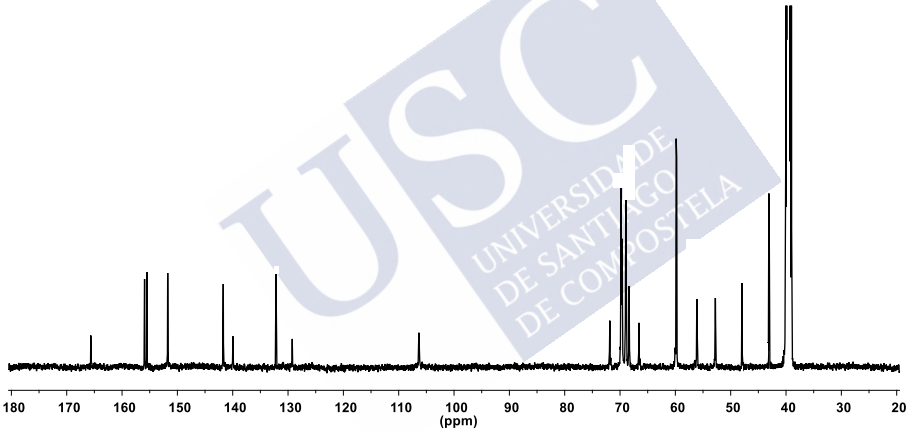


*Figure 101. $^{13}C$ NMR spectrum (125 MHz, DMSO-d6) of 2[G3]-OH.*

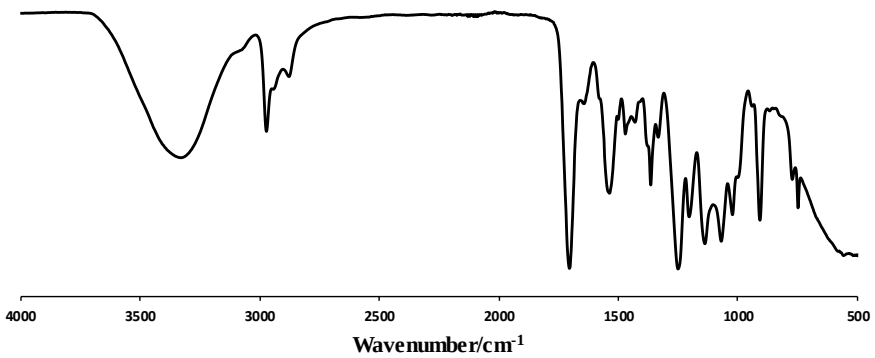


*Figure 102. IR (KBr) spectrum of 2[G3]-OH.*

### 4.5.4 2[G3]-TEG-$NH_2$·HCl

In a Schlenk-flask, Alk-TEG-$NH_2$·HCl (129 mg, 253 τ mol) was added to a solution of 2[G2]-$N_3$ (35 mg, 7 τ mol) in tBuOH/$H_2O$ 5:1 (127 τ L). The reaction was stirred at 120 ºC for 8 h and then was purified by ultrafiltration (4 x 30 mL $H_2O$, Amicon YM3) and lyophilized to afford 2[G3]-TEG-$NH_2$·HCl as a white foam (92 mg, 93%). $^1$H NMR (500 MHz, $D_2O$, 50 ms DOSY filter) δ: 7.16 (br s, 16H), 5.39-5.11 (m, 72H), 4.73-4.56 (m, 36H), 4.27-4.05 (m, 48H), 3.98-3.45 (m, 504H), 3.34-3.12 (m, 144H). $^{13}$C NMR (125 MHz, $D_2O$) δ: 168.9, 157.7, 157.1, 151.9, 142.0, 139.8, 132.7, 129.3, 106.3, 72.1, 69.8, 69.7, 69.4, 69.1, 68.8, 68.4, 66.4, 57.0, 53.8, 48.5, 40.0, 39.0. IR (KBr): 3261, 2935, 1716, 1247, 1113 cm$^{-1}$.

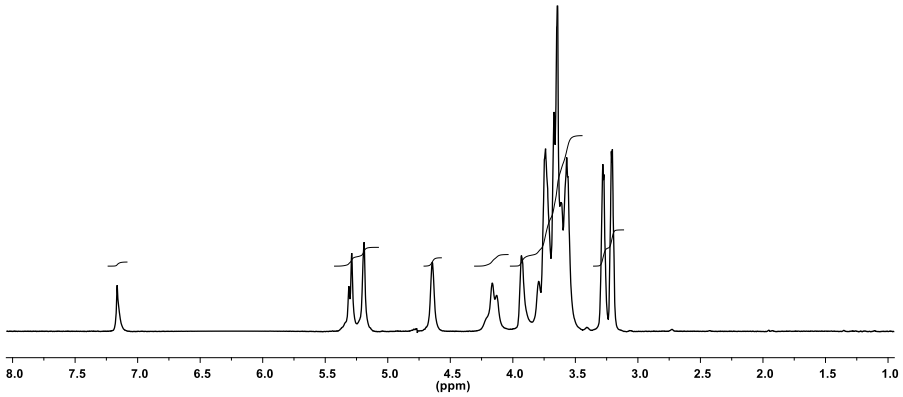


*Figure 103. $^{1}H$ NMR spectrum (500 Hz, $D_2O$) of 2[G3]-TEG-$NH_2$·HCl.*

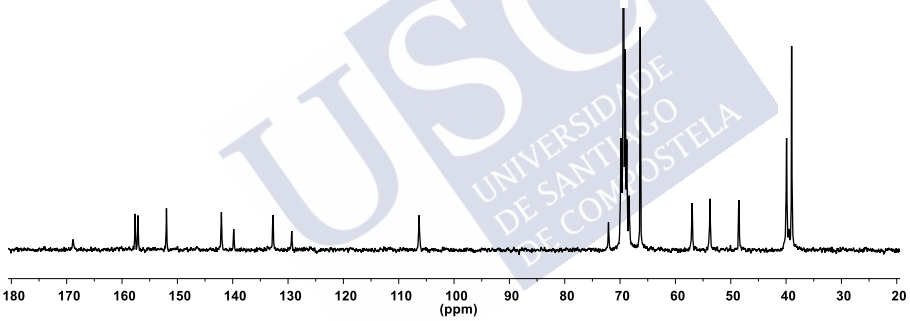


*Figure 104. $^{13}C$ NMR spectrum (125 MHz, $D_2O$) of 2[G3]-TEG-$NH_2$·HCl.*

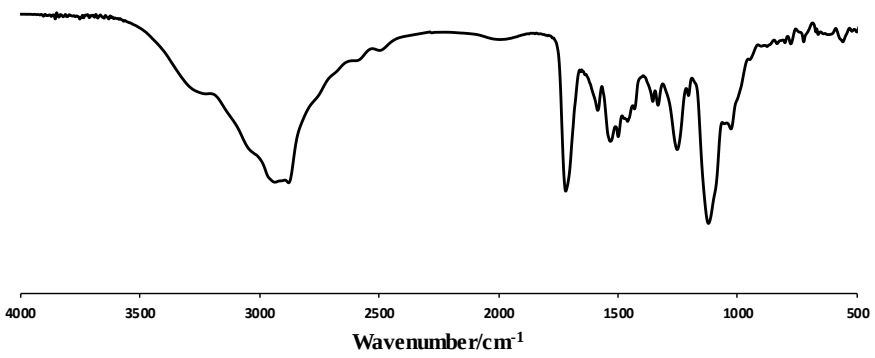


*Figure 105. IR (KBr) spectrum of 2[G3]-TEG-$NH_2$·HCl.*

### 4.5.5 3[G4]-TEG-OH

In a Schlenk-flask, Alk-TEG-OH (148 mg, 309 ɀ mol) was added to a solution of 3[G3]-$N_3$ (50 mg, 2.10 ɀ mol) in tBuOH/$H_2O$ 2:1 (170 ɀ L). The reaction was stirred at 120 ºC for 8 h and then was purified by ultrafiltration (4 x 30 mL $H_2O$, Amicon YM3) and lyophilized to afford 3[G4]-TEG-OH as a pale yellow oil (114 mg, 92%). $^1$H NMR (500 MHz, $D_2O$) δ: 7.24-7.10 (m, 78H), 5.40-5.13 (m, 324H), 4.74-4.58 (m, 162H), 4.26-4.00 (m, 240H), 4.00-3.40 (m, 2658H), 3.34-3.18 (m, 324H). $^{13}$C NMR (125 MHz, $D_2O$) δ: 168.4, 157.6, 157.2, 152.1, 141.9, 139.8, 132.7, 129.2, 106.1, 72.1, 71.6, 69.8, 69.4, 69.2, 69.0, 68.8, 68.5, 68.3, 60.2, 56.8, 53.6, 48.5, 39.9. IR (KBr): 3332, 2876, 1708, 1246, 1100 cm$^{-1}$.

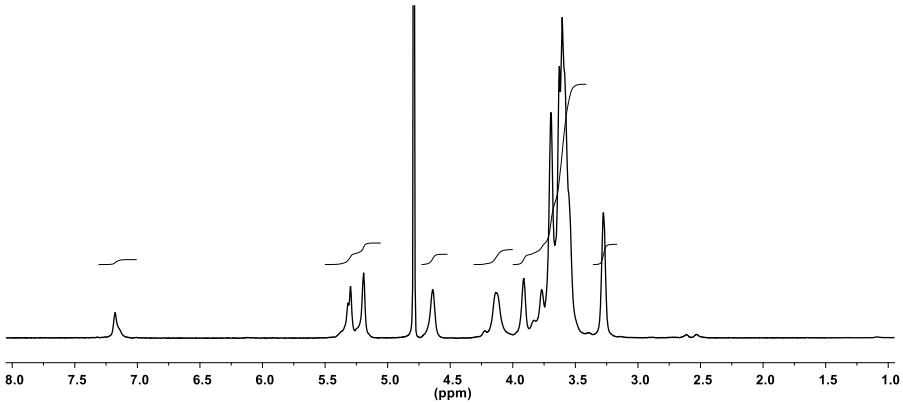


*Figure 106. $^{1}H$ NMR spectrum (500 MHz, $D_2O$) of 3[G4]-TEG-OH.*

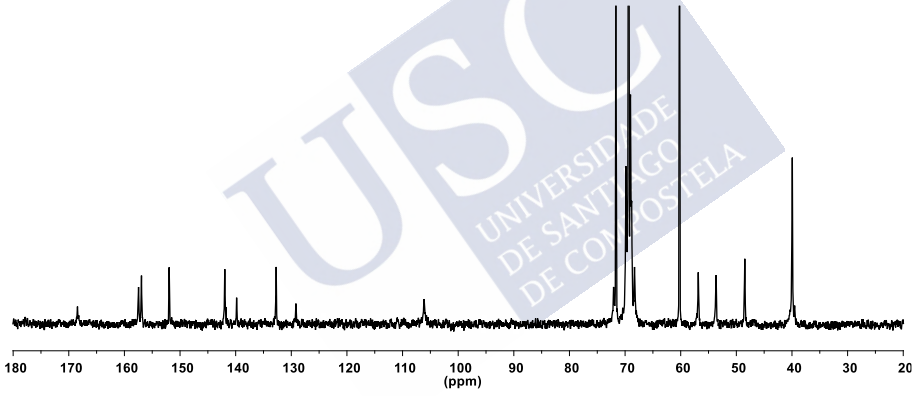


*Figure 107. $^{13}C$ NMR spectrum (125 MHz, $D_2O$) of 3[G4]-TEG-OH.*

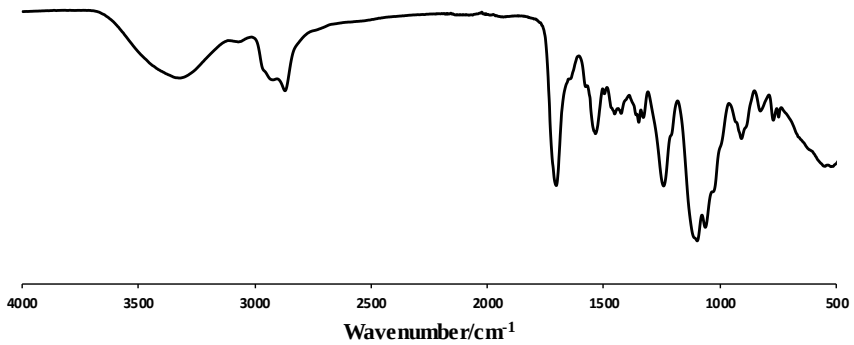


*Figure 108. IR (KBr) spectrum of 3[G4]-TEG-OH.*

### 4.5.6 3[G4]-OH

In a Schlenk-flask, Alk-OH (90 mg, 346 ɾ mol) was added to a solution of 3[G3]-$N_3$ (50 mg, 2.10 ɾ mol) in tBuOH/$H_2O$ 5:1 (170 ɾL ). The reaction was stirred at 120 ºC for 8 h and then was purified by ultrafiltration (4 x 30 mL acetone/$H_2O$ 1:1 and 2 x 30 mL $H_2O$, Amicon YM3) and lyophilized to afford 3[G4]-OH as a white foam (86 mg, 91%). $^1$H NMR (500 MHz, $D_2O$) δ: 7.19-7.03 (m, 78H), 5.36-5.02 (m, 324H), 4.68-4.47 (m, 162H), 4.22-3.97 (m, 240H), 3.96-3.38 (m, 1602H), 3.26-3.04 (m, 324H). $^{13}$C NMR (125 MHz, DMSO-$d_6$) δ: 165.6, 155.9, 155.5, 151.8, 141.7, 140.0, 132.2, 129.3, 106.4, 71.8, 69.9, 69.8, 69.6, 69.0, 68.9, 68.4, 59.9, 56.1, 52.8, 48.0, 43.1. IR (KBr): 3351, 2931, 1643, 1251, 1114 cm$^{-1}$.

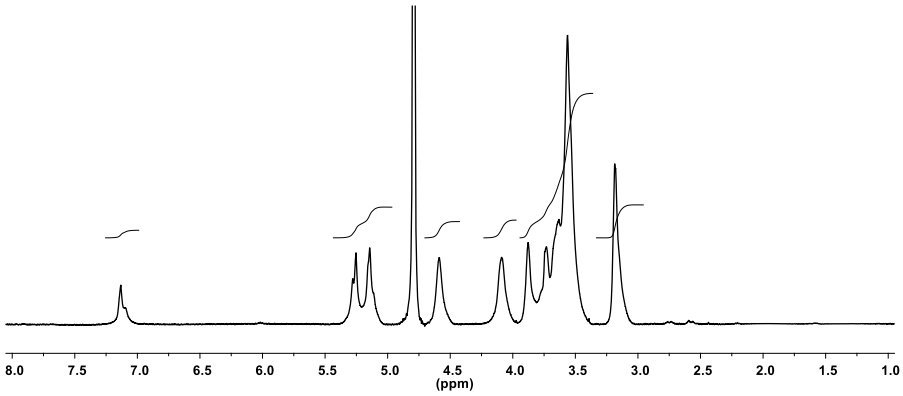


*Figure 109. $^{1}H$ NMR spectrum (500 MHz, $D_2O$) of 3[G4]-OH.*

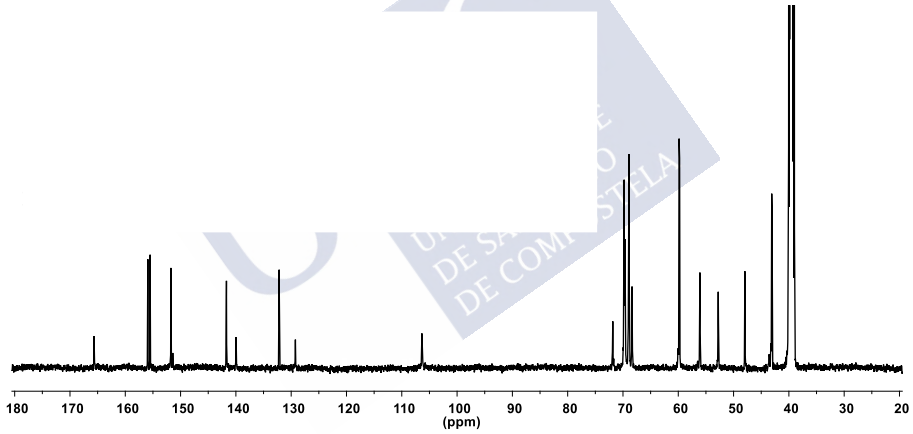


*Figure 110. $^{13}C$ NMR spectrum (125 MHz, DMSO-$d_6$) of 3[G4]-OH.*

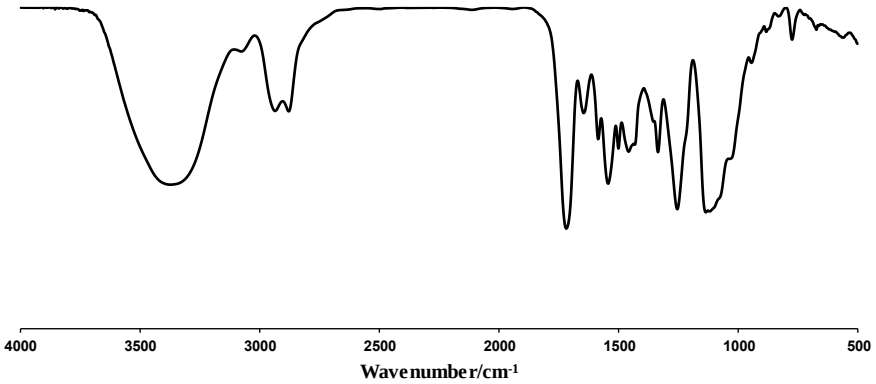


*Figure 111. IR (KBr) spectrum of 3[G4]-OH.*

### 4.5.7 3[G4]-PhOH

In a Schlenk-flask, Alk-PhOH (130 mg, 339 τ mol) was added to a solution of 3[G3]-$N_3$ (50 mg, 2.10 τ mol) in MeOH/$H_2O$ 5:1 (170 τ L). The reaction was stirred at 120 °C for 8 h and then was purified by ultrafiltration (4 x 30 mL acetone/$H_2O$ 2:1 and 2 x 30 mL $H_2O$, Amicon YM3) and lyophilized to afford 3[G4]-PhOH as a white solid (105 mg, 91%). $^1$H NMR (500 MHz, DMSO-$d_6$) δ: 9.25 (br s, 162H), 8.44 (br s, 36H), 7.67 (s, 81H), 7.55 (s, 81H), 7.17 (s, 78H), 6.99 (d, *J*=7.4 Hz, 324H), 6.66 (d, *J*=7.4 Hz, 324H), 5.28-5.00 (m, 324H), 4.59-4.44 (m, 162H), 4.19-3.91 (m, 564H), 3.82-3.41 (m, 1038H). $^{13}$C NMR (125 MHz, DMSO-$d_6$) δ: 166.1, 156.7, 156.4, 155.9, 152.2, 142.1, 140.4, 132.6, 130.8, 129.9, 129.6, 128.8, 115.4, 106.7, 72.3, 70.2, 70.1, 69.3, 68.7, 56.6, 53.4, 48.4, 43.9. IR (KBr): 3336, 2923, 1708, 1517, 1241, 1122 cm$^{-1}$.

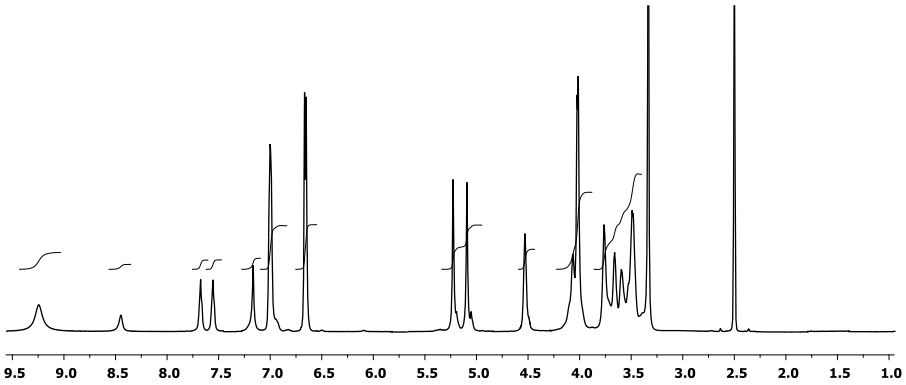


*Figure 112. $^{1}H$ NMR spectrum (500 MHz, DMSO-$d_6$) of 3[G4]-PhOH.*

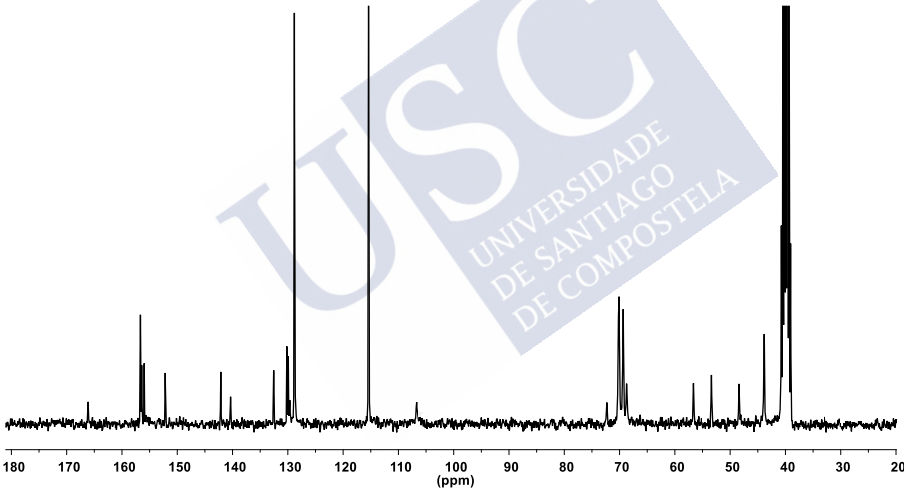


*Figure 113. $^{13}C$ NMR spectrum (125 MHz, DMSO-$d_6$) of 3[G4]-PhOH.*

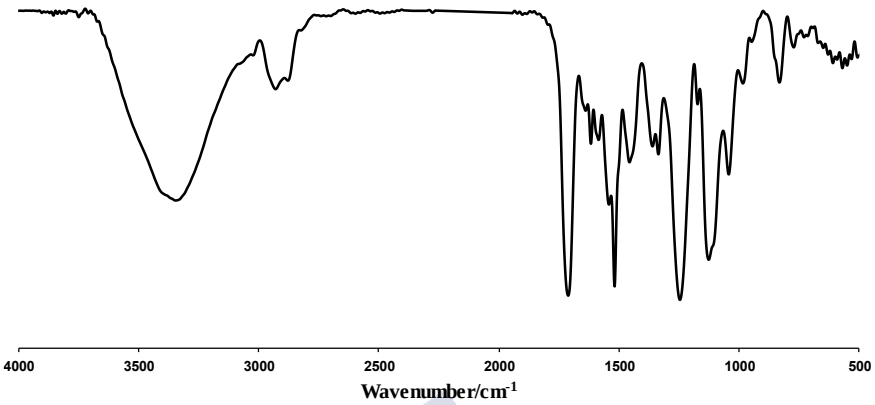


*Figure 114. IR (KBr) spectrum of 3[G4]-PhOH.*

### 4.5.8 3[G]-$OSO_3Na$

In a Schlenk-flask, Alk-$OSO_3H \cdot NH_3$ (145 mg, 319 ɀmol) was added to a solution of 3[G3]-$N_3$ (47 mg, 1.97 ɀmol) in tBuOH/$H_2O$ 1:1 (160 ɀL). The reaction was stirred at 120 ºC for 8 h and then was purified by ultrafiltration (4 x 30 mL 0.1 M NaOH/acetone 1:1 and 2 x 30 mL $H_2O$, Amicon YM3) and lyophilized to afford 3[G4]-$OSO_3Na$ as a white foam (108 mg, 91%). $^1H$ NMR (500 MHz, $D_2O$) δ: 7.17 (br s, 78H), 5.42-5.15 (m, 324H), 4.70-4.57 (m, 162H), 4.31-4.00 (m, 564H), 4.00-3.51 (m, 1038H), 3.47-3.33 (m, 324H). $^{13}C$ NMR (125 MHz, $D_2O$) δ: 168.8, 157.5, 156.9, 151.8, 141.9, 139.6, 132.6, 129.2, 106.1, 72.1, 69.9, 69.5, 69.0, 68.8, 68.3, 68.0, 67.2, 57.1, 53.9, 48.6, 40.0. IR (KBr): 3446, 2935, 1718, 1542, 1255 $cm^{-1}$.

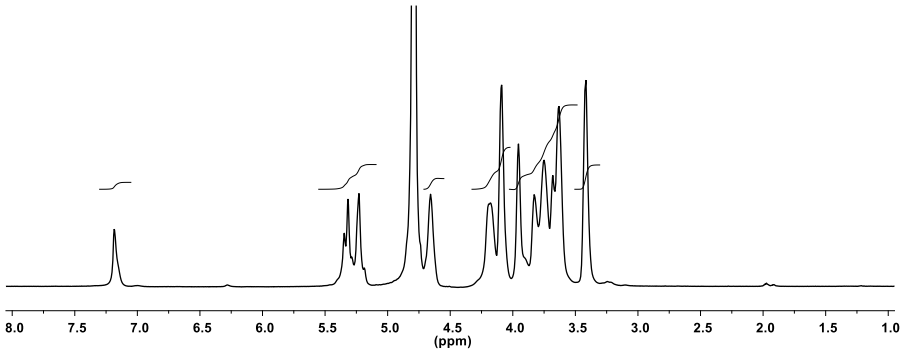


*Figure 115. $^{1}H$ NMR spectrum (500 MHz, $D_2O$) of 3[G4]-$OSO_3Na$.*

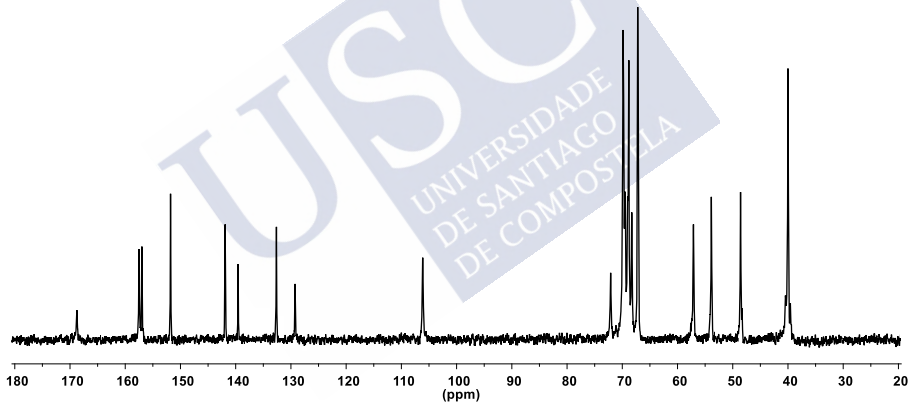


*Figure 116. $^{13}C$ NMR spectrum (125 MHz, $D_2O$) of 3[G4]-$OSO_3Na$.*

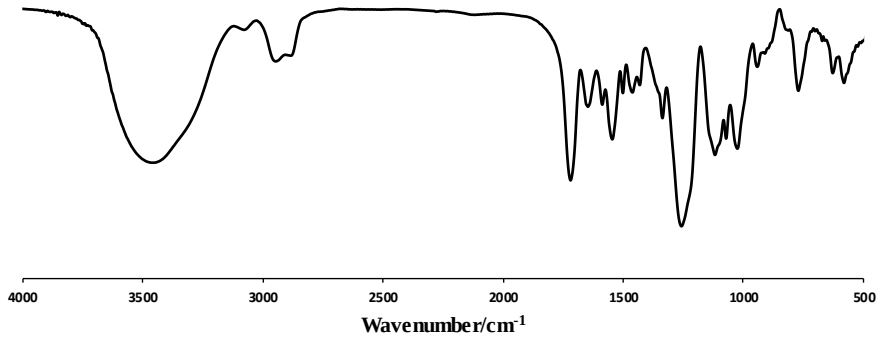


*Figure 117. IR (KBr) spectrum of 3[G4]-$OSO_3Na$.*

### 4.5.9 3[G4]-Man

In a Schlenk-flask, Alk-Man (120 mg, 158 ɀ mol) was added to a solution of 3[G3]-$N_3$ (24 mg, 0.974 ɀ mol) in tBuOH/$H_2O$ 5:1 (160 ɀ L). The reaction was stirred at 120 ºC for 12 h and then was purified by ultrafiltration (4 x 30 mL $H_2O$, Amicon YM3) and lyophilized to afford 3[G4]-Man as a brown foam (78 mg, 93%). $^1$H NMR (500 MHz, $D_2O$) δ: 7.18 (br s, 78H), 5.43-5.15 (m, 324H), 4.90 (s, 162H), 4.76-4.60 (m, 162H), 4.24-4.07 (m, 240H), 4.05-3.48 (m, 3306H), 3.37-3.21 (324H). $^{13}$C NMR (125 MHz, $D_2O$) δ: 168.9, 157.9, 157.4, 152.4, 142.4, 140.3, 133.2, 129.6, 106.7, 100.4, 73.2, 72.6, 71.0, 70.5, 70.3, 70.1, 70.0, 69.7, 69.6, 69.4, 68.9, 67.2, 66.7, 61.4, 60.8, 57.4, 54.3, 49.1, 40.6. IR (KBr): 3315, 1638, 1248, 1061 $cm^{-1}$.

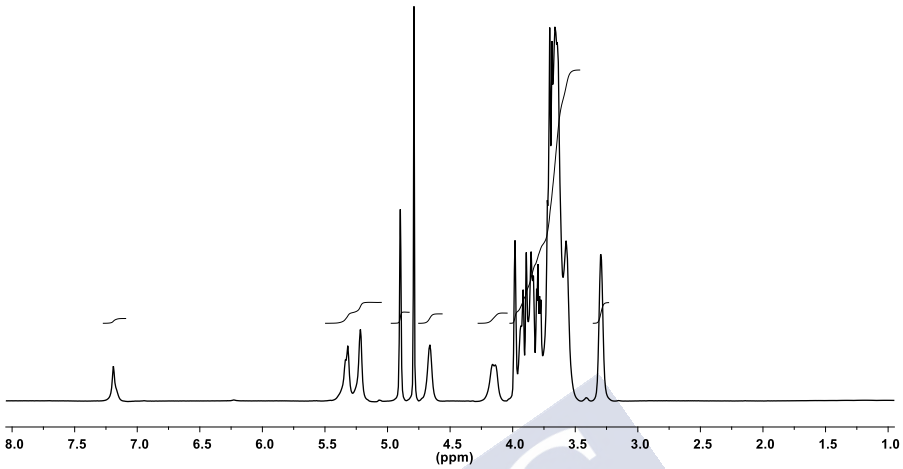


*Figure 118. $^{1}H$ NMR spectrum (500 MHz, $D_2O$) of 3[G4]-Man.*

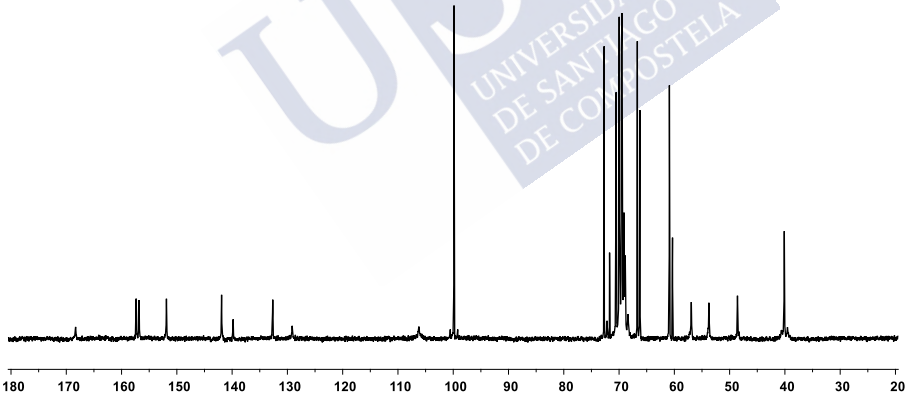


*Figure 119. $^{13}C$ NMR spectrum (125 MHz, $D_2O$) of 3[G4]-Man.*

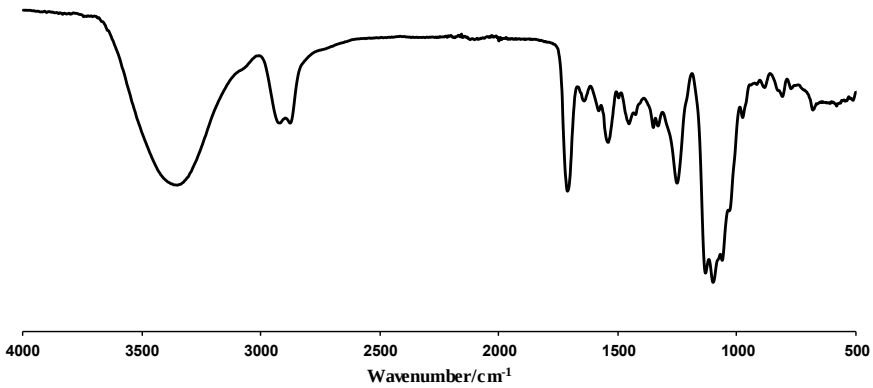


*Figure 120. IR (KBr) spectrum of 3[G4]-Man.*

### 4.5.10 3[G4]-Glu

In a Schlenk-flask, Alk-Glu (135 mg, 177 ɀmol) was added to a solution of 3[G3]-$N_3$ (26 mg, 1.1 ɀmol) in tBuOH/$H_2O$ 1:1 (178 ɀL). The reaction was stirred at 120 ºC for 14 h and then was purified by ultrafiltration (4 x 30 mL $H_2O$, Amicon YM3) and lyophilized to afford 3[G4]-Glu as a beige foam (85 mg, 92%). $^1$H NMR (500 MHz, $D_2O$) δ: 7.16 (br s, 78H), 5.40-5.13 (m, 324H), 4.72-4.58 (m, 162H), 4.52-4.43 (m, 162H), 4.26-3.99 (m, 402H), 3.99-3.36 (m, 3144H), 3.35-3.21 (m, 324H). $^{13}$C NMR (125 MHz, $D_2O$) δ: 168.9, 157.9, 157.4, 152.4, 142.4, 140.3, 133.2, 129.7, 106.7, 102.7, 76.4, 76.2, 73.4, 70.4, 70.1, 69.9, 69.8, 69.6, 69.4, 69.0, 61.3, 57.5, 54.3, 49.1, 40.6. IR (KBr): 3354, 2878, 1710, 1251, 1079 cm$^{-1}$.

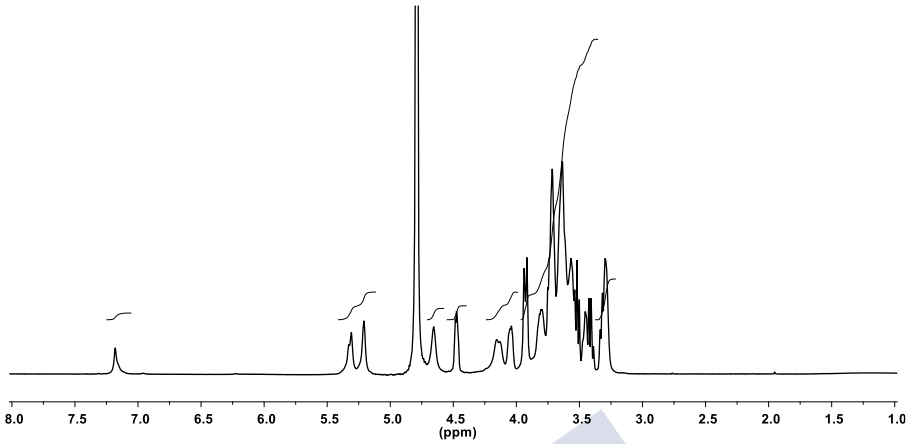


*Figure 121. $^{1}H$ NMR spectrum (500 MHz, $D_2O$) of 3[G4]-Glu.*

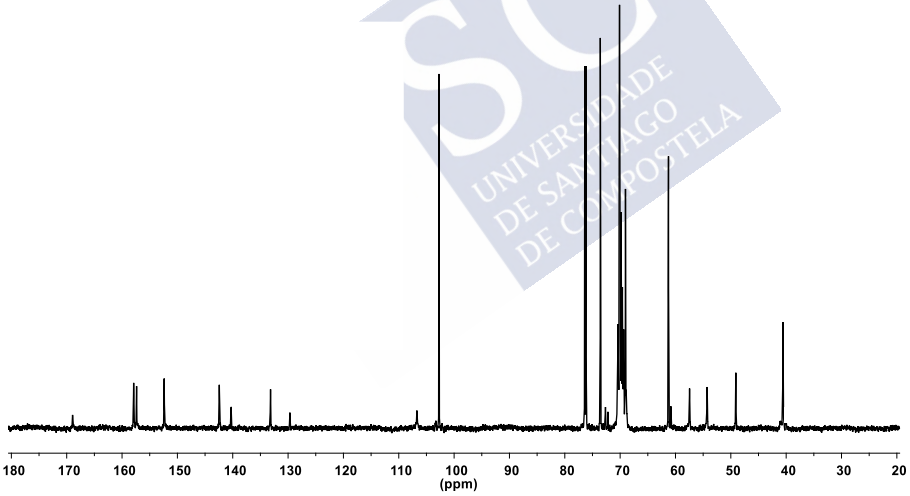


*Figure 122. $^{13}C$ NMR spectrum (125 MHz, $D_2O$) of 3[G4]-Glu.*

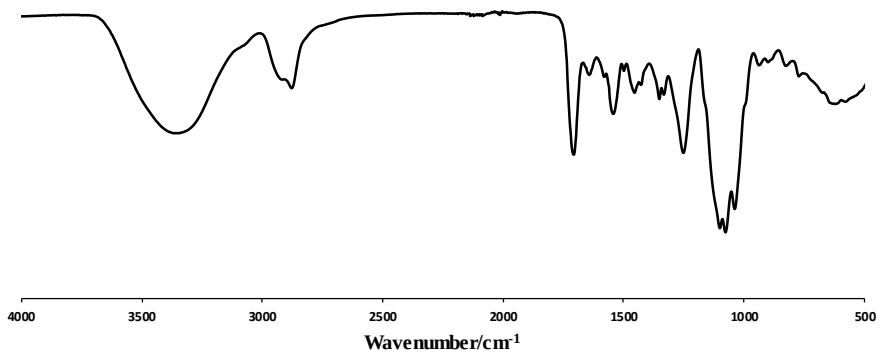


*Figure 123. IR (KBr) spectrum of 3[G4]-Glu.*

### 4.5.11 3[G4]-TEG-$NH_2$·HCl

In a Schlenk-flask, Alk-TEG-$NH_2$·HCl (173 mg, 339 ɀ mol) was added to a solution of 3[G3]-$N_3$ (50 mg, 2.10 ɀ mol) in tBuOH/$H_2O$ 1:1 (170 ɀ L). The reaction was stirred at 120 ºC for 8 h and then was purified by ultrafiltration (4 x 30 mL $H_2O$, Amicon YM3) and lyophilized to afford 3[G4]-TEG-$NH_2$·HCl as a white foam (125 mg, 92%). $^1$H NMR (500 MHz, $D_2O$) δ: 7.16 (br s, 78H), 5.40-5.12 (m, 324H), 4.71-4.55 (m, 162H), 4.29-4.02 (m, 240H), 4.00-3.46 (m, 2334H), 3.34-3.17 (m, 648H). $^{13}$C NMR (125 MHz, $D_2O$) δ: 168.7, 157.6, 157.0, 151.9, 141.9, 139.7, 132.7, 129.2, 106.2, 72.0, 69.8, 69.7, 69.4, 69.0, 68.7, 68.3, 66.2, 56.9, 53.7, 48.5, 39.8, 38.9. IR (KBr): 3383, 2971, 1677, 1201, 1130 cm$^{-1}$.

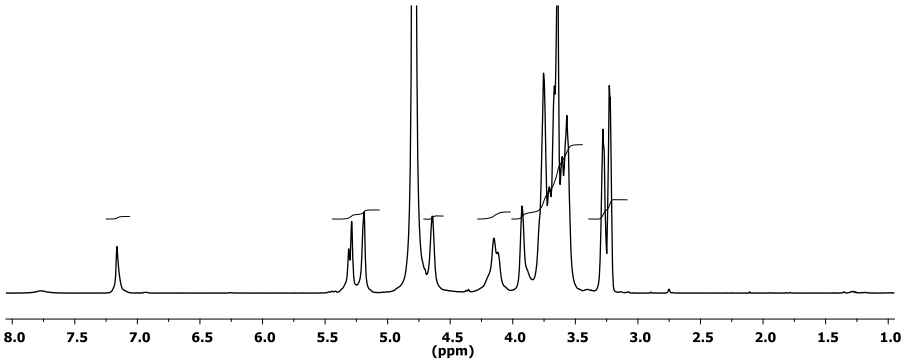


*Figure 124. $^{1}H$ NMR spectrum (500 MHz, $D_2O$) of 3[G4]-TEG-$NH_2$·HCl.*

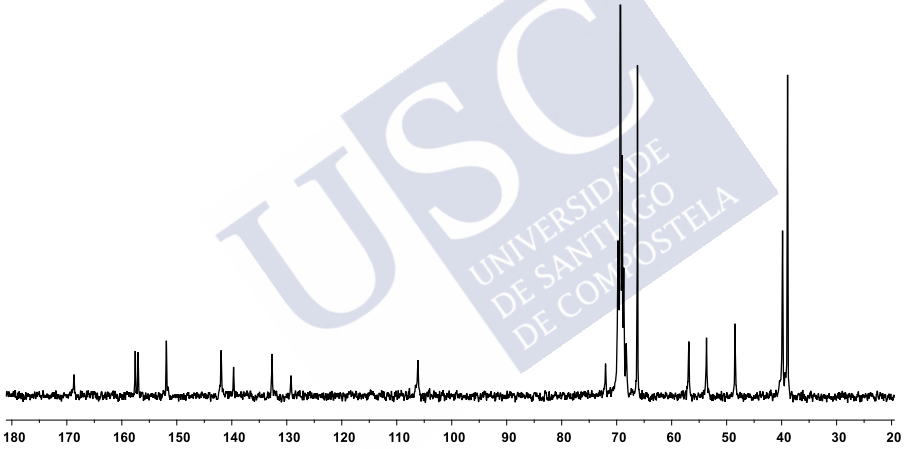


*Figure 125. $^{13}C$ NMR spectrum (125 MHz, $D_2O$) of 3[G4]-TEG-$NH_2$·HCl.*

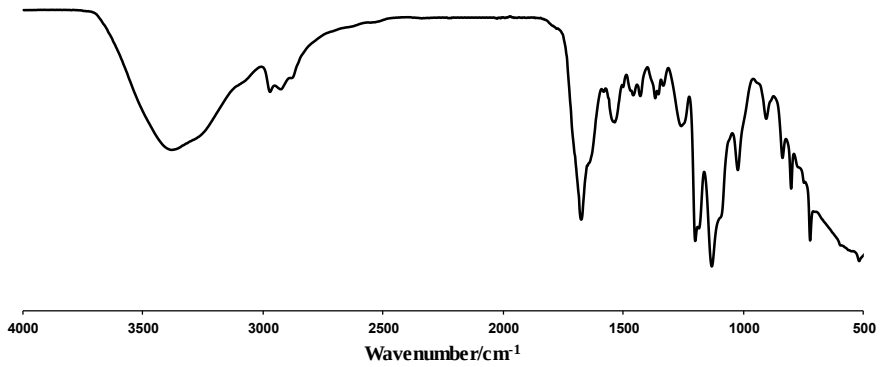


*Figure 126. IR (KBr) spectrum of 3[G4]-TEG-$NH_2$·HCl.*

### 4.5.12 3[G4]-DOTA

In a Schlenk-flask, p-NCS-Bz-DOTA-GA (96 mg, 173 τmol) was added to a solution of Alk-TEG-$NH_2$·HCl (25 mg, 57.6 τmol) and $Et_3N$ (48 τL, 346 τmol) in dry DMSO (30 τL) under argon. After 24 h of stirring at rt, 3[G3]-$N_3$ (4.4 mg, 0.18 τmol) was added. The reaction mixture was stirred at 120 ºC for 32 h and then was purified by ultrafiltration (4 x 30 mL 50 mM PB pH 7.4 and 3 x 30 mL $H_2O$, Amicon YM3) and lyophilized to afford 3[G4]-DOTA as a brown foam (26 mg, 90%). $^1$H NMR (500 MHz, $D_2O$, 50 ms DOSY filter) δ: 7.59-6.97 (m, 648H), 6.97-6.68 (m, 78H), 5.41-5.10 (m, 324H), 4.76-4.57 (m, 162H), 4.52-4.08 (m, 324H), 4.07-2.92 (m, 7356H), 2.55-2.26 (m, 324H), 2.11-1.82 (m, 324H). IR (KBr): 3319, 2872, 1712, 1631, 1540, 1094 $cm^{-1}$.

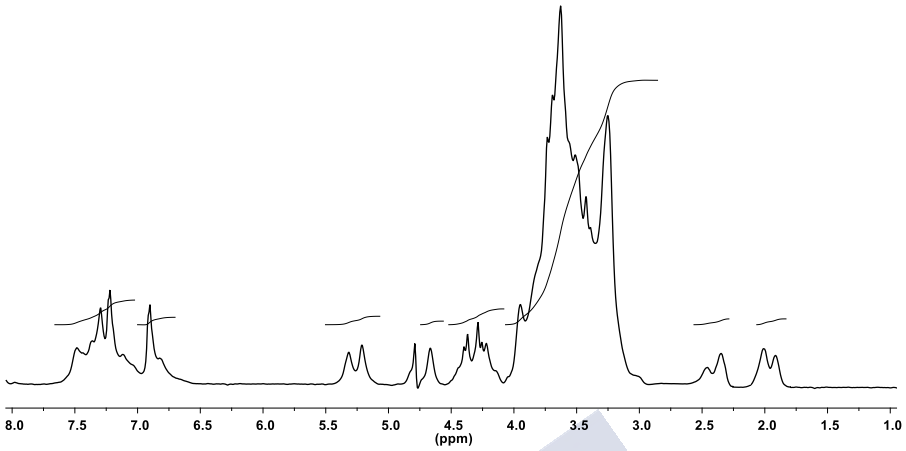


*Figure 127. $^{1}H$ NMR spectrum (500 MHz, $D_2O$) of 3[G4]-DOTA.*

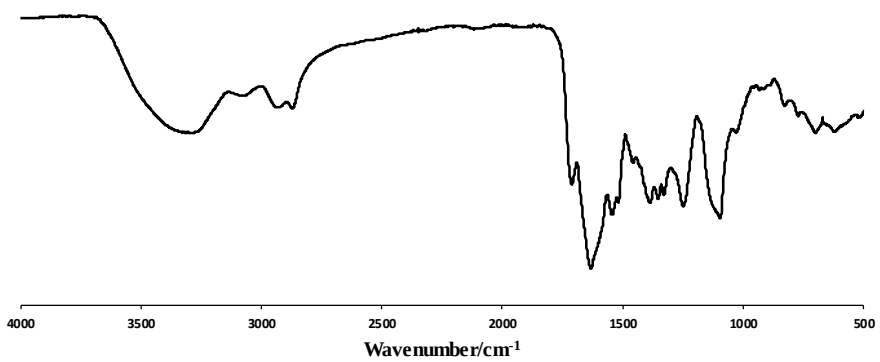


*Figure 128. IR (KBr) spectrum of 3[G4]-DOTA.*

### 4.5.13 3[G4]-(Man)$_{60}$/(Bio)$_{16}$/(FITC)$_5$

In a Schlenk-flask, Alk-Man (38 mg, 50 ɀ mol), Alk-Bio (12 mg, 13.4 ɀ mol) and Alk-FITC (5.1 mg, 4.2 ɀ mol) were added to a solution of 3[G3]-$N_3$ (10 mg, 0.42 ɀ mol) in tBuOH/$H_2O$ 1:1 (68 ɀ L). The reaction was stirred at 120 $^{o}$C for 14 h and then was purified by ultrafiltration (5 x 30 mL $H_2O$, Amicon YM3) and lyophilized to

afford 3[G4]-$(Man)_{60}$/$(Bio)_{16}$/$(FITC)_5$ as a pale red foam (36 mg, 96%). $^1$H NMR (500 MHz, $D_2O$) δ: 7.38-7.05 (m, 104H), 6.71-6.63 (m, 10H), 5.45-5.09 (m, 324H), 4.90 (s, 120H), 4.74-4.55 (m, 162H), 4.54-4.45 (m, 32H), 4.34-4.03 (m, 272H), 4.02-3.42 (m, 4798H), 3.41-3.09 (m, 340H), 2.93-2.64 (m, 64H), 2.30-2.12 (m, 64H), 1.71-1.17 (m, 192H). $^{13}$C NMR (125 MHz, $D_2O$) δ: 176.2, 168.5, 165.1, 157.5, 156.9, 151.9, 141.9, 140.9, 132.7, 129.2, 106.1, 100.1, 72.6, 72.1, 71.6, 70.4, 69.9, 69.5, 69.4, 69.1, 68.8, 68.3, 66.6, 66.2, 62.4, 61.4, 60.8, 60.7, 57.5, 55.8, 54.3, 49.1, 48.8, 40.6, 40.2, 39.9, 39.3, 35.9, 28.5, 28.2, 25.7. IR (KBr): 3326, 2928, 1581, 1025 cm$^{-1}$.

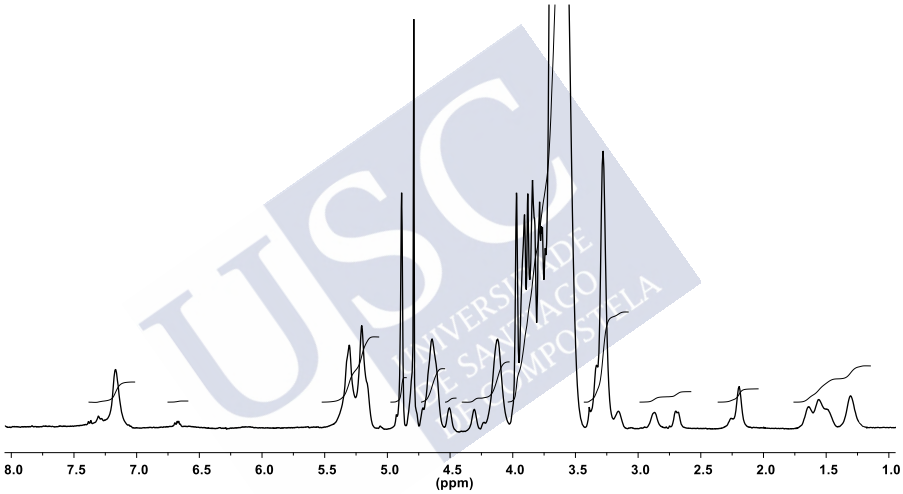


*Figure 129. $^1$H NMR spectrum (500 MHz, $D_2O$) of 3[G4]-$(Man)_{60}$/$(Bio)_{16}$/$(FITC)_5$.*

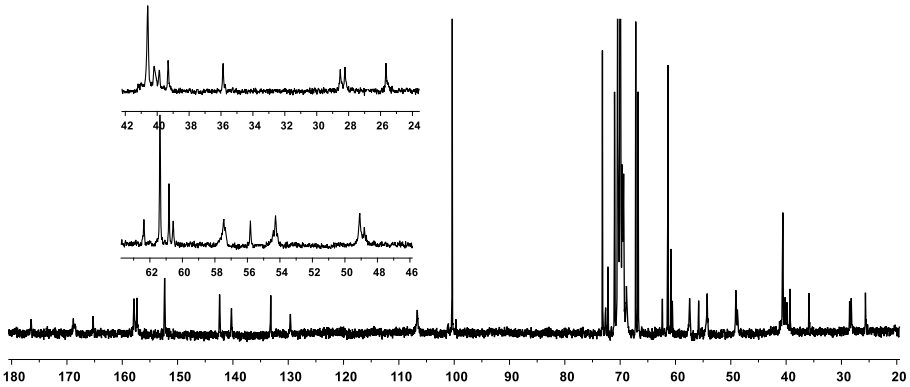


*Figure 130. $^{13}C$ NMR spectrum (125 MHz, $D_2O$) of 3[G4]-$(Man)_{60}$/$(Bio)_{16}$/$(FITC)_5$.*

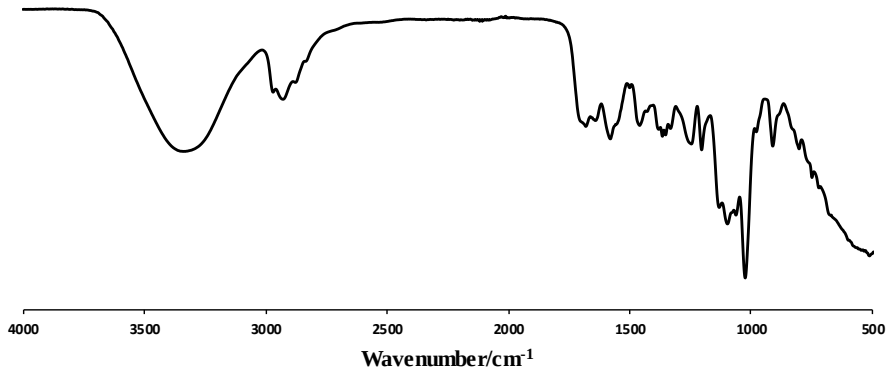


*Figure 131. IR (KBr) spectrum of 3[G4]-$(Man)_{60}$/$(Bio)_{16}$/$(FITC)_5$.*

### 4.5.14 3[G5]-Man

In a Schlenk-flask, Alk-Man (123 mg, 162 ɀ mol) was added to a solution of 3[G4]-$N_3$ (25 mg, 0.346 ɀ mol) in tBuOH/$H_2O$ 5:1 (168 ɀ L). The reaction was stirred at 120 $^oC$ for 12 h and then was purified by ultrafiltration (4 x 30 mL $H_2O$, Amicon YM5) and lyophilized to afford 3[G5]-Man as a brown foam (84 mg, 94%). $^1H$ NMR (500 MHz, $D_2O$) δ: 7.17 (br s, 240H), 5.40-5.13 (m, 972H), 4.89 (s, 486H),

4.75-4.57 (m, 486H), 4.27-4.05 (m, 762H), 4.02-3.45 (m, 10920H), 3.35-3.20 (m, 972H). $^{13}$C NMR (125 MHz, $D_2O$) δ: 168.3, 157.4, 156.8, 151.9, 141.9, 139.8, 132.6, 129.1, 106.2, 99.9, 72.7, 72.2, 71.7, 70.5, 70.0, 69.9, 69.7, 69.6, 69.4, 69.1, 68.9, 68.4, 66.7, 66.2, 60.9, 60.3, 56.9, 53.7, 48.6, 40.1. IR (KBr): 3409, 2927, 1712, 1251, 1095 $cm^{-1}$.

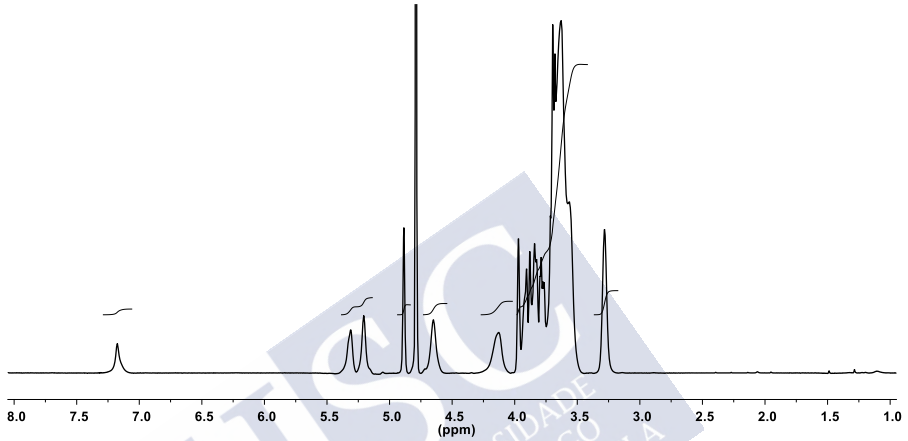


*Figure 132. $^{1}$H NMR spectrum (500 MHz, $D_2O$) of 3[G5]-Man.*

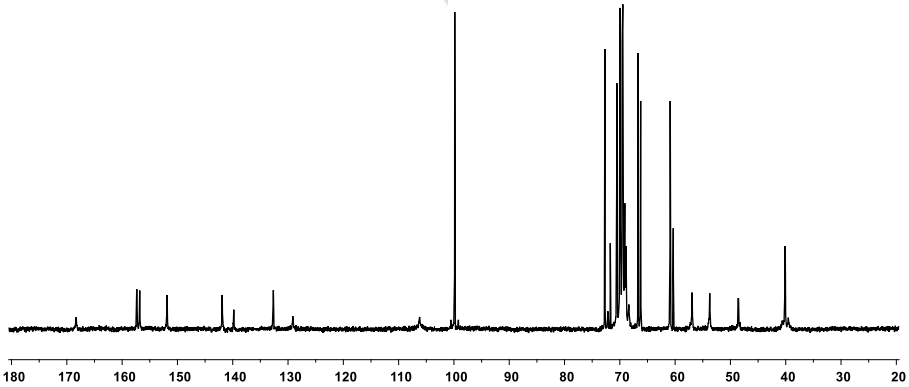


*Figure 133. $^{13}$C NMR spectrum (125 MHz, $D_2O$) of 3[G5]-Man.*

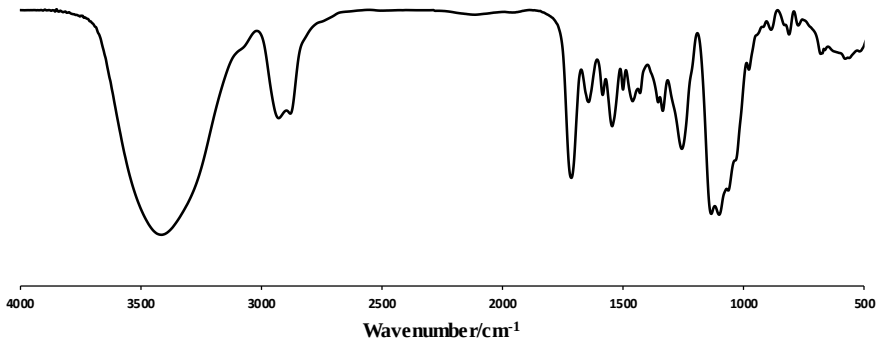


*Figure 134. IR (KBr) spectrum of 3[G5]-Man.*

### 4.5.15 $PEG_{5k}$-[G3]-Cat

In a Schlenk-flask, Alk-Cat (10 mg, 23.5 ɀmol) was added to a solution of $PEG_{5k}$-[G2]-$N_3$ (10 mg, 1.31 ɀmol) in tBuOH/$H_2O$ 1:1 (24 ɀL). The reaction was stirred at 120 ºC for 12 h and then was purified by ultrafiltration (4 x 30 mL acetone/$H_2O$ 3:1 and $H_2O$ 2 x 30 mL, Amicon YM3) and lyophilized to afford $PEG_{5k}$-[G3]-Cat as a brown foam (13 mg, 86%). $^1$H NMR (500 MHz, DMSO-$d_6$) δ: 8.78-8.39 (m, 36H), 7.38-7.25 (m, 18H), 7.24-7.12 (m, 24H), 6.66-6.31 (m, 54H), 5.26-5.01 (m, 36H), 4.59-4.46 (m, 18H), 4.20-3.95 (m, 24H), 3.86-2.98 (m, 634H). IR (KBr): 3318, 2877, 1702, 1361, 1221, 1091 cm$^{-1}$.

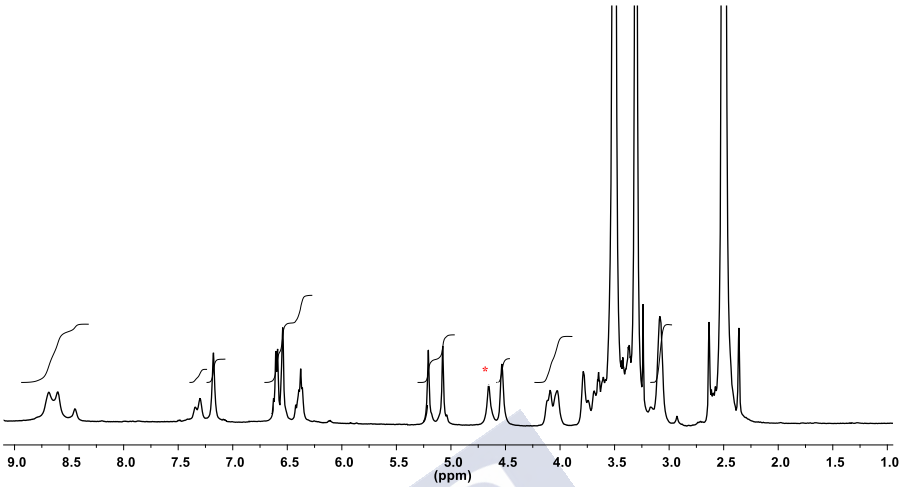


*Figure 135. $^{1}H$ NMR spectrum (500 MHz, DMSO-$d_6$) of $PEG_{5k}$-[G3]-Cat.*

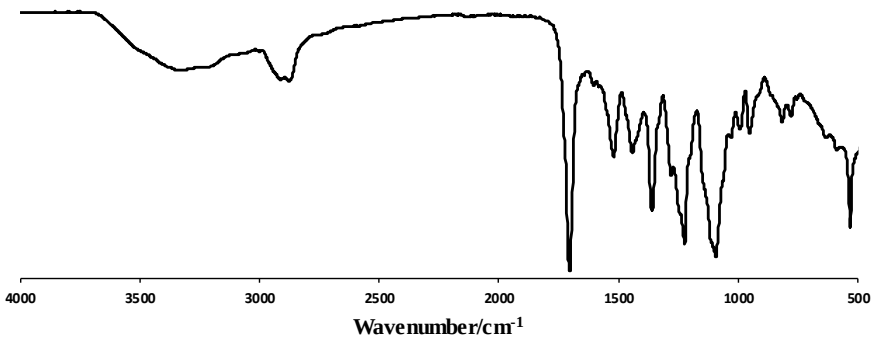


*Figure 136. IR (KBr) spectrum of $PEG_{5k}$-[G3]-Cat.*

### 4.5.16 $PEG_{5k}$-$PGA_{25}$-[G1]-OH

In a Schlenk-flask, Alk-OH (12 mg, 46 ɀmol) was added to a solution of $PEG_{5k}$-$PGA_{25}$-$N_3$ (10 mg, 0.9 ɀmol) in tBuOH/$H_2O$ 1:1 (46 ɀL). The reaction was stirred at 120 °C for 12 h and then was purified by ultrafiltration (4 x 30 mL $H_2O$, Amicon YM3) and

lyophilized to afford $PEG_{5k}$-$PGA_{25}$-[G1]-OH as a pale yellow foam (13 mg, 81%). $^1$H NMR (500 MHz, $D_2O$) δ: 5.41-5.10 (m, 92H), 4.56-4.24 (m, 69H), 3.93-3.51 (m, 568H), 3.32-3.05 (m, 138H), 2.46-2.24 (m, 46H), 2.24-1.89 (m, 96H). IR (KBr): 3295, 2878, 1703, 1649, 1535, 1249, 1076 $cm^{-1}$.

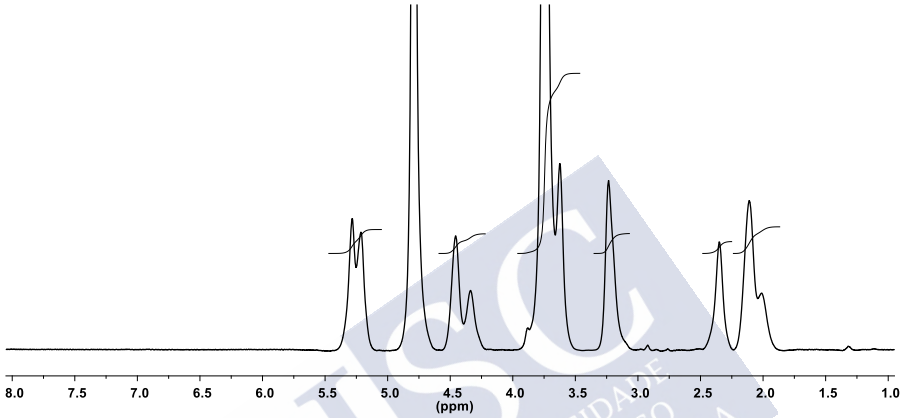


*Figure 137. $^1$H NMR spectrum (500 MHz, $D_2O$) of $PEG_{5k}$-$PGA_{25}$-[G1]-OH.*

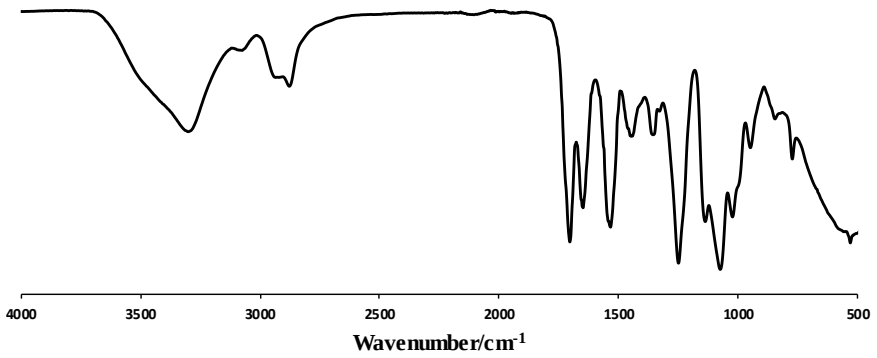


*Figure 138. IR (KBr) spectrum of $PEG_{5k}$-$PGA_{25}$-[G1]-OH.*

## 4.6 Interaction with Con A

A solution of Con A (17 ɀM in 20 mM Tris-HCl, 250 mM NaCl, 1 mM $CaCl_2$, 1 mM $MnCl_2$, pH 6.2) was added in 10 ɀL portions to a solution of the mannosylated dendrimer 3[G4]-$(Man)_{60}$/$(Bio)_{16}$/$(FITC)_5$ (300 ɀL, 1.67 mM in 20 mM Tris-HCl, 250 mM NaCl, 1 mM $CaCl_2$, 1 mM $MnCl_2$, pH 6.2). After each addition, the mixture was allowed to stand for 5 min before the absorbance at 700 nm being recorded and proceed with the next addition. Once the absorbance reached a constant value, a subsequent addition of a saturated solution of α-methyl-D-mannopyranoside (10 ɀL ) recovered the original absorbance value. Same experiment was applied to a 17 ɀM solution of lysozyme in the same buffer as a control protein, not recognizing mannose.

## 4.7 Incubation of Agarose Beads (Streptavidin) with 3[G4]-$(Man)_{60}$/$(Bio)_{16}$/$(FITC)_5$]

A suspension of streptavidin-agarose beads (25 ɀL, 10.1 mg/mL in 10 mM PB pH 7.4, 150 mM NaCl) was added to a solution of fluorescently labelled 3[G4]-$(Man)_{60}$/$(Bio)_{16}$/$(FITC)_5$ dendrimer (1.0 mL, 1.0 mg/mL in 10 mM PB pH 6.5, 150 mM NaCl). The resulting suspension was shaken in the dark for 2 h at 37 ºC. Then, the beads were centrifuged (1000 g, 30 s), washed (10 mM PB pH 6.5, 150 mM NaCl) and centrifuged again. After three additional washing/centrifugation cycles, beads were finally suspended in 10 mM PB pH 7.4, 150 mM NaCl and analyzed by fluorescence microscopy on an Olympus BX-51 microscope equipped with an Olympus DP-71 camera. Excitation of fluorescent streptavidin-agarose beads was carried out in the green channel (blue excitation U-MWB2: excitation filter 460-490 nm, emission filter 520 nm and dichromatic mirror 500 nm). Unfunctionalized agarose beads (no streptavidin) treated with 3[G4]-$(Man)_{60}$/$(Bio)_{16}$/$(FITC)_5$ under identical conditions served as control.

### 4.8 Preparation of $PEG_{5k}$-[G3]-Cat micelles and DOX-loaded $PEG_{5k}$-[G3]-Cat micelles

$PEG_{5k}$-[G3]-Cat was dissolved in 10 mM PB pH 7.4, 150 mM NaCl (1 mg/mL). DOX was dissolved in 150 mM NaCl (1 mg/mL). Both solutions were filtered through 0.45 μm nylon filters.

- Self-assembly of $PEG_{5k}$-[G3]-Cat in solution was confirmed by DLS after 1 h at rt.

- Dox-loaded micelles were prepared by adding the $PEG_{5k}$-[G3]-Cat solution over that of DOX in a volume ratio 2:1. The resulting solution was left in the dark under stirring at 37 ºC for 48 h. Unloaded DOX was removed by dialysis (Spectra/Por® 6, MWCO 1 KDa) against 250 mL of 10 mM PB pH 7.4, 150 mM NaCl for 12 h in the dark at 37 ºC. To determine the EE and DL of DOX, aliquots of the buffer solution were taken at the end of the dialysis (3 × 150 μL) and placed in a 96-well microplate. Then, 500 mM acetate pH 4 buffer (50 μL) was added to each well and the fluorescence of the samples was measured at a microplate reader (exc. 485±20 nm, em. 535±20 nm; Tecan Infinite F200 PRO). The concentration of unloaded DOX in solution was determined by comparison with a standard calibration curve made from the fluorescence emission of fresh solutions of DOX of known concentration prepared under identical conditions. An EE of 87% and DL of 29% were obtained.

# 5 Conclusion

With the aim of exploring new methodologies for the functionalization of GATG dendrimers while taking advantage of their of peripheral decoration with terminal azides, we have focused on the thermal azide-alkyne cycloaddition (TAAC). Using internal alkynes activated with propargylic carbamates, reliable TAAC conditions (temperature, concentration, solvent and time) were optimized with a model system mimicking the GATG periphery. At the same time, a scaling up of the synthesis of GATG dendrimers of the 2G and 3G families was achieved that allowed preparation of G4 dendrimers of both families in gram scale. With these two pieces in hand, internal alkynes functionalized with several ligands of biomedical interest (anionic and cationic groups, biotin, carbohydrates, alcohols, phenol, catechol, fluorophores as FITC, and chelating agents such as DOTA) were efficiently synthesized and used for the TAAC functionalization of several generations of GATG dendrimers and PEG-dendritic block copolymers. The resulting functionalized dendritic structures were reproducibly obtained in very high yields after heating at 120 ºC for 6-8 h followed by easy purifications by ultrafiltration. These materials are envisaged as promising tools for different biological applications, including drug delivery, multivalent recognition and cell internalization.